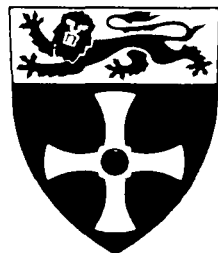


UNIVERSITY OF
NEWCASTLE UPON TYNE



The Role of PARP-1 in the Cellular Response to Topoisomerase I Poisons.

NEWCASTLE UNIVERSITY LIBRARY

204 06047 3

MED Thesis L7756

PhD Thesis

Lisa M. Smith

Feb 2004

Abstract

The role of poly(ADP-ribose)polymerase-1 (PARP-1) in the cellular response to topoisomerase I poisons.

PARP-1 inhibitors enhance DNA topoisomerase I (Topo I) poison-induced cytotoxicity and anti-tumour activity *in vitro* and *in vivo* but the underlying mechanism has not been defined. Two hypotheses have been proposed to explain this a) PARP-I modulates topo I activity via poly(ADP-ribosylation), or b) PARP-1 participates in the repair of topo I-induced DNA lesions. To explore these mechanisms we have investigated the cellular effects of a novel potent PARP-1 inhibitor, AG14361 ($K_i < 5$ nM), in combination with the topo I poisons, camptothecin and topotecan.

PARP-1 null mouse embryonic fibroblasts (MEFs) were 3-fold more sensitive to topotecan than PARP-1 wild type MEFs. AG14361 significantly enhanced topotecan-induced growth inhibition by 3-fold in PARP-1 wild-type cells but not PARP-1 null cells. This confirms that PARP-1 activity promotes survival after topo I poison-induced cytotoxicity and the cellular effects of AG14361 are due to PARP-1 inhibition. AG14316 also increased camptothecin-induced growth inhibition in human K562 cells ~2-fold. AG14361 did not affect topo I-DNA cleavable complexes or topo I relaxation activity. In contrast, AG14361 increased camptothecin-induced DNA strand breaks by 20% and significantly retarded DNA repair following camptothecin removal, (62% inhibition of repair 10 mins). These data indicate a role for PARP-1 in the repair of topo I poison-mediated damage. The repair pathways by which PARP-1 acts to repair this damage was investigated using repair-deficient cells. AG14361 significantly potentiated the cytotoxicity of camptothecin in AA8 repair-proficient and V3 non-homologous end joining-deficient cells, but not the *irs1*SF homologous recombination-deficient or EM9 base excision repair-deficient cells. AG14361 also failed to retard the repair of camptothecin-induced DNA damage in EM9 cells. This suggests that PARP-1 may act via BER and possibly HR to repair topo I poison-mediated DNA damage.

Acknowledgements.

I would like to thank everybody at the NICR for their help, support and friendship throughout my PhD. In particular I must thank, my supervisors, Nicola Curtin, Caroline Austin, and Elaine Willmore, and the members of the Drug Development Lab without whose guidance and support this thesis could not have been completed. A special mention must go to the former residents of 5, Fifth Avenue, for helping in brightening up the worst of days and in escaping from it all. Finally, I must thanks James for putting up with me while writing this, I could not have done it without him.

Abbreviations.

3-AB	3-Aminobenzamide
5-FU	5-Fluorouracil
ATM	Ataxia telangiectasia mutated protein
ATR	Ataxia telangiectasia related protein
BCNU	1,3-(bis(2-chloroethyl)-1-nitrosourea
BER	Base Excision Repair
BRCT	BRCA-1 C-terminus domain
CHO	Chinese hamster ovary
CPT	Camptothecin
CSA	Cockayne syndrome A protein
CSB	Cockayne syndrome B protein
DBD	DNA binding domain
DMEM	Dulbecco's Modified Eagle's medium
DMS	Dimethyl sulfate
DMSO	Dimethyl sulfoxide
DNA	Deoxyribonucleic acid
DNA-PK	DNA-dependant protein kinase
dpm	Disintegrations per minute
DSB	Double strand break
ECL	Enhanced Chemiluminescence
EMS	Ethyl methanesulfonate
ENU	N-ethyl-N-nitrosourea
FITC	Fluorescein isothiocyanate
GI ₅₀	Growth inhibitory IC ₅₀ - Concentration of drug required to inhibit cell growth by 50%
Gy	Gray
HR	Homologous recombination
HRP	Horse-radish peroxidase
IC ₅₀	Concentration of drug required to inhibit by 50%
IR	Ionising Radiation
LC ₅₀	Concentration required to be lethal to half of the population of cells
MEF	Mouse Embryo Fibroblast
MMS	Methyl methanesulfonate
MNNG	N-methyl-N'-nitro-N-nitrosoguanidine
MNU	N-methyl-N-nitrosourea
MRC	Multiprotein replication complex
NAD	Nicotinamide adenine dinucleotide

NER	Nucleotide Excision Repair
NHEJ	Non -homologous end-joining
NLS	Nuclear localisation sequence
OD	Optical density
PARG	Poly(ADP-ribose) glycohydrolase
PARP-1	Poly(ADP-ribose) polymerase-1
PBS	Phosphate Buffered Saline
PF ₅₀	Potential factor
PLDB	Protein-linked DNA break
PNK	Polynucleotide kinase/phosphatase
RE	Relative elution
RNA	Ribonucleic acid
RPA	Replication protein A
SD	Standard deviation
SDS-PAGE	Sodium dodecyl sulphate - Polyacrylamide gel electrophoresis
SEM	Standard Error
SRB	Sulforhodamine B
SUMO	Small ubiquitin-like modifier
TARDIS	Trapped in Agarose DNA immunostaining
TCA	Trichloroacetic acid
TDP-1	Tyrosyl DNA phosphodiesterase-1
Topo-1	Topoisomerase-1
TP	Topotecan
UV	Ultraviolet
XRCC1	X-ray cross-complementing protein-1

Table of Contents.

Chapter 1: Introduction.	1
1.1 Cancer.	2
1.2 Cancer treatment.	3
1.2.1 Surgery.	3
1.2.2 Radiotherapy.	3
1.2.3 Hormone therapy.	4
1.2.4 Gene Therapy.	4
1.2.5 Immunotherapy.	4
1.2.6 Chemotherapy.	4
1.3 Topoisomerases.	6
1.3.1 Human DNA Topoisomerase I	6
1.3.2 Structure of Topoisomerase I.	6
1.3.3 Topoisomerase I mechanism.	8
1.3.4 Regulation of topoisomerase I by other proteins.	9
1.4 Topoisomerase I poisons.	11
1.4.1 Camptothecin .	12
1.4.2 Topotecan.	14
1.4.3 Irintotecan.	14
1.4.4 Topoisomerase I Poison Mechanism of Action.	15
1.4.5 Binding of camptothecin to the cleavage complex.	17
1.4.6 Resistance to topoisomerase I poisons	19
1.5 DNA repair.	21
1.5.1 Base excision repair (BER).	22
1.5.2 Nucleotide excision repair (NER).	25
1.5.3 Double strand break repair.	25
1.6 PARP-1.	27
1.6.1 PARP Homologues.	28
1.6.2 Structure of PARP-1.	29
1.6.3 PARP-1 reaction mechanism.	31
1.6.4 Poly(ADP-ribose) degradation.	32
1.6.5 Acceptors of poly(ADP-ribose).	32
1.6.6 Consequences of poly(ADP-ribosylation).	33
1.6.7 PARP-1 and DNA repair.	34
1.6.8 Role of PARP-1 in cell death.	40
1.7 Development of PARP-1 inhibitors.	41
1.7.1 Chemo and radio-potentiation by PARP-1 inhibitors.	45
1.8 PARP-1 and Topoisomerase I: Background to this project	48
1.9 Aims	50
 Chapter 2: Methods.	 52
2.1 Materials.	53
2.2 Equipment.	53
2.3 General Tissue Culture.	53
2.3.1 Cryogenic Storage of Cell Lines.	54
2.3.2 Cell Lines.	54

2.3.3	Maintenance of cell lines.	57
2.3.4	Subculture of cell lines.	57
2.3.6	Cell counting.	57
2.3.7	Determination of cell doubling time.	58
2.4	Growth inhibition and cytotoxicity assays.	59
2.4.1	Sulforhodamine B (SRB) assay.	59
2.4.2	XTT cell proliferation assay.	60
2.4.3	Cell counting.	61
2.4.4	Clonogenic survival assay.	61
2.4.5	Sloppy agar clonogenic survival assay.	62
2.5	SDS-polyacrylamide gel electrophoresis and Western blotting.	63
2.5.1	Sample preparation.	63
2.5.2	Electrophoresis.	64
2.5.3	Western blotting.	65
2.6	PARP-1 activity assay.	66
2.6.1	Preparation of cells.	66
2.6.2	Preparation of radiolabelled NAD ⁺ .	67
2.6.3	Assay.	67
2.6.4	Calculation of results.	68
2.7	Measurement of Topoisomerase I activity by DNA Relaxation.	68
2.7.1	Preparation of nuclear extracts.	69
2.7.2	Relaxation Assay.	69
2.8	Trapped in agarose DNA immunostaining (TARDIS).	70
2.8.1	Slide Preparation.	71
2.8.2	Microscopy.	71
2.8.3	Analysis of results.	72
2.9	Potassium-SDS assay for detection of enzyme-DNA complexes.	74
2.9.1	Assay.	74
2.9.2	Calculation of results.	75
2.10	Measurement of DNA single strand breaks by alkaline elution.	75
2.10.1	Cell Preparation.	76
2.10.2	Preparation of Filters.	76
2.10.3	Elution.	77
2.10.4	Processing of filters.	77
2.10.5	Calculation of results and relative elution.	78
2.11	Statistical analysis.	78

Chapter 3: Effect of PARP-1 inhibition on topoisomerase I poison-induced cytotoxicity in cells. 81

3.1	Introduction.	82
3.2	Aims.	87
3.3	Results.	88
3.3.1	Characterisation of cell lines.	88
3.3.2	Investigation of growth inhibitory effects of AG14361.	95
3.3.3	Investigation of PARP-1 inhibitory effects of AG14361.	98
3.3.4	Effect of AG14361 on Topo I poison-mediated growth inhibition.	101
3.3.5	Effect of AG14361 on camptothecin-induced cytotoxicity in K562 cells.	108

3.3.6	Effect of AG14361 on survival of K562 cells exposed to camptothecin for 16 hours.	113
3.4	Discussion.	115

Chapter 4: Effect of PARP-1 on topoisomerase I activity.

4.1	Introduction.	121
4.2	Aims	125
4.3	Results.	126
4.3.1	Measurement of the effect of AG14361 on topoisomerase I relaxation activity.	126
4.3.2	Measurement of topoisomerase I poison-stabilised cleavable complexes.	130
	<i>4.3.2.1 Effect of 30 min exposure to camptothecin on levels of cleavable complexes.</i>	131
	<i>4.3.2.2 Effect of AG14361 on camptothecin-stabilised cleavable complex formation.</i>	135
	<i>4.3.2.3 Effect of AG14361 on persistence of cleavable complexes.</i>	137
	<i>4.3.2.4 Effect of PARP-1 stimulation by ionising radiation (IR) on cleavable complex formation.</i>	141
4.3.3	Effect of PARP-1 on levels of camptothecin-stabilised cleavable complexes measured using potassium-SDS precipitation (K-SDS).	143
	<i>4.3.3.1 Effect of AG14361 on levels of camptothecin-stabilised cleavable complexes.</i>	143
	<i>4.3.3.2 Effect of AG14361 on reversal of topo I poison-stabilised cleavable complexes measured by K-SDS.</i>	147
	<i>4.3.3.3 Effect of camptothecin on cleavable complex formation in PARP-1 wild type and null cells.</i>	149
4.4	Discussion.	150

Chapter 5: Effect of PARP-1 on inhibition of topoisomerase I poison-induced DNA single strand breaks.

5.1	Introduction.	158
5.2	Aims.	162
5.3	Results.	163
5.3.1	Effect of AG14361 on camptothecin-induced DNA single strand breaks.	163
5.3.2	Effect of drug scheduling on camptothecin-mediated DNA strand breaks.	170
5.3.3	Effect of AG14361 on repair of camptothecin-induced DNA damage in PARP-1 wild-type and null cells.	181
5.3.4	Repair of camptothecin-induced DNA strand breaks in PARP-1 wild type and null cells.	188
5.4	Discussion.	191

Chapter 6: Effect of PARP-1 inhibition on topoisomerase I poison mediated cytotoxicity in cell lines deficient in DNA repair.	196
6.1 Introduction.	197
6.2 Aims.	203
6.3 Results.	205
6.3.1 Effect of AG14361 on camptothecin-induced cytotoxicity in AA8, EM9 and V3 cell lines.	205
6.3.2 Effect of AG14361 on camptothecin-induced cytotoxicity in the irs1SF (homologous recombination-deficient) cell line.	212
6.3.3 Effect of AG14361 on survival of irs1SF cells treated with camptothecin.	215
6.3.4 DNA damage repair in AA8 and EM9 cell lines.	217
6.4 Discussion	222
 Chapter 7: Discussion and Future Directions.	 228
 Chapter 8: References.	 237

Table of Figures

Figure 1.1 Crystal structure of mammalian DNA topoisomerase I in complex with DNA.	8
Figure 1.2 Unwinding of DNA by topoisomerase I.	9
Figure 1.3 Structure of the Camptothecins.	12
Figure 1.4 "Replication fork collision model" of topoisomerase I poison-mediated cytotoxicity.	16
Figure 1.5 "Transcription collision model"	17
Figure 1.6. Proposed model for camptothecin binding.	18
Figure 1.7 Base excision repair	24
Figure 1.8 Mechanisms of Double Strand Break Repair.	26
Figure 1.9 Schematic representation of the structure of PARP-1.	30
Figure 1.10 Synthesis of poly(ADP-ribose) by PARP-1.	32
Figure 1.11 Mechanism of action of PARP-1.	34
Figure 1.12 Interaction of PARP-1 with components of the BER pathway at sites of DNA damage.	38
Figure 1.13 Role of PARP-1 in cell death..	41
Figure 1.14 Features of a PARP-1 inhibitor.	43
Figure 1.15 Structure of PARP-1 inhibitors	44
Figure 1.16 Co-crystal structure of AG14361 in the catalytic domain of chicken PARP-1	46
Figure 1.17 Effect of AG14361 on topo I poison-induced growth inhibition (A) and tumour growth delay (B).	50
Figure 2.1 Inactivation of PARP-1 by homologous recombination.	55
Figure 2.2 Relaxation of DNA as visualised on an agarose gel.	70
Figure 2.3 The TARDIS assay.	73
Figure 2.4 The potassium SDS assay.	75
Figure 2.5 Sample Elution Plot.	78
Figure 3.1 Growth curves for PARP-1 wild type and null cells.	90
Figure 3.2 Growth curve for the K562 cell line.	91
Figure 3.3 Topo I protein levels in PARP-1 wild type (+/+) and null (-/-) cells.	93
Figure 3.4 PARP-1 protein levels in PARP-1 wild-type (+/+) and null (-/-) cells.	94
Figure 3.5 Effect of AG14361 on growth of PARP-1 wild type and null cell lines.	96
Figure 3.6 Effect of AG14361 on growth of K562 cells.	97
Figure 3.7 Effect of AG14361 on PARP-1 activity in K562 cells.	99
Figure 3.8 Effect of AG14361 on topotecan-induced growth inhibition in PARP-1 wild-type (+/+) and null (-/-) cell lines.	102
Figure 3.9 Effect of AG14361 on topotecan-induced growth inhibition in PARP-1 nullTR and PARP-1 null cell lines.	106
Figure 3.10 PARP-1 protein levels in PARP-1 nullTR cells (-/- TR) and PARP-1 wild type cells (+/+).	107
Figure 3.11 Effect of AG14361 on camptothecin-induced growth inhibition in K562 cells.	110
Figure 3.12 Effect of AG14361 on camptothecin induced growth inhibition in K562 cells.	111

Figure 3.13 Effect of AG14361 on camptothecin induced cytotoxicity in K562 cells.	114
Figure 4.1 Topo I relaxation activity in K562 cells treated with AG14361 for 30 mins.	127
Figure 4.2 Topo I relaxation activity in K562 cells treated with AG14361 for 16 hours.	129
Figure 4.3 Fluorescence of camptothecin-treated K562 cells.	132
Figure 4.4 Effect of camptothecin on levels of cleavable complexes in K562 cells.	133
Figure 4.5 Effect of camptothecin on levels of Hoechst-stained DNA in K562 cells.	134
Figure 4.6 Effect of AG14361 on camptothecin-stabilised cleavable complexes	136
Figure 4.7 Effect of AG14361 on persistence and reversal of camptothecin-stabilised cleavable complexes.	139
Figure 4.8 Effect of PARP-1 stimulation on levels of cleavable complexes in cells treated with camptothecin in the presence or absence of AG14361.	142
Figure 4.9 Effect of 30 min exposure to AG14361 on cleavable complex formation.	145
Figure 4.10 Effect of 16 hour exposure to AG14361 on cleavable complex formation.	146
Figure 4.11 Effect of AG14361 on reversal of topo I poison-mediated cleavable complexes.	148
Figure 5.1 Types of DNA damage caused by topo I poisons.	159
Figure 5.2 Effect of AG14361 on camptothecin-induced DNA single strand breaks.	166
Figure 5.3 Effect of AG14361 on DNA strand breaks formed following 30 min exposure to camptothecin	169
Figure 5.4 Dosing schedule for pre (A) and post (B) exposure to AG14361.	171
Figure 5.5 Effect of pre-exposure to AG14361 on camptothecin-induced DNA strand break levels.	172
Figure 5.6 Effect of post exposure to AG14361 on 30 mins exposure to camptothecin.	174
Figure 5.7 Effect of AG14361 on repair of camptothecin-induced DNA strand breaks.	176
Figure 5.8 Time course of repair of DNA strand breaks induced by 30 mins exposure to 30 nM camptothecin.	177
Figure 5.9 Effect of AG14361 on the repair of camptothecin-induced strand breaks.	179
Figure 5.10 DNA single strand breaks induced by increasing concentrations of camptothecin in PARP-1 null cells.	182
Figure 5.11 Repair of PARP-1 wild type and null cells following treatment with camptothecin.	185
Figure 5.12 Effect of AG14361 on camptothecin-induced single strand breaks in PARP-1 wild type cells.	186
Figure 5.13 Effect of AG14361 on camptothecin-induced single strand breaks in PARP-1 null cells.	187
Figure 5.14 Repair of camptothecin-induced DNA strand breaks in PARP-1 wild type and null cells.	189

Figure 6.1 DNA damage caused in response to topo I poisons.	198
Figure 6.2 Proposed mechanism for the repair of topo I cleavable complexes by an XRCC1-dependent pathway.	200
Figure 6.3 Relative sensitivities of AA8, V3, EM9 and irs1SF cells to camptothecin.	207
Figure 6.4 Effect of AG14361 on camptothecin-induced cytotoxicity in AA8 cells.	208
Figure 6.5 Effect of AG14361 on camptothecin-induced cytotoxicity in V3 cells.	209
Figure 6.6 Effect of AG14361 on camptothecin-induced cytotoxicity in EM9 cell	210
Figure 6.7 Effect of AG14361 on cell survival in the irs1SF cell line.	213
Figure 6.8 Inhibition of PARP-1 activity by AG14361 in the irs1SF cell line.	214
Figure 6.9 Effect of AG14361 on camptothecin-induced cytotoxicity in irs1SF cells.	216
Figure 6.10 Effect of AG14361 on repair of camptothecin-induced DNA strand breaks in AA8 and EM9 cells.	219
Figure 7.1 The role of PARP-1 in topo I poison-mediated cytotoxicity	236

Table of Tables.

Table 1.1 PARP-1 inhibitory activities of PARP-1 inhibitors.	44
Table 2.1 Antibodies used in this study.	66
Table 3.1 Doubling times of cell lines.	91
Table 3.2 PARP-1 activity and its inhibition by AG14361 in K562 and PARP-1 wild type and PARP-1 null cells.	100
Table 3.3 Effect of AG14361 on topotecan-mediated growth inhibition in PARP-1 wild type and null cells.	103
Table 3.4 Effect of AG14361 on topotecan-induced growth inhibition in PARP-1 wild type, PARP-1 null ^{TR} and PARP-1 null cell lines.	107
Table 3.5 Effect of AG14361 on camptothecin-induced growth inhibition in K562 cells	112
Table 3.6 Cell survival of K562 cells treated with camptothecin in the presence or absence of AG14361.	114
Table 4.1 Effect of AG14361 on persistence and reversal of camptothecin-induced cleavable complexes.	140
Table 4.2 Effect of PARP-1 inhibition on cleavable complex formation.	145
Table 5.1 Effect of AG14361 on levels of DNA single strand breaks induced by camptothecin.	167
Table 5.2 Effect of AG14361 on DNA strand breaks formed following 30 mins exposure to camptothecin.	169
Table 5.3 DNA strand break levels in K562 cells treated with AG14361 for 16 hours followed by camptothecin for a further 30 mins.	172
Table 5.4 DNA strand breaks in K562 cells treated with camptothecin for 30 mins followed by AG14361 for a further 16 hours.	174
Table 5.5 Effect of 1 and 16 hour post-exposure to AG14361 following 30 mins exposure to 300 nM camptothecin.	176
Table 5.6 Effect of AG14361 on repair of DNA single strand breaks formed following a 30 min exposure to 30 nM camptothecin.	180

Table 5.7 Repair of camptothecin-induced DNA strand breaks in PARP-1 wild type and null cells.	190
Table 6.1 Cell lines used in this chapter and their characteristics.	205
Table 6.2 Survival of AA8, EM9 and V3 cell lines following a 16 hour exposure to camptothecin in the presence or absence of AG14361.	211
Table 6.3 Effect of AG14361 on camptothecin-induced cytotoxicity in irs1SF cells	216
Table 6.4 Effect of AG14361 on repair of camptothecin-induced DNA strand breaks in AA8 and EM9 cells.	221

Chapter 1

Introduction.

1.1 Cancer

Cancer is a major cause of morbidity in the UK, with one in three people being diagnosed with cancer during their lifetime and a quarter of all deaths attributable to cancer. There are over 200 different types of cancer of which the four main types, lung, breast, prostate and colorectal account for over half of all cases diagnosed. Lung cancer accounts for a quarter of all cancer deaths. A major cause of cancer is exposure to environmental carcinogens, e.g. natural and synthetic chemicals, radiation and viruses. Diet is also a large factor in predicting likelihood of developing cancer. Cigarette smoking has been identified as the single most important cause of preventable disease and premature death in the UK and accounts for one third of all deaths from cancer (www.cancerresearchuk.org).

Cancers are largely caused by changes in the DNA as a result of exposure to agents in the environment or spontaneous events. A single change may have little effect however, these changes accumulate and eventually may activate proto-oncogenes, or inactivate tumour suppressor genes. Some individuals have inherited genetic defects that predispose them to certain forms of cancer, these include some forms of breast cancer characterised by loss of the BRCA1 gene, and loss of the APC gene (adenomatous polyposis coli) found in familial colon cancer (Bale and Brown, 2001). Loss of the p53 tumour suppressor gene in Li-Fraumeni syndrome is associated with the development of tumours at a variety of sites including breast, brain and adrenal gland at and early age (Bale and Brown, 2001). Inherited genetic defects account for a minority of cancer cases and it is generally accepted that cancers are more common in the elderly; 65 % of cancer cases occurring in those over 65 years, due to the accumulation of several genetic changes. It is now recognised that epigenetic changes such as silencing of tumour suppressor genes by promoter hypermethylation and chromatin remodelling (acetylation/methylation) also play a role (Rountree *et al.*, 2001).

Cancer is characterised by uncontrolled cell growth that is the result of accumulating genetic and/or epigenetic changes. Cancer is thought to be clonal in origin with a single altered cell proliferating to form a tumour. The growth of this tumour may be slow and is not necessarily life-threatening. However, due to the inherent genetic instability of tumour cells, accumulating changes cause the development of heterogeneity and some

tumour cells can metastasise from their primary site to form tumours in other tissues. As the tumours grow they develop their own blood supply by the process of angiogenesis. The condition becomes life threatening when the primary tumour and the metastases invade the neighbouring tissues and essential organs.

1.2 Cancer treatment

Cancer treatment most commonly comprises of surgery, radiotherapy and chemotherapy. More recently, immunotherapy, hormone therapy and gene therapy are being developed for use in the treatment of cancer. The type of treatment received depends on the size and location of the tumour. Most anti-cancer therapies target dividing cells. Because of the high turnover of these cells they have less time to repair the damage caused by chemotherapy or radiotherapy, this is detected by the cell and may lead to cell death. Unfortunately, normal cells such as bone marrow and hair follicles also undergo frequent cell division, therefore leading to the side effects of myelosuppression and hair loss. Many cancers are intrinsically resistant to chemo- and radiotherapy or acquire resistance during treatment. Increasing efforts are being made to develop new therapies using new targets and drug combinations to overcome drug-resistance, and to reduce the side effects of the treatments currently in use.

1.2.1 Surgery.

Surgery is the most effective treatment for cancer if the tumour is detected before it has metastasised and if all of the tumour mass can be removed. Therefore primary tumours are normally treated by surgical removal, and this is followed up with chemotherapy, and/or radiotherapy, to remove residual tumour. If the tumour is in an area that is not accessible to surgery other therapies must be used (reviewed by Rosenberg, 2001).

1.2.2 Radiotherapy.

Radiotherapy is often used in combination with surgery or chemotherapy. Radiation therapy is useful if the tumour is in a location where surgery is difficult to perform and if the tumour is locally confined. Radiotherapy is also useful as it can be focussed on the tumour thereby reducing damage to healthy tissues. This therapy can also be used to ensure that all of the tumour is removed following surgery by targeting the radiation to the margins of the tumour. Radiotherapy works by generating reactive oxygen species

that cause significant levels of DNA damage in the target cells. This DNA damage is detected by the cell and can result in cell death (reviewed in Hellman, 2001)

1.2.3 Hormone therapy.

Hormone therapy can be used in the treatment of hormone-dependent breast and prostate cancers. Cells in the breast and prostate require oestrogens or androgens for their proliferation. Therefore inhibition of the synthesis of these hormones or blocking the hormone receptor on the target cells can slow tumour growth and lead to tumour regression. Tamoxifen is one of the most widely used forms of hormone therapy. It is an antioestrogen, that binds to the oestrogen receptor without activating gene transcription and so preventing the normal substrate oestradiol from stimulating proliferation. (reviewed in Erlichman and Laprinzi, 2001)

1.2.4 Gene Therapy.

Gene therapy is being investigated as an approach for cancer therapy. Gene regulation can be achieved using nucleotides that are complementary to the mRNA sequences for over produced proteins. These sequences bind the overproduced mRNA sequence and target it for degradation. An alternative approach is to introduce a gene to replace a defective one or that down regulates growth. An example is the delivery of p53 into tumour cells by adenoviral vectors. This would function to restore the tumour suppressor function of p53 that is often lost in tumour development. Such therapies are still in development. (reviewed in Hwu, 2001)

1.2.5 Immunotherapy.

In order to increase the specificity of the chemotherapy for the malignant cells, the use of antibodies to target drugs to tumours using specific tumour markers is being developed. In antibody directed pro-drug therapy (ADEPT) the drug is given in a form that is inactive. Using antibodies, the enzyme that can activate the pro-drug is targeted to the tumour; therefore the drug only becomes active at the required location. (reviewed in Weiner *et al.*, 2001)

1.2.6 Chemotherapy.

If the tumour has spread from its primary site then systemic therapy, most usually chemotherapy, is required. Chemotherapy can be used on its own or in combination with surgery, radiotherapy or other chemotherapeutics. It can be used in the adjuvant

setting to kill undetected tumour cells remaining following other treatments such as surgery, to slow disease progression and give better quality of life. The drugs used largely act by damaging DNA, inhibiting its synthesis or processing, or interfere with the progression of cells through the cell cycle e.g. tubulin binders. DNA-directed chemotherapy can be divided into agents which interact with DNA directly, i.e. the DNA alkylating agents, and DNA intercalators, agents which inhibit DNA synthesis i.e. the antimetabolites, and agents which interfere with DNA processing e.g. the topoisomerase poisons. Alkylating agents were one of the first classes of drug used to treat cancer. They can be subdivided into the monofunctional agents, such as temozolomide, and the bifunctional agents such as 1,3-(bis(2-chloroethyl)-1-nitrosourea (BCNU) and the platinum agents such as cisplatin. These agents form adducts on DNA bases leading to DNA inter and intra-strand cross-links. Antimetabolites have also been used to treat cancer for the past 50 or more years. These are analogues of natural products involved in DNA synthesis and can be subdivided into nucleoside or base analogues and antifolates. One of the earliest base analogues is 5-fluorouracil (5-FU), This analogue of thymine may be converted to the triphosphate and incorporated into RNA, or through metabolism to deoxynucleotides 5FdUMP and 5FdUTP which can inhibit thymidylate synthase, the rate limiting step for dTTP biosynthesis and hence DNA synthesis, and be incorporated into DNA in place of dTTP (reviewed in Longley *et al.*, 2003). More recent nucleoside analogues include gemcitabine, a cytosine analogue, which following conversion to its triphosphate is inserted into the DNA, causing chain termination. Antifolates such as methotrexate (first introduced in the 1950's) are analogues of folic acid and inhibit the folate-dependent enzymes e.g. dihydrofolate reductase, required for the synthesis of purine and thymine nucleotides (reviewed in various chapters of de Vita, 2001).

Another major class of DNA-directed chemotherapeutic agents are the topoisomerase poisons. These have largely been identified from screening natural products e.g. those derived from fungi and plants used in herbal medicines, and their semi-synthetic derivatives. These agents inhibit the DNA processing activity of topoisomerase I and II converting these essential cellular enzymes into cellular poisons. The topoisomerase II inhibitors, such as doxorubicin (derived from *Streptomyces peucetici*) and etoposide (derived from *Podophyllum peltatum*, mayapple), were the first to be developed and, by stabilising the normally transient topo II-DNA cleavable complex lead to persistent

DNA double strand breaks. The exclusive target of the camptothecins (derived from *Camptotheca acuminata*) such as topotecan and irinotecan now widely used in the treatment of colon and ovarian cancer has been identified as topoisomerase I. Topoisomerase I and its inhibition are described in the following sections.

1.3 Topoisomerases.

The topoisomerases are a family of proteins that catalyse the breakage, unwinding and religation of DNA to relieve torsional strain associated with the processes of replication transcription, recombination and DNA repair. The topoisomerase family is divided into three groups based on their mechanism of action; these are type I-3', I-5' and II. Type 1-3' topoisomerases include human DNA topoisomerase I, and cleave a single strand of DNA via a 3'-phosphotyrosine intermediate relieving torsional strain by one turn. Type 1-5' topoisomerases include bacterial DNA topoisomerase I and cleave single stranded DNA via a 5'-phosphotyrosine intermediate (Champoux, 1978). Type II topoisomerases cleave double stranded DNA via two 5'-phosphotyrosine intermediates (Sander and Hsieh, 1983). They act as a homodimer and lead to unwinding of DNA by two turns and are also able to catenate and decatenate DNA. These type II topoisomerases require ATP as an energy cofactor. The topoisomerases have been reviewed by Wang *et al.*, (1996). As only human DNA topoisomerase I is discussed in this study a detailed description of the other topoisomerases is not included.

1.3.1 Human DNA Topoisomerase I.

Human DNA topoisomerase I (Topo I, EC 5.99.1.2) is a nuclear protein which is present in all cells at levels of between 10^6 and 10^7 molecules per cell (Roca *et al.*, 1995). It is expressed throughout the cell cycle, with a slight increase in activity at S-phase (Heck *et al.*, 1988).

1.3.2 Structure of Topoisomerase I.

Topoisomerase I is a 100 kDa monomeric protein consisting of 765 amino acids encoded by a gene located on chromosome 20q11.2-13.1 (Juan *et al.*, 1988). The structure of DNA topoisomerase I has been extensively reviewed by Berger (1998). Human topoisomerase I comprises of 4 domains; a 24 kDa N-terminal domain, a 56 kDa core domain, divided into subdomains I, II and III, a 7 kDa linker domain and a 6

kDa C-terminal domain (see Figure.1.1) (Champoux *et al.*, 1998, Stewart *et al.*, 1996). The 210 residue N-terminal domain contains 90% polar and 72% charged residues, and is largely disordered, and most inter-species variation is seen in this region. This domain is thought to be important for interactions with other proteins and contains a nuclear localisation sequence, although this domain can be removed from the enzyme without significant effect on the activity of the enzyme. The C-terminal domain is the most conserved region of topoisomerase I across species and contains the active site Tyr 723 residue responsible for catalysis. The core domain is also highly conserved and binds preferentially to supercoiled DNA. Core subdomains I and II form the upper half or "cap" of the clamp-like conformation formed on binding of the topoisomerase I molecule to DNA. Core subdomain III and the C-terminal domain form the lower half of the clamp making interactions with the DNA and wrapping completely around the DNA. The linker domain is between subdomain II and the C-terminal domain, it protrudes out from the core of the molecule, and is thought to control the rotation of the uncleaved strand during relaxation. The linker region is less well conserved and is not essential for catalytic activity (Redinbo *et al.*, 1998, Stewart *et al.*, 1998).

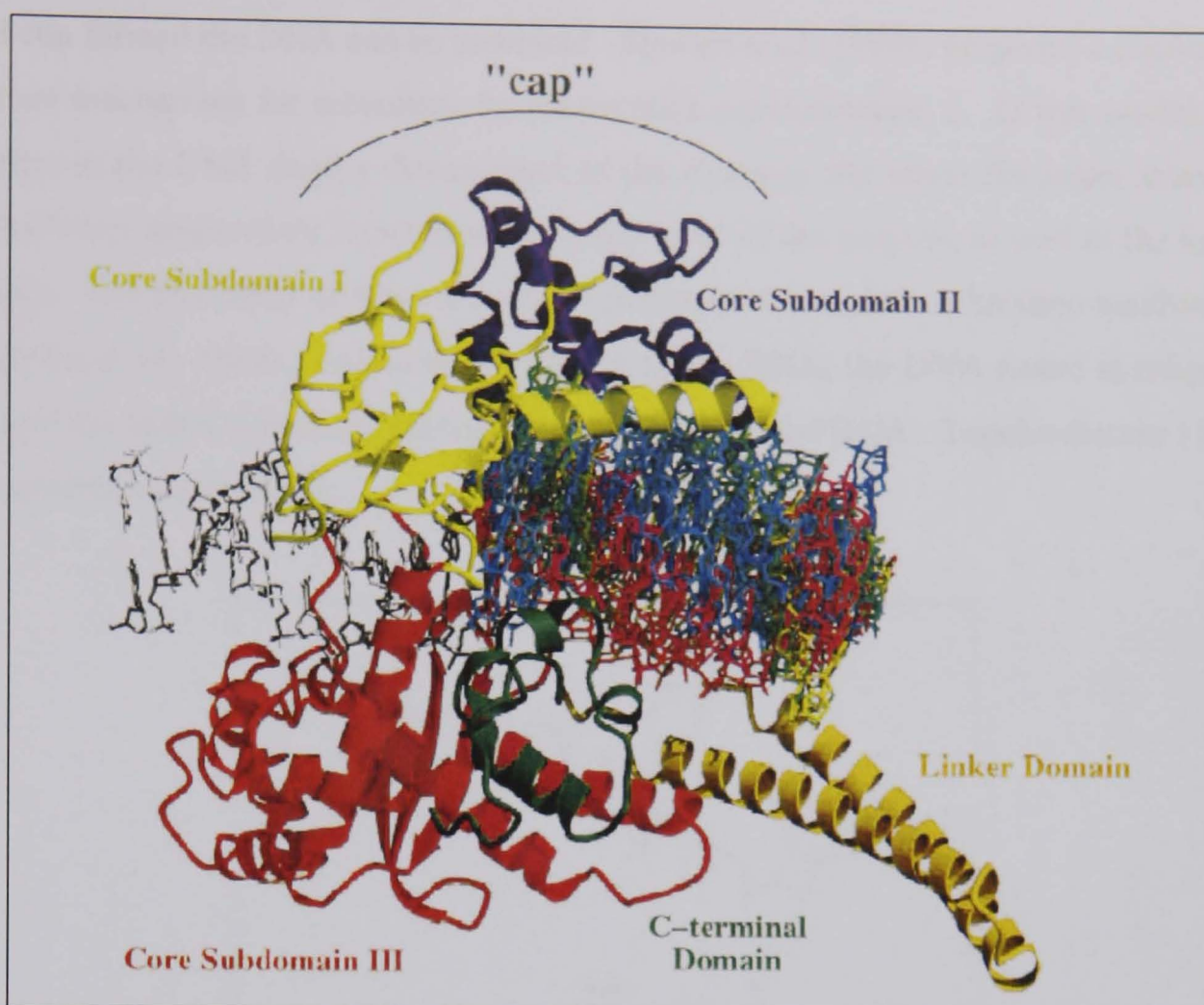


Figure.1.1 Crystal structure of mammalian DNA topoisomerase I in complex with DNA. (from Redinbo *et al.*, 1999)

1.3.3 Topoisomerase I mechanism.

The main role of topoisomerase I is to remove excessive positive supercoils, as well as negative supercoils arising during DNA replication and transcription. The mechanism by which topoisomerase I achieves this is shown in Figure 2. Topoisomerase I wraps completely around the DNA and buries it in a DNA-binding pore of 15-20 Å diameter. Topoisomerase I binds to the DNA over a 10 bp sequence, with the cleavage site centrally placed (Stevensner *et al.*, 1989). The enzyme contacts the DNA almost exclusively by protein-DNA phosphate interactions, and appears to make only one base specific interaction adjacent to the site of cleavage and covalent attachment, using lysine 532 in the core domain III (Stewart *et al.*, 1998). DNA topoisomerase I cleaves one of the DNA strands via a nucleophilic attack of the phosphodiester bond in DNA. This forms a covalent linkage between a tyrosine group (Tyr 723 in human topoisomerase I) at the active site of topoisomerase I and a 3'-phosphate group on the DNA backbone. This is termed the cleavable complex. Once the cleavable complex

has been formed the DNA can be unwound. Stewart *et al.*, (1998) proposed a controlled rotation mechanism for relaxation by mammalian topoisomerase I. In this model, the rotation of the DNA duplex downstream of the cleavage site about the intact strand is controlled or hindered by interactions with the "cap" of the enzyme, as well as the linker domain. The flexibility of these domains was proposed to aid the relaxation mechanism (Redinbo *et al.*, 1999). Following relaxation of the DNA, the DNA strand is religated and the active tyrosine is released from the end of the DNA. Topoisomerase I then dissociates from the DNA.

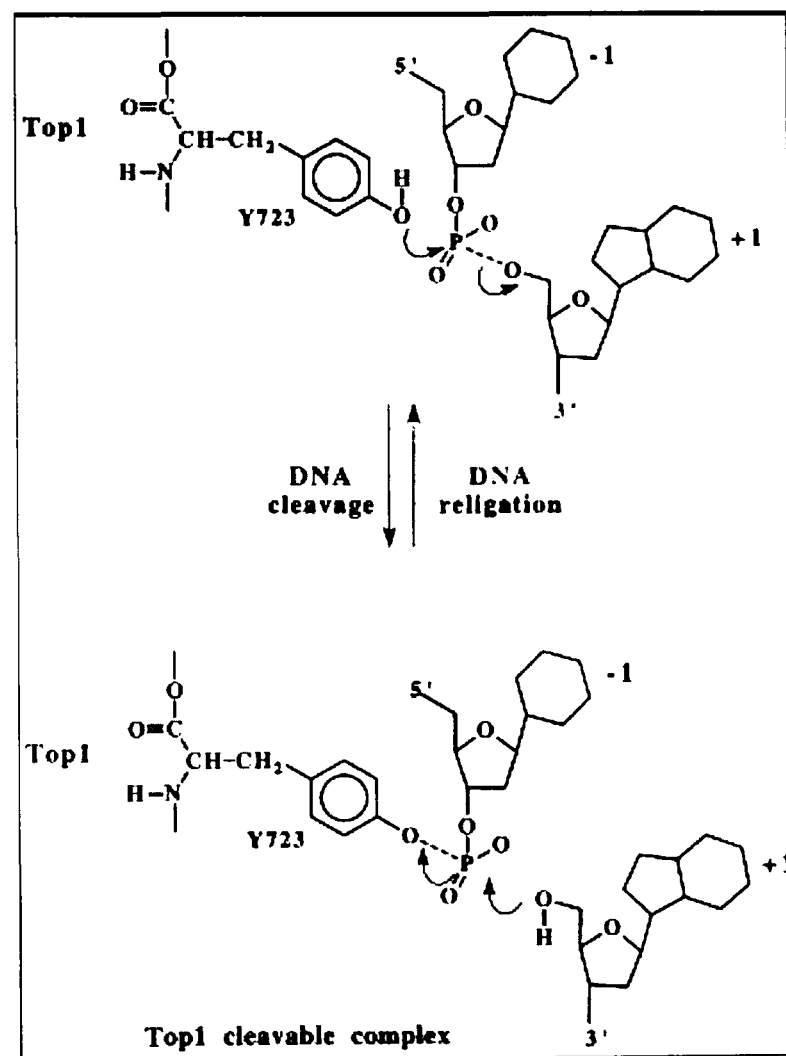


Figure 1.2 Unwinding of DNA by topoisomerase I (from Pommier *et al.*, 1998)

1.3.4 Regulation of topoisomerase I by other proteins.

Topoisomerase I can be modified post-translationally by a number of different mechanisms. Interaction with other proteins may also have an effect on the activity of topoisomerase I. In this section the modifications and interactions that are relevant to this study are discussed.

Phosphorylation.

Topoisomerase I has been shown to be phosphorylated *in vitro* and *in vivo*. *In vitro* experiments have shown that phosphorylation of serine residues enhances activity where as phosphorylation of tyrosine residues, causes inactivation (Tse-Dinh *et al.*, 1984, Pommier *et al.*, 1990). *In vivo* studies have shown that topoisomerase I is phosphorylated in response to a number of different stimuli including epidermal growth factor and insulin (Samuels *et al.*, 1994). Topoisomerase I is phosphorylated by caesin kinase II, and protein kinase C on serine or threonine residues under the influence of different stimuli. Protein kinase C and caesin kinase II may regulate topoisomerase I activity, stabilise the cleavable complex, or influence the recruitment of topoisomerase I to other proteins. The level of phosphorylation may also determine the sensitivity of cells to camptothecin (Pommier *et al.*, 1990).

Poly(ADP-ribosylation).

PARP-1 has been shown to poly(ADP-ribosylate) topoisomerase I *in vitro* and in whole cells, causing inhibition of topoisomerase I relaxation activity (Jongstra-Bilan *et al.*, 1983, Ferro and Olivera, 1984, Krupitza and Cerutti, 1989). This is thought to be due to an increase in the negative charge of topoisomerase I associated with (ADP-ribose) polymers resulting in repulsion of topoisomerase I from DNA. Poly(ADP-ribosylation) of topoisomerase I also occurs following treatment with ionising radiation (Boothman *et al.*, 1998). Poly(ADP-ribosylation) of topoisomerase I is described in detail in chapter 4.

p53.

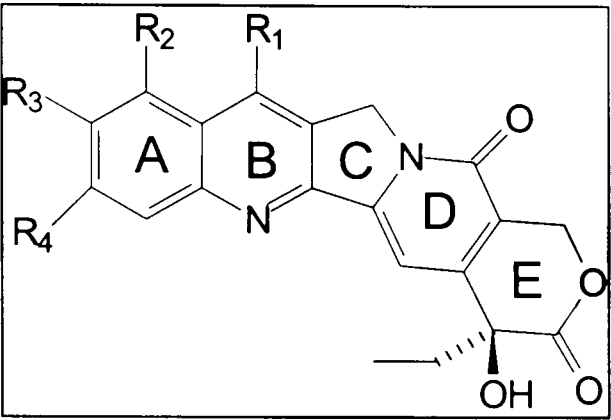
Topoisomerase I interacts directly with the tumour suppressor protein p53, as shown by co-immunoprecipitation studies (Gobert *et al.*, 1996, and 1999). This interaction serves to increase the activity of topoisomerase I. There is a difference in the interaction between topoisomerase I and p53 in cells containing wild type and mutant p53. In HT-29 cells expressing mutant p53, the two proteins are always associated where as in MCF-7 cells with wt p53 the association is tightly regulated, taking place only during periods of genotoxic stress (Gobert *et al.*, 1999). The topoisomerase I-p53 complex has also been shown to be poly(ADP-ribosylated) in response to γ -irradiation (Smith and Grosovsky, 1999). It is thought that the p53 response to DNA damage may involve topoisomerase I.

Ubiquitination and Sumoylation.

Topoisomerase I has been shown to be ubiquitinated and sumoylated in response to treatment with topoisomerase I poisons (Desai *et al.*, 1997, Mao *et al.*, 2000). Ubiquitination of topoisomerase I results in its degradation by the 26S proteasome and may be a factor in determining drug resistance (Desai *et al.*, 2001). Sumoylation involves the conjugation of small ubiquitin-like modifiers (SUMOs) to the target proteins in a process called sumoylation. Sumoylation requires UBC9, an E2 enzyme involved in the formation of a covalent bond with lysine residues on the target protein. It is thought that SUMOs may compete with ubiquitin to target the protein for degradation. Mo *et al.*, (2001) have shown that the sumoylation of topoisomerase I is associated with its nuclear delocalisation, and suggest that SUMO may be an address tag for this process. Sumoylation may act as a rescuing mechanism to prevent further DNA damage mediated via topoisomerase I.

1.4 Topoisomerase I poisons.

Topoisomerase I poisons are an exciting class of chemotherapeutic agents that are used in the treatment of a number of malignancies including colorectal and ovarian cancers. Topoisomerase I poison sensitivity has been reported to be related to the levels of topoisomerase I in the cell and, since topoisomerase I is frequently present at higher levels in some tumour cells compared to normal cells from the same tissue, a degree of selective anti-tumour activity is predicted. For example, colorectal and prostate tumour cells have been shown to have 2 to 35-fold higher levels of topoisomerase I protein corresponding to similar increases in gene expression and catalytic activity compared to normal cells from the same origin (Husain *et al.*, 1994, Madden and Champoux, 1992). Combine this with the fact that tumour cells are dividing and therefore conducting replication and transcription (processes that topoisomerase I is involved in) and this makes topoisomerase I a promising target for anticancer therapy. Topoisomerase I poisons used today are derivatives of the natural product camptothecin, and include topotecan and irinotecan. The structures of these compounds are shown in Figure 1.3 and have been described most recently by Ulukan and Swaan, (2002), and Pizzolato and Saltz (2003).



Compound	R1	R2	R3	R4
Camptothecin	H	H	H	H
Topotecan	H	CH ₂ -N(CH ₂) ₂	OH	H
Irinotecan	CH ₂ -CH ₃	H		H

Figure 1.3 Structure of the Camptothecins.

1.4.1 Camptothecin.

Camptothecin is a plant alkaloid that was first isolated from stem wood of *Camptotheca acuminata* (family *Nyssaceae*) during a National Cancer Institute screen searching thousands of plants for steroids (Wall *et al.*, 1966). All of these extracts were tested for their antiviral, antibacterial and antitumour activity. The extract from *C. acuminata* had significant antitumour activity in a standard *in vivo* test system as well as in murine leukaemic L1210 cells. Therefore this agent was seen as a possible anti-tumour agent.

Camptothecin was approved by the Food and Drug Administration (FDA), for use against colon carcinoma in the 1970s. It was also evaluated against other forms of

cancer and showed impressive antitumour activity in patients with gastrointestinal cancer. However it was shown to cause unpredictable and severe adverse effects including myelosuppression, vomiting, diarrhoea, and severe haemorrhagic cystitis. Because of these findings clinical trials of camptothecin were terminated in 1972 (Moertal *et al.*, 1972).

DNA topoisomerase I was shown to be the sole molecular target of camptothecin in purified systems and in cultured mammalian cells (Hsiang *et al.*, 1985, Hsiang and Liu, 1988). Both of these studies showed that camptothecin increased the level of protein-linked DNA strand breaks, and that these breaks were reversible on removal of camptothecin. Immunoblot analysis of camptothecin-treated cell lysates showed that there was a dose-dependent decrease in the amount of topoisomerase I detectable on the blot with increasing concentrations of camptothecin. The explanation for this was that there was an increase in the number of topoisomerase I-DNA complexes, which were too bulky to run through the gel, presumably due to stabilisation of the cleavable complex. This was proved by the digestion of the extracts with DNase I and subsequent immunoblotting which resulted in the reappearance of topoisomerase I bands. This therefore showed that camptothecin interferes with topoisomerase I by trapping the reversible enzyme-DNA cleavable complex.

Once the intracellular target of camptothecin had been discovered there was renewed interest in this class of compounds. It was shown that administration of the water soluble sodium salt of camptothecin resulted in much less of an antitumour effect, and more severe side effects compared to the natural product of camptothecin (Gottlieb *et al.*, 1970). This was related to the open lactone ring present in this structure (Slichenmyer *et al.*, 1993). Therefore this heralded the development of camptothecin-derivatives, based on structure activity relationships, containing a closed lactone ring. Of these compounds, topotecan and irinotecan were the most promising anticancer agents in phase I clinical trials although exatecan, and rubitecan are currently in phase II clinical trials. Irinotecan and topotecan are described in detail below and all topoisomerase I poisons have been extensively reviewed by Ulukan and Swaan, (2002), Pizzolato and Saltz, (2003), and Koh and Nishio, (2000).

1.4.2 Topotecan

Topotecan (TP, 9-[(dimethylamino)methyl]-10-hydroxy-camptothecin, Hycamtin®) is a water-soluble camptothecin derivative that acts without further modification to inhibit topoisomerase I. Topotecan has impressive anti tumour activity *in vitro* and in tumour xenograft models covering a wide range of tumour types (Houghton *et al.*, 1992, Kingsbury, 1991). The FDA approved it for use in 1996 in patients with cisplatin-refractory ovarian carcinoma and as second-line therapy for non-small cell lung cancer (Takimoto 1997, ten Bokkel Huinink *et al.*, 1997). Topotecan has been accepted for use in these refractory malignancies, however no randomised trial has ever shown a survival benefit with topotecan compared to other therapies. Topotecan is currently in clinical trials for a number of different malignancies on its own and in combination with ionising radiation, paclitaxel, etoposide, cisplatin and cytarabine.

1.4.3 Irinotecan.

Irinotecan (CPT-11, 7-ethyl-10-[4-(1-piperidino)]carbonyloxycamptothecin, Camptosar®) is a potent semi-synthetic water-soluble analogue of camptothecin. Irinotecan acts as a pro-drug and has to be converted *in vivo* into the active compound SN-38. This conversion involves the cleavage of the dipiperidino side chain of irinotecan by carboxylesterase found in the gut and liver (Takasuna *et al.*, 1996). SN-38 is 1000-fold more potent than irinotecan in cells, although the actual concentrations of SN-38 may be 1000-fold lower than irinotecan, therefore irinotecan itself may contribute some way towards anti-tumour activity (Kawoto *et al.*, 1991).

Irinotecan was developed in Japan and was first approved for use against lung cancers in Japan in 1994. Subsequently it was approved for use as a second-line agent against colon cancer in Europe in 1995, and this remains the largest use for this compound today. Irinotecan is being studied for use against other malignancies including mesothelioma, ovarian cancer and some forms of head and neck cancers.

Although the camptothecins have impressive anti-tumour activity there are limitations to the use of these drugs, including the rapid reversibility of the cleavable complex and the instability of the lactone form of camptothecin at physiological pH. Therefore other non-camptothecin topoisomerase I inhibitors are being developed. These compounds are intercalators or minor groove binders and therefore may interact with other proteins.

Non-camptothecins such as rebeccamycin, intoplicine and ecteinascidin, are currently in clinical trials.

1.4.4 Topoisomerase I Poison Mechanism of Action.

Topoisomerase I poisons act by reversibly stabilising the topoisomerase I-DNA complex by inhibiting the religation step of the enzymes catalytic cycle, converting topoisomerase I into a cellular poison (Hsaing *et al.*, 1985, Svejstrup *et al.*, 1991) although there is evidence that the camptothecins may inhibit the cleavage step as well (Kjeldson *et al.*, 1992). This cleavable complex is reversible on removal of drug and is not itself a cytotoxic lesion. Cytotoxicity of topoisomerase I poisons is largely S-phase - specific. D'Arpa *et al.*, (1990), showed that in V79 cells treated with camptothecin, cytotoxicity increased with progression of the cells from G1 to S-phase and decreased on progression to G2. When DNA synthesis was inhibited by treatment with aphidicolin, camptothecin was ineffective. It is thought that the S-phase specific cytotoxic lesion caused by camptothecin is generated following the collision of the camptothecin-stabilised cleavable complex with the progressing replication fork. This collision results in the production of DNA double strand breaks and an irreversible topoisomerase I-DNA complex (Zhang *et al.*, 1990) (Figure 1.4). This damage is detected by the cell and triggers other cellular processes, which lead to cell cycle arrest in the G2 phase, and eventually cell death.

There is also an S-phase independent mechanism of cytotoxicity, demonstrated by the ability of high doses of camptothecin to kill cells treated with aphidicolin to inhibit replication (Goldwasser *et al.*, 1996, Barrows *et al.*, 1998). EM9, base excision repair (BER) deficient cells, have been shown to be hypersensitive to camptothecin even when treated with aphidicolin suggesting that BER might be important for the non-S-phase component of camptothecin-toxicity (Barrows *et al.*, 1998). Wu and Liu, (1997) proposed a "Transcription Collision Model" to explain replication independent-camptothecin toxicity. In this model it is thought that collision between the topoisomerase I cleavable complex located on the template strand and the elongating RNA polymerase results in transcription arrest and the conversion of the cleavable complex into irreversible strand breaks (Figure 1.5). Further explanations for S-phase independent cytotoxicity are discussed in Barrows *et al.*, (1998).

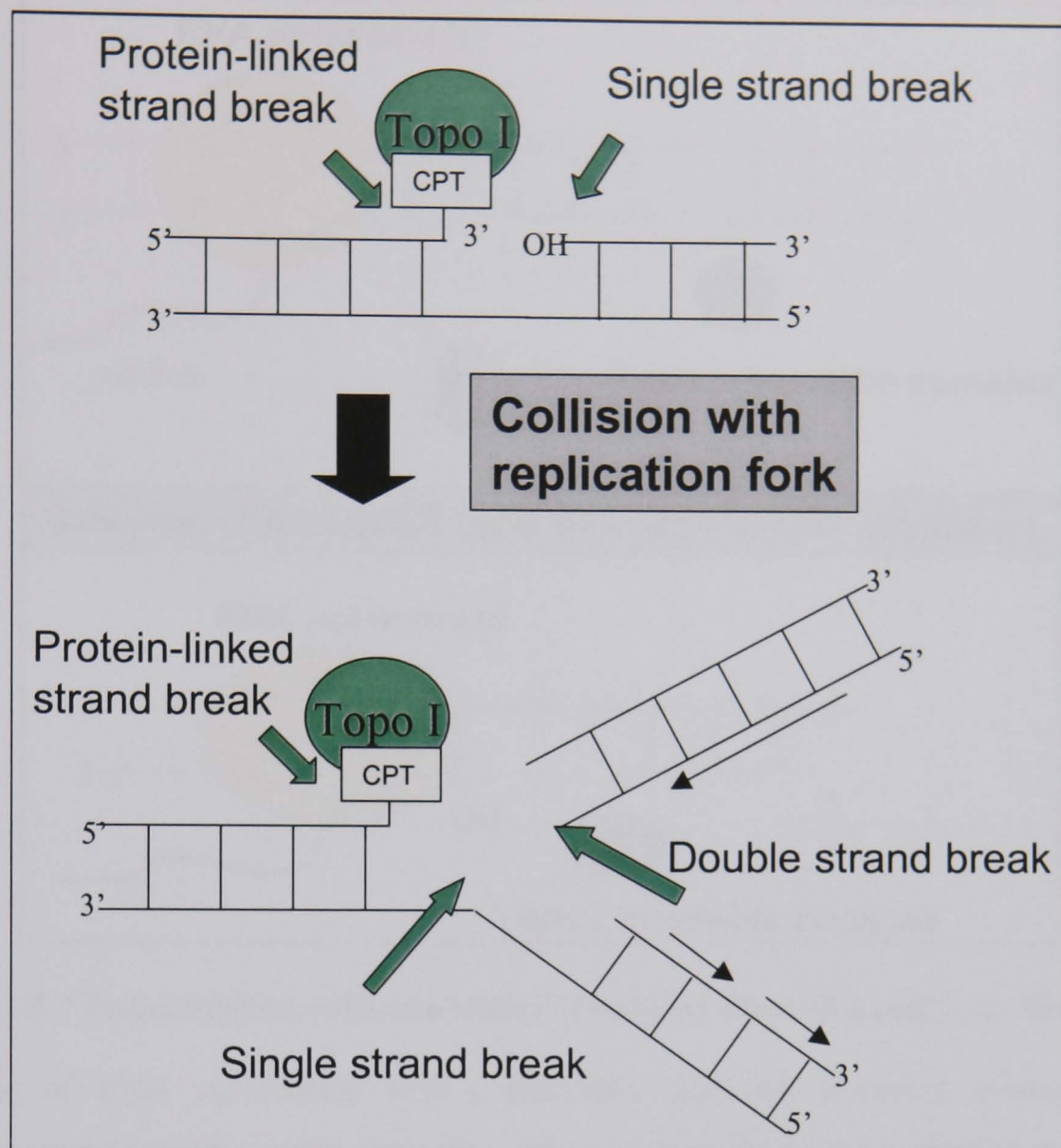


Figure 1.4 "Replication fork collision model" of topoisomerase I poison-mediated cytotoxicity.

The topoisomerase I-DNA complex is stabilised by camptothecin, to form the stabilised cleavable complex and a single strand break. Collision with the progressing replication fork results in the generation of single and double DNA strand breaks.

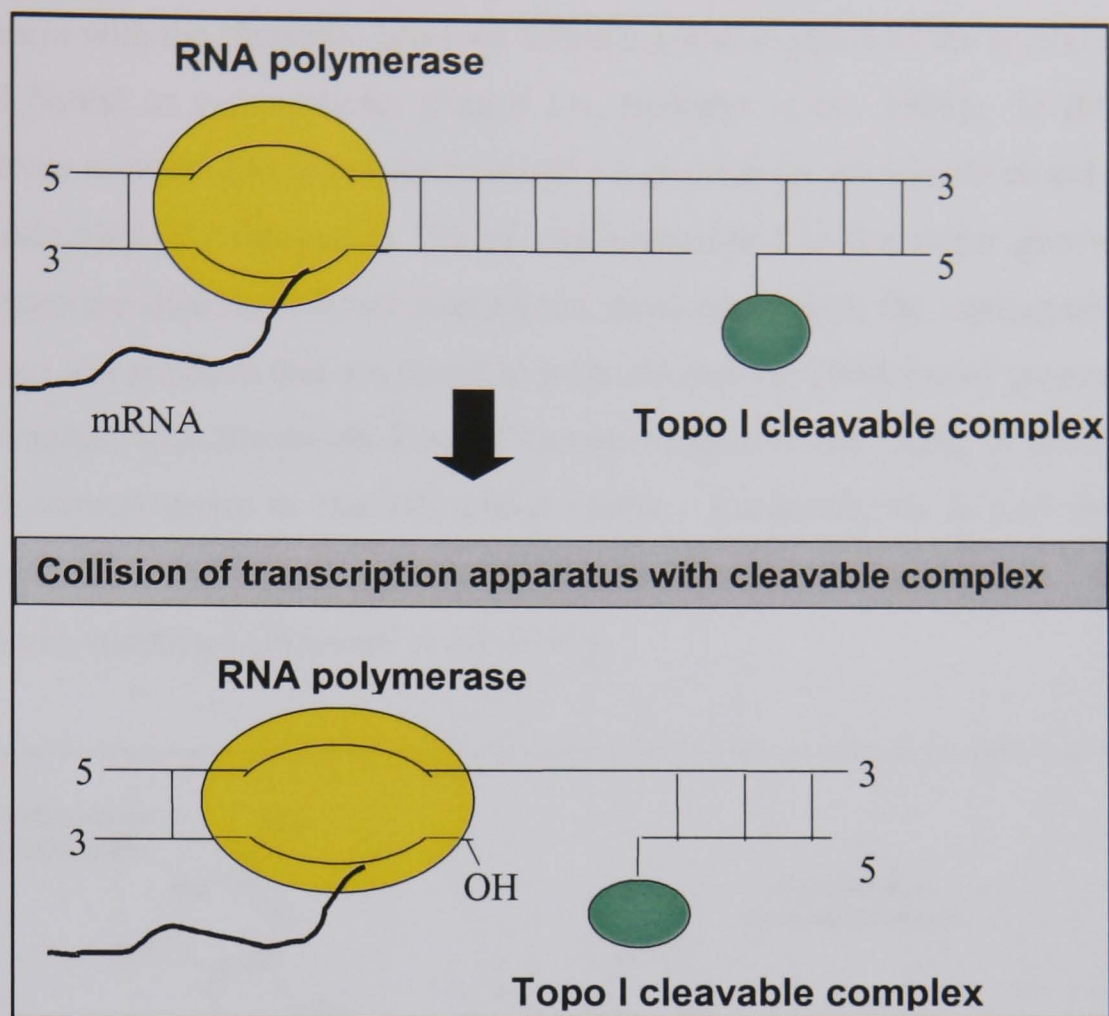


Figure 1.5 "Transcription collision model" (adapted from Wu and Liu, 1997).

Collision of RNA polymerase with a stabilised cleavable complex located on the template strand results in the formation of an irreversible single strand break. The transiently broken 5'-OH end is shown displaced from the duplex by the DNA helix tracking activity of the RNA polymerase.

1.4.5 Binding of camptothecin to the cleavage complex.

Topoisomerase I binds DNA in a sequence specific manner. Under normal conditions a T is preferred at the -1 position i.e. the 3'-terminus of the cleaved DNA. There is no sequence preference at the +1 position i.e. the base at the 5' terminus of the break. Camptothecin only traps topoisomerase I-DNA complexes at certain cleavage sites. In the presence of camptothecin there is a strong preference for a G at the +1 position. This suggests that camptothecin interacts with the G at the 5' terminus of the cleavage site or the C on the non-cleaved strand (Jaxel *et al.*, 1991, Tanizawa *et al.*, 1993).

The stacking model has been proposed as a mechanism for the interaction of camptothecin with the cleavable complex following investigation of the crystal structure of topo I bound to camptothecin (figure 1.6, Redinbo *et al.*, 1998). In this model camptothecin is stacked between the terminal +1 guanine on the scissile strand of DNA and the side chain of asparagine 722 of topoisomerase I in the major groove of the DNA. There are sites for H-bond interactions, particularly with the asparagine 533 and the arginine 364 residues that are found to protrude into the DNA major groove. These residues interact with the double bonded lactone oxygen in the E-ring of camptothecin and the hydroxyl group at the 20S chiral centre. Camptothecin is also thought to interact with the active site of topoisomerase I, as mutations in the catalytic site confer camptothecin-resistance (Fujimori *et al.*, 1995).

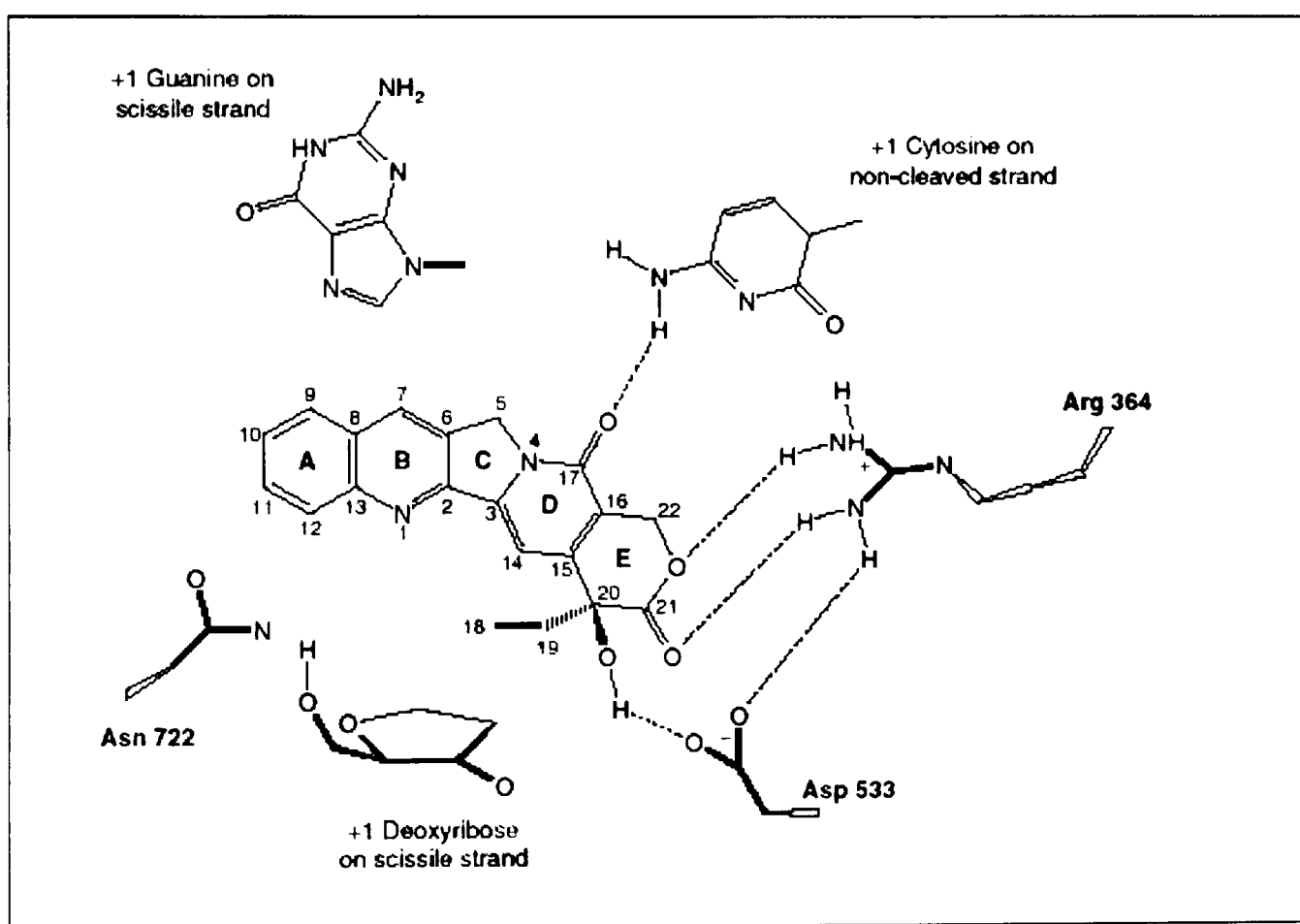


Figure 1.6. Proposed model for camptothecin binding. (A) A schematic representation of the key hydrogen bond and ring-stacking interactions made between the human topoisomerase I-DNA covalent complex and camptothecin in the proposed camptothecin binding mode. The atomic nomenclature for camptothecin is also indicated. (From Redinbo *et al.*, 1998).

1.4.6 Resistance to topoisomerase I poisons

Mechanisms of resistance to topoisomerase I poisons can be divided into 3 categories:

- (i) pre-target events such as accumulation of camptothecin in the cell,
- (ii) drug-target events such as altered topoisomerase I levels, activity and mutation,
- (iii) post-target events such as DNA repair.

Drug accumulation.

Passive diffusion may play a role in the uptake of camptothecins, although it has also been shown that energy-requiring processes may be involved in their accumulation. Several ATP-binding cassette (ABC) proteins are able to pump camptothecin out of the cell and overexpression of P-glycoprotein can confer resistance to topoisomerase I poisons. A screen to identify mutations that lead to camptothecin-resistance in yeast identified two ABC proteins, Snq2 and Pdr5. In addition the Bcrp/Mxr was shown to be overexpressed in cells resistant to topotecan and SN-38, and inhibition of Mrp2 by antisense oligonucleotides increased sensitivity to SN-38 and irinotecan (Saleem *et al.*, 2000).

Topoisomerase I activity.

Topoisomerase I expression has been shown to be a good predictor of cellular or tumour sensitivity as elevated levels of topoisomerase I were related to increased sensitivity to topoisomerase I poisons (Madden and Champoux, 1992, and Husain *et al.*, 1994). However a direct link between topoisomerase I activity and tumour response remains controversial with a number of authors reporting no clear link between the two factors (Goldwasser *et al.*, 1995, Voigt *et al.*, 1997). Voigt *et al.*, evaluated the effect of topoisomerase I activity on the cytotoxic response to topoisomerase I poisons and demonstrated that topoisomerase I activity was not a good single predictor of sensitivity. A correlation between activity in cells and drug response was seen following a 2 hour exposure but not after 24 hours. This correlation was only between cell lines of the same origin and there was no trend when cell lines from different origins were considered. However as these cells were all from a different background there may be many factors determining their differential sensitivities. Similar results were obtained by Goldwasser *et al.*, (1995) using a panel of cell lines with different sensitivities to camptothecin. This study showed that the levels of cleavable complexes

formed in response to camptothecin were the best indicator of the growth inhibitory effects of camptothecin. However, some cell lines displayed differences in growth inhibition that were not accompanied by similar differences in cleavable complex levels. This study also showed that p53 status was not a determinant of response. These authors concluded that the factors determining sensitivity to topoisomerase I poisons are numerous and may depend on other factors downstream of the cleavable complex as well as cleavable complex formation itself. Nevertheless, in studies comparing cells of the same parental background there is a clear link between sensitivity to topoisomerase I poisons and topoisomerase I activity. In such experiments there are fewer differences between the cell lines that may account for differences in sensitivity between parental and derivative cell lines.

Some studies have shown that camptothecin-induced down regulation of topoisomerase I is defective in a number of tumour cell lines (Desai *et al.*, 2001). There was an inverse correlation between the amount of down regulation and the degree of sensitivity in the cell. This suggests a role for topoisomerase I degradation in the development of resistance to topoisomerase I poisons. Ubiquitination and degradation by the 26S proteasome pathway is stimulated in response to treatment with camptothecin, therefore it is possible that this pathway may be involved in cellular resistance to topoisomerase I poisons.

Topoisomerase I mutations are probably not relevant for camptothecin resistance in a clinical setting as mutations in topoisomerase I are not commonly found in resistant tumours and are often a late event in the development of camptothecin resistance in the laboratory. Of the mutations that have been studied, most of these seem to cluster around the catalytic tyrosine 723 residue. For example, in the camptothecin-resistant CCRF-CEM line, mutation of asparagine 722 to serine confers camptothecin-resistance. Resistance inducing mutations are found in other conserved regions of topoisomerase I, these are thought to be brought close to the active site by protein folding (Kubota *et al.*, 1992).

DNA Repair.

The repair of topoisomerase I-DNA complexes has an impact on the sensitivity to camptothecin. The exact nature of the repair of the topoisomerase I-DNA complex is unclear. The first step is thought to involve a 3'-specific tyrosyl DNA phosphodiesterase that specifically cleaves the phosphotyrosyl bond between the enzyme and the DNA (Pouliot *et al.*, 1999). As topoisomerase I is ubiquitinated and sumoylated, mainly while attached to DNA, following treatment with camptothecin, this may also be a mechanism of repair or damage limitation (Desai *et al.*, 2001). The single strand break can be repaired by base excision repair (BER) or nucleotide excision repair (NER). The DNA strand breaks produced on collision with the replication fork may be repaired by either of the double strand break repair pathways, homologous recombination (HR) or non-homologous end-joining (NHEJ). Cells deficient in various components of these pathways have been shown to be hypersensitive to camptothecin. Similarly, some camptothecin resistant cells have been shown to exhibit enhanced NER capacity (Fujimori *et al.*, 1996). The repair of top I poison induced DNA damage is described in detail in chapter 6 and has been reviewed by Pourquier and Pommier (2001).

1.5 DNA repair.

DNA damaging agents cause a number of different types of damage that have to be repaired using different strategies. The normal cellular response to DNA damage is to signal to halt the cell cycle, inhibit transcription, replication and chromosome segregation and either repair the DNA or execute apoptosis. Long-term, failure to repair the DNA or to apoptose may lead to accumulation of mutations and chromosome aberrations, which may cause cancer. Cells have multiple pathways for repairing the various types of DNA damage. Defects in any of these pathways predisposes to malignancies. There are a number of damage repair pathways in mammals. Nucleotide excision repair (NER), and base excision repair (BER) repair damage to single strands of DNA whereas homologous recombination (HR) and non-homologous end-joining (NHEJ) repair double strand breaks. Mismatch repair is responsible for the repair of replication errors such as mismatches, deletions and insertions. DNA damage can also be repaired by direct reversal of the modified base using specific alkyltransferases such as O⁶-methylguanine DNA methyltransferase (MGMT). Only the repair pathways that are relevant to this thesis have been described in detail in the following sections.

1.5.1 Base excision repair (BER).

Base excision repair is the major pathway for the correction of damage caused by X-rays, oxygen radicals, and alkylating agents. The lesions caused by these agents include abasic sites, 8-oxoguanine, and single strand breaks. These lesions may or may not impede transcription or replication but frequently cause small mutations and only affect one of the DNA strands. The BER pathway has been reviewed in detail by Hansen and Kelly (2000), Krokan *et al.*, (2000) and Hoeijmakers (2001).

BER is divided into two sub-pathways determined by the length of the resynthesised patch. The major pathway in mammals is the short patch pathway. Short patch repair deals with the repair of single base alterations. Long patch repair, the minor pathway, involves the resynthesis of 2-8 nucleotides and repairs damage that is not able to be processed by the short patch pathway. However there may be crossover between these pathways. Both pathways are summarised in Figure 1.7.

Damage caused by methylation, deamination, or exposure to reactive oxygen species results in base modification. Such damage is recognised by glycosylases specific for individual base alterations (Lindahl, 1974). These recognise suspect bases, and flip them out of the helix by DNA backbone compression. The base is cleaved out by hydrolysis of the N-glycosyl bond linking damaged bases to the sugar-phosphate backbone to leave an abasic site (Dodson *et al.*, 1994). AP endonuclease 1 (APE1) causes a nick in the DNA strand at the abasic site and generates a 3' hydroxyl and a 5'-deoxyribosephosphate (Kane and Linn, 1981). Following this step, repair can continue by either of the two sub-pathways. The major pathway followed (the short patch pathway (Dianov *et al.*, 1998)), involves the recruitment of DNA pol β to repair the 5'-deoxyribosephosphate (DRP) terminus created by APE1 inserting a single nucleotide to fill the gap. The remaining nick is sealed by DNA ligase III (Srivastava *et al.*, 1998).

Abasic sites can also occur due to spontaneous hydrolysis or exposure to ionising radiation resulting in single strand breaks. Under these circumstances there is no need for the removal of bases, instead it is thought that polynucleotide kinase (PNK) and PARP-1 may be involved and act to trim the ends for repair synthesis PNK or APE-1 modify the DNA so that there are 5'-phosphates and 3'-hydroxyl ends. PARP-1 binds as

a dimer, to the DNA breaks which activate the enzyme leading to addition of PAR polymers to PARP-1 itself and other acceptor proteins. The automodification of poly(ADP-ribose) may recruit XRCC1-DNA ligase III complex. DNA pol β and ligase III then fill and religate the gap.

Under some circumstances repair may not be able to continue via the short patch pathway. For example, DNA pol β may not be able to repair the DRP produced in the short patch pathway if it is reduced or oxidised. Under these circumstances the long patch pathway is used. This is thought to involve the recruitment of PARP-1, PCNA and FEN-1 in addition to the short patch pathway BER components, and stimulates the extension of the gap to 2-8 nucleotides and the cleavage of the flap by FEN-1. DNA pol β and possibly DNA pol δ/ϵ repair the remaining gap and the ends are rejoined by ligase I (Klugland and Lindahl, 1997). As indicated in Figure 1.7, there may be cross over between the long and short patch pathways.

BER protein interactions.

XRCC1 is the scaffold protein of the BER pathway and interacts with many of the proteins involved in this pathway (reviewed by Caldecott, 2003). XRCC1 interacts with PARP-1, pol β and ligase III (Caldecott *et al.*, 1996) and PNK (Whitehouse *et al.*, 2001). XRCC1 binds to the BRCA-1 C-terminal (BRCT) domain of PARP-1 via its own BRCT domain (Masson *et al.*, 1998). It is thought that PARP-1 may recruit XRCC1 to sites of damage as XRCC1 preferentially interacts with ADP-ribosylated PARP-1 (Schreiber *et al.*, 2002). XRCC1 may then recruit the other enzymes in turn. XRCC1 is known to stimulate the kinase and phosphatase activities of PNK, and has been shown to interact with PNK in a yeast-2-hybrid screen (Whitehouse *et al.*, 2001). XRCC1 interacts with DNA pol- β via its N-terminal domain, and it is thought that this complex may surround the DNA and prevent further damage to the undamaged strand (Marintchev *et al.*, 2000). DNA ligase III and XRCC1 interact via their BRCT domains (Nash *et al.*, 1997), and it is thought that this interaction functions to stabilise DNA ligase III and to target it to sites of damage.

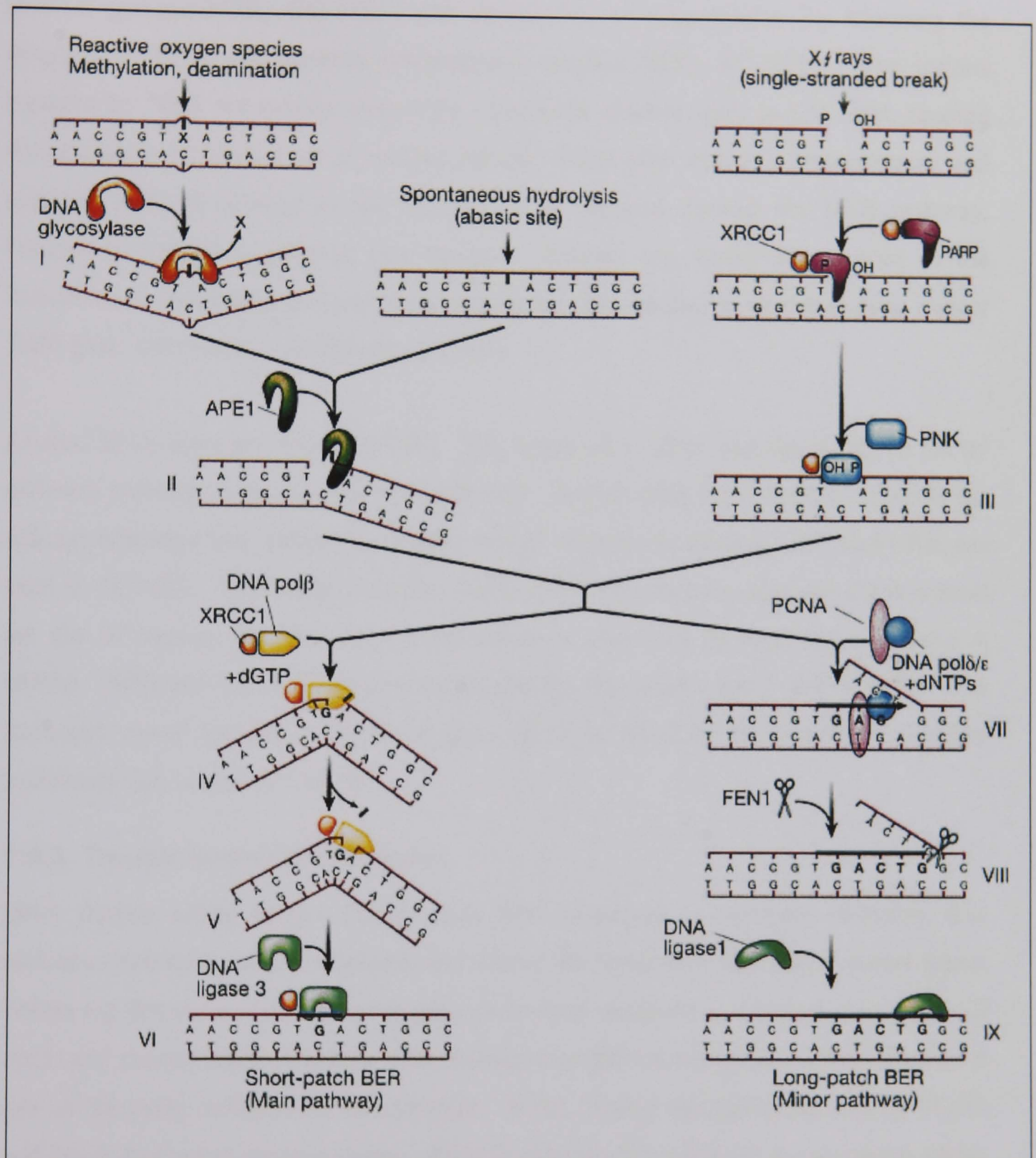


Figure 1.7 Base excision repair. (Picture adapted from Hoeijmakers, 2001). Description of the pathway is included in the text, arrows indicate cross over between the two pathways may occur at these points.

1.5.2 Nucleotide excision repair (NER).

NER repairs DNA damage that distorts the DNA helix, interfering with base pairing (Global genome-NER; GG-NER) and obstruction of transcription by blocking the progress of RNA polymerases (transcription-coupled NER; TC-NER). The lesions repaired by NER are mainly caused by exogenous sources such as UV light, causing distortions in DNA such as thymidine dimers. Polycyclic aromatic hydrocarbons and cisplatin induced damage is also thought to be repaired through the NER pathway. Defects in the NER pathway can result in extreme sun sensitivity as seen in the Xeroderma Pigmentosum syndrome increasing the likelihood of developing cancer 1000-fold. (reviewed in Hoeijmakers, 2001).

Around 25 proteins participate in NER. The detection of DNA damage is carried out by different proteins in each of the sub pathways. In GG-NER XPC-hHR23B detects the damage whereas two proteins associated with Cockayne Syndrome, CSA and CSB, are used in TC-NER. Following detection, XPB and XPD helicases open the DNA around the site of damage and this open intermediate is stabilised by Replication protein A (RPA). XPG and ERCC1/XPF are endonucleases that cleave the 3' and 5' ends of the damaged strand leaving a 24-32 bp gap, which is filled by the regular replication machinery (de Laat *et al.*, 1999).

1.5.3 Double strand break repair.

DNA double strand breaks (DSB) arise from exposure to ionising radiation, free radicals, chemicals such as cisplatin, and during the replication of a single strand break. Following detection of a DSB a complex cascade of reactions is initiated to halt the cell cycle and recruit repair proteins. The Ataxia telangiectasia-mutated (ATM) protein is one of the early initiators of this process. ATM, Ataxia telangiectasia related (ATR) and DNA-dependent protein kinase catalytic subunit (DNA-PKcs) are serine/threonine kinases which phosphorylate histone H2AX in the DNA domain next to the DSB, this may result in modulation of the chromatin structure allowing access of the DNA repair proteins. ATM and ATR also signal the DNA damage by phosphorylating p53, resulting in its stabilisation. p53 halts the cell cycle in G1 by inducing the expression of genes such as p21 (which lead to growth arrest), or bax (leading to apoptosis). There are two mechanisms of DSB repair described in the following sections. When a second

copy of the DNA is available homologous recombination (HR) is the mechanism of choice; otherwise the more error-prone non-homologous end-joining pathway (NHEJ) is used. HR is the most accurate as it uses a template, and NHEJ is more error-prone as end-joining mechanisms may involve the deletion of bases that can lead to mutations. Mammalian cells repair the majority of DSBs by NHEJ, although this pathway may be coupled to HR to generate accurate repair of strand breaks. The mechanisms are shown in Figure 1.8. (Reviewed in Hoeijmakers 2001 and Kanaar *et al.*, 1998).

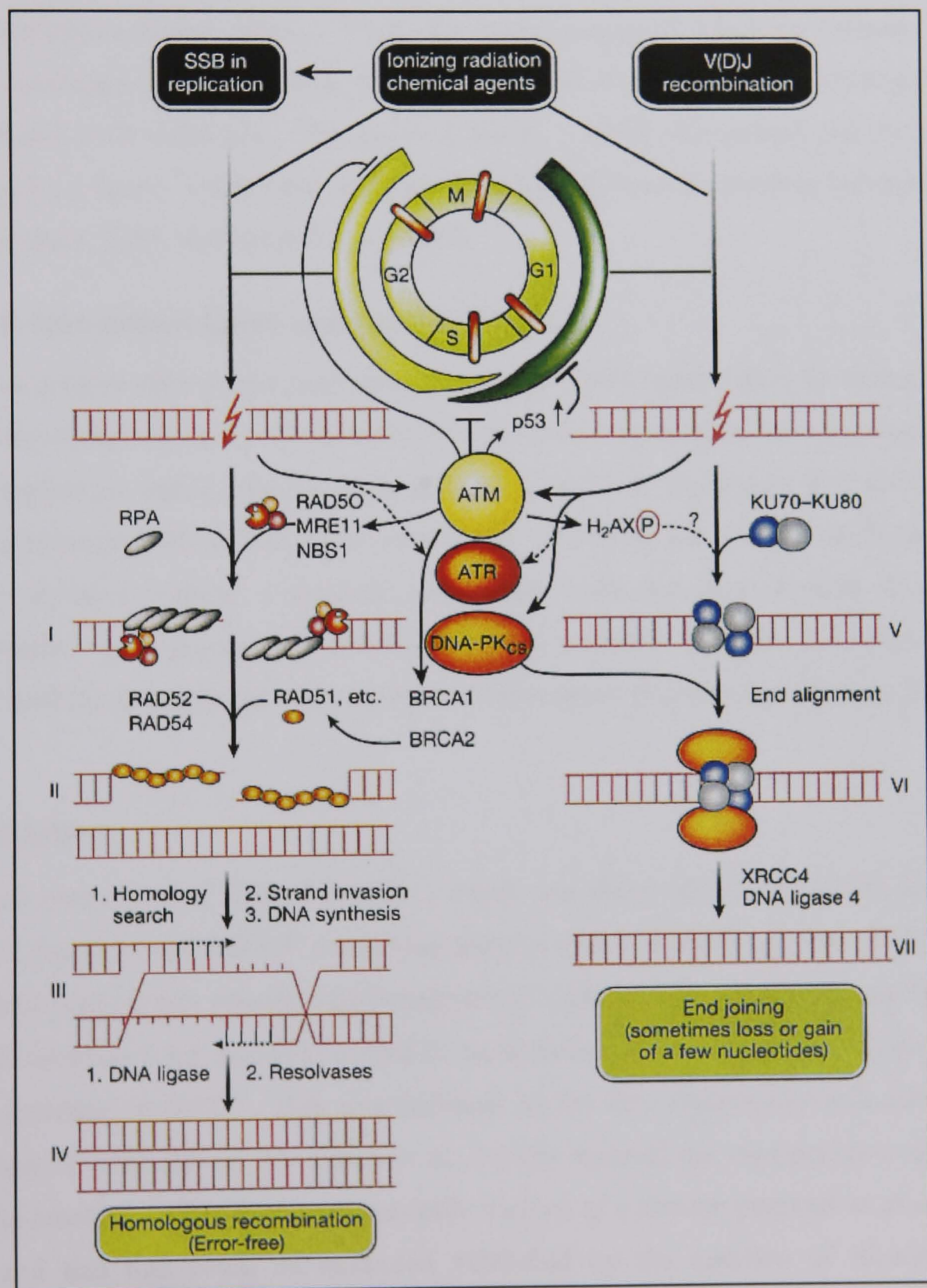


Figure 1.8 Mechanisms of Double Strand Break Repair (Hoeijmakers 2001).

1.5.3.1 Homologous recombination (HR).

This pathway repairs double strand breaks using the sister chromatid as a template to provide a perfect copy. Therefore this pathway is conducted in the S and G2 phases of the cell cycle where the second copy is present. To allow strand invasion into homologous sequences, the 5'-3' exonuclease activity of the RAD50/MRE11/NBS1 complex exposes both of the 3' ends at the double strand break. This complex can be phosphorylated by ATM. RPA aids the assembly of a RAD51 nucleofilament that may include XRCC2, XRCC3, RAD51B, C and D. This nucleoprotein filament searches for the homologous duplex DNA. When the correct sequence has been located, DNA strand exchange creates a joint molecule between the homologous damaged and undamaged DNA duplexes. The gap is filled by a DNA polymerase and the strand rejoined by a ligase. Finally the so-called Holliday junctions are resolved by resolvases (Hoeijmakers, 2001, and Kanaar *et al.*, 1998).

1.5.3.2 Non-homologous end joining (NHEJ).

NHEJ is a more error-prone mechanism of double strand break repair occurring in the G1 phase of the cell cycle. Cells in G1 only have the homologous chromosome to use as a template for repair, which may be difficult to find, and is dangerous to use as may lead to homozygosity for recessive mutations. In NHEJ, the ends of the breaks are simply rejoined without a template, sometimes with the loss or gain of a few nucleotides. This process is carried out by the Ku70/80 complex and DNA-PKcs, which bind the ends that are religated by XRCC4-ligase I (Khanna and Jackson, 2001).

1.6 PARP-1.

A major component of BER is PARP-1, which was discovered in the 1960's although the first description of a NAD^+ consuming enzyme was made by Riott *et al.*, in 1956. In this early study it was observed that treatment of cells with the alkylating agent 2,4,6-triethyleneimino-1,3,5-triazine resulted in the inhibition of glycolysis that was mediated via a depletion in NAD^+ . This was followed by the first reports of the formation of polymers of ADP-ribose. Chambon *et al.*, (1963) reported the incorporation of [^{14}C]-adenine-labelled ATP into an acid-insoluble fraction of a nuclear preparation of chicken liver and that this could be enhanced 1000-fold by the addition of nicotinamide mononucleotide. It has since been shown that the enzyme, poly(ADP-

ribose)polymerase-1 (PARP-1) is activated in response to alkylating agents and is responsible for the synthesis of (ADP-ribose) polymers (Whish *et al.*, 1975).

PARP-1 (EC 2.4.2.30) is a 113 kDa nuclear enzyme containing 1014 amino acids, encoded by a single copy gene at the q41-q42 position of chromosome 1. PARP-1 is found in most eukaryotic cells at levels of between 10^5 and 10^6 copies per cell, in a dimeric form. PARP-1 activity is low under "normal" cellular conditions but is stimulated by more than 500-fold in the presence of DNA strand breaks (Benjamin and Gill, 1980, reviewed by de Murcia *et al.*, 1994).

1.6.1 PARP Homologues.

To date 15 PARP homologues have been identified by sequence homology. PARP-1 was the original poly(ADP-ribosylating) protein identified in the 1960s and has been followed by the discovery of others more recently. The characteristics of the more extensively studied PARP homologues are described below; these have been reviewed in de Murcia and Shall (2000), Smith (2001) and Bouchard *et al.*, (2003).

PARP-2

PARP-2 was discovered after the observation that PARP-1 null cells still showed residual PARP activity following DNA damage (Ame *et al.*, 1999). PARP-2 is a nuclear protein similar to PARP-1 (60 % homology) and is activated in response to DNA damage. This protein is 64.8 kDa and shares considerable homology to the catalytic domain of PARP-1 and has the ability to bind DNA even though it does not have the zinc finger-binding domain found in PARP-1. PARP-2 has been shown to be a member of the BER repair complex, interacting with XRCC1, DNA pol β and DNA ligase III. PARP-2 forms a dimer with itself and PARP-1. PARP-2 null cells have been shown to be deficient in strand break resealing following treatment with MNU, similar to that observed in PARP-1 null cells (Schreiber *et al.*, 2002). Therefore PARP-2 seems to play a role in BER, and may compensate for lack of PARP-1.

PARP-3

PARP-3 is a 60 kDa protein, whose gene is located on chromosome 3. This PARP has neither a DNA binding domain (DBD) or automodification domain. This protein has been shown to localise to the centriole throughout the cell cycle. (Johanssen *et al.*, 1999)

PARP-4 (PH5P or VPARP)

PARP-4 is a multifunctional 192 kDa protein belonging to the inter- α -inhibitor family. This protein has been isolated as one of those found in the Vault ribonucleoprotein particle. This protein contains a PARP catalytic domain. (Jean *et al.*, 1999)

Tankyrase 1 (PARP-5)

Tankyrase is a 142 kDa protein localised in the telomeres. It contains a PARP-1 catalytic fragment. Its function is to negatively regulate the TRF-1 protein involved in telomere elongation. Thus poly(ADP-ribosylation) of TRF-1 by tankyrase-1 functions to regulate telomere length.(Smith 1998, 2000)

Tankyrase 2 (PARP-6)

Tankyrase 2 is more than 80% homologous to tankyrase 1 and has a similar function. It is expressed in the cytoplasm and can be recruited to the telomeres to bind TRF-1. It associates with the Golgi apparatus. Overexpression of this protein leads to necrosis.

Ti PARP

Ti PARP is a 75 Kda PARP that is inducible by 2,3,7,8-tetrachlorodibenzo-p-dioxine.

sPARP-1

This is a short form of PARP-1 possibly resulting from an alternative start site in the PARP-1 gene. It is a 55-kDa protein containing the catalytic domain of PARP-1. It is located in the nucleus and is stimulated by genotoxic stress. Strand breaks are not needed for activation of sPARP.

1.6.2 Structure of PARP-1.

PARP-1 can be divided into three domains by proteolytic cleavage, a 46 kDa, DNA-binding domain, a 22 kDa automodification domain and a 54 kDa C-terminal substrate binding domain (Kamishita *et al.*, 1984). The domain structure of PARP-1 is shown in Figure 1.9 and has been extensively reviewed by reviewed Masutani *et al.*, 2003, and de Murcia and Shall 2000).

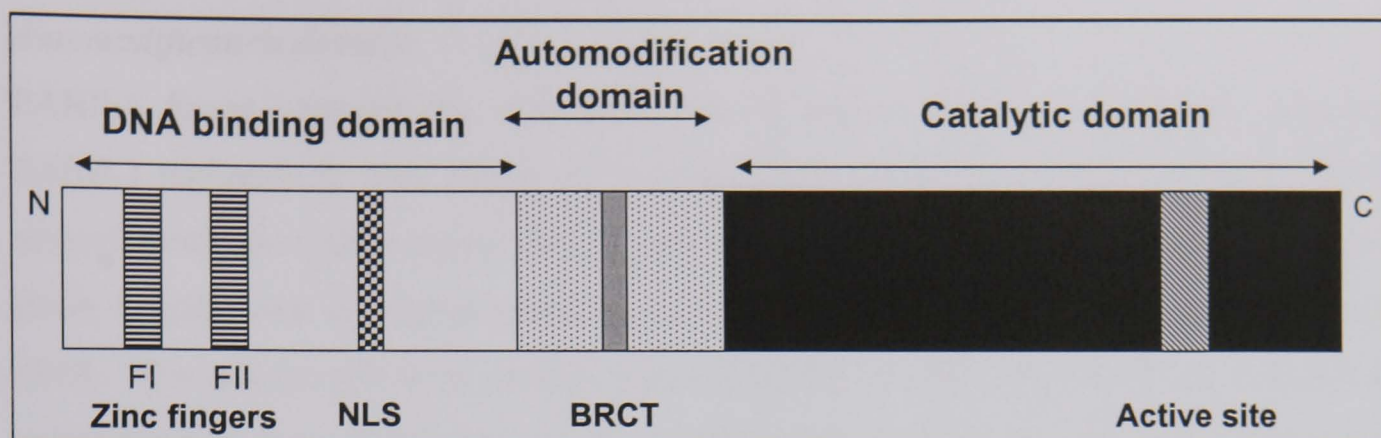


Figure 1.9 Schematic representation of the structure of PARP-1. Adapted from Masson *et al.*, (1998). NLS, Nuclear localisation sequence; BRCT, BRCA1 C-terminus motif.

DNA binding domain.

The N-terminal DNA-binding domain contains two zinc-finger motifs, a basic amino acid sequence, a nuclear localisation sequence, and a cysteine rich sequence. The zinc fingers share the same sequence motif of Cysteine-X₂-Cysteine-X₂₈₋₃₀-Histidine-X₂-Cysteine, where X is any amino acid. This motif binds a zinc atom in a tetrahedral complex using the Cys and His residues. It was originally thought that the second zinc finger was essential for the recognition of the single strand breaks, however it has since been shown that both of the zinc fingers are capable of single strand break recognition (Gradwohl *et al.*, 1990, de Murcia and Shall, 2000). However the first zinc finger is essential for activation of PARP-1 in response to DNA damage, whereas deletion of the second zinc finger does not prevent activation of PARP-1 (Ikejima *et al.*, 1990). This zinc-finger region detects DNA single-strand breaks and interacts with one and a half turns of the DNA helix, protecting seven nucleotides either side of the break independently of DNA sequence (Menissier de Murcia *et al.*, 1989). A basic amino acid sequence present down stream of the zinc fingers also contributes to non-specific DNA binding activity (Ikejima *et al.*, 1990). The DNA binding domain also contains regions for protein-protein interactions. Proteins found to interact with this area of PARP-1 include histones, PARP-1, XRCC1 (Masson *et al.*, 1998), DNA pol α (Dantzer *et al.*, 1999), and the transcription factors TEF-1 and RxR α . The DNA binding domain also contains a bipartite NLS that ensures that PARP-1 is transported through the nuclear membrane into the nucleus.

Automodification domain.

PARP-1 forms homodimers with itself and is able to ADP-ribosylate the adjacent PARP-1 molecule at sites within the automodification domain. This auto poly(ADP-ribosylation) takes place mainly on 15 conserved glutamate residues and interferes with DNA binding due to charge repulsion between the negatively charged polymer and DNA. The automodification domain contains a BRCT motif commonly found in DNA repair and cell cycle checkpoint proteins. This motif binds ubc9 (ubiquitin-conjugating enzyme-9) (Masson *et al.*, 1997), Oct-1 (POU-homeodomain-containing octamer transcription factor-1) (Nie *et al.*, 1998), YY1 (Yin-Yang-1) (Griesenbeck *et al.*, 1999), as well as PARP-1 and PARP-2 (Schreiber *et al.*, 2002).

C-terminal catalytic domain.

The C-terminal domain of PARP-1 is the most highly conserved region of the PARP-1 protein. It is conserved 100% in vertebrates and shows 92 % homology amongst other species. The C-terminal catalytic domain is responsible for all of the catalytic activity associated with the PARP-1 protein; NAD⁺ hydrolysis, initiation, elongation, branching and termination of polymer. Initiation involves the attachment of ADP-ribose to a protein acceptor. Elongation involves the addition of more ADP-ribose polymers, and polymer length can range from a few to 200 residues. It is thought that for every initiation step PARP-1 catalyses over 200 elongation and 5-7 branching reactions.

1.6.3 PARP-1 reaction mechanism.

Poly(ADP-ribosylation) is a post translational modification of nuclear proteins. In response to DNA damage, PARP-1 binds the DNA strand break through the N-terminal DNA binding domain and catalyses the transfer of an ADP-ribose unit from its substrate NAD⁺ to a nucleophilic acceptor protein, releasing nicotinamide. This reaction involves the breakage of the glycosidic bond between the C1' atom of ribose and the nicotinamide in NAD⁺ (Figure 1.10), and the formation of a new glycosidic bond to the nucleophilic acceptor. Glutamic acid, aspartic acid, or lysine residues act as acceptors for poly(ADP-ribosylation) on the target protein. For elongation, the ADP-ribose is added to the 2'-hydroxyl of the nicotinamide ribose (α), or adenine ribose (β) for the formation of branched polymers. In the case of automodification PARP-1 acts as a homodimer where each monomer poly(ADP-ribosylates) glutamate residues on the other PARP-1 molecule (Mendoza-Gonzalez and Alvarez-Gonzalez, 1993; reviewed by de Murcia *et al.*, 1994 and Lindahl *et al.*, 1995).

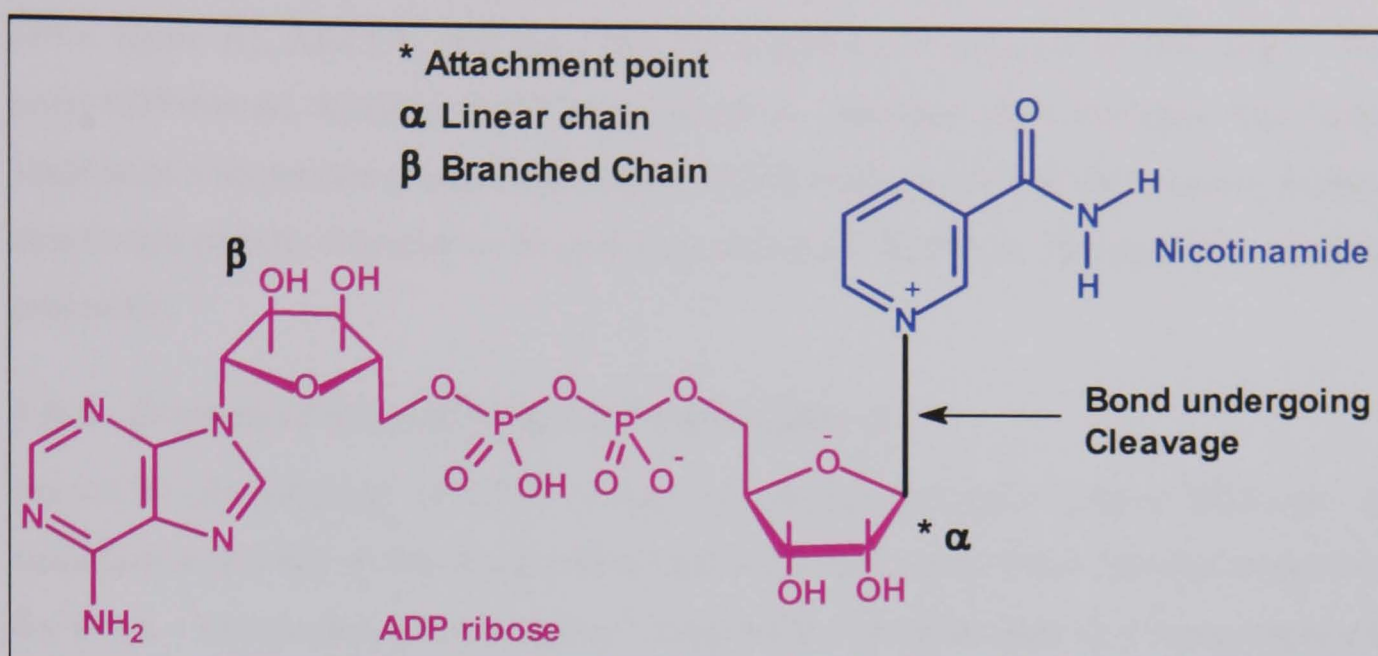


Figure 1.10 Synthesis of poly(ADP-ribose) by PARP-1. Addition of ADP-ribose to growing polymer chain and release of nicotinamide. (Picture provided by N. Curtin, NICR)

1.6.4 Poly(ADP-ribose) degradation.

Poly(ADP-ribose) is degraded within approximately 2-5 minutes of polymer formation by poly(ADP-ribose) glycohydrolase (PARG). PARG specifically splits ribose-ribose bonds of linear and branched forms of poly(ADP-ribose) degrading polymer down to the protein-bound ADP-ribose residue. The last residue may be removed by ADP-ribosyl protein lyase (Hatakeyama *et al.*, 1986), however more recently it has been shown that the last residue may be removed by PARG (Jacobson *et al.*, 2003).

1.6.5 Acceptors of poly(ADP-ribose).

PARP-1 catalyses the formation of poly(ADP-ribose) polymers on PARP-1 itself and a number of other DNA binding proteins. Poly(ADP-ribose) binding can be very strong and covalent poly(ADP-ribose)-histone (H1 and H2B) complexes resist strong acids, detergents and high salt concentrations. The other major acceptors are HMG proteins, lamin B, topoisomerase I, DNA-PK, and p53. The existence of a 20 amino acid poly(ADP-ribose) binding motif consisting of two conserved regions, a cluster rich in basic amino acids and a pattern of basic amino acids interspersed with basic residues has been reported by Pleschke *et al.*, (2000). The discovery of this sequence has allowed screening of proteins for the poly(ADP-ribose) binding motif and has identified

a number of proteins involved in DNA damage that may be poly(ADP-ribosylated). These include p21, xeroderma pigmentosum group A complementing protein, MSH6, DNA ligase III, XRCC1, and the DNA-PKcs and Ku70 subunits of DNA-PK. The poly(ADP-ribose) binding motif was found to interfere with domains that were associated with protein-protein interactions, DNA binding, nuclear localisation, nuclear export and protein degradation suggesting a role for PARP-1 in the regulation of these processes.

1.6.6 Consequences of poly(ADP-ribosylation).

Poly(ADP-ribosylation) of DNA-interacting proteins generally causes inhibition or reduction in activity of the target protein due to the repulsion of the enzyme away from the DNA. This is due to the negative charge of the (ADP-ribose) (1.7 -ve charges per monomer). As shown in Figure.1.11, poly(ADP-ribosylation) of histones or PARP-1, in response to strand breaks, results in their repulsion from DNA and may serve to alter the chromatin conformation allowing access to repair enzymes (the histone shuttle model, Althaus *et al.*, 1994). Poly(ADP-ribosylation) of PARP-1 may act to remove the PARP-1 from the site of the DNA damage again allowing access for repair enzymes. One exception is DNA-PK, where poly(ADP-ribosylation) of DNA-PKcs leads to an increase in activity. It is thought that the poly(ADP-ribosylation) of the catalytic subunit could enhance the interaction between DNA-PKcs and the Ku70/80 heterodimer via the non-covalent poly(ADP-ribose)-binding site on the Ku70 protein (Ruscetti *et al.*, 1998).

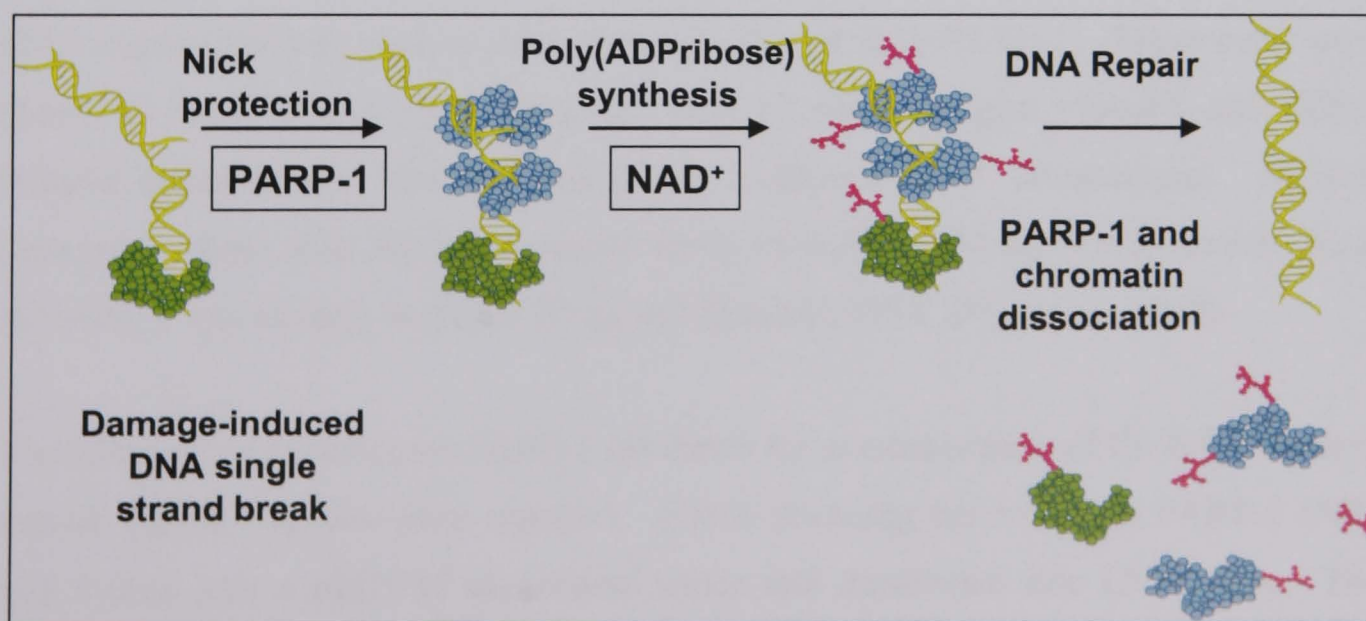


Figure.1.11 Mechanism of action of PARP-1. DNA damage stimulates PARP-1 (blue) and recruits it to the site of damage. PARP-1 poly(ADP-ribosylates) itself and histones (green) causing repulsion from the DNA leading to dissociation of PARP-1 and chromatin remodelling allowing access for DNA repair enzymes to the site of damage. Picture provided by N. Curtin, NICR.

1.6.7 PARP-1 and DNA repair.

The role of PARP-1 in DNA repair was initially proposed following the observation that PARP-1 activity was increased ~500-fold following stimulation by DNA strand breaks (Benjamin and Gill, 1980). More direct evidence followed when it was shown that an early inhibitor of PARP-1, 3-aminobenzamide (3-AB) dramatically slowed the ligation of single strand breaks and greatly increased cytotoxicity induced by the methylating agent dimethyl sulfate (DMS) (Durkacz *et al.*, 1980). Many other authors have shown similar findings using PARP-1 inhibitors such as 3-AB with other alkylating agents, including, methyl methanesulfonate (MMS), N-methyl-N'-nitro-N-nitrosoguanidine (MNNG), ionising radiation, the radiomimetic bleomycin and oxidating agents such as H₂O₂ (reviewed by Griffin *et al.*, 1995). The general conclusion from these studies was that PARP-1 plays a role in BER in some capacity, as damage caused by such agents would normally be repaired by BER.

As the early inhibitors of PARP-1 were shown to affect other cellular processes apart from PARP-1, activity such as *de novo* purine biosynthesis (Milam *et al.*, 1986), more specific molecular approaches were sought to elucidate the role of PARP-1. Antisense RNA expression was used to deplete HeLa cells of 90% PARP-1. These cells were shown to have limited DNA repair in recovery from nitrogen mustard and MMS-induced strand breaks, this corresponded to a reduced NAD⁺ consumption. At later time points these cells displayed normal levels of repair, showing that the involvement of PARP-1 was an early response (Ding and Smulson 1994, Ding *et al.*, 1992).

The effect of trans-dominant PARP-1 inhibition by overexpression of the DNA binding domain (DBD) has also been reported. cDNA encoding the wild-type PARP-1 DBD was cloned into a pECV23 expression vector and transfected into CV-1 cells. The overexpression of the DNA binding domain inhibited PARP-1 activity by competing with it for DNA strand breaks, and irreversibly binding to the DNA. This trans-

dominant inhibition of PARP-1 in intact cells inhibited unscheduled DNA synthesis that occurs during BER and inhibited the repair of MNNG-induced DNA damage (Molinette *et al.*, 1993, Kupper *et al.*, 1995).

PARP-1-deficient mouse and cell studies.

PARP-1 deficient V79 cells derived by selection in NAD⁺ deficient medium were shown to be hypersensitive to a range of alkylating agents, camptothecin, and γ -irradiation (Chatterjee 1990, 1991). Although this suggested a role for PARP-1 in repair, as these cells may also be defective in other NAD-requiring processes and have a vastly reduced proliferation rate, better models were sought. PARP-1 knockout mice have been developed by homologous recombination, and immortalised cell lines have been derived from these mice. This has allowed verification of the previous results and has been reviewed by Shall and de Murcia (2000). Three independent groups have created PARP-1 knockout mice by disruption of the PARP-1 gene at exons 1, 2 and 4 (Masutani *et al.*, 1999, Wang *et al.*, 1995, Menissier de Murcia *et al.*, 1997, respectively). These mice develop normally and are fertile, demonstrating that PARP-1 is dispensable for development. However, all of the PARP-1 knockout animals have a serious defect in response to DNA damage caused by alkylating agents (MNNG, MNU, MMS) and γ -irradiation, which can be attributed to a defect in the BER process. They have a high level of genomic instability, including increased level of sister chromatid exchanges and chromatid breaks (Menissier de Murcia *et al.*, 1997, Wang *et al.*, 1995). PARP-1 deficient mice have been exposed to a number of genotoxic agents that have been shown to stimulate PARP-1 activity. PARP-1 null mice treated with the alkylating agent MNU (75 mg/kg), died within 2-4 weeks of administration, compared to 60% survival of the wild type mice 8 weeks after exposure (Menissier de Murcia *et al.*, 1997). Similarly most of these PARP-1 null mice exposed to 8 Gy of γ -rays died within 4-6 days of exposure compared to 50% at three weeks post exposure for the wild type mice. Similar results were obtained using mice from the Wang laboratory where all of the PARP-1 null mice that had been exposed to 8 Gy of γ -irradiation had died within 10 days of exposure compared to 100% survival of the wild type mice (Wang *et al.*, 1997). The PARP-1 null mice from the de Murcia laboratory have also been shown to be hypersensitive to CPT-11. 64% of PARP-1 null mice had died within 2 weeks of exposure to 140 mg/kg CPT-11 while all of the wild type mice were alive at 8 weeks

(Burkle et al, 2000). Immortalised cell lines derived from these mice have been shown to display a dramatic delay in DNA strand break rejoining following exposure to the DNA alkylating agent MMS. Six hours after treatment with 0.15 mM MMS, 95% of strand breaks were repaired in the wild type cells, whereas only 36 % of the strand breaks were repaired in the PARP-1 null cells although the damage was repaired eventually (Trucco *et al.*, 1998). These data show that in the absence of PARP-1 there is a defect in the repair of those lesions repaired by the BER pathway, therefore adding further support to the proposal that PARP-1 is involved in DNA repair.

The BER pathway consists of two overlapping pathways; long and short patch repair (see section 1.5.1). To determine whether PARP-1 was involved in the long or short pathways the pathways have been reconstructed *in vitro*. The effect of PARP-1 deficient cell extracts on these pathways was investigated. Using two different AP sites, uracil and 8-oxoguanine it was shown that the absence of PARP-1 had dramatic effects on long patch repair of uracil or 8-oxoguanine derived AP sites (> 90% reduction), but only moderate effects on short patch repair (50% reduction). The defect was shown to be associated with the polymerisation step of the pathway and PARP-1 protein and catalytic activity was demonstrated to take part in the repair process (Dantzer *et al.*, 2000).

All of the above data suggests that PARP-1 is involved in the response to DNA damage but an exact role was disputed until interactions with other proteins in the BER pathway were demonstrated. PARP-1 has already been shown to contain a BRCT domain that is a common motif in DNA repair and DNA damage responsive cell cycle checkpoint proteins (Callebaut *et al.*, 1997). Using immunoprecipitation, co-purification and yeast-2-hybrid techniques, PARP-1 has been shown to physically interact with a number of proteins in the BER pathway. PARP-1 has been shown to associate with XRCC1 in a yeast-2-hybrid screen and this has been confirmed in mammalian cells by immunoprecipitation. XRCC1 interacts with the PARP-1 via its BRCT domain. This interaction can be via the BRCT domain or zinc finger domains of the PARP-1 protein. XRCC1 interacts preferentially with automodified PARP-1 and this interaction negatively regulates PARP-1 activity (Masson *et al.*, 1998, Trucco *et al.*, 1998). This suggests that PARP-1 recruits XRCC1 and the interaction of the two proteins serves to remove PARP-1. This proposal was supported by the observation that PARP-1 null

cells were unable to form XRCC1 foci in response to treatment with H_2O_2 and MMS (El-Khamisy *et al.*, 2003). PARP-1 also interacts via its BRCT domain with the C-terminal domain of DNA pol β (Dantzer *et al.*, 2000). An interaction between PARP-1 and DNA ligase III has also been demonstrated by affinity chromatography. PARP-1 binds to the N-terminal region of DNA ligase III. DNA ligase III has also been shown to bind directly to poly(ADP-ribose) and preferentially associates with automodified PARP-1 (Leppard *et al.*, 2003). Thus PARP-1 activation may function to recruit DNA ligase to the BER complex. Further characterisation of the role of PARP-1 in the long patch pathway showed that PARP-1 has also been shown to be involved in strand displacement during DNA synthesis by DNA pol β . This is dependent on the presence of FEN-1. Therefore there may be some interaction between these two proteins to activate long patch repair (Prasad *et al.*, 2001). Therefore as PARP-1 associates with many of the proteins involved in the BER process it is possible that poly(ADP-ribose) synthesis by PARP-1 regulates the BER process, possibly in a cyclic manner, by regulating the association and dissociation of proteins from the BER core complex (figure 1.12, Dantzer *et al.*, 2000).

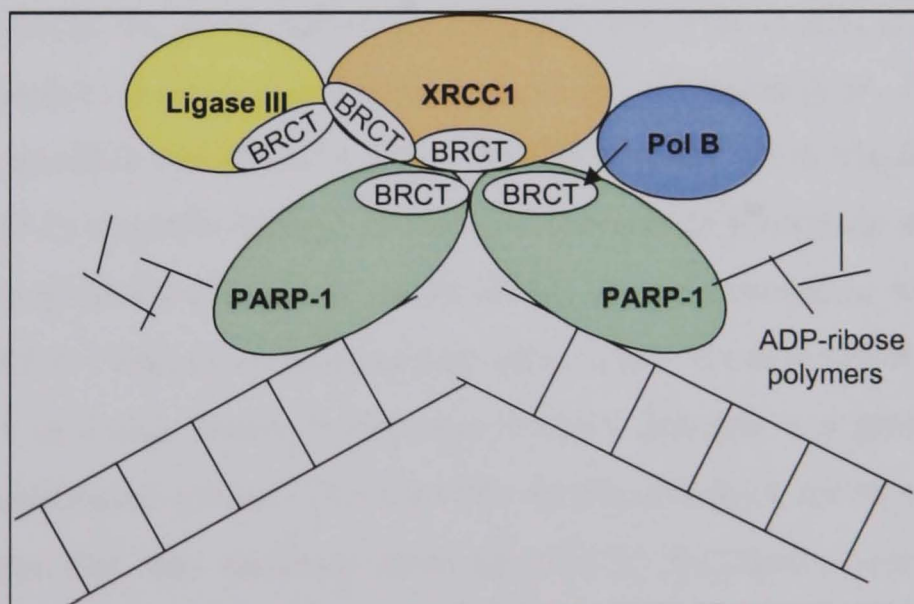


Figure.1.12 Interaction of PARP-1 with components of the BER pathway at sites of DNA damage. PARP-1 binds the break as a dimer via its Zn fingers. PARP-1 makes interactions with XRCC1 via common BRCT domains, PARP-1 also interacts with DNA pol β . Poly(ADP-ribosylation) of PARP-1 removes PARP-1 from the strand breakage site allowing pol β to repair the break and DNA ligase to religate the DNA. Adapted from de Murcia and Shall (2000).

It has also been proposed that PARP-1 might supply ATP to the long patch BER pathway by local production of poly(ADP-ribose) under conditions of ATP shortage. This would involve the degradation of poly(ADP-ribose) by PARG and generation of ADP-ribose units. These could combine with the pyrophosphate liberated by the action of pol β to generate ATP. The production of ATP may be necessary for the completion of the repair process, as ligase III requires ATP (Oei and Zeigler, 2000).

The evidence for the role of PARP-1 in repair is overwhelming although its actual function has not been absolutely defined. PARP-1 may be involved in several steps of the BER pathway. PARP-1 preferentially binds to a sugar phosphate at the 5' margin of a single -stranded DNA nick suggesting that PARP-1 binds a BER intermediate that is formed before a choice of sub-pathway has been made (Lavrik *et al.*, 2001). Therefore PARP-1 may play a role in the selection of pathways. PARP-1 and its catalytic activity are required for BER, its catalytic activity may be required for chromatin remodelling via poly(ADP-ribosylation) of histones. This high concentration of negative charge from the poly(ADP-ribose) may cause repulsion of histones away from the DNA allowing the DNA repair proteins to access the damaged DNA. Poly(ADP-ribosylation) may also be required for activation of the BER proteins such as XRCC1. As PARP-1 preferentially binds to the automodified form of XRCC1 (Masson *et al.*, 1998, Trucco *et al.*, 1998) it is possible that PARP-1 binds the DNA strand break via the zinc fingers and the increase in negative charge caused by automodification may attract XRCC1. XRCC1 may then become attached to the DNA via its interaction with the BRCT domain of PARP-1. These two proteins may then recruit the other BER proteins. The role of PARP-1 as a nick sensor in response to DNA damage may protect DNA from accidental recombination events. This could be by prevention of access of exonucleases or other enzymes that may facilitate recombination by the rapid and tight binding of PARP-1. The negatively charged poly(ADP-ribose) polymers would also repel DNA preventing exchange of DNA sequences (Lindahl *et al.*, 1995). PARP-1 may detect the break and signal for the start up of the repair process, informing the cell of the level of damage via poly(ADP-ribosylation) of other proteins; this process may involve other DNA repair proteins such as DNA-PK and ATM.

There is evidence suggesting that PARP-1 may not have an essential role in BER and that BER can function in the absence of PARP-1. Using an *in vitro* BER system, it was shown that repair of strand breaks was stimulated by NAD^+ and induced poly(ADP-ribose) formation. BER was not efficient in the presence of competitive inhibitors of PARP-1 such as 3-AB or in the absence of NAD^+ . However the repair was still effective when >98% of the PARP-1 activity of the cell extracts used had been depleted by affinity chromatography suggesting that PARP-1 was not essential for BER. Taken together these data suggest that BER can proceed independently of PARP-1, but if PARP-1 is present then it must be active. In the absence of NAD^+ or the presence of 3-AB, PARP-1 is still able to bind to DNA, however as it is unable to poly(ADP-ribosylate) itself it is unable to dissociate, becoming an obstruction to DNA repair. This may suggest that the effects of PARP-1 inhibition may be more severe than lack of PARP-1. However it should be noted that these assay were conducted using plasmid DNA in the absence of histones, and therefore these results may not be representative of chromosomal DNA (Sato and Lindahl 1992, Sato *et al.*, 1993). Other groups have shown that PARP-1 deficient cells are able to conduct BER effectively (Vodenicharov *et al.*, 2000, Allinson *et al.*, 2003). Vodenicharov *et al.*, showed that extracts made from PARP-1 null cells were able to repair plasmid DNA damaged by MNNG or γ -irradiation and similarly that PARP-1 null cells could repair this damage as efficiently as the wild type cells. Allinson *et al.*, showed similar findings, that PARP-1 null cell extracts could efficiently repair abasic sites in DNA, although this was shown to be independent of NAD^+ . The repair in the PARP-1 null cell was also faster than that seen in the wild-type cells. There are a number of explanations for the ability of the PARP-1 null cells to repair SSBs. It may be that PARP-1 itself is not involved in repair but is required to poly(ADP-ribosylate) proteins involved in this process. It is also possible that PARP-2 may be performing the role of PARP-1 in these cells. PARP-2 is stimulated by DNA damage and can also interact with XRCC1, pol β and DNA ligase III in the BER complex. PARP-1 and 2 can act together in heterodimers as well as individual homodimers (Schreiber *et al.*, 2002). It is interesting to note that PARP-1/2 knockout mice are embryonic lethal, suggesting that these two enzymes together play an essential role (Menissier de Murcia *et al.*, 2003).

1.6.8 Role of PARP-1 in cell death.

PARP-1 is activated in response to DNA damage, but the extent of damage determines the eventual fate of the cell (see Figure 1.13). In response to mild DNA damage PARP-1 is activated and is recruited to sites of DNA damage and may serve to recruit other DNA repair enzymes. Indeed 3-AB sensitised Jurkat cells to apoptosis, suggesting that at low levels of DNA damage PARP-1 protects against apoptosis (Payne *et al.*, 1998). At higher levels of DNA damage, the repair machinery is not able to perform repair and apoptosis follows. An early event in apoptosis is the cleavage of PARP-1 into 85 and 23 kDa fragments by caspases; caspase-3 and 7 being the most efficient (Kaufman *et al.*, 1993). The cleavage occurs in the DNA binding domain of PARP-1. The remaining 85 kDa fragment containing the automodification and catalytic domains, has basal PARP-1 activity equivalent to that of the whole enzyme in the absence of stimulation by DNA ends, but is not inducible by DNA strand breaks.

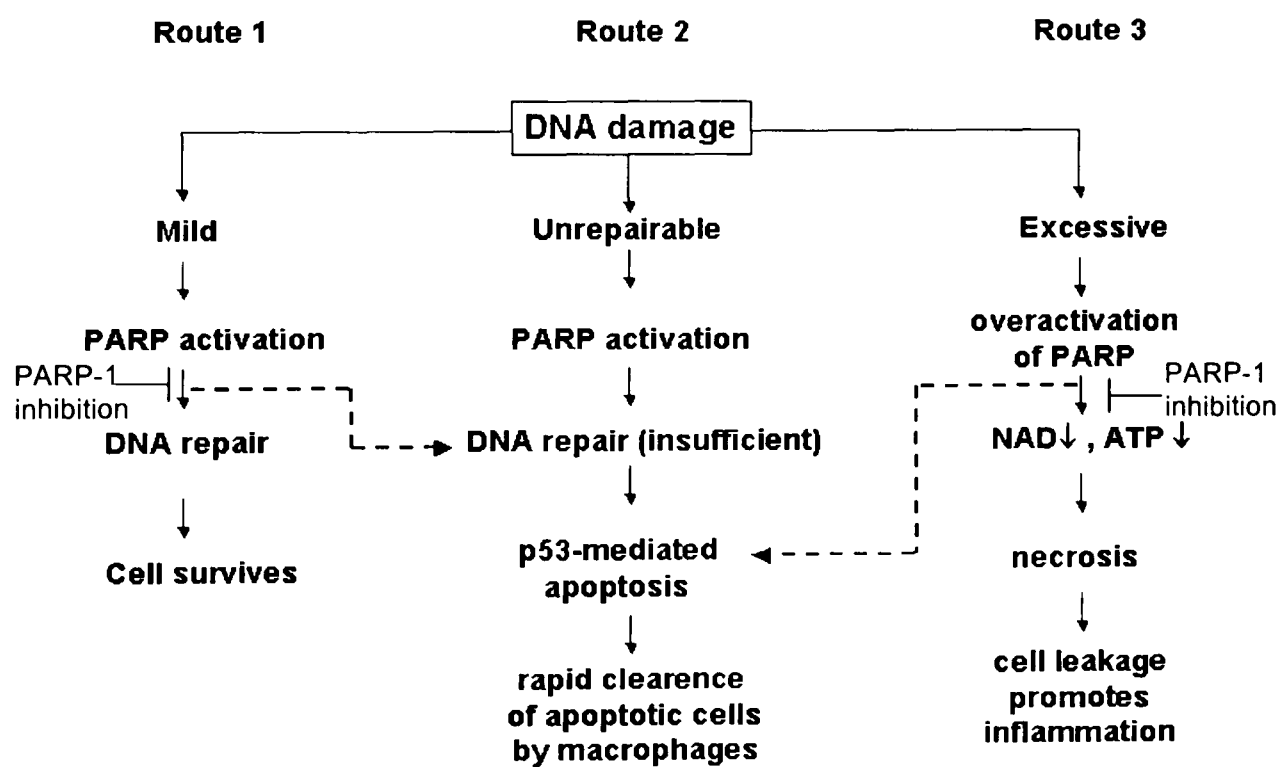


Figure 1.13 Role of PARP-1 in cell death. Picture from Virag and Szabo. (2002). The three different response pathways used to combat varying degrees of DNA damage. The dotted lined represents the crossover between pathways induced by PARP-1 inhibition.

Excessive levels of DNA damage caused by inflammation, or shock lead to PARP-1 hyperactivation. This causes a massive depletion of the NAD^+ pool causing depletion of ATP, and glycolysis and mitochondrial respiration become impaired. ATP is used to try to resynthesise the NAD^+ leading to a futile and lethal cycle. Cell death follows by a

caspase-independent pathway. (the Suicide hypothesis; Berger *et al.*, 1985, Chiarugi 2002, Virag and Szabo 2002). These observations have led to the study of the use of PARP-1 inhibitors for use in myocardial infarction, cerebral ischaemia and insulin dependent-diabetes where there is massive DNA damage leads to over-activation of PARP-1. Use of PARP-1 inhibitors to treat these conditions may reduce the extent of the damaging death response, increasing survival or causing apoptosis (reviewed by Tentori *et al.*, 2002, Southan and Szabo, 2003).

Recent findings have shown that PARP-1 may be involved in caspase-independent form of cell death, involving apoptosis inducing factor (AIF) (Yu *et al.*, 2002). AIF translocates from the mitochondria to the nucleus in response to damage, and this is dependent on PARP-1 activity. This translocation causes nuclear condensation and cell death. AIF also causes the release of cytochrome C from the mitochondria. This pathway may pre-date caspases on an evolutionary scale and has been shown to act following growth factor deprivation and in early development.

1.7 Development of PARP-1 inhibitors.

Early inhibitors were developed to enable the study of the mechanism of PARP-1, These compounds were analogues of the by-product of PARP-1 catalysis, nicotinamide; nicotinamide itself being a weak PARP-1 inhibitor. Benzamide, an isostere of nicotinamide was shown to be an inhibitor of PARP-1 in 1975 (Shall, 1975). Following this the investigation of benzamide analogues led to the discovery of more specific PARP-1 inhibitors including the "benchmark" inhibitor 3-aminobenzamide (3-AB) (Purnell and Whish, 1980). 3-AB was shown to cause 96 % inhibition of PARP-1 and has a K_i of 4 μ M. However, these early benzamide compounds were shown to lack specificity and interfere with other cellular processes such as inhibiting *de novo* purine biosynthesis (Milam *et al.*, 1986, Eriksson *et al.*, 1996, Cleaver *et al.*, 1984). They could not be used clinically as they were far too weak; 3-5 mM 3-AB was required for potentiation *in vitro*.

3-AB has been shown to potentiate the cytotoxicity of a range of alkylating agents, ionising radiation and bleomycin (see section 1.6.7 and 1.7.1). The promising *in vitro* studies using 3-AB prompted further investigation and the development of more potent

PARP-1 inhibitors. The study of a large number of compounds for their potential PARP-1 inhibition by Banasik *et al.*, (1992), aided in the determination of the essential features of a PARP-1 inhibitor. This study showed that a carboxamide group constrained within a ring structure conjugated to an aromatic ring was a common feature of the PARP-1 inhibitors screened. Some compounds were 100-fold more potent than benzamide. The biologically active conformation has the carbonyl group of the carboxamide orientated *anti* to the 3-bond of the heteroaromatic ring (Suto *et al.*, 1991).

The majority of PARP-1 inhibitors are analogues of nicotinamide and are competitive with respect to NAD^+ . Structure-activity studies have indicated which are the desirable features for potent PARP-1 inhibition as summarised in figure 1.14. These include an unsubstituted aromatic or poly aromatic heterocyclic system and the presence of a carboxamide group, as those compounds without this group have no activity. The carboxamide moiety must be constrained to the *anti* conformation, as those derivatives with unrestrained carboxamides were less active. An amide proton is required for putative hydrogen bonding. Finally a non-cleaved bond is required at the position corresponding to the 3-position of the benzamide (Griffin *et al.*, 1995).

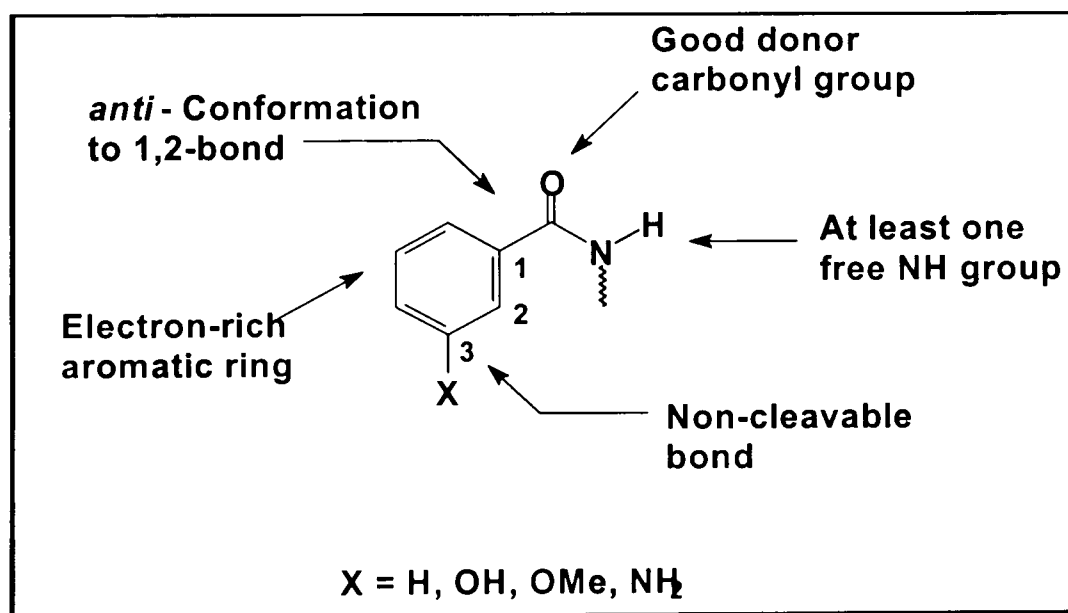


Figure 1.14 Features of a PARP-1 inhibitor. Picture from Griffin *et al.*, 1995

A number of classes of compounds were discovered to have PARP-1 inhibitory activity. These include benzimidazole carboxamides such as NU1085, quinazolinon-4-[3H]-ones such as NU1025 and isoquinoline derivatives such as PD128763. NU1025 and PD128763 incorporate the carboxamide into a ring system to lock the essential groups

in to the optimal conformation. In NU1085, the carboxamide is locked in the favoured conformation through intramolecular hydrogen bonds between the imidazole nitrogen and one of the carboxamide hydrogens (Figure1.15). These inhibitors showed increased affinity for PARP-1 compared to the original compounds but they still required concentrations of 10-100 μ M to achieve chemopotential (Table 1.1) (Boulton *et al.*, 1995, Bowman *et al.*, 1996 and Delaney *et al.*, 2000).

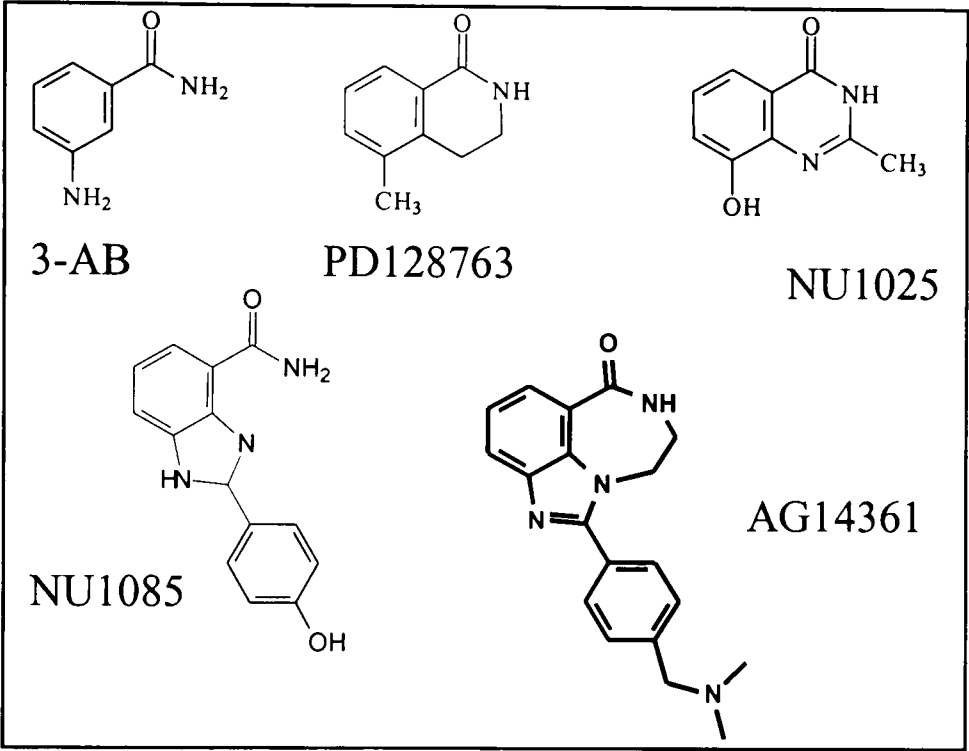


Figure1.15 Structure of PARP-1 inhibitors. AG14361 (the inhibitor used in this thesis) is shown in bold.

	Ki (nM)	Relative potency (Compared to 3-AB)
3-AB	4000	1
PD128763	70	60
NU1025	50	100
NU1085	10	830
AG14361	<<6	>1000

Table 1.1 PARP-1 inhibitory activities of PARP-1 inhibitors (Skalitzky *et al.*, 2003 and N. Curtin, personal communication).

The development of the tricyclic benzimidazoles, aimed to combine the best features of NU1025, NU1085 and PD128763, to form a PARP-1 inhibitor with the restricted

carboxamide in a ring structure, resulted in much more potent PARP-1 inhibitors. The development of these compounds is described by Skalitzky *et al.*, (2003) and Canan Koch *et al.*, (2003). The aim was to design structures that would restrict the benzamide rotation and allow optimum interaction with the PARP-1 protein. These structures locked the carboxamide in the s-trans conformation via a ring connection such as a lactam, to an indole core. Modelling studies have shown that these tricyclic systems allow interaction with PARP-1 via three critical hydrogen bonds of the lactam carbonyl/N-H with glycine-863 and serine 904 in the active site (Figure 1.16). The non-planar conformation of the seven-membered ring may prove to be ideal for interactions between the inhibitor and PARP-1, by allowing the lactam carbonyl and N-H to get closer to the amino acids involved in the H-bonding interactions. Tyrosine residues (907 and 889) nearby may also form π - π -interactions with the indole core and C-2 aryl substituent. The indole N-H participates in hydrogen bonding between the ordered water molecule and the catalytic Glu-988 residue. The flexibility of the Gln-763 accommodates the p-benzylamine substituent. The presence of the inhibitor is also thought to interfere with the intra molecular hydrogen bonding of PARP-1 between Tyr-889 and Asp-766 (Skalitzky *et al.*, 2003, Canan-Koch *et al.*, 2002).

AG14361 (structure shown in bold in Figure 1.15) is a tricyclic benzimidazole that has been chosen for further evaluation in cytotoxicity and *in vivo* studies, and is the subject of this thesis. The interactions made between AG14361 and the catalytic site of chicken PARP-1 and humanised by changing residue 763 from glutamine to glutamate, are shown in figure 1.16. AG14361 satisfies the structural requirements for a PARP-1 inhibitor that have been revealed by structure-activity relationships and discussed in this section. The use of this inhibitor in chemo- and radio-potential studies will be discussed in the following section.

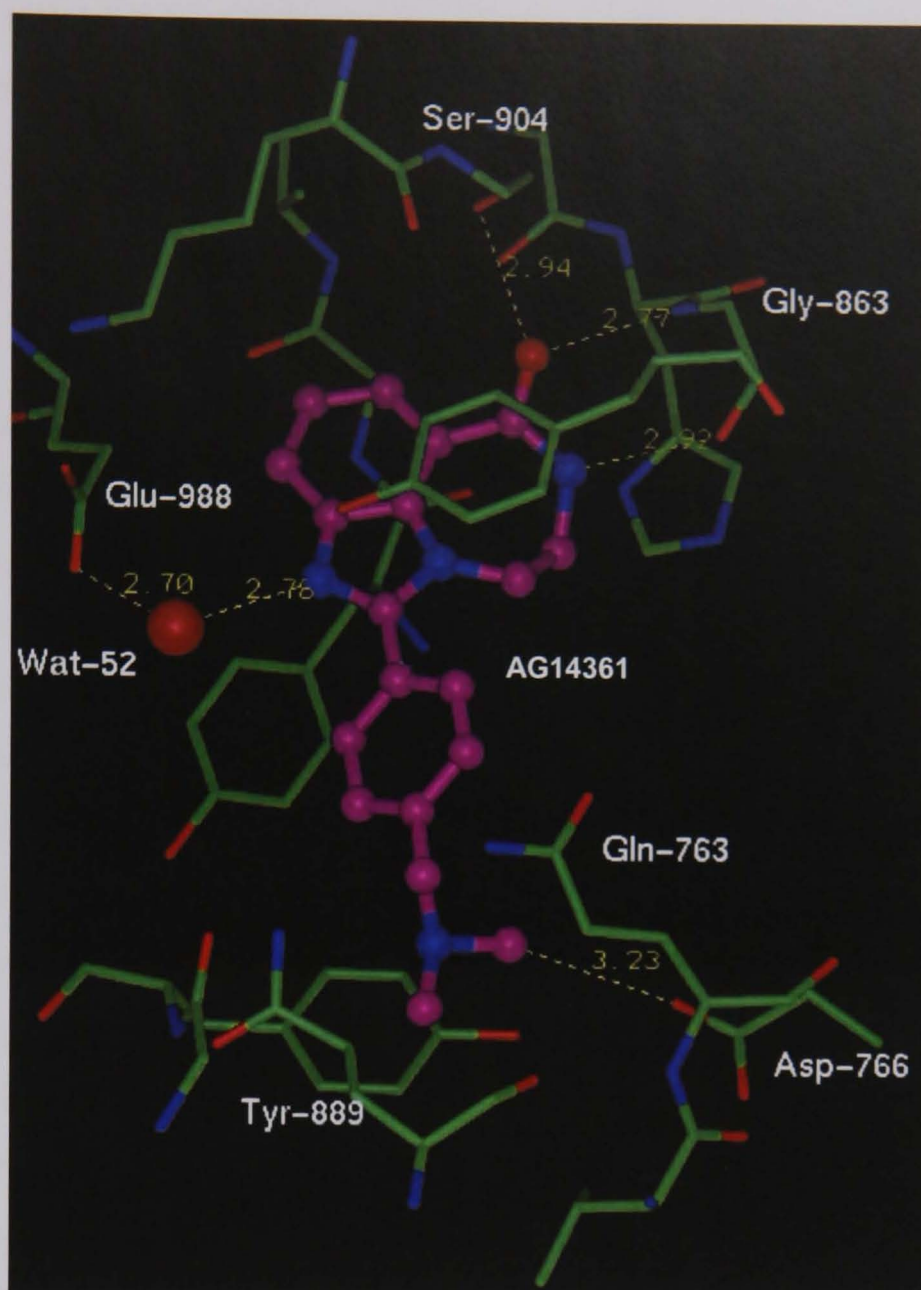


Figure 1.16 Co-crystal structure of AG14361 in the catalytic domain of chicken PARP-1 (provided by K Maegley, Pfizer GRD).

1.7.1 Chemo and radio-potentialiation by PARP-1 inhibitors.

The early PARP-1 inhibitors such as benzamide and 3-AB have been shown to potentiate the cytotoxicity of a number of alkylating agents and ionising radiation. One of the earliest studies by Durkacz *et al.*, (1980) showed that four classes of PARP-1 inhibitor, nicotinamides, methylxanthenes, thymidine and benzamides, potentiated the cytotoxicity of the alkylating agent dimethyl sulfate in L1210 cells. Nicotinamide and 3-AB have also been shown to potentiate X-ray-induced potentially lethal damage in V79 cells (Ben-Hur *et al.*, 1984). Similarly 3-AB potentiates the cytotoxicity of the radiomimetic drug, bleomycin (Huet and Laval, 1985). 3-AB has also been shown to potentiate the cytotoxicity of a number of cytotoxics including MNNG, BCNU, etoposide and cisplatin (reviewed by Griffin *et al.*, 1995) providing opportunity for the

development of PARP-1 inhibitors in combination with other chemotherapeutic agents. As the original inhibitors have been shown to lack specificity, new inhibitors were developed that were more potent and specific with the potential for clinical development. In this section the combination of PARP-1 inhibitor and anticancer agents will be discussed.

6-[5H]-phenanthridinone is a potent PARP-1 inhibitor that was originally shown to have PARP-1 inhibitory activity along with a range of other compounds, by Banasik *et al.*, (1992). Phenanthridinone is an isoquinalone derivative that has been studied in conjunction with a range of cytotoxics including camptothecin in a panel of murine and human tumour cell lines. 6-[5H]-phenanthridinone was shown to enhance the cytotoxicity of SN-38 the active metabolite of irinotecan, taxotere, BCNU and cisplatin. This compound potentiated cytotoxicity of bleomycin in some cell types. Thus this PARP-1 inhibitor did potentiate the activity of chemotherapeutic agents, but this was dependent on the cell type and drug action (Holl *et al.*, 2000).

The dihydroisoquinalone PARP-1 inhibitor PD128763, has been used in combination with a number of alkylating agents and ionising radiation. PD128763 was able to block recovery and increase cell killing following exposure of Chinese hamster V79 cells to X-irradiation (Arundel-Suto *et al.*, 1991). A 7 and 36-fold potentiation of cytotoxicity of the alkylating agent streptozotocin, and the nitroimidazole RSU1069, respectively was also seen in L1210 cells (Seebolt-Leopold *et al.*, 1992). In a separate study, PD128763 has been shown to potentiate the cytotoxicity 4 to 7-fold and increase the number of DNA strand breaks caused by temozolomide (Boulton *et al.*, 1995).

A similar drug screen has been conducted using NU1025 in murine L1210 cells. Here it was found that NU1025 could potentiate the cytotoxicity of MITC (the methylating-species derived from temozolomide), 4-fold as well as a 2.6-fold potentiation of camptothecin, and 1.4-fold potentiation of γ -irradiation, and bleomycin. NU1025 did not potentiate the cytotoxicity of the topoisomerase II poison etoposide, the thymidylate synthase inhibitor, nolatrexed or the cytotoxic nucleoside gemcitabine (Bowman *et al.*, 1998).

Further studies used NU1025 and NU1085 with topotecan and temozolomide in a panel of 12 cell lines that were chosen to be representative of the most common malignancies, lung, colon, ovarian and breast. In this study it was shown that the potentiation of growth inhibition by NU1025 and NU1085 varied between cell lines from 1.5 to 4-fold for temozolomide and 1 to 5-fold for topotecan. Potentiation was independent of tissue of origin and p53 status of the cells (Delaney *et al.*, 2000). NU1025 has been used *in vivo* in combination with temozolomide by Tentori *et al.*, (2002). In this study, NU1025 significantly increased the survival of mice that had been injected intracranially with L5178Y lymphoma cells and treated with temozolomide. Mice treated with temozolomide alone were dead by day 24, whereas those treated with temozolomide and NU1025 were still alive up to 90 days after treatment.

Studies using the more potent inhibitor AG14361 found that 0.4 μ M AG14361 caused a 5.5-fold enhancement of temozolomide-induced growth inhibition in LoVo colorectal carcinoma cells. A 2.1 to 2.3-fold potentiation of growth inhibition was also seen in A549 non-small cell lung carcinoma cells. *In vivo* studies using mice bearing human tumour xenografts also demonstrated that AG14361 could reduce the anti-tumour activity of temozolomide. The most impressive activity was seen using SW620 (colon carcinoma) xenografts, where a 100% complete remission rate was observed when temozolomide was used in combination with AG14361. This remission persisted for 60 days at the lowest dose of AG14361 (5 mg/kg) and until the end of the study at 100 days at the highest dose (15 mg/kg) (Calabrese *et al.*, JNCI in press). In the same study the effect of AG14361 on ionising radiation and topotecan was studied. Recovery from damage caused by irradiation in growth arrested cells (potentially lethal damage) was delayed by 73% in LoVo cells. Irradiation of mice bearing LoVo xenografts caused a 19 day tumour growth delay that could be extended to 37 days by the co-administration of AG14361. AG14361 was able to enhance topotecan-induced growth inhibition in A549 cells, SW620 cells and LoVo cells and delay tumour growth in mice bearing LoVo and SW620 tumour xenografts compared to those mice treated with irinotecan alone (for more details see section 1.8).

The combination of PARP-1 inhibitor, similar to AG14361 but with improved solubility, and temozolomide has recently reached Phase I clinical trials in Newcastle.

1.8 PARP-1 and Topoisomerase I: Background to this project

Previous studies have shown that PARP-1 inhibitors potentiate the cytotoxicity of topoisomerase I poisons (Bowman *et al.*, 2001). Here it was shown that NU1025 could potentiate the cytotoxicity of camptothecin 2 to 3-fold in murine leukaemic L1210 cells. This corresponded to a 2 to 3-fold increase in camptothecin-induced DNA single strand breaks. Similarly Calabrese *et al.*, (JNCI in press) demonstrated that the novel potent PARP-1 inhibitor AG14361 caused a 1.4 to 2-fold potentiation of the growth inhibitory effect of topotecan in human tumour cell lines. *In vivo* xenograft studies showed that the anti-tumour activity of irinotecan could be increased 2 to 3-fold by co-administration of AG14361. These studies are described in more detail in chapter 3 (See Figure 1.17, Calabrese *et al.*, JNCI in press).

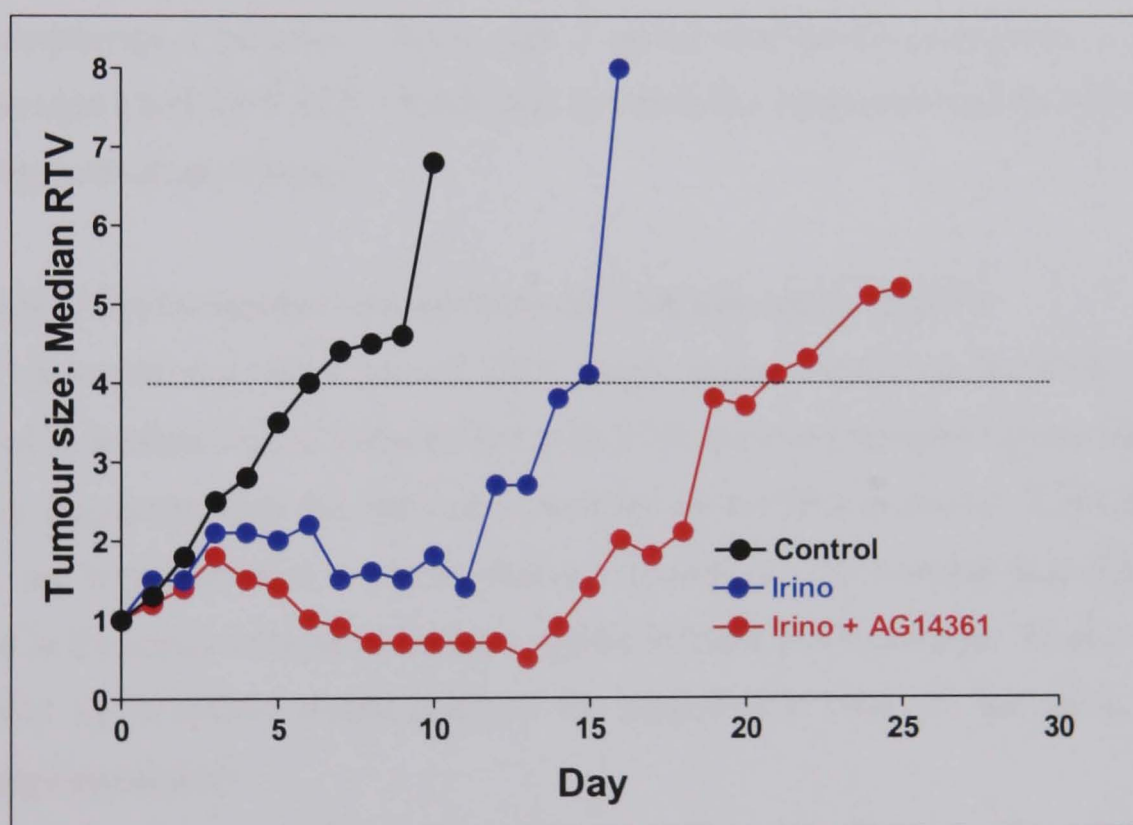
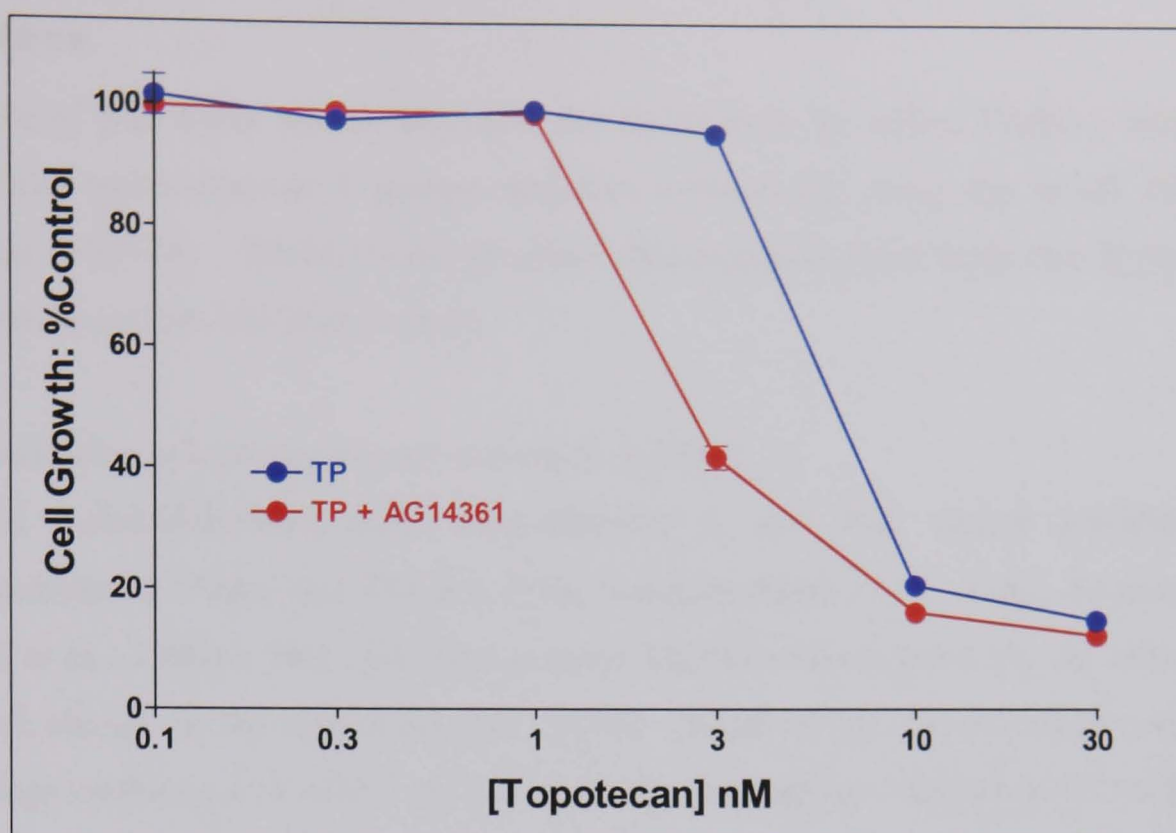


Figure 1.17 Effect of AG14361 on topo I poison-induced growth inhibition (A) and tumour growth delay (B).

(A) Effect of 0.4 μ M AG14361 on growth of SW620 cells treated with increasing concentrations of topotecan for 5 days continuously.

(B) Effect of AG14361 on growth of SW620 tumour xenografts following daily treatment for 5 days with 2.5 mg/kg irinotecan \pm 5 mg/kg AG14316.

Graphs provided by N. Curtin, personal communication.

1.9 Aims

The aim of this study was to elucidate the mechanism by which PARP-1 inhibition potentiates topoisomerase I poison-mediated cytotoxicity using the novel PARP-1 inhibitor AG14361. Based on the previous data available there were two hypotheses proposed to explain this phenomenon.

1. Modulation of topoisomerase I activity by PARP-1.

PARP-1 poly(ADP-ribosylates) topoisomerase I, and this causes inhibition of topoisomerase I (Ferro and Olivera 1984, Jongstra-Bilan *et al.*, 1983, Krupitza and Cerutti *et al.*, 1989). This inhibition is most likely to be mediated via an increase in negative charge on the topoisomerase I protein caused by the (ADP-ribose) polymers. Therefore inhibition of PARP-1 by AG14361 may release topoisomerase I from PARP-1 mediated inhibition, providing more cleavable complex formation and hence targets for topoisomerase I poisons. Since topo I poison-mediated cytotoxicity is directly related to topo I activity PARP-1 inhibition increases the cytotoxicity of topoisomerase I poisons by activation of topo I.

2. Repair of topoisomerase I poison-induced DNA damage by PARP-1.

PARP-1 is involved in the repair of DNA single strand breaks via the BER pathway (reviewed in section 1.6.7). Cells deficient in BER are hypersensitive to topoisomerase I poisons, suggesting that this damage is repaired by the BER pathway. Cells deficient in BER are hypersensitive to camptothecin. Therefore it is possible that PARP-1 is involved in the repair of topoisomerase I poison induced DNA damage. Thus inhibition of PARP-1 by AG14361 would result in the inhibition or delay of the repair thereby increasing cytotoxicity.

PARP-1 wild type and null cells were studied in addition to the use of AG14361. This determined whether inhibition of PARP-1 was equivalent to lack of PARP-1 and investigated the possibility that when PARP-1 was inhibited it may act as a poison, by binding DNA and preventing DNA repair.

The studies described in the following chapters were designed to test these hypotheses to investigate the effect of PARP-1 on topoisomerase I poison-induced cytotoxicity.

**PAGE
MISSING
IN
ORIGINAL**

Chapter 2

Methods.

2.1 Materials.

All reagents were provided by Sigma (Poole, Dorset, UK) unless otherwise stated.

AG14361 (1-(4-dimethylaminomethylphenyl)-8-9-dihydro-7H-2,7,9a-benzo[cd]azulen-6-one) was provided by Agouron/Pfizer Pharmaceuticals GRD, La Jolla, CA, USA. AG14361 was stored as powder at 4°C or as 10 mM stocks in DMSO at -20°C. AG14361 was used at 0.4 µM in all experiments unless otherwise stated.

Topo I poisons, Camptothecin (CPT, Sigma) and Topotecan (TP, Hycamptin© SmithKlineBeecham Pharmaceuticals Philadelphia, PA) were stored as powder at 4°C or as 10 mM stocks in DMSO at -20°C.

All radiolabelled compounds ([³²P]-NAD⁺, [³H]-thymidine and [¹⁴C]-thymidine) were supplied by Amersham (Bucks, UK). Wallac Optiphase HiSafe scintillant (Fisher Chemicals) was used with the radioactive samples prior to counting

Tissue culture media, supplements, antibiotics and trypsin were supplied by Invitrogen (Paisley, UK) unless otherwise stated.

2.2 Equipment.

All tissue culture plastic-ware was purchased from NUNC (Fisher Scientific, Loughborough, UK). Routine centrifugation was carried out using either a MSE Mistral 5000 bench topo centrifuge, or an Eppendorf centrifuge 5417R with 45-30-11 rotor depending on sample size (Fisher Scientific). The pH of buffers and solutions was measured using an Orion Model 420A pH meter (Fisher Scientific). A Titretek Multiscan MCC/340 (Flow Laboratories, Rickmansworth, UK) plate reader was used to measure the absorbance of XTT or SRB stains and BCA reagent in protein assays. Where samples were warmed or mixed a shaking water bath was used (Grant OLS200, Fisher Scientific). Perkin Elmer Lambda 2 UV Vis spectrophotometer was supplied by Perkin Elmer (Beaconsfields, Bucks UK). A Wallac 1409 DSA β-counter (Perkin Elmer) was used to measure levels of radioactivity in samples.

2.3 General Tissue Culture.

All cell lines were maintained at 37 °C in a humidified atmosphere containing 5% CO₂ in a Heraeus incubator (Heraeus, Essex, UK). All manipulation of cell lines was carried out using sterile equipment and reagents within a class II safety cabinet.

All cell lines were routinely tested for mycoplasma using an enzyme immunoassay (*Mycoplasma* Detection Kit, Roche Diagnostics, Sussex, UK) for the detection of the most common *mycoplasma/acholeplasma* species found in cell cultures. Testing was conducted at approximately 3 month intervals and the cells used in this study were found to be free of *mycoplasma* at all times.

2.3.1 Cryogenic Storage of Cell Lines.

Cells were kept in liquid nitrogen for long-term storage in the presence of DMSO. DMSO is a cryoprotective agent, which prevents the formation of ice crystals within the cells on freezing which would damage the cells. Cells were spun down at 1500 rpm for 5 mins and resuspended in freezing medium (DMEM or RPMI containing 10% (v/v) DMSO and 20% (v/v) foetal calf serum) to give a final concentration of approximately 1-2 million cells per ml. Cryovials containing 1 ml of cell suspension were then frozen at -80°C for ~24 hours before transfer into liquid nitrogen stores (-180°C). This slow freezing reduces the amount of damage sustained by the cell.

To retrieve cells from the frozen stocks the cells were thawed rapidly in a water bath, to 37°C, thus reducing the amount of damage to the cells. The cell suspension was then centrifuged, the medium was aspirated off to remove the DMSO, and the cells were resuspended in a large volume of fresh medium. The cells were then seeded into flasks at the appropriate cell density. Cell lines were passaged at least twice before they were used in any experiment to ensure that they were growing optimally.

2.3.2 Cell Lines.

PARP-1 wild type and null cell lines.

Immortalised PARP-1 wild-type and null mouse embryo fibroblasts (MEFs) cell lines were derived by isolation of embryos from the PARP-1 wild type and null mice by E. Notriani at the University of Newcastle upon Tyne using standard methodology (Robertson *et al.*, 1987) and continuous cell culture. PARP-1 wild type and null mice were kindly provided by Gilbert de Murcia (Ecole Supérieure de Biotechnologie de Strasbourg, France). Deletion of the PARP-1 gene was achieved by homologous recombination (Mennissier de Murcia *et al.*, 1997) (see Figure 2.1). It was found that whereas the PARP-1 null cells expressed wild type p53, the PARP-1 wild type cells expressed high levels of transcriptionally inactive mutant p53, which was the result of a

base change at codon 278 which corresponded to an Asp to Glu substitution. This mutation was found to be within a conserved region of the DNA binding domain of p53 (P. Jowsey PhD thesis, 2003).

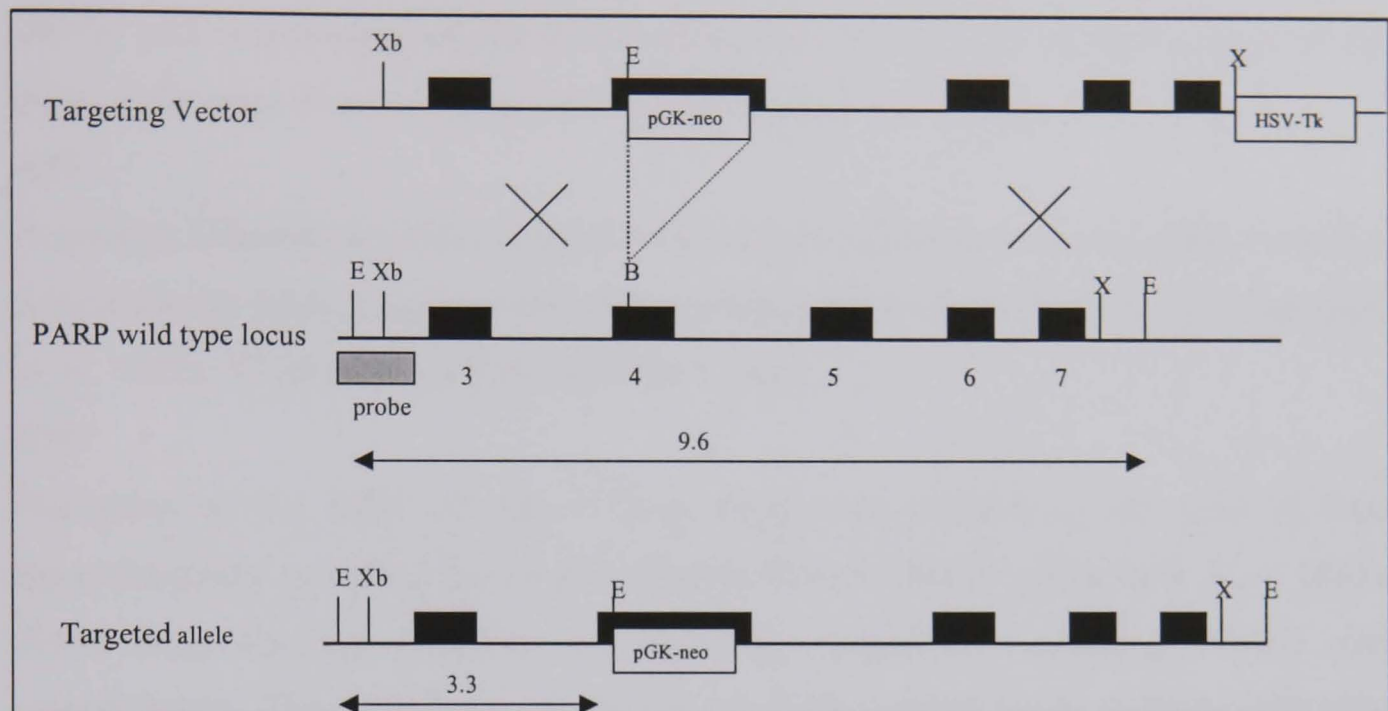


Figure 2.1 Inactivation of PARP-1 by homologous recombination.

Gene inactivation was achieved by insertion of PGK-*neo* into the fourth exon of the PARP-1 gene. EcoRI (E) restriction was used to detect the targeted gene as indicated. (B, BamHI; X, XhoI; Xb, XbaI; pG-neo, neomycin-resistance gene driven by the pGK promotor; HSV-Tk, thymidilate kinase gene driven by the herpes simplex virus promoter). Diagram adapted from Menissier de Murcia *et al.*, (1997).

PARP-1 null^{TR}

PARP-1 null^{TR} cells are PARP-1 null cells that have been re-transfected with human PARP-1, to create a PARP-1 wild-type cell line that expresses wild-type p53. PARP-1 null cells were transfected with the pPARP31 plasmid using FuGENE 6. These cells were also co-transfected with a plasmid containing a neomycin resistance gene, to enable selection of transfectants. These PARP-1 null^{TR} cells have been shown to express PARP-1 protein, which was activated in response to DNA double strand breaks. This activity could be inhibited by AG14361. Southern blotting was used to show that the original PARP-1 gene was still inactivated, by the presence of the 3.3 kb fragment (data not shown, P.Jowsey PhD thesis 2003).

K562.

The K562 cell line is an erythroleukaemic line derived from pleural effusion of a 53 year old female Caucasian with chronic myelogenous leukaemia. (Lozzio and Lozzio, 1975). p53 is homozygously deleted in these cells via an N-terminal truncation of the gene. Cells were obtained from the ATCC (Manassas VA, USA).

AA8.

A parental Chinese hamster ovary cell line that was isolated as a spontaneous clone that is functionally heterozygous at the adenine phosphoribosyltransferase locus (Thompson *et al.*, 1980). Cells were obtained from the ATCC.

EM9.

Derivative of the AA8 cell line. These cells were isolated on the basis of their hypersensitivity to killing by ethyl methanesulfonate (EMS) (Thompson *et al.*, 1980). These cells are hypersensitive to alkylating agents, UV radiation, X-rays and camptothecin. They also have a reduced rate of DNA-strand break rejoining following treatment with X-rays, EMS or methyl methanesulfonate (MMS), as well as a high baseline frequency of sister chromatid exchange compared to the parental AA8 cell line (Thompson *et al.*, 1982). It had been demonstrated that this hypersensitivity could be corrected by complementation with XRCC1, thus these cells were deficient in base excision repair (Thompson *et al.*, 1990). The gene coding for XRCC1 in the EM9 cells has been shown to contain a C to T base change in codon 221, which introduces a termination codon one third of the way into the sequence. This results in the expression of a truncated XRCC1, which does not contain either of the BRCT domains (Shen *et al.*, 1998). Cells were obtained from the ATCC.

V3.

Derivative of the AA8 cell line that does not express DNA-PKcs due to an inactivating mutation in the C-terminal region of one allele of the DNA-PKcs gene (XRCC7). This results in a deficiency in NHEJ (Blunt *et al.*, 1995). Cells were a kind gift from P. Jeggo, University of Sussex.

irs1SF.

A derivative of the AA8 cell line with a mutated XRCC3 gene. This results in inactivation of HR (Tebbs *et al.*, 1995). These cells have been shown to be hypersensitive to AG14361 (S Kyle, personal communication). Cells were a kind gift from T. Helleday, University of Sheffield.

2.3.3 Maintenance of cell lines.

PARP-1 mouse embryo fibroblasts (MEFs) were grown as monolayers in plastic tissue culture flasks. They were maintained in Dulbeccos Modified Eagle's medium containing non-essential amino acids and glutamine. This was supplemented with 10 % (v/v) foetal calf serum, 100 units/ml penicillin, 100 µg/ml streptomycin, 15 mM hepes and 1 mM sodium pyruvate.

K562 cells were grown as suspensions in RPMI 1640 plus L-glutamine, supplemented with 10 % (v/v) foetal calf serum, 100 units/ml penicillin, 100 µg/ml streptomycin.

AA8, EM9, V3 and IRS1SF cell lines were maintained as monolayers in RPMI 1640 plus L-glutamine supplemented with 10 % (v/v) foetal calf serum and 100 units/ml penicillin, 100 µg/ml streptomycin.

All cell lines were passaged twice a week or when 80% confluent.

2.3.4 Subculture of cell lines.

K562 suspension cells were subcultured by dilution of a volume of cell suspension in fresh medium to maintain the culture at a density of between 1×10^5 and 1×10^6 cells/ml, up to passage ~25.

Monolayer cell lines had to be removed from the tissue culture dishes prior to subculture or use in cell assays. To achieve this the medium was aspirated from the cells and the cells were washed in Dul A (Dulbecco's Phosphate Buffered Salts, modified without Ca^{2+} and Mg^{2+}). An appropriate volume (enough to cover the cells) of 0.25% trypsin in DulA/EDTA (0.02% (w/v), disodium salt) was added and the cells were incubated at 37°C until the cells had detached from the plate. Fresh medium was added to neutralise the trypsin and dilute the cell suspension to the desired cell density.

2.3.6 Cell counting.

To enable the seeding of the cells at known cell densities the number of cells in a suspension was measured using a haemocytometer or a Coulter counter.

Haemocytometer.

A haemocytometer consists of two mirrored counting chambers on a glass slide. A coverslip is placed on to the haemocytometer to form a counting chamber with a depth of 0.1 mm. The chamber is divided into 9 x 1 mm² squares. Therefore the volume of each square is 1 x 10⁻⁴ ml. Cell suspensions can be added to this chamber using a pasteur pipette, and cells counted under a microscope (Olympus CK2 Microscope). By counting the cells seen in the 1 mm² squares and taking the dilution factor into account the number of cells in the original suspension can be calculated using the equation below.

$$\text{Mean cell count per 1mm}^2 \text{ square} \times \text{dilution factor} = \text{cells/ml} \times 10^4$$

Coulter Counter.

In clonogenic and cell counting assays a Coulter counter was used to determine cell numbers. The Z1 Coulter counter (Beckman Coulter, Bucks) is an electronic cell counter. Cells were firstly fixed in an equal volume of Carnoys fixative (75% methanol, 25% acetic acid (v/v)). The fixed cell suspension was then diluted 1/10 in Isoton (Becton Dickinson, Oxford, UK) and transferred to the counting chamber of the Coulter counter. Electrolyte is drawn through a small orifice, across which a current passes. The entrance of a cell into the aperture, displaces its own volume of electrolyte and modulates the current flowing between two electrodes across the aperture. The machine detects this as a voltage pulse that is proportional in height to the volume of electrolyte displaced and therefore cell size. Voltage pulses are counted by the machine to give an accurate determination of cell number. Aperture size can be altered to account for differences in cell size and was used at 8-24 µm for the cells used in this study. Using this aperture size gave reproducible cell counts that were consistent with those obtained using a haemocytometer.

2.3.7 Determination of cell doubling time.

To measure cell doubling times cells were harvested and diluted into suspensions that contained 200, 500, 1000, 2000, 5000 and 10000 cells/ml. These were seeded into rows on seven 96-well plates. At 24 hour intervals a plate was fixed and growth was measured using the SRB assay, or XTT assay described in the next section. Absorbance values obtained from the assays were plotted against time using GraphPad Prism

software (San Diego CA, USA) and the doubling time of the cells calculated using linear regression on the exponential part of the plot.

2.4 Growth inhibition and cytotoxicity assays.

A variety of methods were used to assess the growth inhibitory and cytotoxic effects of drugs on cells. The choice of which assay to use was determined by the cell type, i.e. whether monolayer or suspension and the desired biological endpoint. The assays base their determination of growth on the amount of protein bound to a plate, cell number, metabolic activity or cell viability. As cytotoxic agents may prevent growth but may or may not affect cell viability it is important to use more than one type of assay to determine the effect of the drug on the cells.

In preparation for all of these assays, cells were seeded into dishes at a known cell number that did not become confluent during the course of the experiment and were therefore growing exponentially throughout the period of drug exposure. Monolayer cells were seeded a day before drug exposure to allow the cells to adhere to the plates. Cells were exposed to various concentrations of camptothecin or topotecan in the presence or absence of 0.4 μ M AG14361; control cells were exposed to an equivalent concentration of DMSO to account for any growth inhibitory effects of DMSO. The final concentration of DMSO in an experiment was always less than 1% to prevent any growth inhibitory effects of DMSO from interfering with drug effects. In some experiments the drug was removed from the cells after a period of time and cells were washed with Dul A. Specific details of each experiment are included in figure legends.

2.4.1 Sulforhodamine B (SRB) assay.

Staining with SRB is a rapid, sensitive and inexpensive method for measuring cellular protein content of adherent cells. SRB is an aminoxanthene dye that binds basic amino acid residues under acidic conditions; this is reversible under alkali conditions allowing quantification of the dye. Therefore absorbance of SRB measured at 570 nm is directly proportional to the amount of cellular protein in the well. This method has limitations in that an increase in cell size in response to a drug could be interpreted as an increase in cell number, and therefore is only accurate as long as the cell size remains constant (Skehan *et al*, 1990).

Cells were seeded and exposed to drugs as required. After the desired time, usually corresponding to 3 cell doublings, cells were fixed with 50% (w/v) trichloroacetic acid (TCA), and cooled at 4°C for at least 1 hour. The medium was removed and the plates washed five times in water, then dried at 60°C. Plates were then stained in 0.4% (w/v) SRB dissolved in 1% (v/v) acetic acid and left for 20 mins before washing in 1% (v/v) acetic acid and drying at 60 °C. Stain was solubilised using 10 mM Tris base (pH 10.5) before reading on a Titretek Multiscan MCC/340 plate reader at 570nm.

Average absorbance values were obtained for each drug treatment and expressed as a percentage of the related untreated or AG14361-treated control. Growth inhibitory IC₅₀ values (GI₅₀, the concentration that results in 50% growth inhibition) were calculated using a point to point curve on GraphPad Prism software. The potentiation factor (PF), a measure of the increase in growth inhibition in the presence of AG14361, was also calculated as stated below.

$$PF_{50} = \frac{GI_{50} \text{ drug alone}}{GI_{50} \text{ drug} + AG14361}$$

2.4.2 XTT cell proliferation assay.

This assay determines the growth and viability of cells using a tetrazolium salt that is metabolised by mitochondrial dehydrogenases in active cells to form a spectrally different formazan salt. The conversion of the yellow XTT to the orange formazan dye therefore only occurs in viable and metabolically active cells (Scudiero *et al.*, 1988). This assay was used for determination of cell doubling times of suspension cells.

Cells were exposed to drugs for the required duration. The XTT assay was conducted as instructed using the Cell Proliferation Kit II (Roche Diagnostics, GmbH). The XTT reagent (1 mg/mL) was mixed with the electron-coupling reagent (phenazine methosulfate) at a ratio of 50/1 (v/v). 50 µl of the XTT reagent mixture was added to each well of the 96-well plate and incubated in a humidified atmosphere for 4 hours at 37°C, 5% CO₂ to allow the dye to be metabolised. The 4 hour incubation time had been previously optimised for use with the K562 cells by A. Jobson, CAMB, University of Newcastle upon Tyne. The absorbance was then read on a Titretek Multiscan MCC/340

spectrophotometer at 450 nm. To determine doubling times the mean absorbance for each cell density was plotted against time and doubling time calculated using linear regression on the exponential part of the plot using GraphPad Prism software.

2.4.3 Cell counting.

Growth inhibition can be measured by counting the number of cells present after the drug treatment and comparing this with untreated control. This assay does not give a measure of the viability of these cells, just the number of cells. This assay was most suitable for use with suspension cells. Cell lines were treated and left to grow for the desired period of time, then fixed using an equal volume of Carnoys fixative (75% methanol, 25% acetic acid, (v/v)). The fixed cell suspensions were diluted 1 in 10 in Isoton, before a 1 ml sample was counted in duplicate using a Z1 Coulter counter (Beckman Coulter, Bucks) as described in section 2.3.6.

Mean cell numbers for each sample were calculated and expressed as a percentage of an untreated or AG14361-treated control. GI₅₀ values were calculated using the GraphPad Prism software as described in section 2.4.1.

2.4.4 Clonogenic survival assay.

Clonogenic assays measure the cytotoxicity of a drug i.e. cell kill. Some agents may cause cytostatic effects, inhibiting cell growth, however the cells still remain viable and are able to reproduce when returned to drug-free medium, therefore these agents do not necessarily kill the cell. As the clonogenic assay involves drug exposure followed by a long colony forming period in drug free medium this assay exclusively measures cell viability. This assay also allows the measurement of very low levels of cell survival e.g. at much higher concentrations of drug than the growth inhibition assays, as greater numbers of cells can be exposed and seeded to account for several orders of magnitude of cell kill (reviewed in Brown and Boger-Brown, 1999).

Following drug exposure, monolayer cell lines were trypsinised and then counted by Coulter counter as described in section 2.3.6. The cells were diluted in fresh medium to give a suspension of 1×10^4 cells/ml. The cells were then seeded at low densities onto 60 mm dishes (100 and 200 cells for controls and increasing to 10,000 for the highest drug concentrations). This ensured that there were cells surviving to form colonies at each

dose level. The plates were grown for 7 days for AA8, EM9 and V3 cell lines and 10 days for irs1SF cells.

When colonies were visible they were fixed using Carnoys fixative, and then stained with 0.4% (v/v) crystal violet in water. Colonies containing more than 30 cells were counted. Plates containing less than 10 colonies or over 300 colonies were not included. Each colony is assumed to be derived from a single cell and therefore the colony count is an estimate of the number of cells that survived the drug treatment. The plating efficiency of the cells was calculated as the percentage of colonies formed on the plates compared to the number of cells originally seeded. The clonogenic survival of drug treated-cells was calculated as the plating efficiency of treated cells expressed as a percentage of the plating efficiency of the DMSO alone or AG14361-treated controls. Mean percent survival curves were plotted and LC₅₀ values (concentration that results in 50% cell kill) calculated using GraphPad Prism software using a point to point curve plot.

2.4.5 Sloppy agar clonogenic survival assay.

The sloppy agar technique enables clonogenic assays to be performed with cells that grow in suspension e.g. K562 rather than monolayers. The cells are trapped in an agarose matrix to hold the cells in suspension allowing colony formation without migration through the gel. To visualise the colonies in the gel the tetrazolium dye MTT (methylthiazolotetrazolium) is used. MTT is a yellow dye that is reduced to a blue formazan by mitochondrial reductases in the cell in viable cells. The blue colonies can then be counted to determine cell survival.

K562 cells were treated, counted and diluted to a cell density of 1×10^4 cells/ml as described in the clonogenic assay (section 2.4.4). Using this suspension a known number of cells was transferred into 8 ml polyurethane tubes. Three cell densities were used per drug concentration, typically in the range of 100-200 for controls and up to 10000 at the highest drug concentrations. The cell suspension was then made to 1 ml with fresh medium and then to a final volume of 7 mls with 0.15% SeaKem ME agarose firstly diluted in PBS, then diluted in pre-warmed RPMI to give a final concentration of 0.125% agarose. The tubes were mixed by inversion, cooled to room temperature to allow the agarose to set and the lids loosened, and holes punctured in them to allow gas

flow. The tubes were then incubated at 37°C in a humidified atmosphere for 10-12 days to allow colony formation.

When colonies were visible the cell suspensions were poured out of the tubes into dishes containing 1 ml freshly prepared MTT (0.5 mg/ml in sterile water). Cells were left to stain overnight in the dark at 37°C in a humidified atmosphere. Survival was measured by colony counting. Only dishes containing greater than 10 and less than 300 colonies were counted. Mean percent survival was calculated as described in section 2.4.4.

2.5 SDS-polyacrylamide gel electrophoresis and Western blotting.

This is a method that can be used to visualise proteins in a cell extract. Proteins are separated on the basis of size by running them through a SDS-polyacrylamide gel. The proteins are then transferred to nitrocellulose under the influence of an electrical current. The protein of interest can be detected using antibodies specific for that protein followed by the use of the appropriate horseradish peroxidase-conjugated (HRP) secondary antibody. Enhanced chemiluminescence (ECL) can then be used to visualise the presence of the protein on X-ray film. The band corresponding to the protein of interest can then be quantified if desired using densitometry.

2.5.1 Sample preparation.

Preparation of Whole cell lysates.

Cells were grown to 80% confluence before being lysed by addition of SDS lysis buffer (6.25 mM Tris HCl pH 6.8, 2% SDS, 10% glycerol) and harvested by cell scraping. The lysate was sonicated for 10 seconds using a MSE Soniprep Sonicator 150 (Fisher Scientific) and heated to 90°C for 5 mins. If the lysates were still sticky after this, the procedure was repeated to ensure that all of the cells were lysed.

Preparation of Nuclear extracts.

For the detection of topo I protein nuclear extracts were prepared. This was recommended by TopoGen (Colombo OH), the suppliers of the topo I antibody, in order to achieve the best results with their product. $1-2 \times 10^7$ cells were required per sample. The medium was decanted from exponentially growing cells and washed with TD buffer (100 mM NaCl, 20 mM KCl, 0.5 mM Na₂HPO₄, 20 mM Tris). The cells were

then scraped into 2 ml TD buffer and then spun at 1000 xg for 10 mins at 4°C. The supernatant was discarded and the pellet was resuspended in 2 ml Buffer A (100 mM NaCl, 50 mM KCl, 0.1 mM EDTA, 20 mM Tris-HCl, pH7.5, 0.1 mM PMSF, 10% Glycerol, 0.2% NP-40, 0.1% Triton-X 100). The extract was then incubated on ice for 10 mins. The nuclei were then pelleted by centrifugation at 1000 xg for 10 mins at 4°C. The supernatant was then discarded and the nuclei resuspended in 180 µl Buffer A. The extracts were inspected for nuclei under the microscope. Finally 20 µl 10 % SDS was added to the nuclei. Following this the extracts were sonicated and heated as for whole cell extracts.

BCA Protein assay.

To determine the amount of protein in each sample therefore enabling equal amounts of protein to be loaded onto the gel, a protein assay was conducted on all samples. The Pierce BCA Protein Assay Kit (Pierce, Rockford IL) was used. This assay is based on the reduction of Cu^{2+} to Cu^{1+} by protein in an alkaline medium (Biuret reaction). BCA (bicinchoninic acid) chelates with the Cu^{1+} in a ratio of 2:1 to form a purple reaction product. The absorbance of this product can be measured on a spectrophotometer at 560 nm. To conduct the assay a standard curve of known concentrations of BSA (0.125-2 mg/ml) is set in quadruplicate on a 96-well plate. Samples are applied to the plate in quadruplicate, these may be diluted 1/10 in lysis buffer if necessary. The BCA reagent was mixed in a ratio of 25:1 reagent A to reagent B and 200 µl added to each well. The plate was incubated at 37°C for ~30 mins. The absorbance of the wells was measured at 560 nm on a plate reader. Protein concentration was calculated by comparison to the standard curve and correction for the dilution of the samples.

The cell lysates were diluted in the relevant buffer (SDS lysis buffer or TD buffer) to the desired protein concentration and 5% (v/v), 0.5% (w/v) bromophenol blue and 5% β-mercaptoethanol were also added. Samples were heated to 80°C for 5 mins to allow reduction of the protein and ensure that the samples were homogeneous.

2.5.2 Electrophoresis.

Samples and molecular weight markers (SeeBlue Pre-Stained Standard; Invitrogen, Paisley, UK) were loaded onto 5-20% Tris-glycine SDS-PAGE pre-cast gels (Invitrogen). Typically between 20 and 50 µg protein was loaded per sample. 5 µl pre-

stained markers were added to provide a ladder of molecular weight standards to aid identification of the protein. Gels were run at 120-200V for 1-1.5 hours in Tris-Glycine running buffer (25 mM Tris, 200 mM Glycine 0.1% SDS) in a NOVEX Mini cell gel rig (Invitrogen) and a Bio-Rad PowerPac 300 (BioRad, Herts UK).

2.5.3 Western blotting.

The proteins were transferred to nitrocellulose membrane (Hybond C, Amersham, Bucks, UK) in transfer buffer (25 mM Tris, 100 mM Glycine, 20% Methanol) at 30V overnight, using a Bio-Rad Mini Protean II Blot Module. The membrane was then blocked in 5% (w/v) dried milk in TBS Tween (50 mM Tris, 150 mM NaCl, with 0.05% Tween 20 added on day of use) for 1 hour. The antibodies used in this thesis are described in Table 2.1. The primary antibody was applied to the membrane diluted 1/1000 in 5% milk in TBS Tween and mixed for at least an hour using a Roller mixer SRT1 (Stuart Scientific, UK). The membrane was washed three times in TBS Tween before application of the appropriate secondary antibody, at 1/1000 dilution, in 5% milk (as above). These were mixed for 1 hour as above. The membrane was washed in TBS Tween for at least one hour with frequent changes of TBS Tween to reduce non-specific binding of the antibody. Proteins were detected using an ECL kit (Amersham) or Pierce SuperSignal West Pico Chemiluminescent Substrate (Pierce) depending on the protein being detected. The ECL reagent was added to the membrane for the required length of time and the excess removed. The membrane was then exposed to Fuji Medical X-ray film Super RX for a number of exposure times to ensure that the protein bands are visible. The film was then developed using a Fuji X-ray film processor RGII. Equal loading of the membrane was determined either by re-probing the membrane with anti-actin antibody AC-40 (DAKO, Ely, UK), or by staining with Ponceau S.

Densitometry.

Bands that were visible on a film were quantified using densitometry. A Fuji LAS-3000 camera (Raytech, Milton Keynes, UK) was used and data obtained using AIDA version 3.28 according to manufacturers instructions. The density of the protein band was given in arbitrary units.

Antibody	Details
Topo I	Polyclonal anti-human topo I isolated from Scleroderma patients (#2012) supplied by TopoGen.
PARP-1	Rabbit polyclonal anti PARP-1 (H-250) supplied by Santa Cruz Biotechnology , Santa Cruz, CA.
Actin	Mouse monoclonal anti-actin (AC-40) supplied by Sigma.
2° antibody to human 1° antibody	HRP-conjugated goat anti-human antibody supplied by Sigma.
2° antibody to rabbit 1° antibody	HRP-conjugated goat anti-rabbit antibody supplied by DAKO.
2° antibody to mouse 1° antibody	HRP-conjugated goat anti-mouse antibody supplied by DAKO.

Table 2.1 Antibodies used in this study.

2.6 PARP-1 activity assay.

This method measures PARP-1 activity stimulated by exogenously added DNA ends by the incorporation of [³²P]-NAD⁺ into acid insoluble ADP-ribose polymer using a modification of the method by Halldorsson *et al.*, (1978). The amount of radiolabel incorporated into the polymer is directly proportional to PARP-1 activity. This assay should only detect PARP-1 activity as a blunt ended double stranded oligonucleotide is used. PARP-2, another member of the PARP family that is stimulated in response to DNA strand breaks, is not stimulated by the type of DNA strand break represented by the oligonucleotide used here (G. de Murcia, personal communication). As the oligonucleotide used to stimulate PARP-1 and the NAD⁺ cannot enter intact cells, the cells were permeabilised prior to assaying for PARP-1 activity. In this study digitonin was used to permeabilise the cells.

2.6.1 Preparation of cells

Exponentially growing cells (approx. 15x10⁶/per treatment) were treated with various concentrations of AG14361 for 10 mins and harvested by trypsinisation where necessary (monolayer cultures). Cell suspensions were counted and pelleted by centrifugation as described in earlier sections. Cells were washed once in ice cold Dul A and then centrifuged at 15000 rpm for 5 mins at 4°C. Cells were resuspended in 0.15

mg/ml digitonin (Boehringer-Mannheim, Mannheim, Germany) in Dul A to a density of 3×10^7 cells/ml, and left on ice for 10 mins. Permeabilisation was stopped by addition of 9 volumes of isotonic buffer (40 mM Hepes, 130 mM KCl, 4% Dextran, 2 mM EGTA, 2.3 mM MgCl, 225 mM Sucrose pH 7.8; plus DTT to a final concentration of 2.5 mM added immediately prior to use). The extent of permeabilisation was verified by trypan blue exclusion; permeabilised cells take up the dye and this can be seen under the microscope. Cell counts were taken of each sample to allow calculation of the amount of NAD^+ incorporated per cell.

2.6.2 Preparation of radiolabelled NAD^+ .

An approximately 6 mM NAD^+ solution was prepared freshly on the day of assay. The exact concentration of this solution was calculated by measuring the OD of a 1/100 dilution of this stock solution at 260 nm in a 1 cm silica cell on a Perkin Elmer Lambda 2 UV Vis spectrophotometer (Molar extinction coefficient for NAD/NADH at 260 nm = 18000). The NAD^+ stock was then diluted to give a 600 μM NAD^+ solution. To this approximately 10 $\mu\text{Ci}/\mu\text{l}$ [^{32}P]- NAD^+ was added depending on the current specific activity of the radiolabel.

The oligonucleotide used in this assay was the palindromic sequence CGGAATTCCG synthesised by J Lunec (NICR, Newcastle upon Tyne). It was stored as a 200 $\mu\text{g}/\text{ml}$ solution in 10 mM Tris / EDTA pH 7.8 at -20°C .

2.6.3 Assay.

The reaction mixture containing a final concentration of oligonucleotide 2.5 $\mu\text{g}/\text{ml}$, 75 μM NAD^+ / [^{32}P]- NAD^+ , made to a final volume of 50 μl in water was prepared in 10 mL plastic test tubes (NUNC). The permeabilised cells were warmed to 26°C for 7 mins in a shaking water bath. 300 μl of pre-warmed cell suspension (3×10^6 cells/ml) was added at regular timed intervals to the pre-prepared reaction mixture. The tubes were vortexed and incubated at 27°C for 5 minutes with constant shaking. The reaction was stopped after 5 mins by the addition of 2 ml ice cold 10% trichloroacetic acid (TCA) (10 % (w/v) TCA, 10% (w/v) sodium pyrophosphate). 10% TCA was added to blanks prior to cell addition, this enabled correction for non-specific binding of radiolabel to the filter.

Samples were left on ice for at least an hour to allow precipitation of acid insoluble material including poly(ADP-ribosylated) proteins.

To separate the TCA-precipitated poly(ADP-ribosylated) proteins from the reaction mixture the samples were filtered through a Millipore filtration unit. Glass microfibre filters (GF/C 25mm; Whatman, Kent UK) were soaked in 10% TCA (as above) and placed rough side up on the filtration apparatus. Samples were applied to the filters and washed five times in 1% TCA (1% TCA, 1% sodium pyrophosphate) under gentle suction pressure, before they were air-dried. Filters were placed in 10 ml Optiphase HiSafe scintillant. Radioactivity on the filters was assayed using the Wallac 1409 DSA β -counter and counting for 2 minutes. Triplicate controls containing 5 μ l of 600 μ M NAD⁺/[³²P]-NAD⁺ in 10 ml scintillant were also counted.

2.6.4 Calculation of results.

The mean of the blanks was subtracted from the sample counts to remove non-specific background. The pmol NAD⁺ incorporated per sample was calculated by comparison with mean dpm of the standards (5 μ l of 600 μ M NAD⁺ is equivalent to 3000 pmol). This was then adjusted to account for the cell numbers in each sample, allowing the result to be given in the format pmol NAD⁺ incorporated/ 10^6 cells/5 mins.

2.7 Measurement of Topoisomerase I activity by DNA Relaxation.

Topoisomerase activity can be determined by measuring the relaxation of plasmid DNA. This measures the cleavage, unwinding and religation of DNA by topo I. The relaxation assay measures topoisomerase I activity by following the relaxation of negatively supercoiled DNA based on the different mobility of the supercoiled and relaxed plasmid DNA in agarose-gel electrophoresis. The assay is specific for topoisomerase I by virtue of omission of Mg⁺ and ATP from the assay which are required by other members of the topoisomerase family. To determine topoisomerase I activity, ATP is omitted because ATP is required for topoisomerase II activity. Exclusion of Mg⁺ from the assay buffer allows detection of type 1-3 enzymes (Stewart, 2000)

2.7.1 Preparation of nuclear extracts.

To ensure sufficient levels of protein in the cell preparation to allow quantification, 10^6 - 10^7 cells were used per sample. Following drug treatment the cells were pelleted at 800 x g for 3 mins at 4°C and resuspended in 3ml ice-cold TEMP buffer (10 mM Tris-HCl pH 7.5, 1 mM EDTA, 4 mM MgCl₂, 0.5 mM PMSF). This was repeated and the samples were then incubated on ice for 10 mins. Following this, cells were homogenised using a Dounce homogeniser. The cells were then inspected to ensure that nuclei were present under the microscope. The nuclei were then pelleted at 1500 x g for 10 mins in the cold and washed again in TEMP. The remaining pellet was resuspended in less than 4 pellet volumes of TEP buffer (TEMP without MgCl₂). An equal volume of 1 M NaCl was added and then the samples were left on ice for 30-60 mins. The samples were then centrifuged at 15000 x g for 15 mins 4°C. The supernatant was removed and used in the relaxation assay.

The protein concentration of each sample was determined using the Pierce protein assay as described in section 2.5.1, so that equal amounts of protein could be used in each reaction.

2.7.2 Relaxation Assay.

Each extract was diluted in TEMP buffer to give samples with a protein concentration of 0.1 µg/µl, this concentration had been shown to contain topo I activity in initial studies for this thesis. 1-8µl of sample extract or pure topoisomerase I (2 µl, TopoGen) was mixed with 2 µl R buffer (10 mM Tris-Cl, pH 7.5, 100 mM KCl, 1 mM PMSF and 1.0 mM β-mercaptoethanol, buffer supplied with pure topoisomerase I by TopoGen), 1µl negatively supercoiled PUC19 plasmid DNA (1 µg/µl) and made to a final volume of 20 µl with water. The reaction components were pooled by centrifugation. After incubation at 37°C for 30 mins the reaction was stopped with 1/4 volume of stop buffer (0.5% SDS, 0.1% bromophenol blue and 25% glycerol). The samples were then loaded onto an agarose gel (0.8% in TBE; 89 mM Tris borate, 20 mM EDTA, pH 8.0). The gel was run for ~3 hours. DNA on the gel was visualised by staining with 0.25 µg/ml ethidium bromide in TBE for 30-60 mins. A permanent image was visualised using a UV transilluminator and captured on camera with the GelDoc system. Supercoiled DNA has different mobility to relaxed DNA in agarose-gel electrophoresis; the

supercoiled DNA will travel further down the gel from the relaxed DNA as shown in Figure 2.2. Thus enzyme activity can be compared between samples.

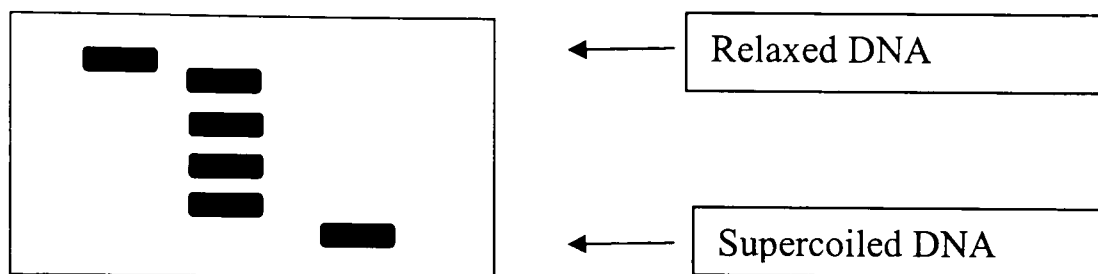


Figure 2.2 Relaxation of DNA as visualised on an agarose gel.

Relaxed DNA is less mobile than the supercoiled form therefore can be separated on a gel. Intermediate DNA species can be detected as the DNA unwinds as shown.

2.8 Trapped in agarose DNA immunostaining (TARDIS).

The TARDIS assay is an immunohistochemical method for the detection of drug-stabilised topoisomerase-DNA cleavable complexes with isoform specific antibodies in individual cells. This assay is an adaptation of the assay used by Frank *et al.*, (1996) for the detection of melphalan-DNA adducts in cells. It has been used to detect topoisomerase I and II α and β stabilised cleavable complexes in a number of cell lines formed in response to a wide range of topo I and II poisons. (Willmore *et al.*, 1998, 2002, Errington *et al.*, 1999, Padget *et al.*, 2000(a), 2000(b))

The TARDIS assay does not use fixing techniques and therefore avoids co-precipitation of proteins that may hinder the access of antibodies. It relies on the immobilisation of cellular DNA in agarose and subsequent lysis of the cell to leave the DNA and covalently associated proteins. As topo I is covalently bound to DNA in the cleavable complex and can be stabilised by camptothecin, levels of the stabilised cleavable complex can be detected by the use of an antibody specific for topoisomerase I, and an appropriate FITC-conjugated secondary antibody. DNA is detected using a fluorescent Hoechst stain. Image analysis allows the quantification of topo I-associated fluorescence associated with DNA corresponding to individual cells. This method is summarised in Figure 2.3.

2.8.1 Slide Preparation.

Following appropriate drug treatment, cells were harvested by centrifugation at 3000 rpm in an MSE Mistral 5000 centrifuge. 50 μ l of cell suspension was mixed with 50 μ l 2% (w/v) agarose ("Sea Prep" ultra low melting-point agarose; BMA Rockland, ME) in PBS. This was smeared onto slides that had been pre-coated with 0.5% (w/v) low melting point agarose in water. Slides were placed on ice briefly to solidify the agarose, prior to incubation in lysis buffer, (10% SDS, 0.5 M potassium phosphate, 0.5 M EDTA, plus protease inhibitors; 1 mM PMSF, 1 mM benzamidine, 2 μ g/ml leupeptin, 2 μ g/ml pepstatin, 1 mM DTT added immediately prior to use) for 30 mins at room temperature, to lyse the cells and remove the cell membrane and soluble proteins. The slides were then transferred into 1 M NaCl (plus protease inhibitors as above) for a further 30 mins to remove non-covalently bound nuclear proteins, leaving only the drug-stabilised topo I complexes. The slides were washed three times in PBS before addition of the primary antibody. To detect Topo I complexes a polyclonal human antibody to human topoisomerase I was used (#2012, TopoGen). For use it was diluted 1/1000 in PBS containing 0.1% (v/v) Tween 20 and 1% (w/v) BSA. Once the antibody had been added, the slides were incubated in a dark humidified atmosphere at room temperature for one hour. The slides were washed in PBST (PBS + 0.1% Tween 20 (v/v)) before addition of the secondary antibody in a dark humidified atmosphere at room temperature, for an hour. The secondary antibody was an FITC-conjugated goat anti-human immunoglobulin G (Fab specific) (Sigma). It was diluted 1/100 in PBST + 1% (w/v) BSA. After exposure to antibodies the slides were washed twice in PBST and once more in PBS. Immediately prior to visualisation the slides were stained with Hoechst 33258 (10 μ M in PBS) for 5 mins to stain the DNA. Coverslips were placed carefully onto each slide and secured using nail varnish.

2.8.2 Microscopy

A detailed description of the method for the microscopy and image analysis is described by Frank *et al.*, (1996). Hoechst (blue) and FITC (green) associated fluorescence were visualised separately using an epifluorescence microscope (Olympus BH2-RFCA, Technical Lamp Supplies Ltd, Slough, UK) and appropriate optical filters (Omega Optical, Brattleboro USA). Images were visualised using a 10x objective and captured using a cooled slow-scan charge-coupled device (CCD) camera (Astrocam, Cambridge,

UK). A field of view was focussed under a blue filter to visualise the DNA and the image was captured using a 5 second exposure. The same field of view was then captured using a green filter and a 20 second exposure. 6-8 pairs of images were captured per dose from replicate slides to obtain data from 100-150 cells.

2.8.3 Analysis of results

Images were analysed using Imager 2 software (Astrocam, UK) based on Visilog 4 (Neosis, France). The images were background corrected using slides containing PBS alone to correct for stray light and camera background. All of the sample images were subjected to blue and green shade correction to compensate for differences in the lamp intensity and non uniformities in light transmission using slides containing 3 μ M fluorescein and 0.4 mM 4-methylumbelliferone. The corrected blue Hoechst image was used to define the areas containing the DNA in each cell and create a binary image. A series of functions were performed to remove objects on the edge of the image and remove small particles. The blue and green fluorescence intensities corresponding to the area occupied by the DNA were integrated. The values stated are integrated fluorescence, which is defined as the number of pixels in the cell multiplied by the surface of the cell. Integrated fluorescence data for each cell was plotted as scatter plots. Mean fluorescence was also plotted using GraphPad Prism software.

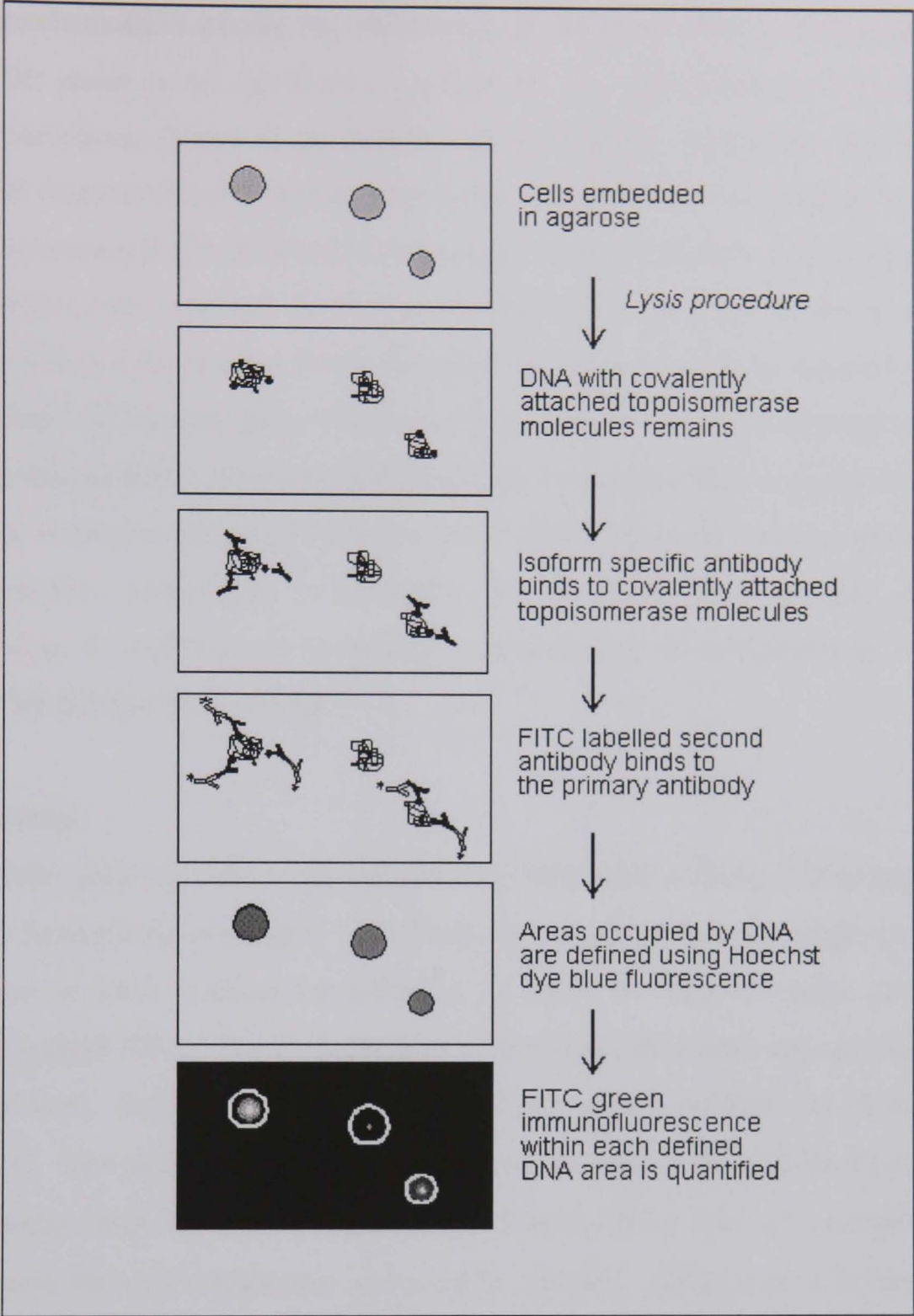


Figure 2.3 The TARDIS assay. Diagram from Padget *et al.*, (2000a)

2.9 Potassium-SDS assay for detection of enzyme-DNA complexes.

The K-SDS assay is an established method for the quantification of protein-DNA covalent complexes (Rowe *et al.*, 2000). The assay relies on the fact that SDS binds protein and dissociates non-covalent protein-DNA complexes but is unable to dissociate covalent interactions. On addition of potassium chloride insoluble crystals of potassium dodecyl sulfate form which co-precipitate free protein and protein covalently attached to the DNA. Using radiolabelled DNA, the levels of protein covalently bound to DNA can be quantified. As camptothecin stabilises the covalent complex formed between topo I and DNA this method enables the quantification of protein-DNA complexes formed in response to treatment with topo I poisons which will correspond to an increase in topo I-DNA cleavable complexes. Increases in the level of cleavable complexes corresponding to exposure to increasing concentrations of camptothecin, have been measured by Beidler *et al.*, (1996).

2.9.1 Assay.

Exponentially growing cells were radiolabelled with 0.04 $\mu\text{Ci/mL}$ [^{14}C]-thymidine (53 mCi/mol; Amersham) overnight. The label was removed by centrifugation and cells were grown in fresh medium for a further ~4 hours to chase the label into the high molecular weight DNA. Equal numbers of cells were treated with appropriate drugs for the desired time. Following drug exposure the cells were centrifuged at 1500 rpm for 5 mins at 4°C. The cells were lysed in 2 ml lysis solution (1.25% SDS (w/v), 0.4 mg/mL herring sperm DNA (Promega, Hants, UK), 5 mM EDTA (pH 8.0) heated to 65°C. This removes the cell membranes and soluble proteins. After a 10 min incubation at 65°C in a waterbath the KCl concentration was adjusted to 65 mM by addition of 352 mM KCl. The lysates were vortexed for 10 secs to fragment DNA. The lysate was cooled on ice for 10 mins to allow precipitation of the protein-DNA complexes, and then centrifuged for 10 mins at 10000g at 4°C. The pellet was resuspended in 1 ml wash buffer (10 mM Tris HCl, pH8.0, 0.1 mg/mL herring sperm DNA, 100 mM KCl, 1 mM EDTA) and heated at 65°C for 10 mins with occasional mixing by inversion to resuspend the pellet. The samples were then cooled on ice for 10 mins to allow precipitation. The precipitate was recovered by centrifugation as before. The wash step was repeated. The washed pellet was resuspended in water pre-heated to 65°C and

added to 5ml Optiphase HiSafe scintillant. Samples were counted on a Wallac 1409 DSA β -counter for 2 mins.

2.9.2 Calculation of results.

The average dpm for triplicate samples was calculated and then expressed as a percentage of the relevant controls.

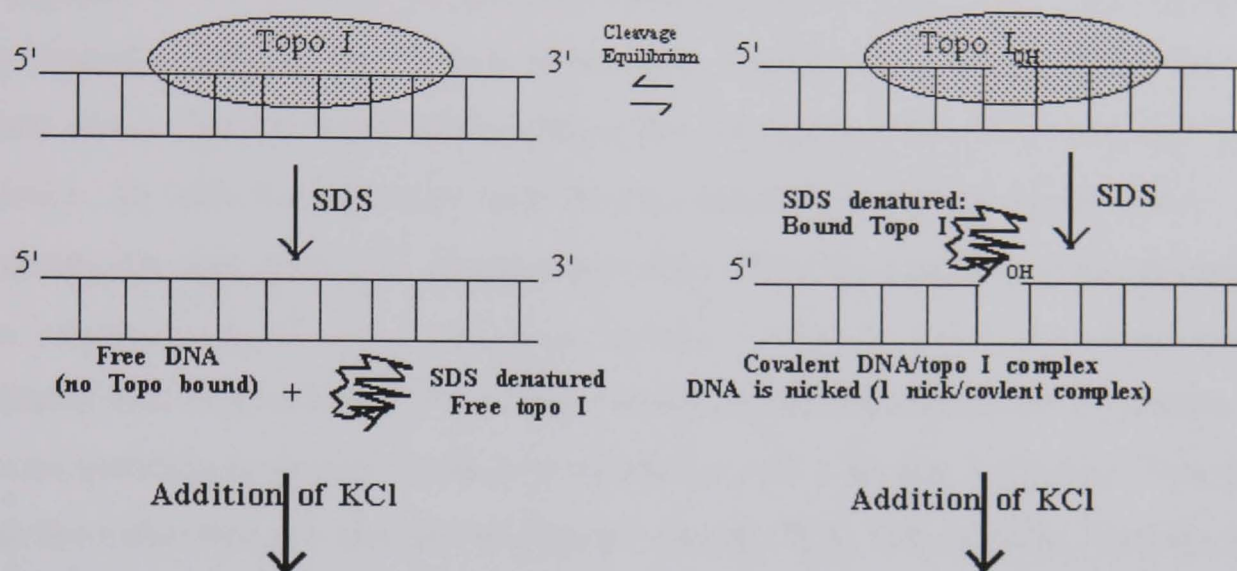


Figure 2.4. The potassium SDS assay.

Topo I binds to DNA covalently and forms a transient cleavable complex. On addition of SDS the topo I is denatured. Upon addition of KCL the SDS bound DNA is precipitated. Adapted from www.TopoGen.com.

2.10 Measurement of DNA single strand breaks by alkaline elution.

Alkaline elution provides quantitative analysis of DNA single strand breaks. Radiolabelled DNA from drug treated cells can be separated according to fragment size using polycarbonate filters which are neither protein or DNA adsorbent. This impedes the passage of larger DNA molecules allowing smaller ones to elute first. Therefore an increase in strand breaks will be signified by an increase in the rate of elution. Double strands of DNA are separated and apurinic/pyrimidinic (AP) sites are revealed by cleavage at high alkaline pH (pH 12.2), therefore revealing both single strand breaks and AP sites. In this study protein adsorption was minimised by the use of low protein adsorption polycarbonate filters, the presence of SDS in the lysis and elution buffer and using a lysis buffer containing proteinase K. Elution of the DNA fragments over time was measured by scintillation counting of eluted fractions. To increase the precision of

the assay the samples were co-eluted with an internal standard consisting of irradiated DNA. Comparison of the elution rate of the sample with the internal standard DNA enables correction for variation in pump channel efficiency (Kohn *et al.*, 1981).

2.10.1 Cell Preparation.

Cells were seeded at a density that ensured at least 4×10^5 cells per sample on the day of the experiment for both the sample and internal standard (IS) cells. Monolayer cells were seeded at least 24 hours prior to labelling so that they had adhered to the tissue culture dish. Sample cells were labelled for 24 hours with [^{14}C]-thymidine (0.016 $\mu\text{Ci/mL}$). IS cells were labelled with ^3H -Thymidine (0.1 $\mu\text{Ci/mL}$) for 24 hours. [^3H]-thymidine damages DNA to a greater extent than [^{14}C]-thymidine, therefore the samples were labelled with the least damaging isotope. After 24 hours the unincorporated radiolabel was removed from the cells by changing the medium on the monolayer cells and resuspending suspension cells in fresh medium for a further 2-4 hours. This was to chase the radiolabel into the high molecular weight DNA, thus ensuring that any strand breaks that were detected were in the mature DNA.

Sample cells were treated as described in figure legends and control cells were treated with equivalent concentrations of DMSO. Cells were kept on ice to prevent repair and in the dark to prevent accumulation of further damage that may be caused by lighting etc, prior to elution.

Prior to elution the IS cells were irradiated using a Gammacell 1000 elite irradiator (Nordion International Inc, Kanata, Canada) with a dose of 3 Gy to give uniform strand breaks in these cells.

2.10.2 Preparation of Filters.

Polycarbonate filters (2.0 μm pore size, 25 mm diameter, Whatman) were moistened in ice-cold PBS (1/10 dilution of 10x PBS without magnesium) and placed shiny side up onto 25 mm Swinnex polyethylene filtration funnels (Fisher Scientific). A rubber gasket was applied to the filter before the top was screwed into place to prevent leakage. Foil was wrapped around the barrel to prevent light penetration that could lead to further DNA damage. 50 ml syringe barrels were attached to the Swinnex apparatus. Cold

PBS was passed through the apparatus to ensure an even flow of liquid and air locks were removed. When there was ~10 ml PBS remaining in the barrel the flow was stopped using a clip. The apparatus was kept at 4°C until use.

2.10.3 Elution

Equal numbers of cells (usually 4×10^5) from both the sample and IS cells were added to the PBS remaining in the barrels of the filter apparatus, at 4°C, in subdued lighting. The samples were allowed to drip freely through the apparatus. When all of the liquid had passed through, the syringe barrels were removed and the filters were washed twice with lysis buffer (69 mM SDS, 25 mM EDTA pH 10). The flow was stopped and the funnels filled with lysis buffer containing 0.5mg/ml proteinase K (Roche Diagnostics) and left for 1 hour at room temperature. Lysis of the cells removed the cell membranes and proteins bound to DNA. The filters were washed with 20 mM EDTA (pH 10) before being attached to elution apparatus via silicone tubing running through a peristaltic pump (Watson Marlow 205S, Watson Marlow, Falmouth, UK) to a fraction collector (LKB 2211 Superfrac Pharmacia LKB Technology, Sweden). The swinnex apparatus was topped up with elution buffer (2 mM EDTA-acid form, 1 M tetrapropylammonium hydroxide (tetP), pH 12.0 with tetP and the syringe barrels reattached and filled with 30 ml elution buffer. The pump was set at 2 ml/hr and the fraction collector set at 90 min/fraction with 9 fractions per sample. The fractions were collected into scintillation vials containing 15 ml scintillant.

2.10.4 Processing of filters

When the filters had eluted the tubes were washed with 0.4 M NaOH. The filters were removed from the apparatus, and put into scintillation vials containing 0.4 ml 1 M HCl and baked for an hour at 60°C. This depurinates the DNA. To neutralise the acid, 2.5 mL of 0.4 M NaOH was then added to the filter for a further hour at room temperature to convert the apurinic sites into strand breaks and thus fragmenting the DNA. Scintillant was then added and the tubes capped and shaken. The radioactivity in the vials was then counted using the liquid scintillation counter. Samples were counted for 60 seconds to detect ^{14}C and ^3H .

2.10.5 Calculation of results and relative elution.

For each sample the total amount of radioactivity applied to the filter was calculated by addition of the counts from the individual fractions. The number of counts remaining on the filter after elution of each fraction was calculated and then converted into the fraction of the counts remaining. Values were calculated for both the sample and the IS cells and plotted on a double log scale with reverse x-axis for fraction ³H retained and standard y axis for fraction ¹⁴C retained. Relative elution, i.e. the ratio of the rate of elution of the DNA after treatment compared with untreated control, as shown in Figure2.52.5 was calculated as described by Fornace and Little (1977) using the equation below. To calculate the RE the relative retention (RR) is required; this is the fraction of sample DNA retained when 50% of the IS DNA has been eluted. The RR can be calculated using GraphPad Prism software.

Relative elution = [log Control RR – log sample RR]

RR : Relative retention

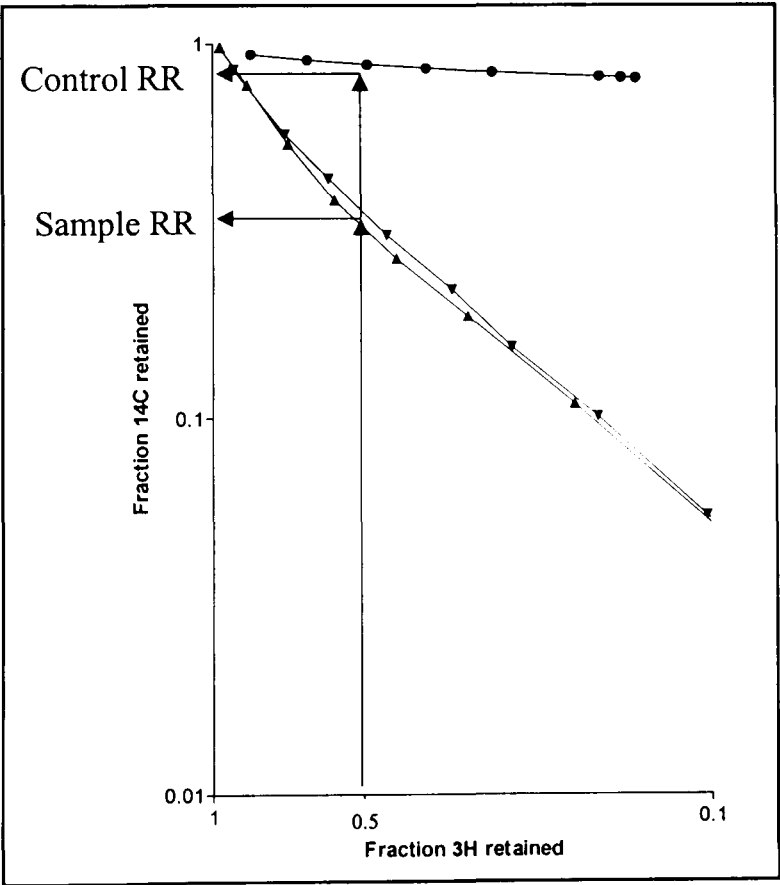


Figure2.5 Sample Elution Plot.

2.11 Statistical analysis.

All experiments were repeated at least three times unless other wise stated and generally contained duplicate samples within the experiment, unless other wise stated. Mean and standard errors were calculated using Microsoft Excel software. The Student's 2-tailed

t-test was used to determine statistically significant differences between data sets. In this study p values at the 95% confidence level are given unless otherwise stated. A paired test was conducted if the two sample sets were paired i.e. a series of identical experiments with treated and controls within the same experiment e.g. K562 cells treated with camptothecin alone compared to K562 cells treated simultaneously with camptothecin + AG14361 in each of three independent experiments. An unpaired t-test was used to determine the difference between cell lines in unrelated experiments.

**PAGE
MISSING
IN
ORIGINAL**

Chapter 3

**Effect of PARP-1 inhibition on topoisomerase I
poison-induced cytotoxicity in cells.**

3.1 Introduction.

The effect of PARP-1 inhibition on topo I poison-mediated cytotoxicity was described in an early study by Mattern *et al.*, (1987). This study showed that pre-incubation with 5 mM 3-AB for 16 hours increased the cytotoxicity of camptothecin approximately 1.5-fold (LD_{50} camptothecin = 0.3 μ M, camptothecin + 3-AB = 0.2 μ M). These data corresponded to an increase in the number of protein-linked DNA strand breaks and single strand breaks. This study also showed that a 60 min incubation with 3-AB prior to exposure to camptothecin had no effect on cytotoxicity. Therefore this has shown that PARP-1 inhibition could enhance topo I poison-mediated cytotoxicity, but only under certain conditions. From this study it was proposed that 3-AB exerted its effect by blocking the poly(ADP-ribosylation) of topo I, thus increasing topo I activity in the cell.

Potential of topo I poison-mediated cytotoxicity by 3-AB has also been described by Beidler *et al.*, (1996). In this study camptothecin resistant and revertant cell lines derived from the human nasopharyngeal KB cell line were used. The resistant KB cells were established by exposure to increasing concentrations of camptothecin for 8 months, when resistant clones were isolated. The partial revertant line was established by culturing the resistant cells in camptothecin-free media for 5-6 months. The resistant cells were shown to be 32 to 54-fold resistant and the revertant cells were 2.5 to 3.2-fold resistant compared to the KB cell line depending on the concentration of camptothecin used in the establishment of the cell line. This was not due to the down-regulation of topo I protein expression or activity, as the levels of protein and topo I activity were similar in both resistant and revertant lines. It was shown that incubation with 1 mM 3-AB for 4 hours increased camptothecin-induced cytotoxicity 6-fold in the resistant cell line but not the parental or revertant KB cell lines, implicating a role for PARP-1 in camptothecin resistance. A subsequent study by Park *et al.*, (2002) showed that levels of the BER scaffold protein XRCC1 were 5-fold higher in the resistant cell line although levels of other BER proteins including PARP-1 remained unchanged. The increased level of XRCC1 was related to the degree of resistance in the cell and potentiation by PARP-1 inhibition. These authors demonstrate that revertant cells that had been transfected with XRCC1 at similar levels as the resistant cell lines were 2-2.5 fold more resistant to camptothecin and that 3-AB could reverse this resistance. This

suggests that the role of PARP-1 in camptothecin resistance may involve the BER pathway.

Conclusions drawn for studies using 3-AB are compromised by the lack of specificity of 3-AB. 3-AB has been shown to interfere with other cellular processes such as *de novo* purine biosynthesis as well as inhibiting PARP-1 (Milam *et al.*, 1986). Therefore more specific and potent PARP-1 inhibitors have been used to try to clarify the role of PARP-1 in the response to cytotoxic drugs (see section 1.7).

6-[5H]-phenanthridinone is a potent PARP-1 inhibitor that was originally shown to have PARP-1 inhibitory activity along with a range of other compounds, by Banasik *et al.*, (1992). Phenanthridinone is an isoquinalone derivative that has been studied in conjunction with a range of cytotoxics including camptothecin in a panel of cell lines. 6-[5H]-phenanthridinone was shown to enhance the antiproliferative activity of SN-38, the active metabolite of irinotecan (Weltin *et al.*, 1997). However, this inhibitor was found to act differently depending on the tumour or cell line used (see section 1.7).

As many of the early PARP-1 inhibitors lacked specificity and potency, there has been increased interest in developing novel PARP-1 inhibitors. The Experimental Therapeutics group at the University of Newcastle upon Tyne has developed a number of more specific and potent compounds, as described in section 1.7. One of these inhibitors, NU1025, has been studied in combination with camptothecin in L1210 cells (Bowman *et al.*, 2001). Exposure to 200 μ M NU1025 potentiated the cytotoxic effects of a 16 hour exposure to camptothecin by 2.1 to 2.5-fold. This potentiation of cytotoxicity by NU1025 was shown to correlate to a 2.5-fold increase in the level of DNA single strand breaks. The ability of camptothecin-induced strand breaks to activate PARP-1 was also measured. Concentrations of 120 nM and 1 μ M camptothecin caused significant activation of PARP-1. These data demonstrated that PARP-1 was involved in topo I-mediated cytotoxicity, most probably through increased DNA strand breakage as PARP-1 was activated by camptothecin-induced damage and inhibition of PARP-1 enhanced levels of strand breaks and cytotoxicity.

Delaney *et al.*, (2000) investigated the effect of NU1025 and another more potent PARP-1 inhibitor, NU1085, in combination with topotecan in a panel of human cell lines. The cell lines used were representative of the 4 most common malignancies; lung, breast, ovary and colon and had varying p53 status. It was found that NU1085 potentiated topotecan-mediated cytotoxicity by 1.5 to 4 fold in 11 out of 12 of the cell lines. There was only one cell line that was not potentiated (LS147T; ovarian) but this cell line was already extremely sensitive to topotecan. The cytotoxicity of these drugs was also studied by colony formation in 3 of the cell lines (LoVo, A549 and OAW-42). These cell lines gave results consistent with the growth inhibition data. Taken together these data suggest that inhibition of PARP-1 can potentiate the growth inhibitory effects of topotecan independently of cell type or p53 status.

More recently a range of even more potent PARP-1 inhibitors have been developed using a combination of structure activity relationships and crystal-based drug-design (Canan-Koch *et al.*, 2003, Skalitzky *et al.*, 2003. A range of benzimidazole-4-carboxamides and tricyclic lactam indoles with Ki values of less than 10 nM have been screened for their effect on topotecan induced growth inhibition by Calabrese *et al.*, (2003). In this study it was found that cellularly active compounds could elicit a 2-fold potentiation of growth inhibition caused by topotecan.

Following this study, a related PARP-1 inhibitor, the tricyclic benzimidazole AG14361, was investigated, in combination with topotecan in three human tumour cell lines. Potentiation of topo I poison-induced growth inhibition was determined by SRB assay following 5 day exposure to topotecan with and without at 0.4 μ M AG14361. AG14361 potentiated the growth inhibitory effect of topotecan in LoVo (colon carcinoma), SW620 (colon carcinoma) and A549 (NSCLC) by 1.7, 1.4 and 2 fold respectively. 0.4 μ M AG14361 is < 5% GI₅₀ in these cells, therefore was not growth inhibitory, and did not alter gene expression, but did inhibit PARP-1 by greater than 85% (Calabrese *et al.*, JNCI in press).

In vivo studies in mice bearing human xenografts showed that co-administration of AG14361 increased the antitumour activity of irinotecan 2 to 3-fold without a detectable increase in whole animal toxicity. In mice bearing LoVo tumour xenografts, 2.5 mg/kg

irinotecan daily for 5 days caused tumour growth delay of 4 days. Co-administration of AG14361 at 5 or 15 mg/kg AG14361 increased the tumour growth delay to 9 days or 11 days respectively. Similarly, in mice bearing SW620 xenografts the irinotecan-induced tumour growth delay of 8 days was increased to 14 or 16 days by co-administration of AG14361 at 5 or 15 mg/kg (Calabrese *et al.*, JNCI in press).

Another potent PARP-1 inhibitor CEP-6800 ($K_i = 5$ nM) has been used *in vitro* and *in vivo* in combination with topo I poisons. 1 μ M CEP-6800 was shown to potentiate the cytotoxicity of camptothecin in HT-29 colorectal tumour cells *in vitro* (Miknyoczki *et al.*, 2003). *In vivo* studies were conducted using irinotecan resistant HT-29 human colon carcinoma xenografts in nude mice. Treatment with irinotecan or CEP-6800 alone had no effect on tumour growth delay. However combination of irinotecan (10 mg/kg) and CEP-6800 (30mg/kg) resulted in a 38% reduction in tumour volume compared to irinotecan alone, starting on day 19 extending to day 33, with a maximum tumour volume reduction of 66%.

PARP-1-deficient cells have also been used to examine the effect of PARP-1 on topo I poison-mediated cytotoxicity. Cells deficient in PARP-1 activity have been shown to be hypersensitive to topo I poisons. PARP-1 deficient cells have been derived from V79 Chinese hamster cells by exposure to increasing concentrations of MNNG. The strategy behind this was based on the ability of PARP-1 activation to cause cell death by depletion of NAD^+ and ATP in response to high levels of DNA damage. Therefore the cells isolated from colonies surviving this treatment, called ADPRT 54 and ADPRT 351, were deficient in PARP-1 and displayed between 5-11% PARP-1 activity compared to parental V79 cells. These cell lines were approximately 3-fold hypersensitive to exposure to camptothecin for 1 hour, the LC_{50} values for ADPRT 54 and 351 being 0.4 and 0.6 μ M respectively, compared to 1.5 μ M for the parental V79 cells (Chatterjee *et al.*, 1989, Chatterjee *et al.*, 1990). The process of selection that these cells underwent was harsh and may have caused other defects apart from the PARP-1 deficiency, particularly considering the doubling time for these cells is >72 hours. Such a long doubling time may alter the response to S-phase acting drugs such as camptothecin although the cells would be more likely to be resistant to camptothecin.

However, despite the limitations of this model system, this is still one of the original demonstrations of hypersensitivity to camptothecin of PARP-1 deficient cells.

More recently three strains of PARP-1 knockout mice have been created by homologous recombination and cell lines have derived from them. PARP-1 null mice with disruptions in exons 1, 2 or 4 of PARP-1 have been created (Masutani *et al.*, 1997, Wang *et al.*, 1995 and Menissier de Murcia *et al.*, 1997, respectively). Using the mice created by the de Murcia laboratory, it has been shown that a single i.p. dose of 140 mg/kg irinotecan killed 64% of the PARP-1 null mice after just 2 weeks. In comparison, none of the wild-type mice were affected, even 8 weeks after exposure to the drugs (de Murcia and Shall, 2000). As these mice were rendered PARP-1 null by homologous recombination, it can be assumed that this is the only defect in the mice and therefore their hypersensitivity to camptothecin is linked to their lack of PARP-1.

3.2 Aims.

The aim of this chapter was to investigate the effects of PARP-1 inhibition by AG14361 on topo I poison-mediated growth inhibition and cytotoxicity in PARP-1 wild type, PARP-1 null and the K562 human leukaemic cell lines. The differential sensitivity of PARP-1 wild type and null cells in response to exposure to the topo I poison, topotecan, alone was investigated. This was to confirm previous studies with PARP-1 inhibitors showing that loss of PARP-1 activity results in increased sensitivity to topo I poisons. The differential effect of AG14361 on topo I poison-induced cytotoxicity in PARP-1 wild type compared to null cells was also investigated. This was to confirm that the potentiation of topo I poisons is due to PARP-1 inhibition rather than some unrelated effect of the inhibitors; therefore showing the specificity of AG14361 for PARP-1.

The effects of PARP-1 inhibition on camptothecin-induced growth inhibition and cytotoxicity were investigated in the K562 cell line. The K562 cells were used as a model system as these cells have been previously characterised for their response to camptothecin (Padget *et al.*, 2000a). In order to conduct further studies presented in later chapters, the levels of sensitivity to camptothecin and the degree of potentiation induced by AG14361 in these cells was determined. Camptothecin was used instead of topotecan as it has a near identical mode of action as topotecan, cost implications and its abundant use in cell culture based studies allowing direct comparison with the literature.

3.3 Results

3.3.1 Characterisation of cell lines.

A number of cell lines were obtained for this study. PARP-1 wild type and PARP-1 null mouse embryo fibroblasts (MEFs) were established by E. Notriani (University of Newcastle upon Tyne) derived from PARP-1 $-/-$ mice and their wild type counterparts provided by G de Murcia; CNRS Strasbourg (Menissier de Murcia *et al.*, 1997 (for further details see section 2.3). Human chronic myelogenous leukaemia K562 cells (Lozzio and Lozzio 1975) were provided the ATCC (Manassas VA). Prior to conducting experiments using these cell lines a number of parameters needed to be established.

3.3.1.1 Determination of cell doubling time.

Determination of doubling times was carried out so that cells could be seeded at densities that did not become confluent during the course of the experiment and to ensure that cells were growing exponentially at the time of drug exposure. This was essential due to the strong S-phase specificity of camptothecin (D'Arpa *et al.*, 1990). Doubling times for cells were determined as described in section 2.3.7. Briefly, 96-well plates were seeded with cells at a range of cell densities. Growth of monolayer cells was determined by fixing the cells with TCA and staining with SRB and measuring absorbance of SRB at 570 nM as described previously by Skehan *et al.*, (1990) (see section 2.4.1). Growth of suspension cells was measured using the XTT Cell Proliferation Kit by measurement of absorbance of XTT at 450 nM (see section 2.4.2). Doubling times were calculated from the exponential part of the growth curve using GraphPad prism (see section 2.3.7). Representative growth curves for PARP-1 wild type and null cells and K562 cells are shown in Figure 3.1 and Figure 3.2 respectively. These results showed that the optimal seeding densities for 5 day exposures were 1000 and 2000 cells/ml for K562 and PARP-1 MEF cells respectively, as wells seeded with 5000 and 10000 became confluent and those seeded with 200 and 500 grew slowly. Doubling times for PARP-1 wild type, PARP-1 null and K562 cells are shown in Table 3.1. Previously published data on doubling times of the K562 cells suggest a 19.6 hour (NCI website http://dtp.nci.gov/docs/misc/common_files/cell_list.html) or 23 hour (Kanofsky and Sima 2000) doubling time for these cells, consistent with data presented here. PARP-1 cells that have been isolated from the same strain of PARP-1 wild type

and null mice as the cells used here have been shown to double every 24 hours and 36 hours respectively (Trucco *et al.*, 1998). The doubling times for PARP-1 wild type cells used in this study agree with these published data, however the PARP-1 null cells used here grew faster. It must be noted that these are not the same cell line just similar cells derived from the same mice. Therefore slight differences in doubling times could be due to non-identical cell lines.

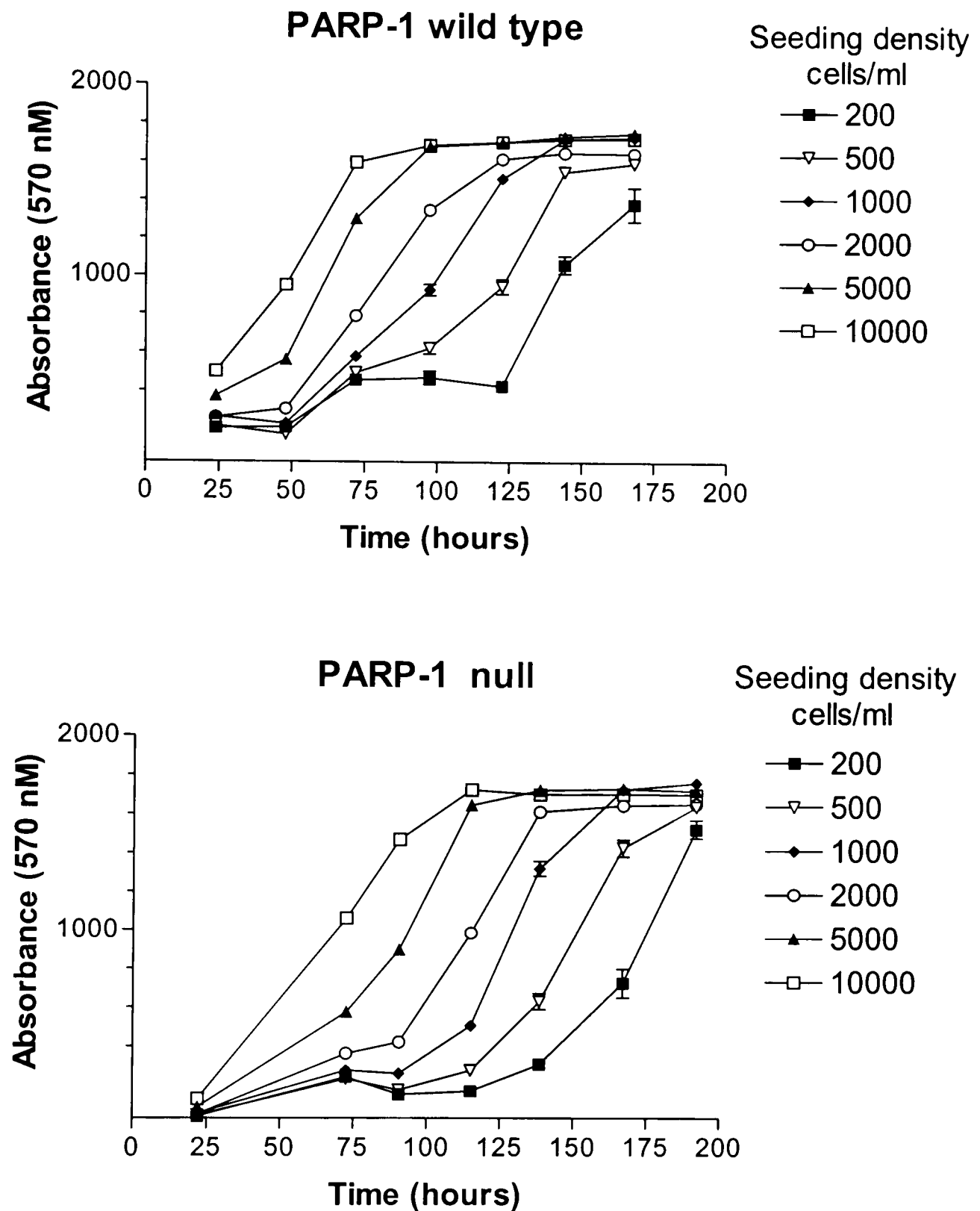


Figure 3.1 Growth curves for PARP-1 wild type and null cells.

Cells were seeded at 200, 500, 1000, 2000, 5000 and 10000 cells/ml in 96 well plates. Plates were fixed at 24 hour intervals and cell densities estimated using the SRB assay. Growth was measured by absorbance of SRB at 570 nM (See section 2.4.1). Representative growth curves for each cell line are shown.

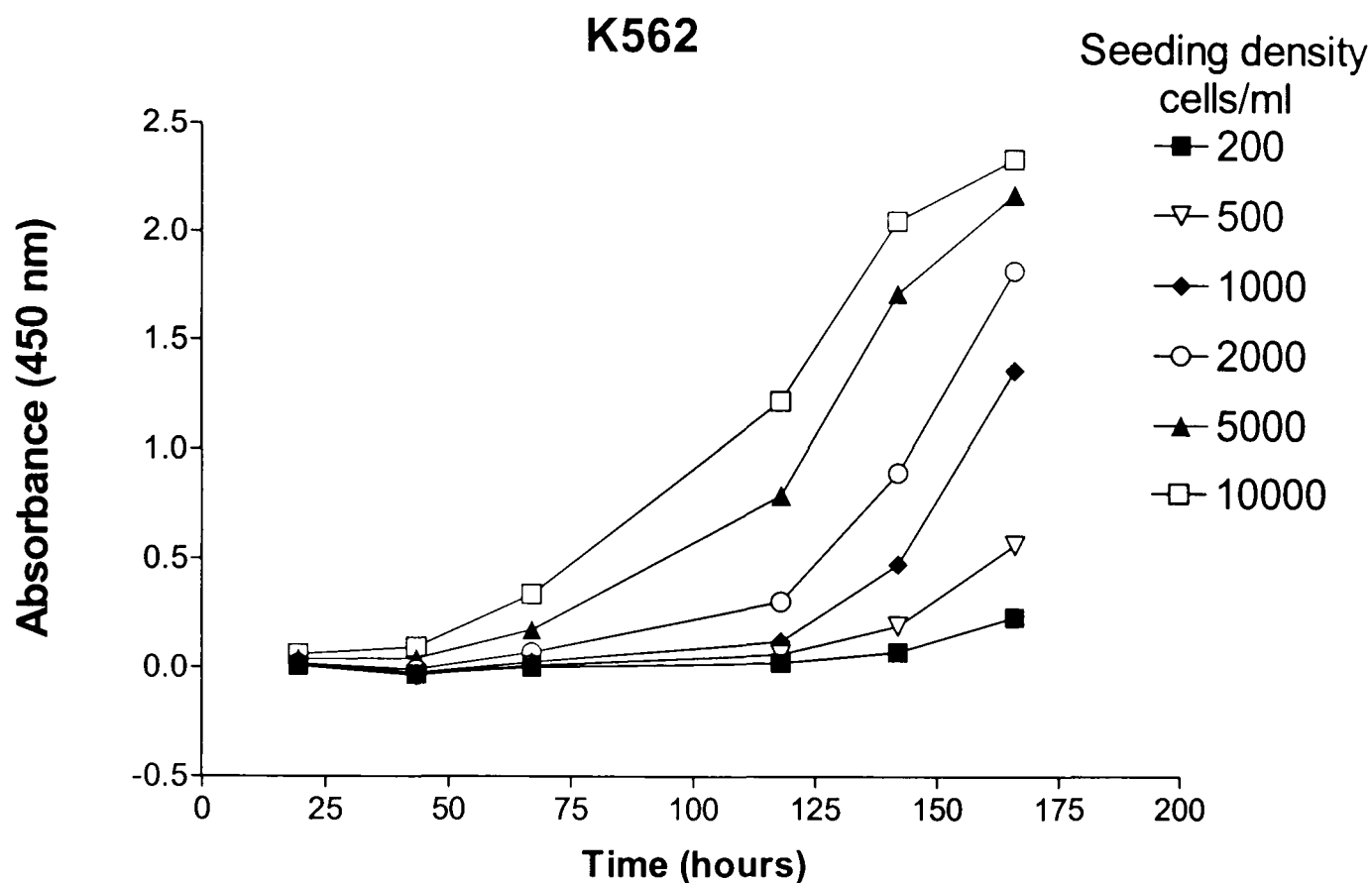


Figure 3.2 Growth curve for the K562 cell line.

Cells were seeded at 200, 500, 1000, 2000, 5000 and 10000 cells/ml in 96 well plates. XTT reagent was added at 24 hour intervals and left for 4 hours before measurement of absorbance of XTT at 450nm (see section 2.4.2). Representative growth curves are shown.

Cell Line	Doubling time (hours)
PARP-1 wild type	25.3 ± 1.9
PARP-1 null	26.6 ± 1.0
K562	20.2 ± 1.1

Table 3.1 Doubling times of cell lines.

Mean doubling times of cell lines determined from 3 independent growth curves per cell line ± SEM. Values were calculated as described in section 2.3.7

3.3.1.2 Drug Target Protein Levels.

Western blotting was used to determine the protein levels of the drug targets topo I and PARP-1, in exponentially growing, asynchronous cultures of K562 and PARP-1 MEF cell lines.

Topoisomerase I

Topo I protein levels in the cells were measured because a decrease in the expression of topo I protein has been described as a common mechanism of resistance to topo I poisons (Chang *et al.*, 1992, Tanizawa, *et al.*, 1993). Therefore, for the comparison of topo I poison-induced growth inhibition between cell lines was important to determine the levels of topo I protein in these cell lines. Topo I levels were determined in nuclear extracts prepared from PARP-1 wild type and null cells, by Western blotting using human anti topo I antibody #2012 (as described in section 2.5). Figure 3.3 shows that there were similar levels of topo I protein in the PARP-1 wild type and null cells. Multiple bands sometimes appeared and were due to protein degradation. The bands on the gel were quantified using a Fuji LAS-3000 camera and Aida version 3.28 as described in section 2.5.3. Using densitometry the topo I associated bands were shown to measure 10.0×10^5 and 9.5×10^5 arbitrary units for PARP-1 wild type and PARP-1 null cell lines respectively. Therefore there was no notable difference in topo I levels between these cell lines. A loading control is absent as a suitable protein for use with nuclear extracts could not be optimised. Equal loading was confirmed by Ponceau S staining of the membrane (data not shown).

PARP-1.

To determine the levels of PARP-1 in the PARP-1 wild type and null cells, whole cell extracts were prepared as described in section 2.5.1. Equal amounts of protein (30µg) from the extracts were run on SDS PAGE gels and blotted onto nitrocellulose prior to being probed with rabbit anti PARP-1 antibody (DAKO). Figure 3.4 shows the presence and absence of PARP-1 protein in PARP-1 wild type and null cells respectively, an actin loading control is also shown.

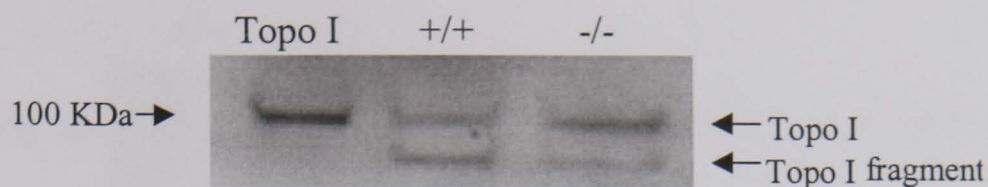


Figure 3.3 Topo I protein levels in PARP-1 wild type (+/+) and null (-/-) cells.

20 μ g nuclear extract from each cell line was loaded/lane. Presence of topo I was determined by Western blotting (see section 2.5). Human polyclonal anti topo I primary (#2012, TopoGen) and HRP-linked anti-human secondary (Amersham) were used. Purified topo I is shown to enable identification of the protein band. Equal loading was confirmed using Ponceau S stain (not shown). All bands are topo I and its degradation products. A typical blot is shown.

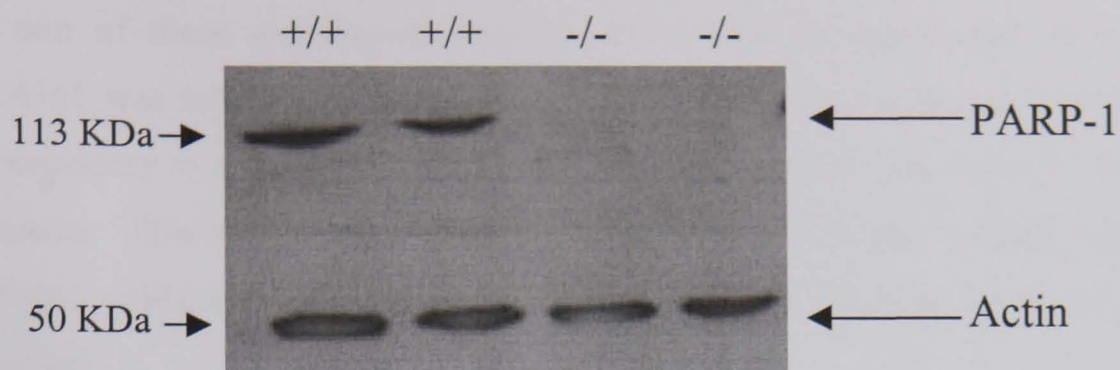


Figure 3.4 PARP-1 protein levels in PARP-1 wild-type (+/+) and null (-/-) cells.

30 μ g protein from whole cell lysates was loaded per lane in duplicate. Western blotting was conducted according to section 2.5. Blots were probed with anti PARP-1 (rabbit polyclonal anti-PARP-1 (H-250) antibody (Santa Cruz Biotechnology) and monoclonal anti actin (AC-40; Sigma) and the appropriate secondary antibody.

3.3.2 Investigation of growth inhibitory effects of AG14361

The aim of these experiments was to ensure that an appropriate concentration of AG14361 was selected for subsequent studies. For chemopotential experiments it was necessary to use AG14361 at a non-toxic concentration that had no intrinsic growth inhibition. This would ensure that any enhancement of topo I poison cytotoxicity by AG14361 could not be attributed to additive AG14361-induced cytotoxicity or growth inhibition.

In a previous study on the chemo and radio-potentiating effects of AG14361, growth inhibition assays were conducted using a concentration of 0.4 μ M AG14361 inhibitor (Calabrese *et al.*, JNCI in press). AG14361 was not growth inhibitory to PARP-1 wild type or null cell lines at concentrations below 10 μ M AG14361 (Figure 3.5 Calabrese *et al.*, 2003, JNCI in press). 0.4 μ M AG14361 therefore potentially represents a concentration that has maximal PARP-1 inhibition with little or no growth inhibition. For the purposes of this study it was important to verify that 0.4 μ M was also a suitable concentration for use in K562 cells.

In order to confirm that AG14361 was not growth inhibitory at the concentrations used in chemopotential studies, exponentially growing K562 cells were exposed to increasing concentrations of AG14361. K562 cells were exposed to AG14361 for 16 hours to correspond with exposure period used in chemopotential assays used later in this chapter. Growth inhibition was determined by cell counting (section 2.4.3). Figure 3.6 shows that AG14361 did not significantly inhibit the growth of K562 cells at 0.4 μ M ($p = 0.2$ paired t-test compared to untreated cells) and indeed significant growth inhibition was not observed below 10 μ M AG14361. Thus 0.4 μ M was confirmed to lack growth inhibitory activity per se. However, it was also important to confirm that this concentration of AG14361 inhibited PARP-1 activity in the cell lines under investigation.

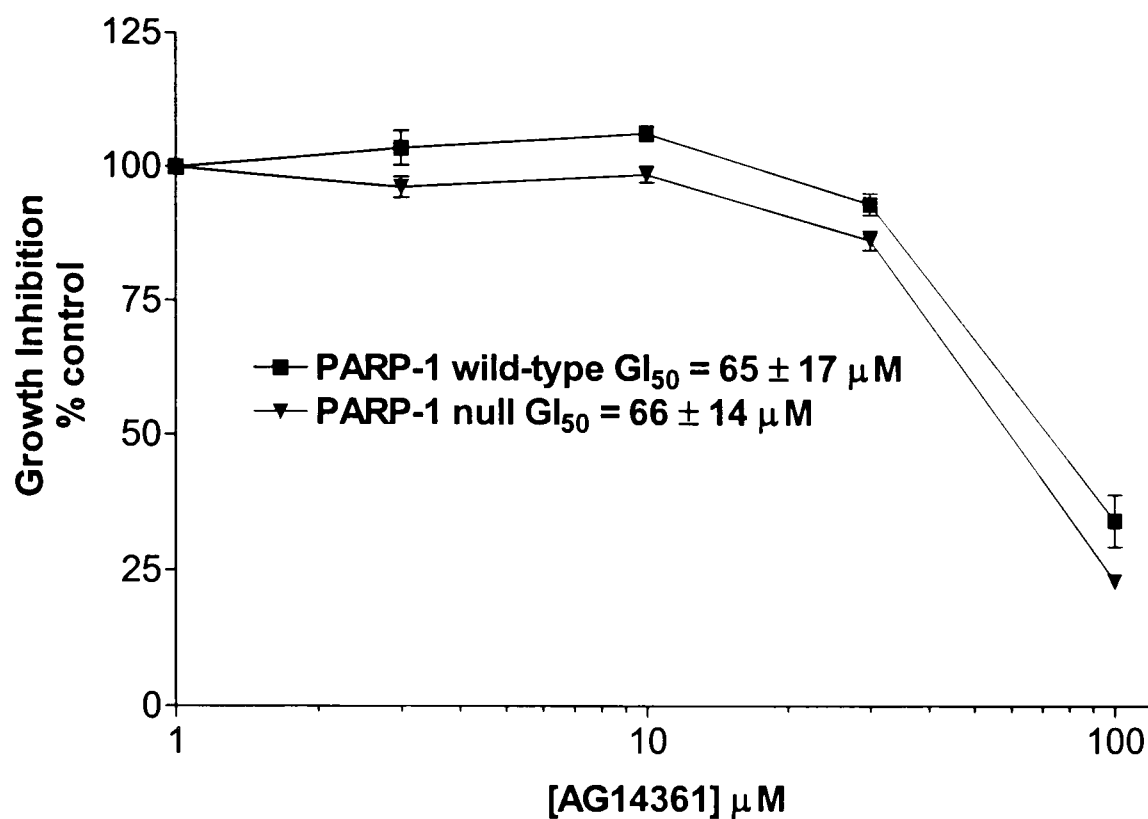


Figure 3.5 Effect of AG14361 on growth of PARP-1 wild type and null cell lines.

Cells were exposed to 0, 1, 3, 10, 30 or 100 μM AG14361 for 5 days. Growth inhibition was measured by SRB assay, section 2.4.1. Data are the mean of 3 independent experiments \pm SEM, IC_{50} values are the mean of individual IC_{50} values from each experiment (Calabrese *et al.*, JNCI in press).

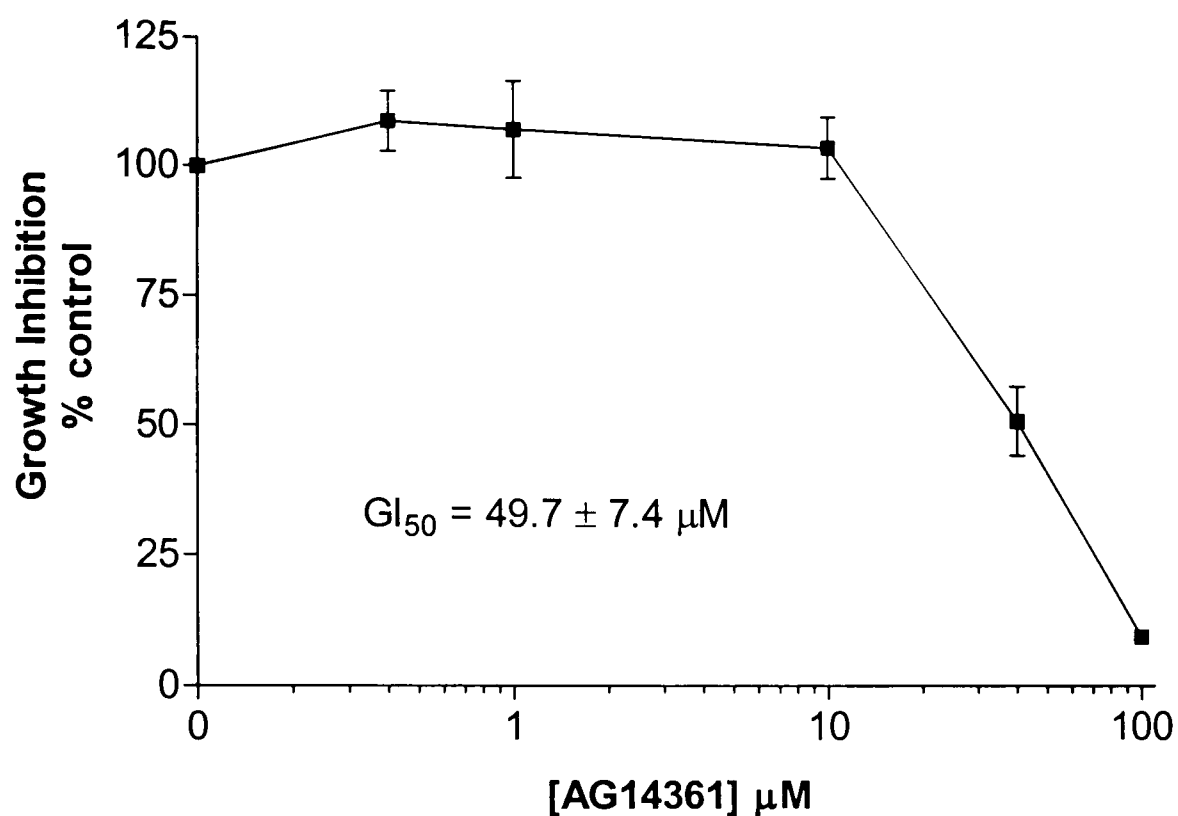


Figure 3.6 Effect of AG14361 on growth of K562 cells.

K562 cells were exposed to 0, 0.4, 1, 10, 40 or 100 μM AG14361 for 16 hours followed by 5 days growth in drug free medium. Cells were then fixed and growth inhibition was measured by cell counting as described in section 2.4.3. Data was expressed as a percentage of a DMSO-treated control. Data are the mean of 3 independent experiments \pm SEM.

3.3.3 Investigation of PARP-1 inhibitory effects of AG14361.

To ensure that PARP-1 activity is sufficiently depleted by 0.4 μ M AG14361 in the cell lines used, PARP-1 activity was measured as described in section 2.6. Briefly, cells were pre-treated for 10 mins with a range of concentrations of AG14361 before permeabilisation and assaying for PARP-1 activity. This methodology ensures that any inhibition observed was caused by inhibitor that had been transported into the cells. The permeabilised cells were incubated with [32 P]-NAD and an oligonucleotide to stimulate PARP-1. Incorporation of radiolabel into acid-insoluble ADP-ribose polymers was measured by scintillation counting. Figure 3.7 shows that 0.4 μ M AG14361 reduced PARP-1 activity in K562 cells by $90 \pm 0.07\%$. A summary of PARP-1 activity data for PARP-1 wild type, null and K562 cell lines is given in Table 3.2. In the PARP-1 wild type cells 0.4 μ M AG14361 was sufficient to reduce PARP-1 activity to less than 5% of normal activity. PARP-1 null cells were found to have ~10% PARP-1 activity, possibly due to PARP-2, and this could be fully inhibited by 0.4 μ M AG14361

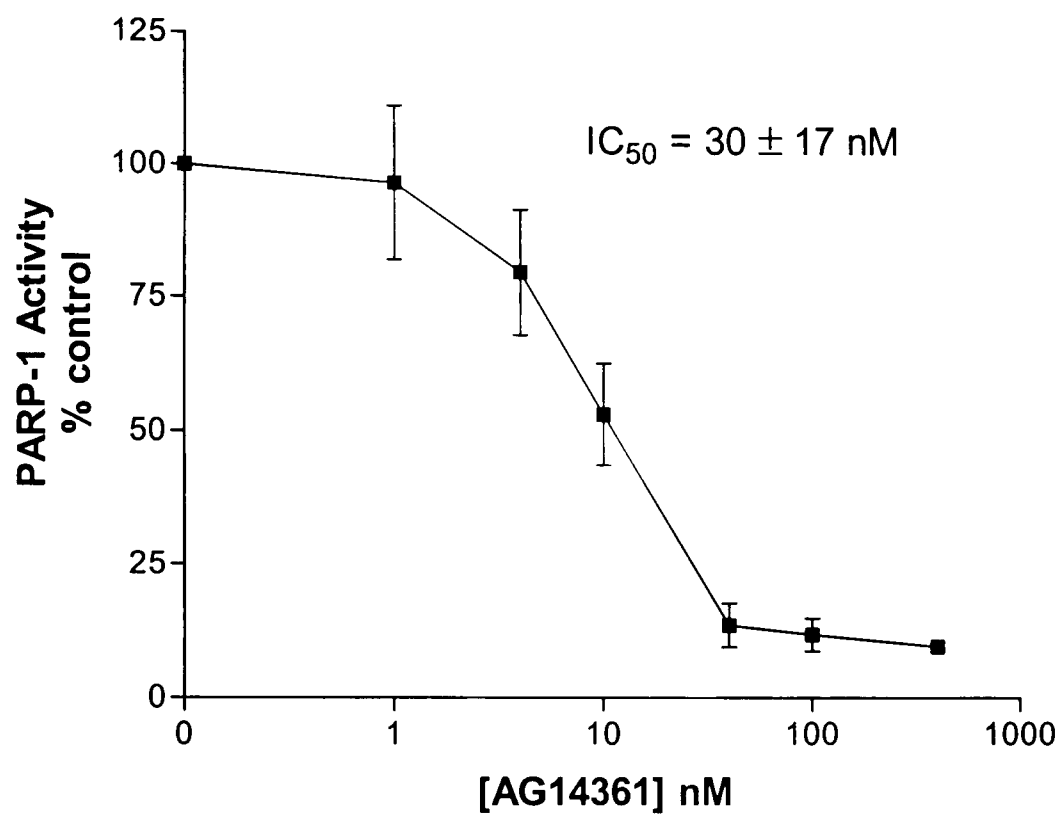


Figure 3.7 Effect of AG14361 on PARP-1 activity in K562 cells.

Exponentially growing K562 cells were exposed to 0, 1, 4, 10, 40, 100, 400 nM AG14361 for 10 mins. PARP-1 activity was measured as described in section 2.6 and activity was expressed as a percentage of a DMSO-treated control. Data are the mean of 3 independent experiments \pm SEM.

Cell Line	PARP-1 activity (pmol/10⁶ cells)	% inhibition by 0.4 μM AG14361	GI₅₀ AG14361 (nM)
K562	233 \pm 39	91 \pm 0.1	30 \pm 17
PARP-1 wild type	160 \pm 40	96 \pm 3	22 \pm 3
PARP-1 null	10 \pm 3	98 \pm 3	15 \pm 4

Table 3.2 PARP-1 activity and its inhibition by AG14361 in K562 and PARP-1 wild type and PARP-1 null cells.

Data are mean \pm SEM for at least 3 independent experiments. PARP-1 wild type and null cell line data reproduced with permission (Veuger *et al.*, manuscript in press Oncogene 2003).

3.3.4 Effect of AG14361 on Topo I poison-mediated growth inhibition.

3.3.4.1 PARP-1 wild type and null cell lines.

To confirm that PARP-1 plays a role in the cellular response to topo I poisons and that AG14361 potentiates topo I poisons through its effect on PARP-1, the effect of AG14361 on topotecan-induced cell growth inhibition was investigated in PARP-1 wild type and null cells.

Exponentially growing PARP-1 wild type and PARP-1 null cell lines were exposed continuously for 5 days to increasing concentrations of topotecan in the presence or absence of 0.4 μ M AG14361, and cell growth inhibition determined by SRB assay (Figure 3.8). The data summarised in Table 3.3 show that the PARP-1 null cells were 3-fold more sensitive to topotecan than wild-type cells, this differential sensitivity was statistically significant ($p = 0.00045$ unpaired t-test). It was also found that the growth inhibitory effect of topotecan in wild-type cells was enhanced 2 to 3-fold by co-incubation with 0.4 μ M AG14361 and that this enhancement was statistically significant ($p = 0.002$ paired t-test). There was a modest potentiation of topotecan-induced growth inhibition by AG14361 in PARP-1 null cells ($p = 0.03$ paired t-test) possibly due to inhibition of PARP-2 by AG14361. However this result was not reproduced in later experiments (see section 3.3.4.3). There was no significant difference in growth inhibition between PARP-1 null cells treated with topotecan alone ($GI_{50} = 20.8$) and PARP-1 wild type cells treated with topotecan and AG14361 ($GI_{50} = 19.5$; $p = 0.9$ unpaired t-test), nor was there a statistically significant difference in growth inhibition between PARP-1 wild type and PARP-1 null cells treated with both topotecan and AG14361 (GI_{50} (wildtype) = 19.5 v (null) 15.6, $p=0.25$, unpaired t-test). This suggests that absence of PARP-1 and chemical inhibition of PARP-1 have an approximately equivalent effect on cell growth following exposure to topotecan.

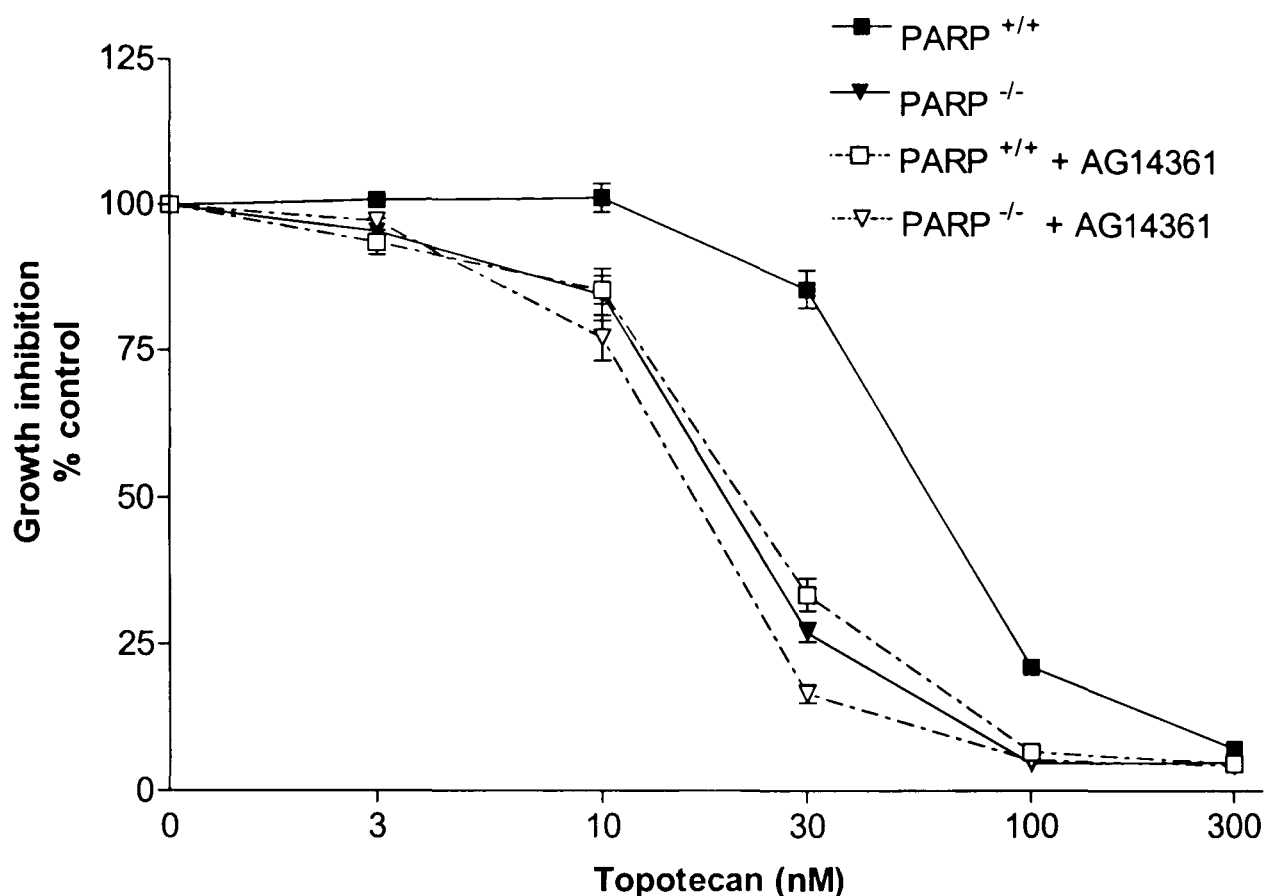


Figure 3.8 Effect of AG14361 on topotecan-induced growth inhibition in PARP-1 wild-type (+/+) and null (-/-) cell lines.

Cells were exposed to 0, 3, 10, 30, 100 and 300 nM topotecan in the presence or absence of 0.4 μ M AG14361 for 5 days continuously. Growth inhibition was measured using the SRB assay (see section 2.4.1) and growth was expressed as a percentage of the related DMSO or 0.4 μ M AG14361-treated control. Data are expressed as a percent of untreated control from 3 independent experiments \pm SEM.

	GI ₅₀ Topotecan (nM)	GI ₅₀ Topotecan + 0.4 μM AG14361 (nM)	PF ₅₀
PARP-1 wild-type	65.0 ± 7.0	19.5 ± 4.3 ^{** (a)}	3.4 ± 0.4
PARP-1 null	20.8 ± 2.0 ^{** (a), NS (c)}	15.6 ± 0.6 ^{*(b)}	1.4 ± 0.1
Sensitivity ratio	3 ± 0.2	1.3 ± 0.5	

Table 3.3 Effect of AG14361 on topotecan-mediated growth inhibition in PARP-1 wild-type and null cells.

Mean IC₅₀ values from 3 independent experiments are given ± SEM. PF₅₀ is the potentiation factor, the ratio of GI₅₀ drug alone: GI₅₀ drug plus PARP-1 inhibitor calculated from GI₅₀ values from individual experiments.

^{**} p< 0.001 paired t-test.

⁺ p <0.05 paired t-test.

NS not significant

^a compared to PARP-1 wild-type treated with topotecan alone.

^b compared to PARP-1 null treated with topotecan.

^c not significantly different from PARP-1 wild type treated with topotecan + AG14361.

3.3.4.2 p53 status of PARP-1 cell lines.

During the course of this study the PARP-1 wild type cell line used here was found to be expressing a mutant p53 (P. Jowsey, PhD thesis 2003). These cells contained a single base change from G to C in codon 278 conferring an Asp to Glu substitution (GAC to GAG codon change). This mutation is located within a conserved region of the DNA binding domain, and rendered p53 unable to act as a transcriptional transactivator. The PARP-1 null cells expressed wild type p53. Loss of p53 is known to cause resistance to topo I poisons and this could be responsible for the relative resistance of the PARP-1 wild type cells compared to the PARP-1 null cells. It was therefore desirable to investigate the effect of PARP-1 on topo I poison sensitivity in cells with the same p53 status.

3.3.4.3 Studies using PARP-1 null^{TR} and PARP-1 null cells.

In an attempt to compare topo I poison mediated cytotoxicity in the presence, absence or inhibition of PARP-1 in cell lines that were p53 wild type, another set of cells were acquired. Previous studies within the NICR led to the stable transfection of PARP-1 into the PARP-1 null cell line. This retransfected cell line, called PARP-1 null^{TR} had previously been shown to express wild type PARP-1 and wild type p53 (P.Jowsey personal communication; for details see section 2.3.2).

The PARP-1 null^{TR} cell line was used to determine whether the differences in p53 status of the cell lines had any impact on the differential response to topotecan. Exponentially growing PARP-1 null^{TR} and PARP-1 null cells were exposed to 0 - 300 nM topotecan in the presence or absence of 0.4 μ M AG14361 for 5 days before measurement of growth inhibition by SRB assay (see section 2.4.1). The effect of PARP-1 inhibition on topotecan induced growth inhibition in these cells is shown in Figure 3.9. The results, summarised in Table 3.4, show that there was no significant difference between the PARP-1 null^{TR} and the PARP-1 null cells in their response to topotecan ($p = 0.9$ paired t-test). There was a modest potentiation of topotecan-induced growth inhibition by AG14361 in the PARP-1 null^{TR} cells ($p = 0.06$ paired t-test), similar to that observed in the untransfected PARP-1 null cells (Table 3.3 and Table 3.4). The PARP-1 null^{TR} cells were approximately 3 times more sensitive to topotecan than the original PARP-1 wild type cells shown in Table 3.3. These data indicate that retransfection of PARP-1 in to

PARP-1 null cells did not affect their hypersensitivity to topotecan. This unexpected result was investigated further by determining the levels of PARP-1 protein in the PARP-1 null^{TR} cells using Western blotting. The blot in Figure 3.10 illustrates that the PARP-1 null^{TR} cells did not express levels of PARP-1 comparable to those levels seen in the wild type cells. This blot is not ideal, however, other members of the NICR have observed a reduced level of PARP in the retransfected PARP null cells. It is therefore possible that the reason for the hypersensitivity of the PARP-1 null^{TR} cells to topotecan is due to a reduced expression of the PARP-1 gene compared to PARP-1 wild type cells. This may be due to lack of selection pressure since the transfected pPARP31 plasmid contains the neomycin resistance gene and the PARP-1 null genotype was created by homologous recombination and insertion of pGK-neo into the PARP-1 gene. Therefore G418 selection used on these cells could not ensure that only the transfected cells would survive.

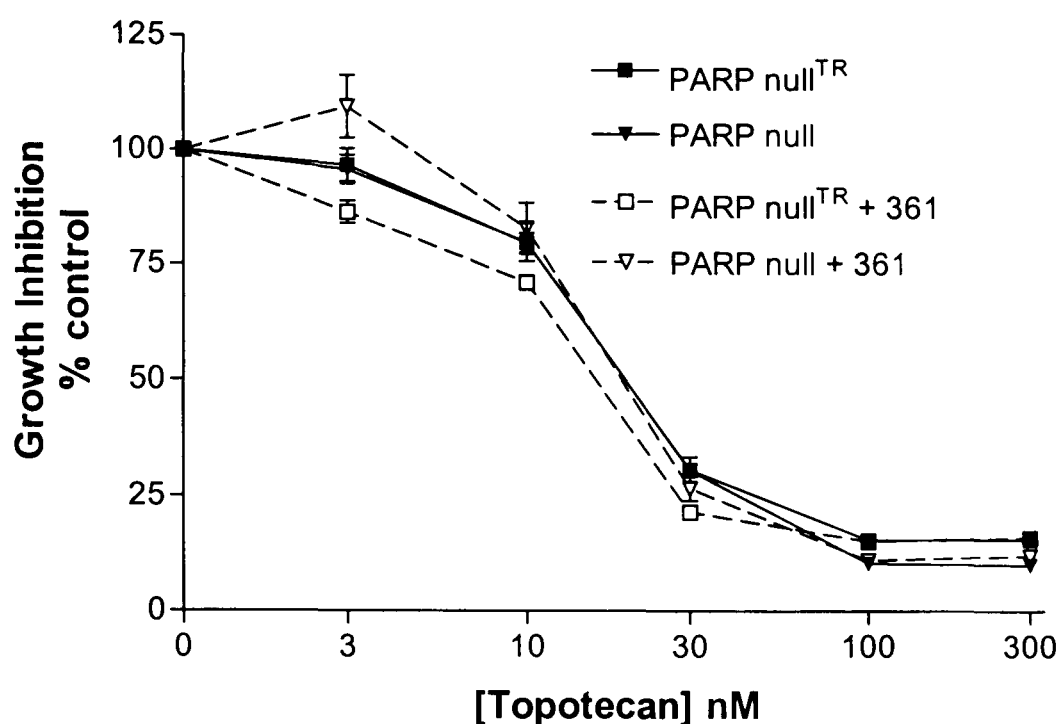


Figure 3.9 Effect of AG14361 on topotecan-induced growth inhibition in PARP-1 null^{TR} and PARP-1 null cell lines.

Exponentially growing cells were exposed to 0, 3 10, 30, 100, 300 nM topotecan in the presence or absence of 0.4 μ M AG14361 for 5 days continuously. Growth inhibition was measured by SRB assay (see section 2.4.1) and growth was expressed as a percentage of the related DMSO or 0.4 μ M AG14361-treated control. Data are the mean of 3 independent experiments \pm SEM.

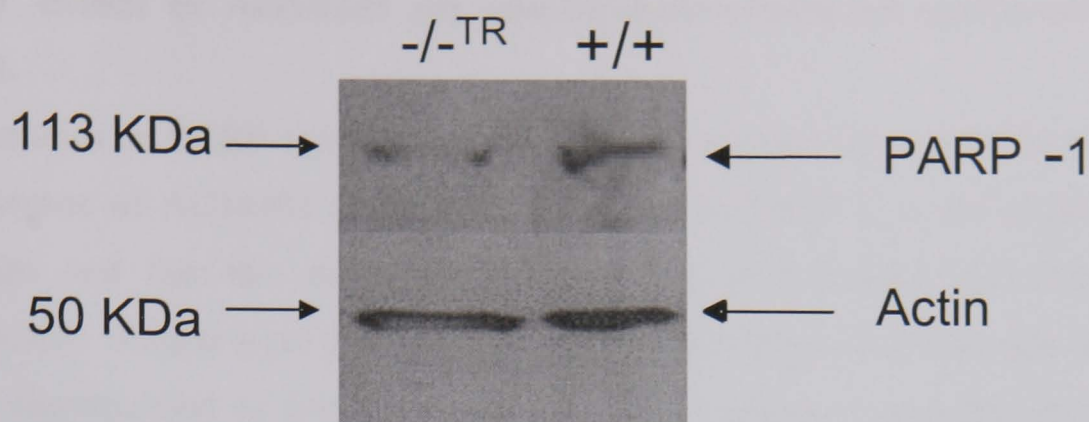


Figure 3.10 PARP-1 protein levels in PARP-1 null^{TR} cells (-/-^{TR}) and PARP-1 wild type cells (+/+).

30µg of whole cell lysate was loaded per well. Proteins were separated and detected using Western blotting as in section 2.5. PARP-1 was detected using rabbit anti-PARP-1 antibody (Santa Cruz Biotechnology) and the appropriate secondary antibody.

Cell Line	GI ₅₀ Topotecan (nM)	GI ₅₀ Topotecan + AG14361 (nM)	PF ₅₀
PARP-1 null ^{TR}	22.2 ± 0.7	18.5 ± 0.5 *	1.20 ± 0.07
PARP-1 null	22.0 ± 0.7	21.5 ± 1.3	1.03 ± 0.07
PARP-1 wild type	65.0 ± 7.0	19.5 ± 4.3	3.4 ± 0.4

Table 3.4 Effect of AG14361 on topotecan -induced growth inhibition in PARP-1 wild type, PARP-1 null^{TR} and PARP-1 null cell lines.

Growth inhibition was measured by SRB assay see section 2.4.1. Data are the mean of 3 independent experiments ± SEM.

* p = 0.06 paired t-test; compared to topotecan alone.

3.3.5 Effect of AG14361 on camptothecin-induced cytotoxicity in K562 cells.

The studies on PARP-1 wild type and null cells treated with topotecan in the presence or absence of AG14361 indicated both a role for PARP-1 in the response to topo I poisons and that the chemopotentiating effect of AG14361 was due to PARP-1 inhibition. Studies were then focussed on a human tumour cell line that has previously been characterised in response to another topo I poison, camptothecin (Padget *et al.*, 2000). Although camptothecin is not used clinically (due to unpredictable toxicity), its use in the subsequent experiments is justified on the grounds of its near identical mode of action to clinically used topo I poisons, and its abundant use in cell culture-based studies allowing direct comparisons with studies in the literature.

The growth inhibitory effect of camptothecin on human chronic myelogenous leukaemia (CML) K562 cells in the presence or absence of 0.4 μ M AG14361 was investigated. Two exposure times were used with the K562 cells. A 30 min exposure was used as this is a time corresponding to the peak in levels of camptothecin-stabilised cleavable complexes in K562 cells (Padget *et al.*, 2000). A 16 hour exposure was also used as this had been used in previous studies by Mattern *et al.*, (1987) and Bowman *et al.*, (2001), and also allowed the majority of cells to have gone through one S-phase of the cell cycle. This is important because of the S-phase specific toxicity of camptothecin (D'Arpa *et al.*, 1990). Cells were exposed to camptothecin in the presence or absence of 0.4 μ M AG14361 for 30 mins or 16 hours before removal of the drug and incubation in drug free medium or medium containing 0.4 μ M AG14361 for a further 5 days. In initial studies the XTT assay was used to determine growth inhibition but this assay, whilst suitable for determining growth of untreated cells gave very variable data with drug exposure, possibly due to the phenomenon of "unbalanced cell growth" of drug treated cells. Growth inhibition was therefore measured by direct counting measured aliquots of cell suspension using a Coulter counter (section 2.4.3). Figure 3.11 and Figure 3.12 show the effect of AG14361 on camptothecin-induced growth inhibition. The growth data summarised in Table 3.5 show that a significant 2-fold potentiation of camptothecin by AG14361 was observed after a 16 hour exposure to camptothecin ($PF_{50} = 1.94$; $p = 0.01005$). However, after a 30 min exposure to camptothecin, AG14361 failed to potentiate the anti-proliferative activity of

camptothecin, thus, there was no significant overall potentiation ($PF_{50} = 1.11 \pm 0.02$; $p = 0.7$ paired t-test). Although following a 30 min exposure to 100 nM camptothecin cell growth inhibition was significantly enhanced by AG14631 1.9 ± 0.04 fold ($p = 0.005$ paired t-test).

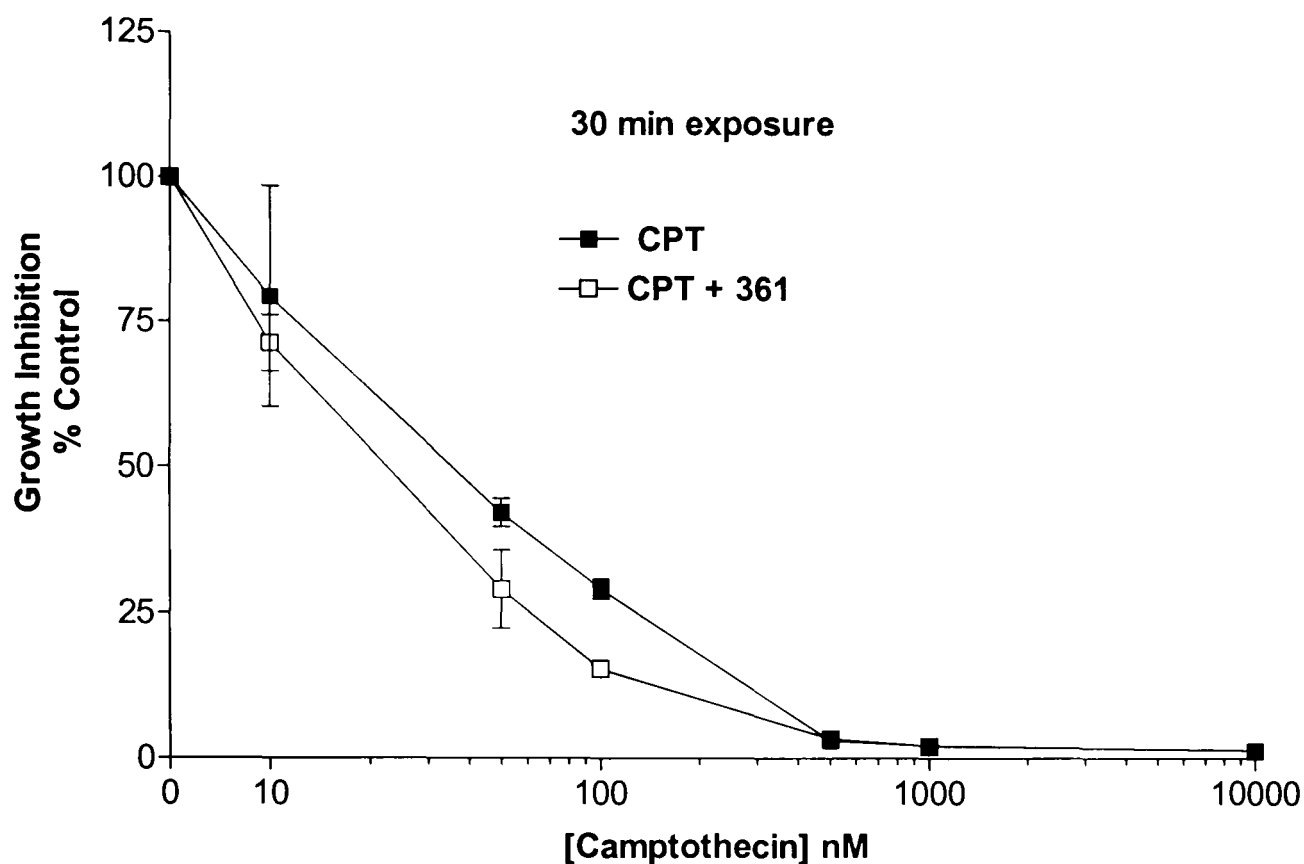


Figure 3.11 Effect of AG14361 on camptothecin-induced growth inhibition in K562 cells.

Exponentially growing cells were exposed to 0, 10, 50, 100, 500, 1000 and 10000 nM camptothecin \pm 0.4 μ M AG14361 for 30 mins and grown for 5 days in drug-free medium or medium containing AG14361. Cell growth was measured by cell counting (see section 2.4.3) and expressed as a percentage of the relevant DMSO or 0.4 μ M AG14361 alone control. Graph shows the mean of 3 independent experiments \pm SEM.

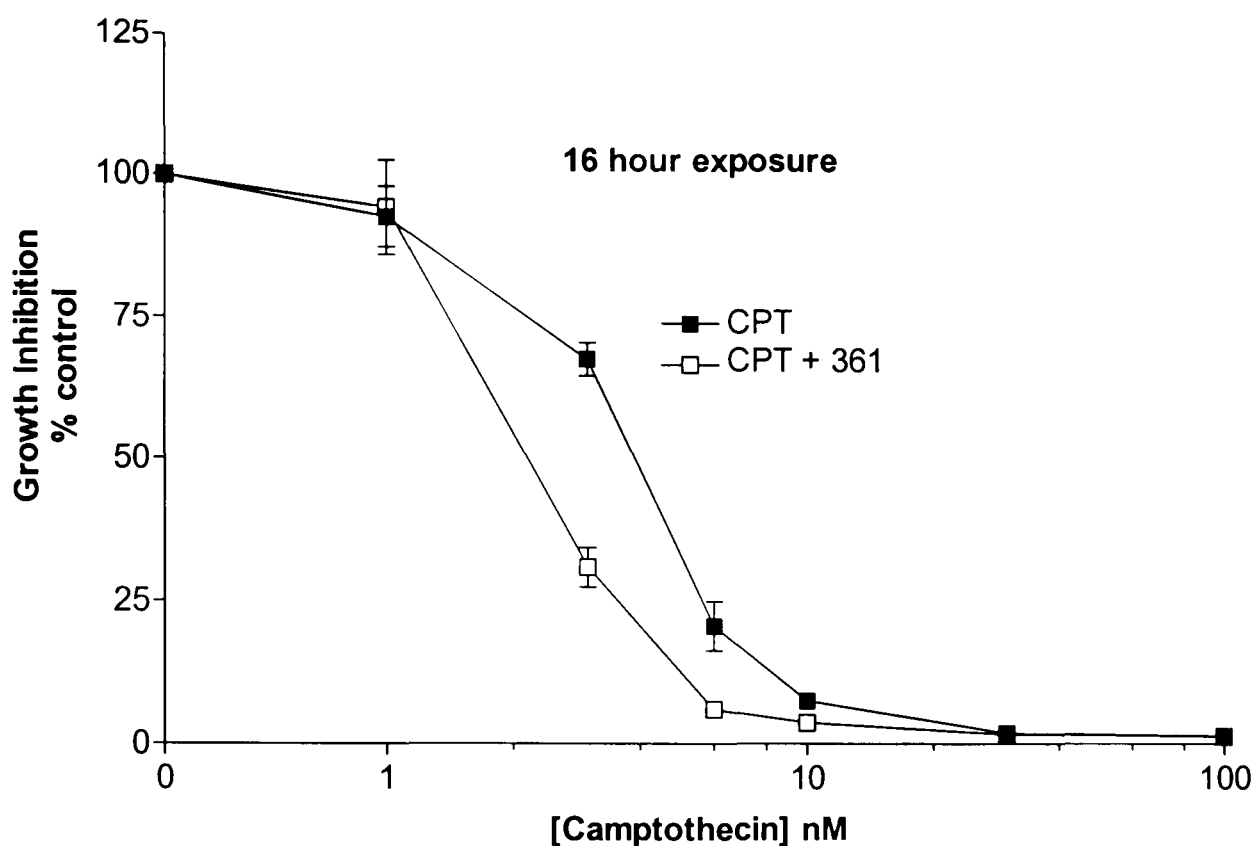


Figure 3.12 Effect of AG14361 on camptothecin induced growth inhibition in K562 cells.

Cells exposed to 0, 1, 3, 6, 10, 30, and 100 nM camptothecin \pm 0.4 μ M AG14361 for 16 hours and grown for 5 days in drug free or medium containing 0.4 μ M AG14361. Cell growth was measured by cell counting (see section 2.4.3) and expressed as a percentage of the relevant DMSO or 0.4 μ M AG14361 alone control. Data are the mean of 4 independent experiments \pm SEM.

Time (hours)	GI ₅₀ Camptothecin (nM)	GI ₅₀ Camptothecin + AG14361 (nM)	PF ₅₀
0.5	40 ± 5.3	38 ± 6.5 ^a	1.11 ± 0.2
16	4.7 ± 0.4	2.4 ± 0.1 [*]	1.9 ± 0.2

Table 3.5 Effect of AG14361 on camptothecin-mediated growth inhibition in K562 cells.

Cells were exposed for 0.5 or 16 hours before removal of drug and growth in drug free medium or medium containing AG14361 for a further 5 days. Growth inhibition was measured by SRB assay and IC₅₀ values calculated as described in section 2.4.1. Data are the mean of 4 independent experiments ± SEM.

(^{*}) significantly different from camptothecin alone p< 0.05 paired t-test.

(^a) not significantly different from camptothecin alone.

3.3.6 Effect of AG14361 on survival of K562 cells exposed to camptothecin for 16 hours.

Growth inhibition assays cannot distinguish between a general retardation of growth in the entire cell population and killing of a proportion of the cells. To determine if the effect of camptothecin and its potentiation by AG14361 was cytotoxic as well as cytostatic, the clonogenic survival of K562 cells in response to exposure to camptothecin in the presence or absence of AG14361 was also investigated. The clonogenic assay described in section 2.4.4, uses a different biological end-point to growth inhibition assays relying on the ability of the treated cells to be able to reproduce from a single cell to form a colony. K562 cells were exposed to camptothecin in the presence or absence of AG14361 for 16 hours before the cells were plated out at known cell numbers. The survival of these cells is shown in Figure 3.13. Camptothecin induced cytotoxicity was significantly increased 1.75-fold by 0.4 μ M AG14361 compared to treatment with camptothecin alone. These results are in good agreement with the results shown in the growth inhibition assay in Figure 3.12. The bi-phasic appearance of the survival curve is characteristic of curves produced in response to S-phase specific agents, and suggests that not all of the cells have been through one cell cycle while exposed to camptothecin, as would be expected as K562 cells double every 24 hours. This could be investigated further using different exposure times.

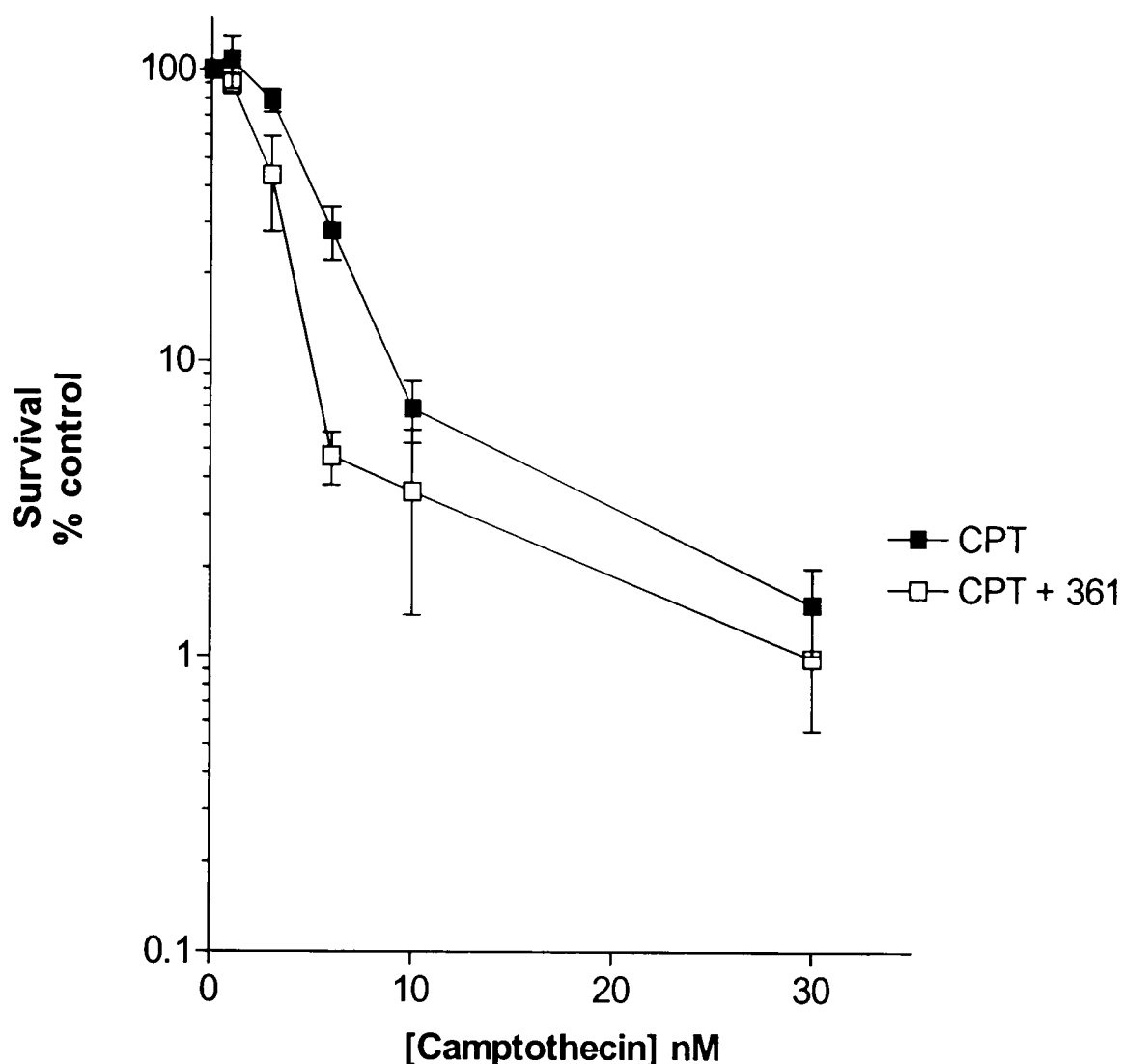


Figure 3.13 Effect of AG14361 on camptothecin induced cytotoxicity in K562 cells. Exponentially growing cells were exposed to 0, 1, 3, 6, 10, and 30 nM camptothecin for 16 hours. Cytotoxicity was measured using the sloppy agar clonogenic assay as described in section 2.4.5 and expressed as a percentage of the relevant DMSO or 0.4 μ M AG14361 alone control. Data are pooled data from 4 independent experiments \pm SEM.

	LC ₅₀ camptothecin (nM)	LC ₅₀ camptothecin + AG14361 (nM)	PF ₅₀
K562	4.86 \pm 0.37	2.77 \pm 0.55 *	1.92 \pm 0.34

Table 3.6 Cell survival of K562 cells treated with camptothecin in the presence or absence of AG14361.

LC₅₀ values are means \pm SEM for 4 independent experiments. PF₅₀ was calculated from individual IC₅₀ values for each experiment.

* p = 0.05 paired t-test compared to camptothecin alone.

3.4 Discussion.

The aim of this chapter was firstly to verify the role of PARP-1 in cellular survival and proliferation following exposure to topo I poisons using PARP-1 wild type and null cells. Secondly, to demonstrate that PARP-1 is the principle cellular target for the novel PARP inhibitor AG14361 and that the enhancement of the antiproliferative activity and cytotoxicity of topo I poisons by AG14361 is due to its PARP-inhibitory effect. The effect of AG14361 on camptothecin-mediated cytotoxicity in K562 cells was also investigated to verify that this was a suitable model for further investigations, as described in subsequent chapters of this thesis.

PARP-1 null cells were shown to be 2 to 3-fold more sensitive to topotecan than the wild type cells (Figure 3.8, Table 3.3). This suggests that there is a role for PARP-1 in the cellular response to topotecan. This was not due to differences in levels of topo I protein as Figure 3.3 shows that these cell lines have similar levels of topo I protein. During the course of these studies the PARP-1 wild type cell line were found to carry a p53 mutation in the PARP-1 wild type cell line that was not present in the PARP-1 null line. The difference in the p53 status in these cells could account for the differential sensitivity of the PARP-1 wild type and null cells to topo I poisons. It has also been shown previously that p53 status is not a good predictor of topo I poison cytotoxicity in a panel of cell lines, therefore it does not necessarily follow that a cell line expressing mutant p53 would be more or less sensitive than those expressing wild type p53 (Goldwasser et al., 1995). Furthermore, studies in the NICR have failed to show an effect of p53 status on growth inhibition by topotecan. Using the HCT116 (wt p53) and HCT116 N7 (p53 degraded by the human papilloma virus E6 protein) human colorectal carcinoma cell lines it was shown that there was no significant difference in topotecan-induced cytotoxicity between these two cell lines (GI_{50} topotecan HCT116 = 4.8 ± 1.7 ; GI_{50} topotecan HCT116 N7 = 5.1 ± 3.6) (G.Swaissland unpublished data).

Whether p53 mutation or loss confers resistance to topo I poisons or not, this does not appear to be by a pathway that involves PARP-1. Delaney *et al.*, (2000) demonstrated that the potentiation of growth inhibition on topotecan by NU1025 in 12 human tumour cell lines was independent of the p53 status of the cell. There was also no

difference in the potentiation of growth inhibition of HCT116 and HCT116 N7 cells exposed to topotecan and AG14361 compared to topotecan alone (PF_{50} HCT116 = $1.7 \pm 0.7 \mu\text{M}$; HCT116 N7 = $2.1 \pm 1.0 \mu\text{M}$) (G. Swaisland unpublished data). The data presented in this chapter clearly show that AG14361 potentiates topotecan in p53 mutant PARP-1 wild type cells and also camptothecin in the p53 null K562 cells. Taken together these data suggest that the difference in p53 status of the PARP-1 wild type and PARP-1 null cells, although not ideal, should not alter the interpretation of the results presented in this study.

In order to eliminate the added complication of differences in p53 status, an alternative PARP-1 wild type and null cell line was investigated. The alternative wild type line had been derived from the same PARP-1 wild type and null mice as the cells originally used here, but by Gilbert de Murcia's Laboratory, (Strasbourg). During the course of this study these cells were also found to have a p53 mutation that was different from the one found in the original cells. Following this, attempts were made to retransfect the PARP-1 null cells with PARP-1 to make a PARP-1 wild-type cell that expressed wild-type p53. These cells, called PARP-1 null^{TR} in this study, had been fully validated and shown to express wild type p53 and PARP-1 protein by other workers in this lab prior to use (P Jowsey, PhD thesis 2003). However, these PARP-1 null^{TR} cells behaved more like the PARP-1 null untransfected cells in that they were shown to be 2-3 fold more sensitive to topotecan compared to the original PARP-1 wild type cells and there was minimal potentiation of growth inhibition caused by topotecan in the presence of AG14361 compared to topotecan alone Figure 3.9. Further investigation revealed that the PARP-1 null^{TR} cells were not expressing PARP-1 at levels comparable to the wild type cell line and this could be the reason for the lack of potentiation of growth inhibition by AG14361 Figure 3.10. This apparent loss of expression of PARP-1 in the transfectants may have been due to the fact that the plasmid containing the PARP-1 gene expressed the neomycin resistance gene. The PARP-1 null mice were generated through recombination with a neomycin resistance gene. Thus selection in G418 containing medium would not confer a selection advantage to cells retransfected with PARP-1.

In this chapter it has been shown that, at the concentrations used in this study (0.4 μ M), AG14361 did not significantly inhibit growth in any of the cell lines used here (Figure 3.5, Figure 3.6). 0.4 μ M AG14361 was sufficient to inhibit the activity of PARP-1 in these cells by at least 90% of normal activity (Figure 3.7, Table 3.2). Thus 0.4 μ M was a suitable concentration to use in this study. The observation that greater than 90% PARP-1 inhibition can be achieved at concentrations that cause less than 10 % growth inhibition is a strong indication that at 0.4 μ M AG14361 PARP-1 is the principle target for AG14361. Previous studies have shown that, in A549 cells, exposure to 0.4 μ M AG14361 for 17 hours did not change the expression of any of the 6800 genes studied. Exposure to the GI₅₀ concentration (14 μ M), the expression of 62 genes, including p21, were altered >2-fold (Calabrese *et al.*, JNCI in press).

AG14361 enhanced the growth inhibitory effects of topotecan 2 to 3-fold in PARP-1 wild-type cells (Figure 3.8, Table 3.3). This was a similar level of potentiation to that seen in other cell lines in response to AG14361 (Calabrese *et al.*, JNCI in press) and with the differential sensitivities of the PARP-1 wild type and null cells as described in this chapter. A similar degree of potentiation of camptothecin-induced growth inhibition has been seen using NU1025 and other PARP-1 inhibitors in the studies by Delaney *et al.*, (2000) and Bowman *et al.*, (2000).

There was no significant increase in growth inhibition when PARP-1 null cells were exposed to topotecan and AG14361 compared to topotecan alone (Figure 3.5). This indicates that AG14361-mediated potentiation of topotecan is primarily due to inhibition of PARP-1, rather than non-specific effects, in agreement with a lack of effect on gene expression (Calabrese *et al.*, JNCI in press).

The GI₅₀ for topotecan alone in PARP-1 null cells was not significantly different from that seen when PARP-1 wild type cells treated with AG14361 (Table 3.3). Thus a concentration that inhibits PARP-1 by greater than 90% is equivalent to genetic ablation of PARP-1 activity in terms of enhancing sensitivity to topo I poisons.

The effect of AG14361 on camptothecin in K562 (p53 null) cells was also investigated. Experiments showed that 0.4 μ M AG14361 inhibits PARP-1 activity by >90% in these

cells and that this concentration of AG14361 does not affect proliferation of K562 cells, similar to observations in the other cell lines (Table 3.2). AG14361 was also shown to potentiate the effect of topo I poisons 2-fold in K562 cells after a 16 hour exposure which is comparable to the 2 to 3-fold potentiation in the PARP-1 wild type cells (table 3.5). However after a 30 min exposure growth inhibition was not potentiated by AG14361 at the concentration of camptothecin corresponding to the GI_{50} , although there was significant potentiation at 100 nM camptothecin (figure 3.11). There was approximately 10-fold difference in the concentration required to achieve the same level of cytotoxicity between the 30 min and 16 hour time point. A similar observation was made by Goldwasser *et al.*, (1995) using a 1 and 24 hour exposure where there was a 40-fold difference in the dose required to cause the same level of cytotoxicity. It has already been shown that PARP-1 is inhibited after a 10 min exposure to AG14361 (Figure 3.7) and that the stabilised cleavable complexes are maximal after 30 mins exposure to camptothecin (Padget *et al.*, 2000). Therefore this would suggest that the potentiation of topo I poisons is not a direct effect of PARP-1 inhibition, i.e. a downstream effect of lack of PARP-1. This would suggest that the effect that PARP-1 exerts accumulates over time e.g. in regulating the formation and reversal of cleavable complexes via modulation of activity of topo I molecules by poly(ADP-ribosylation), or the creation or repair of the single strand breaks. Taken together this suggests that longer exposure to PARP-1 inhibitors is required to achieve maximal potentiation of cytotoxicity and growth inhibition. This has been suggested previously by Mattern *et al.*, (1987), using camptothecin and 3-AB. Here it was demonstrated that a 60 min exposure to 3-AB prior to treatment with camptothecin was not sufficient to potentiate cytotoxicity, however potentiation was seen after a 16 hour pre-treatment.

In summary the data presented in this chapter shows that: -

- PARP-1 is involved in the response to topo I poisons as shown by the hypersensitivity of cells lacking PARP-1 activity to topotecan.
- AG14361 can be used to potentiate topo I poisons at a concentration that inhibits PARP-1 activity by 90% without affecting cellular proliferation and survival *per se*.
- AG14361 is specific for PARP-1 as potentiation of growth inhibition was seen in PARP-1 wild type cells and not PARP-1 null cells.

The data presented in this chapter and data from similar studies in the literature, shows that the lack or inhibition of PARP-1 activity increases sensitivity to topo I poisons 2 to 3-fold in cell cultures and in human tumour xenografts.

Chapter 4

Effect of PARP-1 on topoisomerase I activity.

4.1 Introduction.

In the previous chapter inhibition or loss of PARP-1 activity was shown to increase topo I poison-mediated cytotoxicity. Two hypotheses have been proposed to explain this phenomenon; (1) that PARP-1 modulates topo I activity, and (2) that PARP-1 is involved in the repair of topo I poison-mediated DNA damage. In this chapter the first hypothesis was tested, investigating whether PARP-1 inhibition by AG14361 could alter topo I activity.

Poly(ADP-ribosylation) of topo I is thought to result in the repression of topo I by virtue of the negatively charged poly(ADP-ribose) polymers causing the topo I to be repelled from the negatively charged DNA. Inhibition of PARP-1 by preventing poly(ADP-ribosylation) of topo I should therefore de-repress topo I. Increased topo I expression is associated with increased sensitivity to topo I poisons (Madden and Champoux, 1992, Husain *et al.*, 1994). Presumably this is because of the greater potential for cleavable complex formation and hence stabilisation by topo I poisons.

Inhibition of topo I activity by PARP-1 activity was first shown *in vitro* by Ferro *et al.*, (1983). In this paper it was found that there was a modest DNA topoisomerase activity associated with a purified PARP-1 preparation. This was demonstrated by the ability of this preparation to relax supercoiled plasmid DNA. This topo activity was equivalent to < 30 units/ml topoisomerase in the presence of NAD^+ and DNA i.e. when PARP-1 was active. However if NAD^+ or DNA were omitted from the reaction, topo I was not inhibited and activity was 625-750 units/ml. The implication from this study was that poly(ADP-ribosylation) inhibited topo I activity.

Poly(ADP-ribosylation) of topo I has also been described by Jongstra-Bilan *et al.*, (1983). Topoisomerase activity was detected in a preparation of poly(ADP-ribosylated) proteins. This was shown to be associated with topo I, as the activity was not dependent on the presence of ATP, which is required for topo II activity. As well as confirming the findings of Ferro *et al.*, (that under conditions of poly(ADP-ribosylation) topo I is inhibited) it was shown that inhibition of relaxation activity of topo I by PARP-1 was reversed by nicotinamide and 3-AB, confirming that inhibition of topo I was dependent on PARP-1 activity rather than a protein-protein interaction between topo I and PARP-

1. This paper also showed a shift in the molecular weight of topo I protein to a higher weight in the presence of DNA-associated PARP-1 and radiolabelled NAD^+ . This shift corresponded to an increase in the amount of radiolabel associated with the topo I protein band on the gel and could be inhibited by nicotinamide, signifying that the topo I protein was being poly(ADP-ribosylated). These results confirmed that the topo I protein was an acceptor of poly(ADP-ribose) polymers from PARP-1, and that this modification could inhibit topo I activity.

In the studies by Ferro *et al.*, (1983) and Jongstra-Bilan *et al.*, (1983), topo I that had co-purified with ADP-ribosylated proteins had been used. This topo I activity corresponded to between 0.1 and 1% of the total cellular topo I. Therefore it was important to show that this small fraction was characteristic of the total topo I in the cell. Ferro and Olivera, (1984) showed that the major topo I activity purified from calf thymus could be poly(ADP) ribosylated by purified PARP-1 and this inhibited topo I activity. This topo I was representative of the major topo I activity in the cells and therefore confirmed their previous results. The authors went on to postulate that the increase in the negative charge of topo I caused by the addition of the negative poly(ADP-ribose) polymers would eventually repel topo I from the DNA, thus inhibiting topo I activity (Ferro and Olivera, 1984).

Poly(ADP-ribosylation) of topo I has also been demonstrated in intact cells. Krupitza and Cerutti (1988) showed that topo I was poly(ADP-ribosylated) in an extract of acid insoluble proteins from the JB6 (clone 41) mouse epidermal cell line. Stimulation of PARP-1 by generation of DNA strand breaks following exposure of cells to active oxygen (produced by a xanthine-xanthine oxidase system) increased the amount of polymer associated with the topo I protein by 6-fold, and this could be inhibited by the PARP-1 inhibitor, benzamide (100 μM). Therefore there is evidence that PARP-poly(ADP-ribosylates) topo I in intact cells.

The poly(ADP-ribosylation) of topo I has been investigated by other authors by measuring the levels of topo I covalently bound to DNA in the cleavable complex but their findings are contradictory. Mattern *et al.*, (1987) showed that the number of protein-linked DNA single strand breaks (PLDB) in L1210 treated with 1-10 μM

camptothecin could be increased 1.6-fold in the presence of 5 mM 3-AB. These protein-linked DNA strand breaks were most likely to be camptothecin-stabilised topo I cleavable complexes. Given the earlier evidence that poly(ADP-ribosylation) down-regulated topo I activity, Mattern *et al.*, concluded that the increase in PLDBs was most likely to be due to loss of poly(ADP-ribose) from the topo I in the presence of 3-AB resulting in de-repression of topo I activity. Conversely, the levels of protein-linked DNA strand breaks formed in camptothecin-sensitive or resistant KB cell lines treated with camptothecin were not altered by 3-AB even though camptothecin toxicity could be potentiated in the resistant cell lines (Beidler *et al.*, 1996). The experimental conditions were not identical in these two studies. Mattern *et al.*, exposed cells for 16 hours to 5 mM 3-AB prior to a 1 hour pulse with 1-10 μ M camptothecin whereas, Beidler *et al.* exposed cells for 24 hours to 1 mM 3-AB prior to a 30 min pulse with 5 μ M camptothecin before estimating protein-linked DNA breaks. Moreover, different methods were used to detect the protein-linked strand breaks. Mattern *et al.*, used a lysis buffer containing sarkosyl whereas Beidler used SDS. Topo I-DNA complexes can dissociate in the presence of sarkosyl, however complexes are stabilised when cells are lysed in SDS (Covey *et al.*, 1987). The levels of protein-linked DNA breaks reported in the study by Mattern *et al.*, may therefore underestimate cleavable complex levels. The increase in protein-linked DNA breaks in the presence of 3-AB could therefore reflect either an increased level of complex formation or a decrease in their dissociation in the presence of sarkosyl. Both scenarios would be consistent with poly(ADP-ribosylation) causing reduced affinity of topo I for DNA.

Activation of PARP-1 by DNA damage may cause a reduction of cellular topo I activity. Topo I activity following treatment with IR was found to be reduced 2 to 4-fold in normal cells and ~20-fold in tumour cells with elevated topo I activity. Exposure to IR did not change topo I protein or RNA levels (Boothman *et al.*, 1994). This inhibition of topo I was thought to be associated with poly(ADP-ribosylation) of topo I protein because it was prevented by the PARP-1 inhibitors 3-AB or PD128763. A small band shift of about 3 kDa was observed when topo I protein was separated on 2D-gels following treatment with IR. This was thought to correspond to a mono(ADP-ribosylation) of the topo I protein. Therefore, these data implicate a role for an ADP-ribosylating protein in modulation of topo I activity in response to IR and provides

further evidence to support the hypothesis that PARP modifies topo I inhibiting topo I activity.

A more recent study using TK6 human lymphoblastoid cells has shown that topo I and p53 form a complex that is poly(ADP-ribosylated) following 1Gy of γ -irradiation (Smith and Grosovsky, 1999). Immunoprecipitations of extracts of γ -irradiated TK6 cells were performed using topo I monoclonal antibody. Western blots of these immunoprecipitates were probed for poly(ADP-ribose) polymer, and these revealed a number of proteins that could be co-immunoprecipitated with topo I and also poly(ADP-ribosylated). One of the proteins identified was p53 and thus it was suggested that p53 and topo I form a complex and this complex could be poly(ADP-ribosylated). ADP-ribosylation of topo I was not detectable in untreated cells, however in response to irradiation, poly(ADP-ribosylation) of topo I was complete within a minute of exposure. p53 is also poly(ADP)ribosylated in response to irradiation. Therefore it is possible that poly(ADP-ribosylation) of p53 in the complex as well as topo I itself may account for the inhibition of topo-1 activity following γ -irradiation.

Topo I is a component of the multiprotein replication complex (MRC). Analysis of purified MRC complexes showed that PARP-1 co-purified with some of the core proteins of the 18-21S multiprotein replication complexes from HeLa cells, as well as with the same proteins from a MRC from a different cell line. Immunoblot analysis of the MRC proteins for poly(ADP-ribosylated) proteins revealed that 15 proteins were poly(ADP-ribosylated). These proteins included topo I, DNA pol- α and PCNA. This provides further evidence for the poly(ADP-ribosylation) of topo I, in another biological setting (Simbulan-Rosenthal *et al.*, 1996).

Alternative pathways for the modulation of topo I activity by PARP-1 have been proposed. Topo I is phosphorylated by caesin kinase-2 (CK-2) or protein kinase C which results in an increase in the activity of topo I. Phosphorylation of topo I is associated with increased sensitivity to camptothecin (Pommier *et al.*, 1990). A study was conducted using LY-S camptothecin-resistant, X-ray-sensitive and the LY-R camptothecin-sensitive, X-ray resistant murine lymphoma cells. Topo I was phosphorylated to a much lesser extent in the LY-S cells than the LY-R cells (Staron *et*

al., 1994, 1995). Investigations into this revealed that the LY-S cells had impaired CK-2 activity, approximately 1.7-times lower than the LY-R cells. The LY-S cells also had 5-times higher poly(ADP-ribose) activity than the LY-R cells. Treatment of these cells with benzamide inhibited PARP-1, and increased the phosphorylation of topo I by CK-2. There may be a number of reasons for this. PAR polymers, whose structures are different in the two cell lines (the LY-S cells make significantly shorter polymers than the LY-R cells, Kleczkowska, *et al.*, (2002)), may affect the formation of CK-2 oligomers, or poly(ADP-ribosylation) of topo I may impede the phosphorylation of topo I by CK-2, or negatively charged proteins may inhibit CK-2 directly. These data suggest that as well as direct modulation of topo I by poly(ADP-ribosylation), PARP-1 may modulate topo I activity via phosphorylation (Staron *et al.*, 1996).

Taken together these studies indicate that PARP-1 activity can repress topo I in cell-free and intact cell systems, with and without IR-mediated stimulation of PARP-1 activity, and that the repression of topo I activity can be due to direct poly(ADP-ribosylation) of topo I, or mediated through an effect on p53 or CK-2. Therefore the potentiation of topo I poison-mediated cytotoxicity by AG14361 could be due to topo I de-repression and an increase in the number of targets for topo I poisons. Thus, if there was an effect on topo I activity by the inhibition of PARP-1 it could be determined through measurement of topo I enzyme activity and levels of cleavable complexes formed in response to topo I poisons in the presence or absence of AG14361.

4.2 Aims

The aim of the work described in this chapter was to determine whether inhibition of PARP-1 by AG14361 has any effect on topo I activity and if this is responsible for the potentiation of topo I poison induced cytotoxicity and growth inhibition by AG14361.

In this chapter topo I relaxation activity and cleavable complex formation were measured following exposure of K562 cells to AG14361 for 30 mins or 16 hours to correspond to the time-points used in the growth inhibition and cytotoxicity assays in chapter 3. Levels of cleavable complexes have been measured using the TARDIS assay and K-SDS precipitation.

4.3 Results.

4.3.1 Measurement of the effect of AG14361 on topoisomerase I relaxation activity.

Topo I enzyme activity can be measured using a variety of different methods. In this section the relaxation activity of topo I has been measured. The relaxation assay measures the ability of topo to convert supercoiled purified plasmid DNA into the relaxed form, therefore measuring the breakage, unwinding and religation of the DNA. This assay can measure the relaxation activity of human topo II α and β as well as topo I. The assay is made specific for topo I relaxation activity by exclusion of ATP and Mg^{2+} from the assay. ATP is required for topo II activity. Omission of Mg^{2+} ensured that type I-5' topoisomerase activity is not measured (for more detail see section 2.7).

The effect of AG14361 on topo I relaxation was investigated in the K562 cell line. K562 cells were exposed to 0.4 μM AG14361 in medium for 30 mins or 16 hours at 37°C before preparation of cell extracts according to section 2.7.1. A protein assay was conducted on the extracts to ensure that equal amounts of cellular protein were used in all samples (as section 2.5.1). Serial dilutions of cell extract were made such that the lowest concentration of cell extract corresponding to detectable relaxation activity and the highest concentration of extract corresponding to undetectable relaxation activity could be determined.

30 min exposure

Extracts of cells exposed to AG14361 for 30 mins were incubated with purified plasmid DNA for 30 mins after which the reaction was terminated and the reaction products separated on an 0.8% agarose gel. Figure 4.1 shows that there was very little difference in relaxation activity between untreated cells and cells treated with 0.4 μM AG14361 for 30 mins. This was shown by the presence of a band corresponding to supercoiled DNA in the 0.1 μg protein sample for extracts from both control and AG14361-treated cells. However, at 0.2 μg protein both AG14361-treated and control cell extracts had detectable topo I activity i.e. the band corresponding to supercoiled DNA was no longer visible and instead there were only bands corresponding to relaxed DNA. This suggests that a 30 min exposure to 0.4 μM AG14361 did not affect topo I relaxation activity.

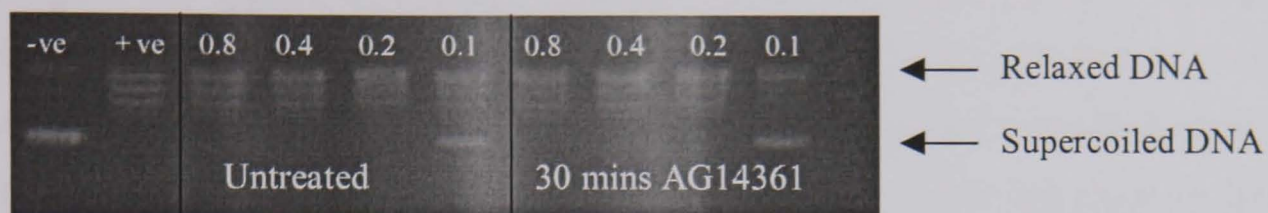


Figure 4.1 Topo I relaxation activity in K562 cells treated with AG14361 for 30 mins.

Nuclear extracts were prepared from K562 cells treated with or without 0.4 μ M AG1436 for 30 mins. These were incubated with 1 μ g supercoiled plasmid DNA for 30 mins. The reaction products were separated on an agarose gel as described in section 2.7.2, (-ve) is a negative control containing water and corresponds to supercoiled DNA, (+ve) is a positive control containing 4 units of purified topoisomerase I corresponding to relaxed DNA. Numbers correspond to cellular protein in each reaction, i.e. 0.8, 0.4, 0.2 and 0.1 μ g cellular protein. Gel shown is one representative of 3 independent experiments.

To further measure the effect of the PARP-1 inhibitor on topo I activity a longer exposure to AG14361 was also investigated. It has been shown in section 3.3.3 that PARP-1 activity was reduced within 10 minutes of exposure to AG14361 in these cells. Therefore any effects of PARP-1 inhibition should be seen soon after exposure to AG14361. Poly(ADP-ribose) glycohydrolase is reported to degrade polymer rapidly; the half life of polymers being less than a minute in cells treated with alkylating agents (Alvarez-Gonzalez and Althaus, 1989). However, in the cytotoxicity assays (section 3.3.5) a 30 min exposure to AG14361 was insufficient to significantly potentiate camptothecin, but a 16 hour exposure increased camptothecin cytotoxicity 2 to 3-fold. This suggests that a prolonged PARP-1 inhibition may be required to reduce poly(ADP-ribosylation) levels sufficiently to modulate topo I activity. To allow direct comparison with cytotoxicity assays in K562 cells the effect of a 16 hour exposure to AG14361 on topo I relaxation activity was investigated.

16 hour exposure

K562 cells were exposed to 0.4 μ M AG14361 for 16 hours before preparation of extracts and measurement of topo I relaxation activity as before. The relaxation of plasmid DNA by these extracts is shown in Figure 4.2. This figure shows that topo I activity was undetectable at 0.1 μ g cellular protein and detectable at 0.2 μ g cellular protein, in both the control and treated samples. This therefore shows that there was no detectable difference in topo I relaxation activity in the presence or absence of AG14361. It should be noted that activity was undetectable at the same level of protein in this experiment and the one shown in Figure 4.1 confirming that there was no difference in activity following short or long term PARP-1 inhibition.

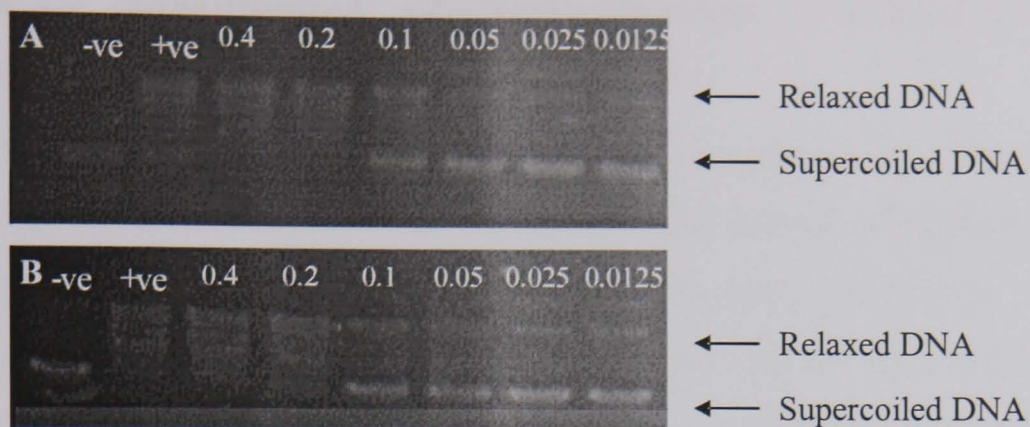


Figure 4.2 Topo I relaxation activity in K562 cells treated with AG14361 for 16 hours.

Nuclear extracts were prepared from K562 cells treated with 0.4 μ M AG1436 (A) or a DMSO treated control (B) for 16 hours and with supercoiled plasmid DNA for 30 mins and the reaction products run out on an agarose gel as described in section 2.7.2 (-ve) is a negative control containing water, (+ve) is a positive control containing 4 units of purified topoisomerase I. Numbers correspond to cellular protein in the reaction, ie 0.4, 0.2, 0.1, 0.05, 0.025, 0.0125 μ g protein. Figure is of one gel that is representative of at least 3 experiments.

4.3.2 Measurement of topoisomerase I poison-stabilised cleavable complexes.

Transient cleavable complexes are formed as a part of the catalytic cycle of topo I, and topo I poisons stabilise these complexes. The number of stabilised cleavable complexes is therefore related to the amount of active topo I present in the cell. Therefore to investigate the effect of PARP-1 on topo I activity the effect of AG14361 on the levels of complexes as well as the reversal of these stabilised complexes was measured. If DNA-bound topo I was a target for poly(ADP-ribosylation) then this may promote its dissociation from DNA, providing the cell with the means to remove stabilised topo I-DNA complexes.

Cleavable complex levels were measured using the TARDIS (Trapped in agarose DNA immunostaining) assay. This assay has been developed at the University of Newcastle upon Tyne for the detection of topo I, II α and II β -associated cleavable complexes. It has been used to detect complexes stabilised by a variety of topo I, II and dual poisons, in human and murine cell lines (Willmore *et al.*, 1998, 2002, Errington *et al.*, 1999, Padget *et al.*, 2000b). This assay had been used previously to measure the levels of stabilised cleavable complexes formed in response to camptothecin in K562 cells (Padget *et al.* 2000a), and was therefore selected for use in the present study with K562 cells.

TARDIS is an immunofluorescent assay that measures the levels of topo I covalently bound to DNA in individual cells. Briefly, cells were treated with camptothecin \pm AG14361 for varying times and then mixed with agarose and spread onto microscope slides. The cells were then lysed leaving just the DNA, and proteins covalently bound to DNA including any drug-stabilised topo I cleavable complexes trapped in the agarose matrix. The presence of DNA-bound topo I was quantified using microscopy to measure fluorescence associated with the FITC-conjugated secondary antibody bound to the topo I-specific primary antibody (for more details see section 2.8). Fluorescence of DNA in the cell was measured by staining with Hoechst 33258 and this was used to define the areas occupied by the DNA for each cell. Thus the fluorescence associated with topo I bound to DNA for each cell could be calculated.

4.3.2.1 Effect of 30 min exposure to camptothecin on levels of cleavable complexes.

Experiments were conducted to validate the assay compared to previous data. A 30 min exposure to camptothecin had previously been shown to be optimal for measuring the maximum levels of cleavable complexes in K562 cells treated with camptothecin. Reproducible high levels of cleavable complexes had been measured previously using the TARDIS assay at 10 μ M camptothecin (Padget *et al.*, 2000a). Therefore K562 cells were exposed to a range of concentrations up to 10 μ M camptothecin for 30 mins. Representative images of camptothecin-treated K562 cells are shown in Figure 4.3. This figure shows that the blue Hoechst associated staining and therefore DNA content of the cell was unchanged by camptothecin exposure. FITC-associated fluorescent (green) labelling of topo I-DNA complexes was undetectable in the control cells and it was barely detectable at the lowest concentration (0.01 μ M) of camptothecin. However, a progressive increase in fluorescence was seen following exposure to 0.1 to 10 μ M camptothecin. Figure 4.4 shows a scatter plot of the FITC-fluorescence associated with individual cells treated with camptothecin, and a plot of the mean values for triplicate experiments. These data show that there was a camptothecin concentration-related increase in the number of cleavable complexes formed after 30 mins exposure. Figure 4.5 shows the scatter and mean plot for Hoechst-associated fluorescence for the same data sets as shown in Figure 4.4 confirming that DNA staining was unaffected by camptothecin. These data are consistent with other data produced using the same drug and cell line (Padget *et al.*, 2000a, and A. Jobson personal communication). These data also showed that a reproducible signal could be achieved using 10 μ M camptothecin, therefore this was the concentration chosen for use in all of the subsequent experiments.

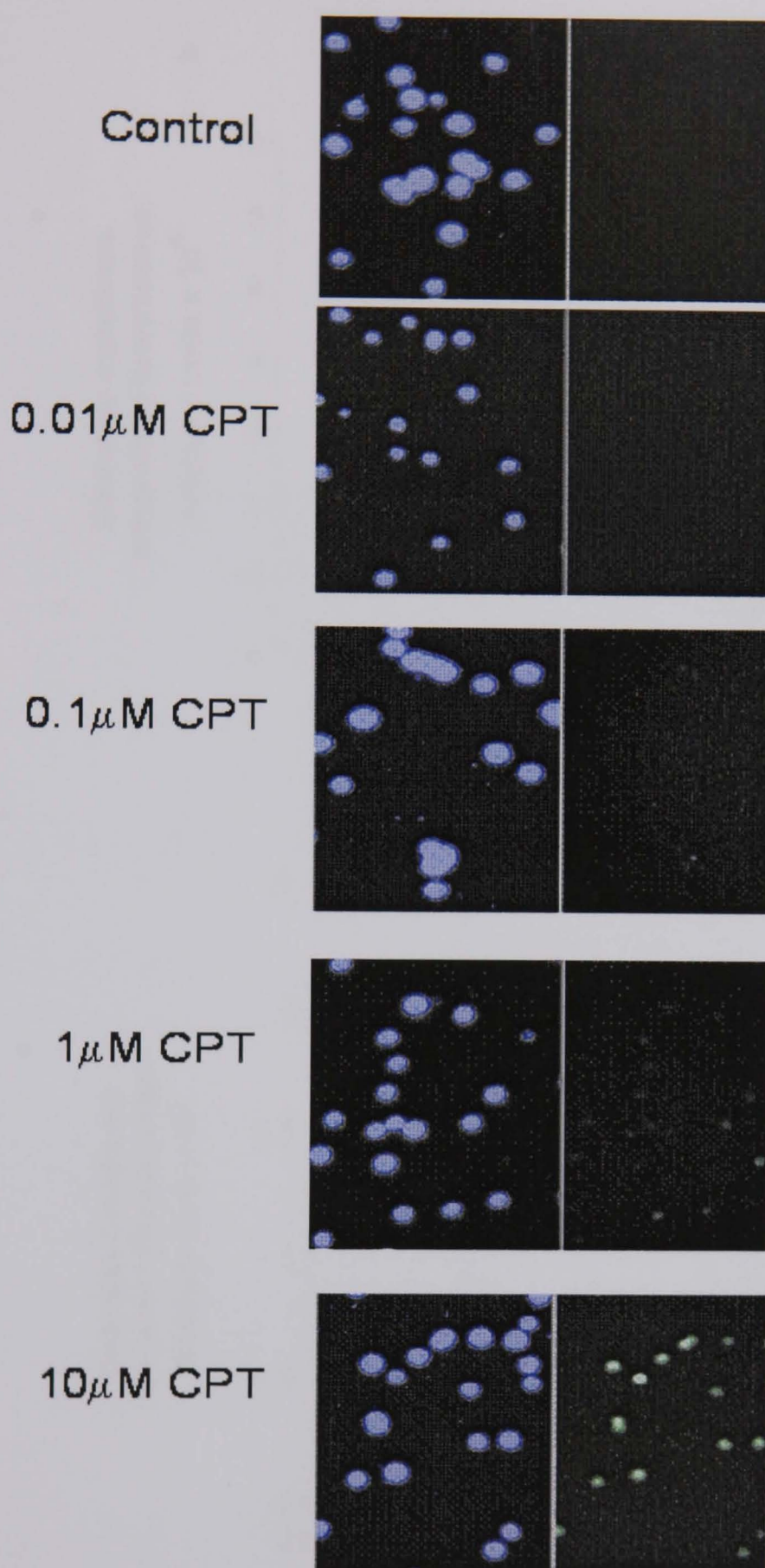


Figure 4.3 Fluorescence of camptothecin-treated K562 cells.

Cells were exposed to 0, 0.1, 1 and 10 μM camptothecin for 30 mins. Fluorescence was measured by the TARDIS assay (section 2.8). Blue images represent Hoechst-stained DNA and green images represent the corresponding FITC-stained immunofluorescence, which directly reflects topo I-cleavable complex levels. Images are typical of those seen in 3 independent experiments.

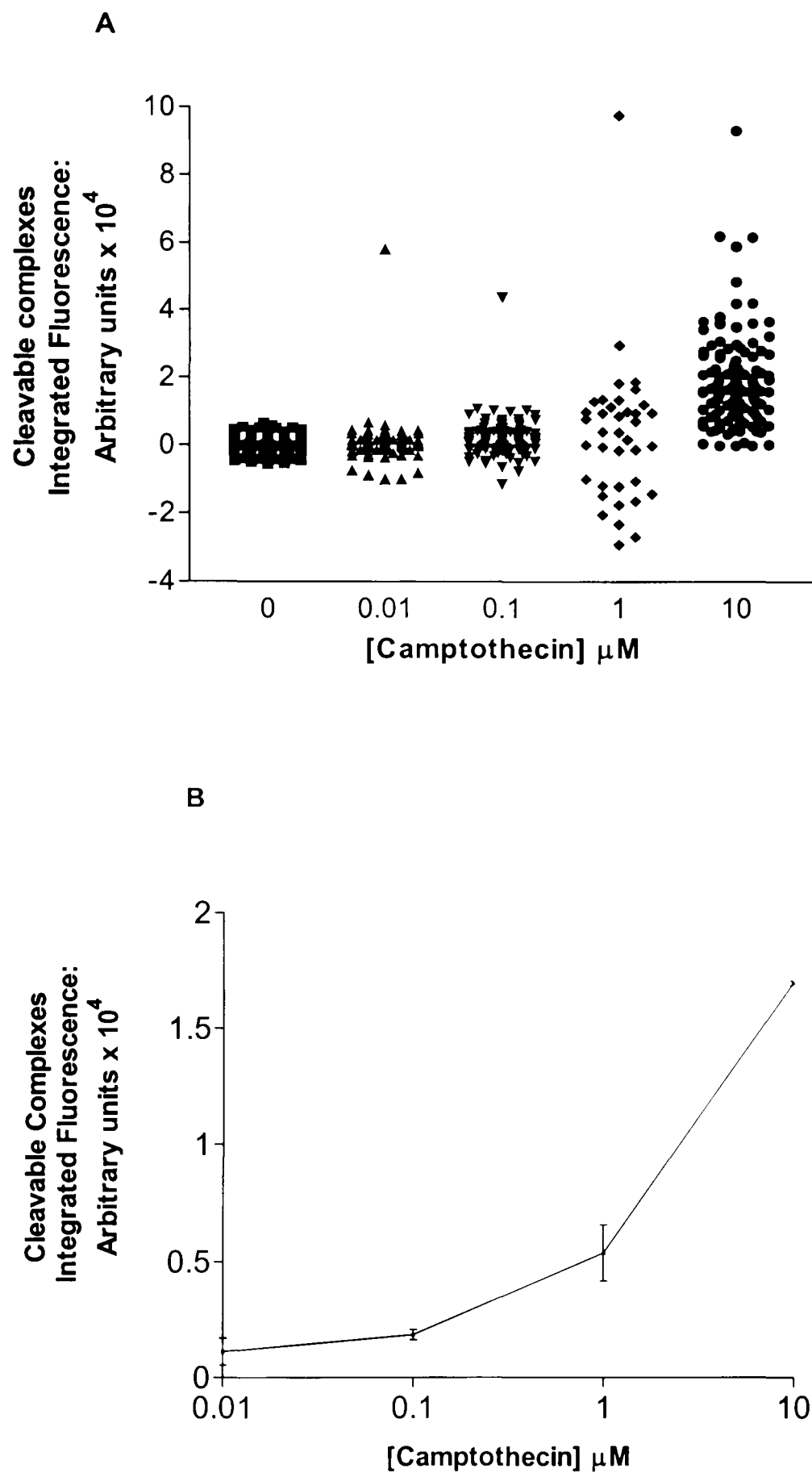


Figure 4.4 Effect of camptothecin on levels of cleavable complexes in K562 cells. Cells were treated with camptothecin for 30 mins before measurement of cleavable complex levels using the TARDIS assay (section 2.8). **A** is a representative scatter showing FITC-associated fluorescence in each cell from one experiment. **B** is a plot of mean FITC associated integrated fluorescence for 3 independent experiments \pm SEM.

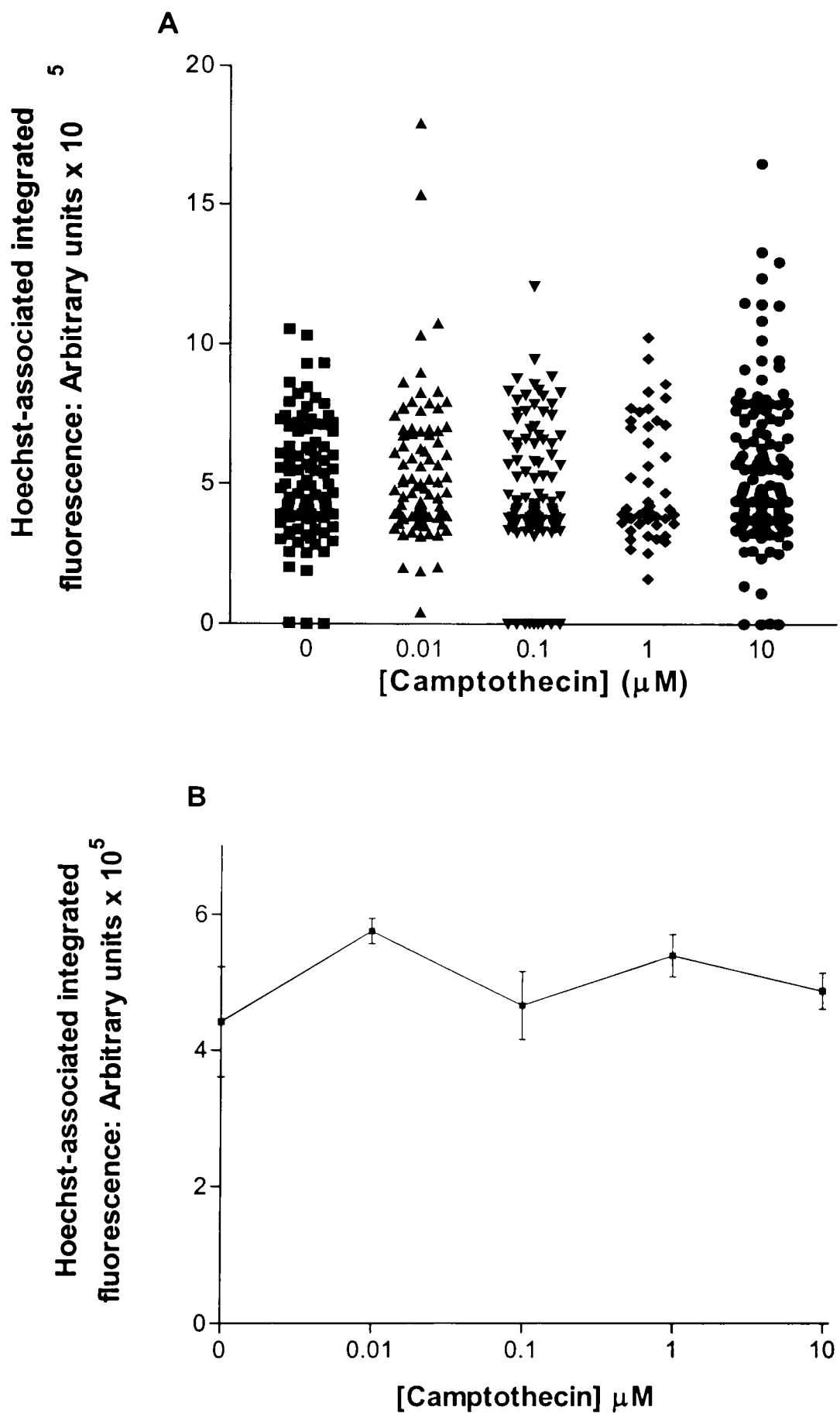


Figure 4.5 Effect of camptothecin on levels of Hoechst-stained DNA in K562 cells.

Cells were treated with camptothecin for 30 mins before measurement of the amount of DNA per cell by Hoechst staining using the TARDIS assay. **A** is a representative scatter plot showing Hoechst fluorescence in individual cells. **B** is a plot of mean Hoechst fluorescence for 3 independent experiments \pm SEM.

4.3.2.2 Effect of AG14361 on camptothecin-stabilised cleavable complex formation.

Measurement of topo I relaxation activity in cell extracts that had been treated with AG14361 showed that there was no significant difference in activity compared to untreated cells. However this only means that total nuclear topo I relaxation activity is apparently not inhibited by poly(ADP-ribosylation) and that exposure to AG14361 does not increase topo I relaxation activity in this artificial system. A real effect of poly(ADP-ribosylation) status on topo I activity may not be detected in this system if ADP-ribose polymers are lost during the preparation of the nuclear extract. However, this assay may not be sensitive enough to detect small changes in activity. Therefore the more specific TARDIS assay was used to detect changes in levels of camptothecin-stabilised cleavable complexes in the presence or absence of AG14361.

30 min exposure to camptothecin ± AG14361

To investigate whether PARP-1 inhibition by AG14361 had any effect levels of cleavable complexes formed as a result of exposure to camptothecin, K562 cells were exposed to 10 µM camptothecin for 30 mins in the presence or absence of 0.4 µM AG14361. Cleavable complex levels were measured using the TARDIS assay (section 2.8). Figure 4.6 shows mean levels of cleavable complex-associated fluorescence in these cells from 7 independent experiments. Means were calculated from each experiment and averaged. This shows that there was no significant difference between cells treated with camptothecin in the presence of AG14361 compared to cells treated with camptothecin alone ($p = 0.74$ paired t-test). There was no increase in levels of cleavable complexes in cells treated with AG14361 alone compared to untreated cells (data not shown). These data show that PARP-1 inhibition had no effect on levels of camptothecin-induced cleavable complexes which is inconsistent with the original hypothesis.

In these experiments a 30 minute exposure to camptothecin was used because it was shown previously that the levels of cleavable complexes measured in K562 cells using the TARDIS assay are only maintained for 90 mins, and after this time levels of complexes decrease even in the presence of drug (Padget *et al.*, 2000a).

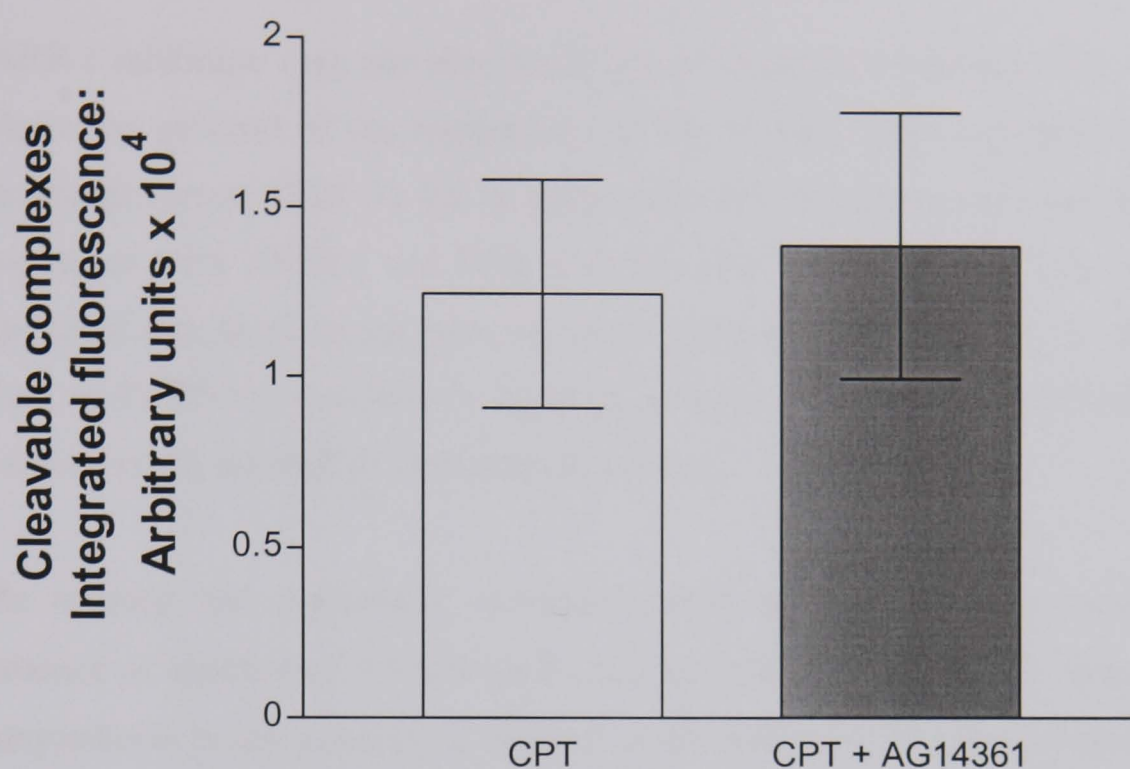


Figure 4.6 Effect of AG14361 on camptothecin-stabilised cleavable complexes. K562 cells were treated with 10 μ M camptothecin in the presence or absence of 0.4 μ M AG14361 for 30 mins. Levels of cleavable complexes were measured using the TARDIS assay as described in section 2.8. Data are the mean of FITC-associated fluorescence values obtained from 7 independent experiments \pm SEM.

4.3.2.3 Effect of AG14361 on persistence of cleavable complexes.

PARP-1 inhibition may not alter the levels of cleavable complexes, but it may have a role in the reversal of the complexes. It has recently been reported that the tyrosyl phosphodiesterase (TDP-1) that is responsible for the removal of cleavable complexes co-purifies with XRCC1 and PNK activities (Plo *et al.*, 2003). This may provide a functional link between the removal of the cleavable complex and the BER pathway. Thus, as PARP-1 is involved in the BER pathway, it is possible that PARP-1 could be involved in the reversal of cleavable complexes.

The reversal and persistence of camptothecin-induced cleavable complexes in the presence or absence of 0.4 μ M AG14361 was studied. K562 cells were treated with camptothecin in the presence or absence of AG14361 for 30 mins, after which the drug was removed and replaced with fresh medium or fresh medium containing 0.4 μ M AG14361 for a further 30 mins. A representative scatter plot is shown in Figure 4.7 and mean data from all experiments is shown in Table 4.1. These data demonstrate that there was a significant increase in the level camptothecin-stabilised cleavable complexes in those cells treated with camptothecin + AG14361 followed by a reversal period of 30 mins in medium containing AG14361, compared to those treated with camptothecin + AG14361 followed by a reversal period of 30 mins in fresh medium ($p = 0.028$, paired t-test). This may suggest that PARP-1 plays a role in the reversal of topo I poison stabilised cleavable complexes. However, there was no significant increase in the persistence of cleavable complexes in those cells treated with camptothecin alone followed by reversal in AG14361 compared to reversal in fresh medium. Therefore it is difficult to draw a definitive conclusion from these results. Reversal of the complexes was $\sim 70\%$ complete after 30 mins in fresh medium in the presence or absence of AG14361, consistent with the findings of Padget *et al.*, (2000a) using camptothecin treated K562 cells. Data were expressed as % camptothecin control to correct for inter-assay variability, data could not be expressed as % untreated control, as these values were negative in some of the experiments. Negative fluorescence values is a phenomenon often observed in untreated cells and lower doses and reflects the way that the image analysis procedure was carried out. It is related to the use of a mean background fluorescence value, which is subtracted from the sample fluorescence. This

background takes into account the variability in the field of view. Thus the subtraction of the mean value from untreated controls may result in negative values.

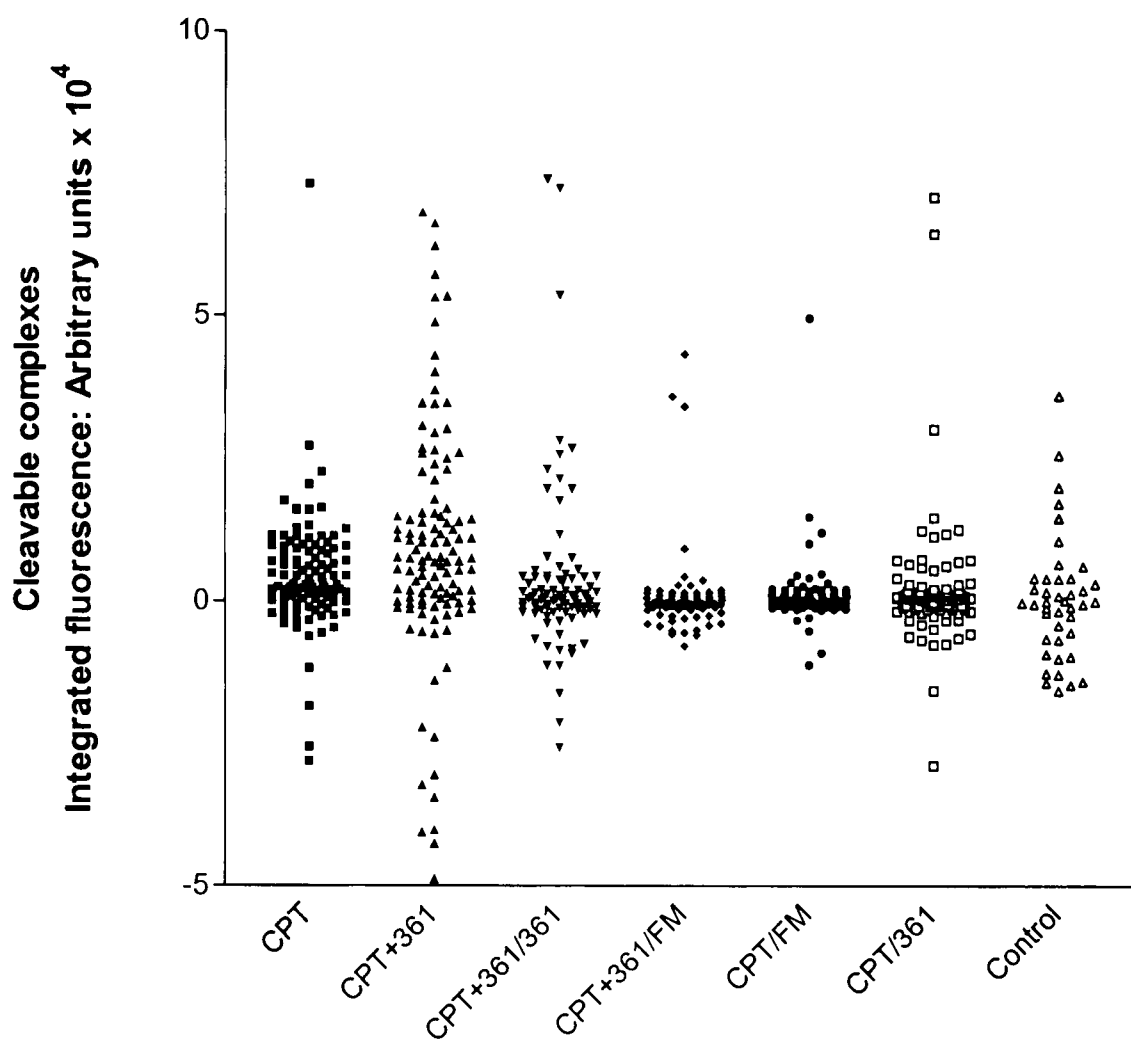


Figure 4.7 Effect of AG14361 on persistence and reversal of camptothecin-stabilised cleavable complexes.

K562 cells were exposed to 10 μ M camptothecin in the presence or absence of 0.4 μ M AG14361 (CPT, and CPT + 361) for 30 mins before removal of the drug and replacement with fresh medium (/FM) or medium containing AG14361 (/361) for a further 30 mins. An untreated control is also shown. Cleavable complexes were measured using the TARDIS assay. Data are the FITC-associated fluorescence for individual cells from one representative experiment.

Conditions	Cleavable complexes Mean % Camptothecin alone control \pm SEM
Untreated control	25 \pm 21
Camptothecin followed by incubation in fresh medium	38 \pm 25
Camptothecin followed by 30 min incubation in medium containing AG14361	34 \pm 11
Camptothecin + AG14361	108 \pm 40
Camptothecin + AG14361 followed by 30 min incubation in fresh medium	24 \pm 14
Camptothecin + AG14361 followed by 30 min incubation in medium containing AG14361	42 \pm 16*

Table 4.1 Effect of AG14361 on persistence and reversal of camptothecin-induced cleavable complexes.

K562 cells were treated with 10 μ M camptothecin in the presence or absence of 0.4 μ M AG14361 for 30 mins followed by drug removal and a post incubation in the presence or absence of AG14361 for a further 30 mins. Table shows mean integrated fluorescence values expressed as a percentage of the camptothecin alone control for each experiment. Data are the mean of 4 independent experiments \pm SEM.

* significantly different from cleavable complex levels in cells incubated with fresh medium after a 30 min incubation in camptothecin + AG14361 (p = 0.028 paired t-test)

4.3.2.4 Effect of PARP-1 stimulation by ionising radiation (IR) on cleavable complex formation.

It was possible that reason that there was no effect of AG14361 on camptothecin-induced complexes was because PARP-1 was not maximally stimulated. If PARP-1 activity is at a basal level in the cells, AG14361 may not have a detectable effect. However, stimulation of PARP-1 activity by IR-induced DNA breaks, should mean that there is a marked difference in poly(ADP-ribosylation) levels between irradiated cells (high PARP-1 activity) and AG14361-treated irradiated cells (less PARP-1 activity). Therefore, the effect of IR-stimulation of PARP-1 on levels of cleavable complexes in response to treatment with camptothecin in the presence or absence of AG14361 was investigated.

K562 cells were irradiated with 6 Gy, this dose was chosen as it corresponds to the LC₉₀ for L1210 cells and causes significant PARP-1 activation in whole cells as measured by NAD⁺ depletion (Bowman *et al.*, 2001). Immediately after irradiation cells were treated with 10 µM camptothecin in the presence or absence of 0.4 µM AG14361 for a further 30 mins and cleavable complexes were measured using the TARDIS assay. The results in Figure 4.8 demonstrate that there was no significant difference between the levels of cleavable complexes in cells treated with camptothecin and IR, camptothecin and AG14361, and camptothecin, AG14361 and IR compared to camptothecin alone ($p = 0.2$ paired t-test). Therefore stimulation of PARP-1 did not significantly reduce levels of camptothecin-stabilised cleavable complexes and AG14361 did not increase the levels of camptothecin-stabilised cleavable complexes relative to irradiated cells.

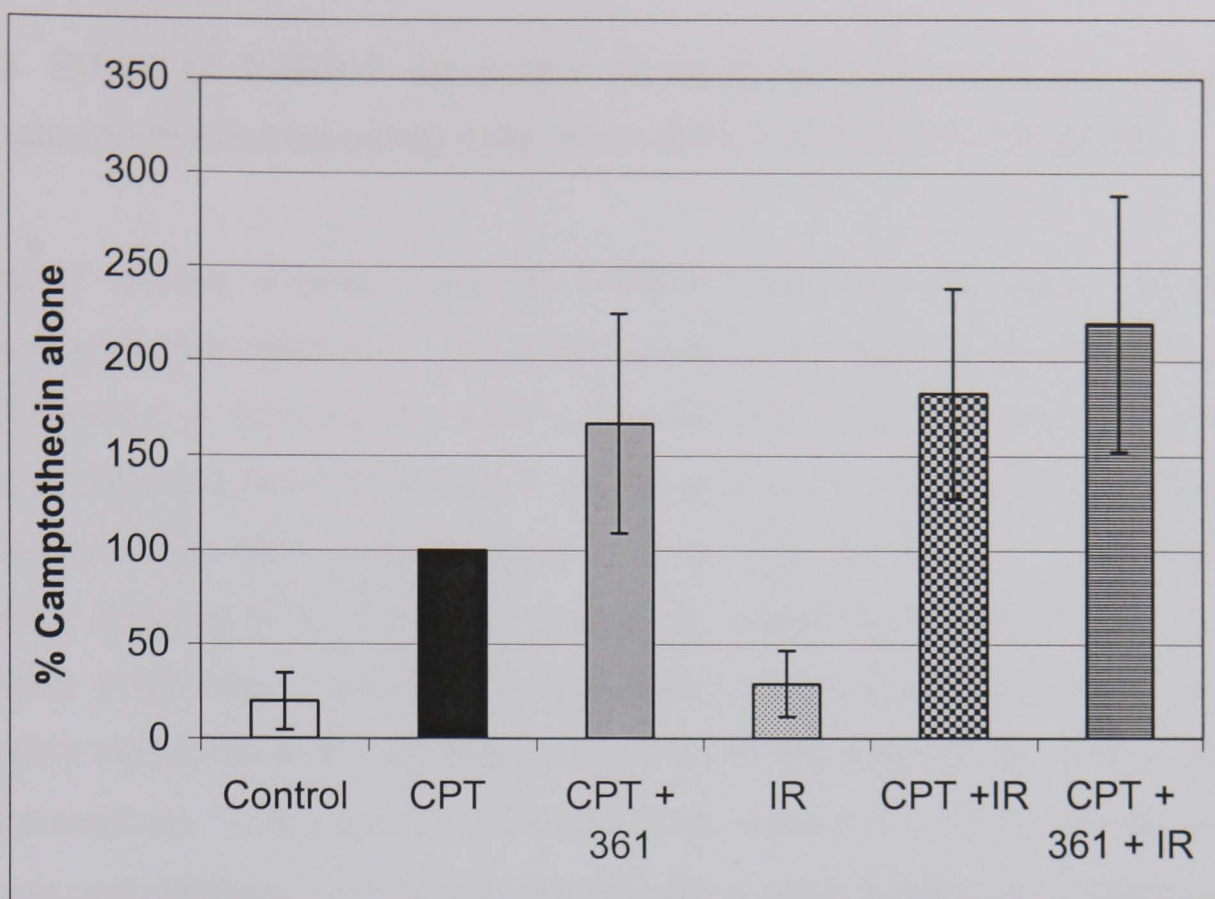


Figure 4.8 Effect of PARP-1 stimulation on levels of cleavable complexes in cells treated with camptothecin in the presence or absence of AG14361.

K562 cells were irradiated with 6 Gy IR before exposure to 10 μ M camptothecin in the presence or absence of 0.4 μ M AG14361 for 30 mins. Cleavable complexes were measured using the TARDIS assay. Integrated fluorescence values for individual experiments were expressed as a percentage of the camptothecin alone control for each experiment. Mean data from 3 independent experiments \pm SEM are shown.

4.3.3 Effect of PARP-1 on levels of camptothecin-stabilised cleavable complexes measured using potassium-SDS precipitation (K-SDS).

To verify the data obtained using the TARDIS assay, a second assay, was used to measure cleavable complexes. The K-SDS precipitation assay is not as specific as the TARDIS assay in detecting topo I-DNA cleavable complexes, as it does not use topo I-specific antibodies but instead detects any covalent protein-DNA complex. However, increases in cleavable complex levels seen in cells treated with camptothecin is generally assumed to be due to an increase in camptothecin-stabilised topo I-DNA cleavable complexes. This assay is more widely used and has been shown to detect cleavable complexes following longer exposures to camptothecin (A. Jobson personal communication). In this section, K562 cells were exposed to 1 or 10 μM camptothecin as these concentrations were shown to give good reproducible signals in the presence or absence of 0.4 μM AG14361 for 30 mins or 16 hours using the K-SDS assay in preliminary experiments. A 30 min exposure was used to allow comparison with data obtained using the TARDIS assay, a 16 hour exposure was used to investigate the effect of longer exposures and allow comparison with the cytotoxicity studies presented in section 3.3.5.

To conduct the K-SDS assay K562 cells were labelled with ^{14}C -thymidine to allow quantification of the results. These cells were then treated with camptothecin and AG14361 as appropriate. The cells were then lysed with SDS to dissociate non-covalent protein-DNA complexes. Addition of potassium chloride leads to the formation of insoluble potassium dodecyl sulfate crystals, which precipitate the protein-DNA covalent complexes, leaving protein-free DNA in solution. This allows purification of the complexes through a series of wash steps and quantification by scintillation counting (see section 2.9).

4.3.3.1 Effect of AG14361 on levels of camptothecin-stabilised cleavable complexes.

The effect of AG14361 on levels of covalent protein-DNA complexes formed after a 30 min exposure to camptothecin measured by K-SDS is shown in Figure 4.9 and Table 4.2. These figures show that there was an increase in complex levels corresponding to

the increasing concentration of camptothecin but the levels of complexes were not significantly increased or decreased in the presence of AG14361. There was no significant change in complex levels when cells were exposed to AG14361 alone compared to untreated cells.

To determine whether it was necessary to expose cells for a longer in order to detect any changes in cleavable complexes the effect of a 16 hour exposure to camptothecin was investigated. The levels of cleavable complexes in K562 cells exposed to camptothecin in the presence or absence of AG14361 for 16 hours are shown in

Figure 4.10 and Table 4.3. These data also show an increase in the level of cleavable complexes with increasing concentration of camptothecin and again the levels of camptothecin-stabilised complexes were not affected by the presence of AG14361.

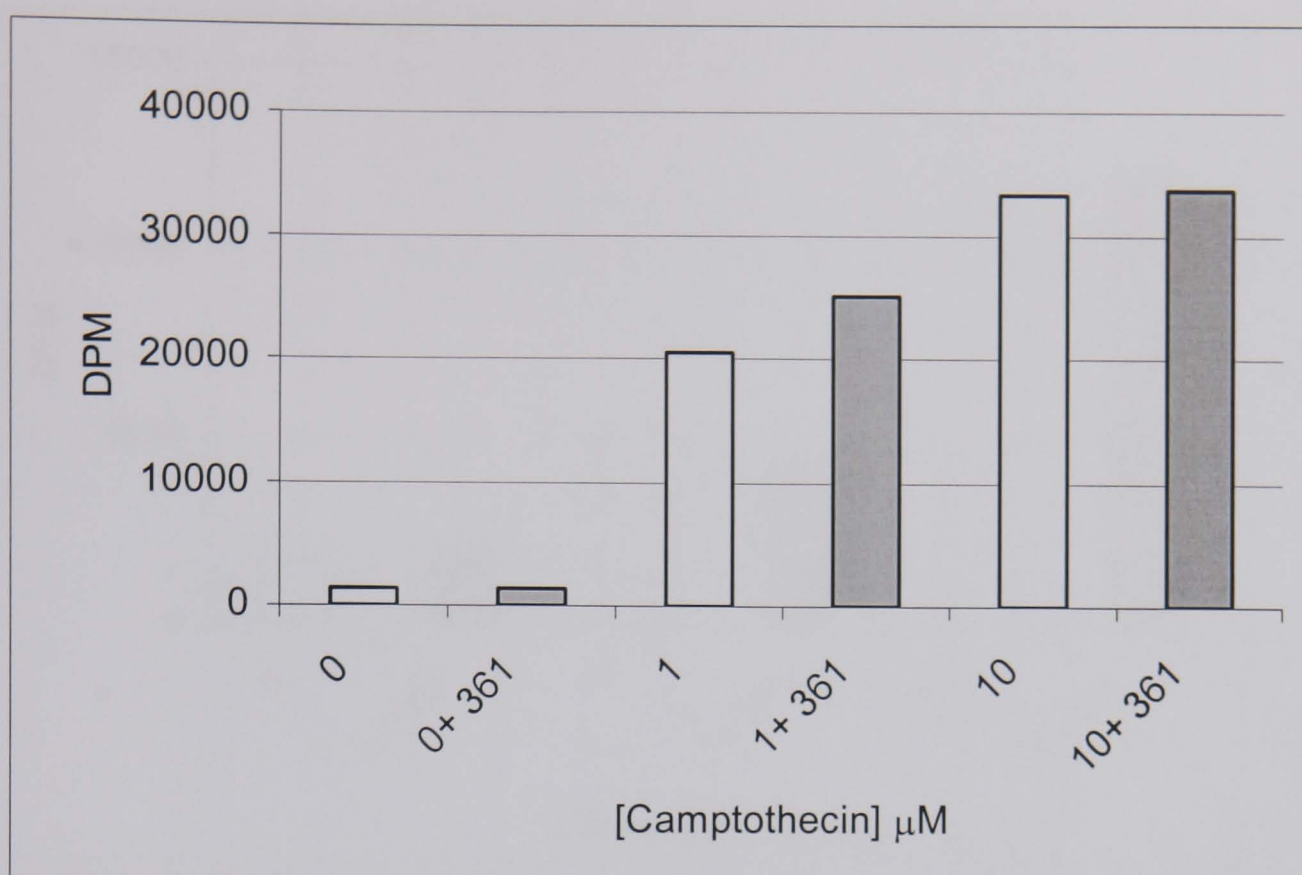


Figure 4.9 Effect of 30 min exposure to AG14361 on cleavable complex formation.

K562 cells were exposed to 0, 1 or 10 μM camptothecin for 30 mins in the presence or absence of 0.4 μM AG14361 before measurement of protein-DNA complexes using the K-SDS assay (see section 2.9). Bar chart shows mean [¹⁴C]-associated radioactivity data from 3 samples from one representative experiment.

[Camptothecin] μM	Protein-DNA complexes		Fold increase
	Camptothecin alone	Camptothecin + AG14361	
1	798 ± 351	934 ± 463	1.17 ± 0.77
10	1202 ± 620	1311± 621	1.09 ± 0.75

Table 4.2 Effect of PARP-1 inhibition on cleavable complex formation.

K562 cells were exposed to camptothecin in the presence or absence of 0.4 μM AG14361 for 30 mins. Levels of cleavable complexes were expressed as a percent of the DMSO or 0.4 μM AG14361-treated control as appropriate. Mean data from 3 independent experiments are given ± SEM.

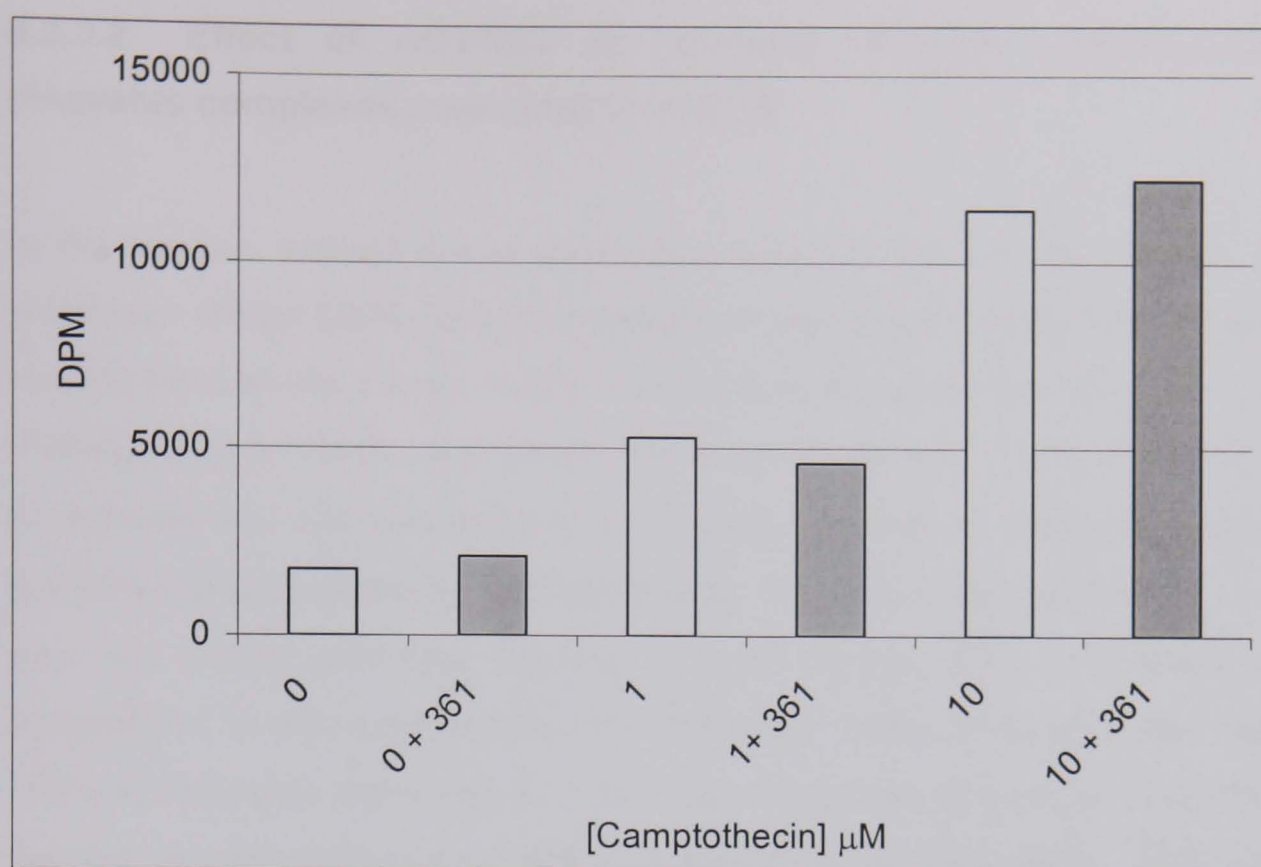


Figure 4.10 Effect of 16 hour exposure to AG14361 on cleavable complex formation.

K562 cells were exposed to 0, 1 or 10 μM camptothecin for 16 hours in the presence or absence of 0.4 μM AG14361 before measurement of cleavable complex levels using the K-SDS assay (see section 2.9). Bar chart shows mean [¹⁴C]-associated radioactivity data from 3 samples from one representative experiment

[Camptothecin] μM	Protein-DNA complexes		Fold increase
	Camptothecin alone	Camptothecin + AG14361	
1	206 ± 46	194 ± 29	0.94 ± 0.25
10	457 ± 94	516 ± 62	1.13 ± 0.27

Table 4.3 Effect of AG14361 on cleavable complex formation.

K562 cells were exposed to camptothecin in the presence or absence of 0.4 μM AG14361 for 30 mins. Levels of cleavable complexes were expressed as a percent of the DMSO or 0.4 μM AG14361-treated control as appropriate. Mean data from 3 independent experiments are given ± SEM

4.3.3.2 Effect of AG14361 on reversal of topo I poison-stabilised cleavable complexes measured by K-SDS.

In the previous sections it was shown that AG14361 had no effect on the levels or persistence of topo I-DNA cleavable complexes measured using the TARDIS assay. To confirm these results a more widely used method, the potassium-SDS assay was used. Previous work by Beidler and Cheng (1995) had shown that < 20% complexes formed by exposure to 5 μ M camptothecin for 60 mins remained 30 mins after camptothecin was removed as measured by the K-SDS assay. To ensure that protein-DNA complexes were still present after drug removal, a shorter reversal time of 10 mins was used compared to 30 mins used with the TARDIS assay. Initial studies had also shown that ~50% of complexes had reversed 10 mins after camptothecin removal in the K562 cells therefore this was deemed a suitable time point for these experiments. K562 cells were treated with 10 μ M camptothecin for 30 mins and allowed to reverse for 10 mins in fresh medium or medium containing AG14361. The results in Figure 4.11 show that there was no significant difference in the levels of cleavable complexes remaining after 10 minutes in drug free medium ($56.0 \pm 9.6\%$ remaining) or medium containing AG14361 ($56.7 \pm 8.4\%$ remaining).

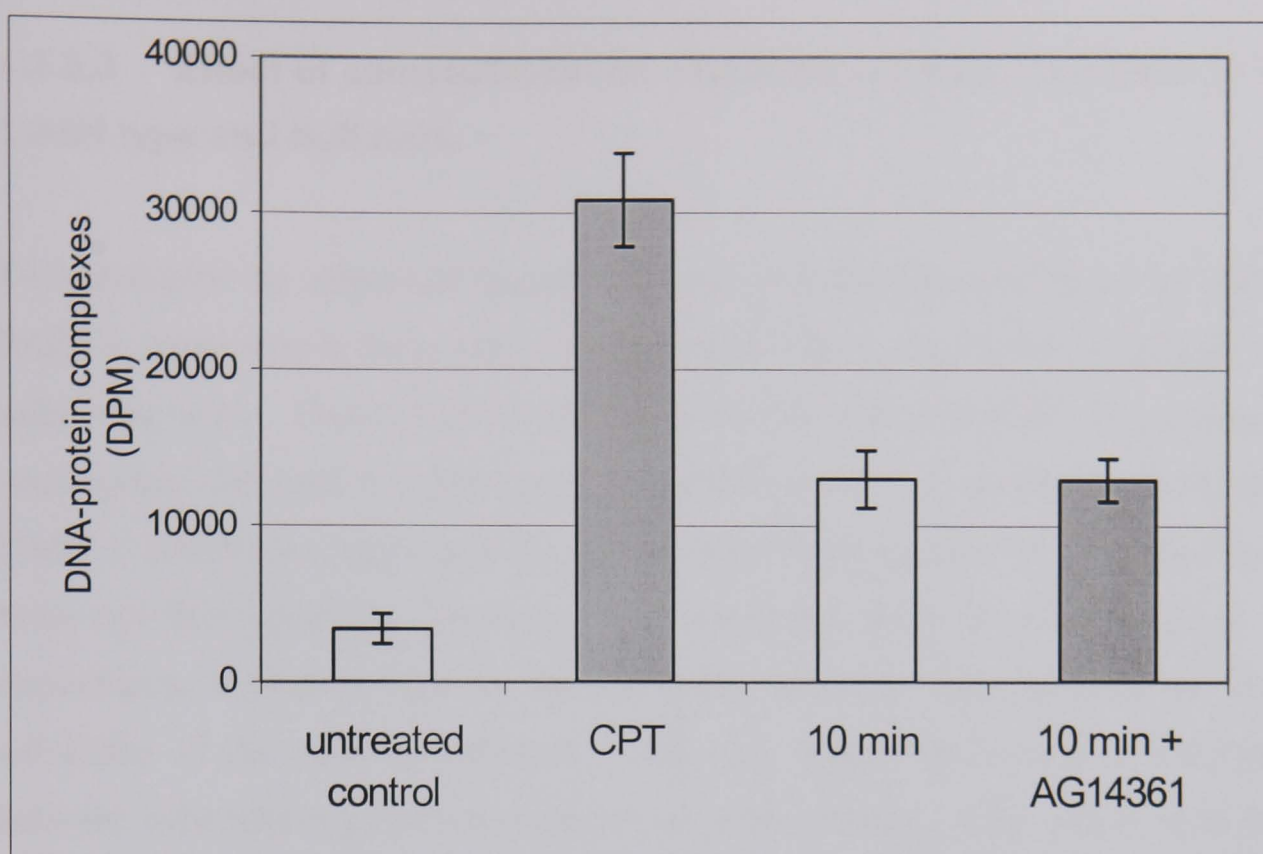


Figure 4.11 Effect of AG14361 on reversal of topo I poison-mediated cleavable complexes.

K562 cells were treated with 10 μ M camptothecin in the presence or absence of 0.4 μ M AG14361 for 30 mins and then allowed to reverse for 10 mins in drug free medium or medium containing 0.4 μ M AG14361. A control sample treated with camptothecin and not allowed to repair (CPT) and a DMSO control were included for comparison. Cells treated with camptothecin + AG14361 and not allowed to repair are not shown but were not significantly different to those cells treated with camptothecin alone. Cleavable complexes were measured by K-SDS as described in section 2.9. Graph shows mean [14 C]-associated radioactivity (DPM) from three independent experiments \pm SEM.

4.3.3.3 Effect of camptothecin on cleavable complex formation in PARP-1 wild type and null cells.

To investigate the effects of camptothecin on cleavable complexes in the absence of PARP-1 rather than in the presence of inhibited PARP-1, the PARP-1 wild type and null cells were used. This allowed investigation of the role of PARP-1 in protein-protein interactions with topo I, which might modulate its activity, distinct from the effect of PARP-1 activity on topo I activity. These cells were exposed to camptothecin for 30 mins and then cleavable complexes were measured using the K-SDS assay. Initial experiments showed a lack of reproducibility between replicate samples, and large variability in the untreated controls. This was thought to be due to washing steps between radiolabelling and resuspension of these adherent cells, which were different from the previous experiments using the K562 suspension cells. Many alterations in methodology were tried but unfortunately due to time limitations a conclusive result could not be obtained. Given more time alternative methods for the measurement of cleavable complexes in these cells would have been investigated.

4.4 Discussion.

The purpose of this chapter aimed to investigate the effects of AG14361 on topo I activity. Previous authors have demonstrated that topo I activity can be inhibited by poly(ADP-ribosylation) and it is thought that this is due to the increase in negative charge conferred on the topo I by ADP-ribose units, causing the repulsion of topo I away from the DNA (reviewed in section 4.1).

The effect of AG14361 on topo I activity has been explored using three different techniques. Topo I activity was determined using an assay to measure the DNA relaxation activity of topo I. The DNA relaxation assay measures the ability of topo I in cell extracts, to nick, unwind and religate plasmid DNA, converting DNA from the supercoiled to relaxed form. Topo I activity was also measured indirectly through the measurement of the cleavable complexes formed in response to treatment with topo I poisons using two different methods. The number of cleavable complexes formed during the catalytic cycle of topo I are proportional to the activity of the topo I in the cell. The transient topo I-DNA cleavable complex can be stabilised by topo I poisons, and are rapidly reversed on the removal of the drug (Covey *et al.*, 1989, Padget *et al.*, 2000a). Therefore the quantification of the levels of cleavable complexes following drug treatment is a good measure of the activity of the topo I in the cell.

The first method used to detect cleavable complexes was the TARDIS assay, a specific immunofluorescent assay that measures the levels of topo I covalently bound to DNA in individual cells, using topo I-specific antibodies (Padget *et al.*, 2000a). The second method was the K-SDS precipitation assay which measures the level of covalent protein-DNA complexes (Rowe, 2000). This method has been more widely used but is not necessarily specific for the topo I-DNA complexes above any other covalent protein-DNA complex as antibodies are not used. This method precipitates any protein that is covalently bound to DNA. However, it can be assumed that any increase in complex levels observed in response to treatment with topo I poisons will be due to an increase in topo I-DNA cleavable complexes.

The effect of AG14361 following two different drug exposures of 30 mins and 16 hours were investigated using the relaxation assay and K-SDS. These time points correspond to those used in the cytotoxicity assays in chapter 3. Only the 30 min time point was investigated using the TARDIS assay as it had previously been shown that the levels of complexes decreased in these cells following 1.5 hours exposure to camptothecin without drug removal, (Padget *et al.*, 2000a). It had previously been shown that there was a more than 50% decrease in levels of cleavable complexes in the presence of camptothecin following a 5 hour exposure, compared to a 30 mins exposure. The results presented in this thesis also show that there was a massive reduction in cleavable complexes detected by K-SDS following a 16 hour exposure to camptothecin compared to those detectable after just 30 mins. Therefore it was assumed that after 16 hours the cleavable complex levels would barely be detectable using this assay.

In this chapter it has been shown that topo I relaxation activity was not altered in K562 cells following 30 mins exposure to AG14361 compared to an untreated control. AG14361 did not increase the levels of cleavable complexes formed following a 30 min exposure to camptothecin as measured by both the TARDIS and K-SDS assays. This was not entirely unexpected as a 30 min exposure to AG14361 failed to potentiate camptothecin cytotoxicity (section 3.3.5). However, topo I relaxation activity and levels of cleavable complexes were not affected following exposure to AG14361 for 16 hours either. Therefore it would seem that the potentiation of camptothecin-induced cytotoxicity by AG14361 is not related to changes in relaxation activity of topo I or the level of cleavable complexes formed in response to treatment with camptothecin.

These results are not consistent with the early published data on the effect of PARP-1 on topo I activity. Jongstra-Bilan *et al.*, (1983) and Ferro and Olivera (1984) found that PARP-1 inhibits topo I relaxation activity and that this inhibition could be reversed by nicotinamide and 3-AB. However, these early studies were conducted using highly purified topo I and PARP-1 proteins in the presence of NAD⁺ and small double stranded DNA to stimulate PARP-1 activity. As these assays were conducted with purified enzymes, and do not take into account the role of other cellular factors that might affect topo I-DNA interactions, such as histones, these experiments may not be representative of the situation in the cell. The data presented in this thesis is consistent the findings of Boothman *et al.*, (1994) who investigating the effect of PARP-1 inhibition by PD-

128763 in U1-Mel radio-resistant melanoma cells. In this study it was shown that there was no change in topo I relaxation activity in these cells following a 5 hour exposure to concentrations up to 3 mM PD-128763.

Similarly, studies conducted Beidler *et al.*, (1996) agree with the data presented in this chapter. Biedler and co-workers showed that in KB cells an incubation of up to 24 hours with 1 mM 3-AB had no effect on topo I cleavable complexes as measured by K-SDS precipitation. Nor did the presence of 3-AB for up to 24 hours increase the level of cleavable complexes formed by a 30 min pulse with 5 μ M camptothecin in parental KB cells or their camptothecin-resistant derivatives. Therefore they concluded that PARP-1 inhibition did not alter the levels of topo I protein available for complex formation following camptothecin exposure.

The possibility that the difference between basal (unstimulated) PARP-1 activity and PARP-1 activity in the presence of AG14361 in K562 cells was too small to detect an effect of PARP-1 on topo I activity was investigated as had been previously by Boothman *et al.*, (1994). These authors showed that 3-AB did not alter the activity of topo I unless the cells had been treated with IR prior to treatment with camptothecin. In theory, treatment with IR would create DNA strand breaks that would stimulate PARP-1 activity. This might result in maximal stimulation of PARP-1 and higher levels of poly(ADP-ribosylation) on topo I resulting in its inhibition. Therefore treatment with IR and camptothecin should result in lower levels of cleavable complexes than treatment with camptothecin alone. Use of AG14361 could therefore prevent this inhibition and result in the formation of higher levels of cleavable complexes when used in combination with camptothecin and IR. Following the observation that there was no change in levels of topo I activity in response to treatment with AG14361 in this thesis, it was thought that PARP-1 may not be maximally stimulated under the conditions used. Therefore cells were exposed to camptothecin following treatment with IR. However, the results shown in Figure 4.8 demonstrate that this was not the case and that stimulation of PARP-1 had no significant effect on levels of cleavable complexes compared to treatment with camptothecin alone. The discrepancy between these studies may be related to the use of confluence arrested cells in the study by Boothman and exponentially growing cells in this study causing the cells to respond differently. Topo

I poisons and IR cause synergistic cell killing in various human tumour cells and this is associated with an increase in the level of protein-DNA complexes formed (Boothman *et al.*, 1992). This is in conflict with the experimental data suggesting that PARP-1 activation by IR results in a reduction in topo I cleavable complex formation. However the data presented in this chapter does not support the proposals that topo I cleavable complexes are increased or decreased by IR nor that PARP-1 inhibition has an effect on complex formation in irradiated or non-irradiated cells.

In the study reported here the levels of protein-DNA complexes were significantly reduced following a 16 hour exposure to camptothecin compared to that seen at 30 mins. A decrease in the level of cleavable complexes over time despite the continued presence of a topo I poison has been observed by a number of other authors (Beidler *et al.*, 1995, Danks *et al.*, 1996, Padget *et al.*, 2000a). Beidler *et al.*, (1995) showed a time-dependent decrease in the level of protein-linked DNA strand breaks (PLDB) when KB cells were exposed to 5 μ M camptothecin and that the most rapid loss of PLDB was seen in the first 6 hours of exposure. Reversal of topotecan-stabilised complexes in human SJ-G5 anaplastic astrocytoma cells in the presence of drug has also been observed by Danks *et al.*, (1996). This was shown to be related to redistribution of the topo I from the nucleoli within 60 mins of exposure to topotecan and was accompanied by a small but significant decrease in the amount of topo I in the nucleus coupled with a simultaneous 50-100% increase in the levels of the 67 kDa topo I fragment in the cytoplasm. Subsequent authors have reported that this nuclear delocalisation is related to sumoylation of the protein. SUMO's are small ubiquitin-like modifiers that conjugate to target proteins and may act as a tag for delocalisation (Mo *et al.*, 2001, Rhallabandi *et al.*, 2002, Desai *et al.*, 2001 and 1997). Therefore it is possible that the decrease in complexes seen here at 16 hours compared to 30 mins is due to redistribution of topo I in response to drug treatment.

Interestingly, PARP-1 has also been shown to delocalise following treatment with the RNA synthesis inhibitor 5,6,-dichloro-1- β -ribofuranosyl-benzimidazole (DRB) (Desnoyers *et al.*, 1996). PARP-1 is distributed throughout the nuclei but is concentrated in the nucleoli. On treatment with concentrations of DRB that inhibited uridine incorporation by 75%, PARP-1 was found to be distributed evenly throughout

the nucleus. Similar results were found using actinomycin D. Topo I has been shown to translocate in response to the same inhibitors as those causing delocalisation of PARP-1. However the translocation of PARP-1 was seen to precede that of topo I, and PARP-1 was not degraded as has been seen for topo I in some cell types. This may have implications when determining the exact role of PARP-1 in the response to topo I poisons and will be important when considering the scheduling of administration of topo I poisons and PARP-1 inhibitors.

The reversal of cleavable complexes was studied at two time points. 30 mins after drug removal in the TARDIS assay and 10 mins after drug removal using K-SDS precipitation. Cleavable complexes are known to reverse rapidly following removal of drug, therefore these time-points were chosen based on previous data and initial experiments (Beidler *et al.*, 1995, Padget *et al.*, 2000a). Using the TARDIS assay a variety of combinations of AG14361 and camptothecin exposures were used to determine whether AG14361 increased the persistence of the cleavable complex after camptothecin removal. Inclusion of AG14361 after camptothecin removal did not increase the induction of complexes, nor did the inclusion of AG14361 in the camptothecin exposure and reversal incubation increase persistence compared to samples treated with camptothecin alone. However, there was a significant increase in the persistence of the cleavable complexes formed when cells were treated with AG14361 and camptothecin followed by incubation in AG14361 alone compared to those treated with AG14361 and camptothecin followed by incubation in fresh medium. This may suggest that AG14361 is involved in the persistence of camptothecin-stabilised cleavable complexes, however it must be noted that there was no significant difference between either of these samples and those cells treated with camptothecin and allowed to repair in fresh medium. Therefore care must be taken in the interpretation of these results. Results obtained using the K-SDS assay showed that AG14361 did not increase the persistence of camptothecin-stabilised cleavable complexes. These results suggest that PARP-1 is not involved in the reversal of topo I-cleavable complexes, apart from the one anomalous result showing significant persistence, obtained with the TARDIS assay. To be confident of this result other experiments need to be conducted. The K-SDS is probably not specific enough to detect such small differences, therefore other assays such as the ICE bioassay or non-de-proteinising alkaline elution could be used.

Evidence to support the role of PARP-1 in the persistence of cleavable complexes has been published recently by Plo *et al.*, (2003). In this study it was shown that the tyrosyl DNA phosphodiesterase that is primarily responsible for the removal of the cleavable complex, co-immunoprecipitates with XRCC1. Such a functional association suggests that the BER pathway may repair the damage caused by processing of the cleavable complex. As PARP-1 is involved in BER it is possible that PARP -1 is involved in the removal of topo I poison-stabilised cleavable complexes.

Although all of the methods here have looked at topo I, it is possible that poly(ADP-ribosylation) of other proteins could affect topo I activity. Histones, for example are poly(ADP-ribosylated), and this results in loosening of chromatin that may increase the access of topo I to DNA, increasing activity. Therefore inhibition of PARP-1 could reduce topo I activity. Of course these two actions could also offset each other. However the data presented in this chapter suggests that topo I may not be poly(ADP-ribosylated) or if it is, it does not affect activity, and that if histones are modified by poly(ADP-ribose) then this does not effect topo I access to DNA.

The data presented in this chapter show that PARP-1 inhibition seems to have little effect on topo I activity, in contradiction to the early publications on this area of research. Much of the early published data was produced using purified systems which are not representative of the cellular environment. Therefore, after using one of the most potent PARP-1 inhibitors available and three different methods of measuring topo I activity under a variety of conditions in whole cells and extracts, it can be concluded that AG14361 has no effect on topo I activity or levels of cleavable complexes. There was a suggestion that AG14361 did lead to the persistence of cleavable complexes using the TARDIS. However, these data should be treated with caution until further work can be carried out. Therefore based on these data it can be concluded that potentiation of topo I poison mediated growth inhibition or cytotoxicity by AG14361 is not due to an increase in topo I activity by AG14361.

Summary.

- 30 min or 16 hour exposure to AG14361 does not effect the relaxation activity of topo I.
- AG14361 does not increase the level of camptothecin-stabilised cleavable complexes measured by the TARDIS and K-SDS assays.
- Stimulation of cellular PARP-1 activity by irradiation does not modulate topo I activity.
- AG14361 may increase the persistence of camptothecin-stabilised DNA strand breaks after removal of camptothecin however further investigation is required.

Chapter 5

Effect of PARP-1 on inhibition of topo I poison-induced DNA single strand breaks.

5.1 Introduction.

In this chapter the role of PARP-1 in the repair of topo I poison-mediated DNA damage was investigated. In the previous chapters a role for PARP-1 in topo I poison mediated cytotoxicity and growth inhibition has been demonstrated. Two hypotheses were proposed to explain this, (i) modulation of topo I activity by poly(ADP-ribosylation) of topo I or (ii) repair of topo I poison-mediated DNA damage by PARP-1. The effect of PARP-1 inhibition on topo I activity was investigated in chapter 4 and it was shown that AG14361 had little effect on topo I activity under the conditions studied. Therefore in this chapter the second hypothesis was investigated; that PARP-1 was involved in the repair of topo I poison induced DNA damage.

Topo I poisons cause a number of different DNA damage lesions, as shown in Figure 5.1, and this may implicate a number of pathways in the repair of topo I poison-mediated DNA damage. The evidence for the involvement of PARP-1 in the repair of DNA single strand breaks via the BER pathway is overwhelming (see section 1.6.7). There is also very good evidence showing the importance of BER in topo I poison-mediated cytotoxicity (described in this chapter and chapter 6). To investigate if PARP-1 is involved in the repair of topo I poison-induced DNA single-strand breaks, the effect of AG14361 on camptothecin-induced single-strand breaks was determined.

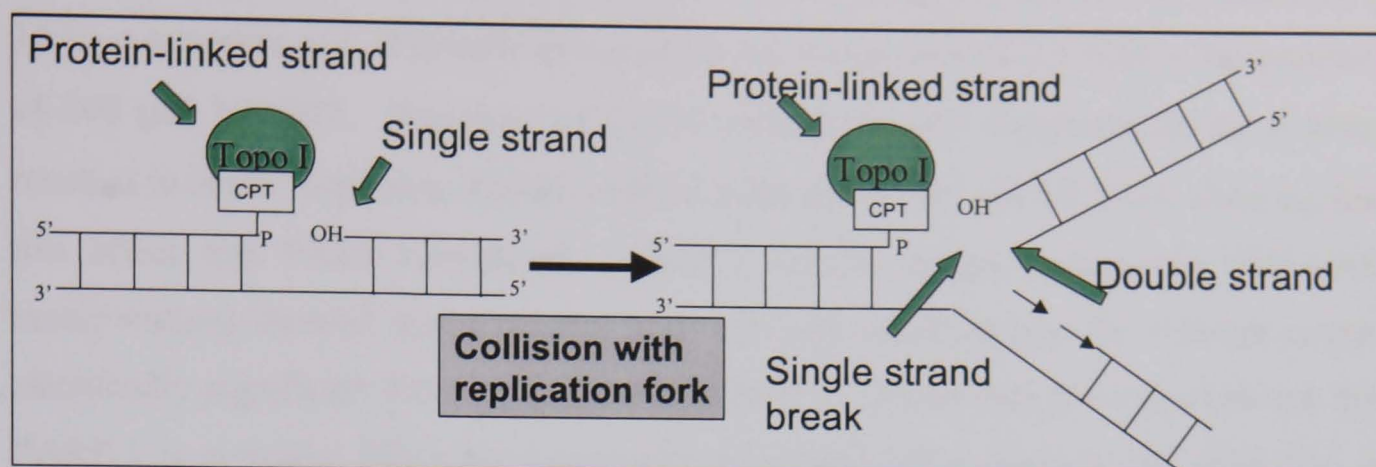


Figure 5.1 Types of DNA damage caused by topo I poisons.

Topo I binds to DNA to form a protein-linked DNA strand break that can be stabilised by topo I poisons such as CPT, and a single strand break. Collision with the progressing replication fork converts the single strand break into a double strand break and leaves a single strand break on the lagging strand.

The role of PARP-1 in BER has been reviewed in section 1.6.7. PARP-1 inhibition results in potentiation of cytotoxicity caused by alkylating agents and IR, whose damage is repaired by the BER pathway. The potentiation of cytotoxicity by PARP-1 inhibitors is related to a decrease in strand break rejoining (Durkacz *et al.*, 1980, Bowman *et al.*, 1998). Similarly, PARP-1 deficient cells are hypersensitive to alkylating agents and IR, and are defective in repair of damage caused by these agents (Menissier de Murcia *et al.*, 1997, Masutani *et al.*, 1999, and reviewed in Shall and de Murcia, 2000). It has also been demonstrated *in vitro* that in the absence of PARP-1 long patch BER is ineffective and short patch repair is impaired by 50% (Dantzer *et al.*, 2000). In addition to this, PARP-1 co-immunoprecipitates with XRCC1, DNA ligase V1, FEN-1 and DNA pol- β , proteins known to be involved in BER (Dantzer *et al.*, 2000, Masson *et al.*, 1998, Lavrik *et al.*, 2001). Thus, there is good evidence for a role for PARP-1 in BER. The exact nature of this role is still in dispute due to many conflicting reports, some suggesting that BER is efficient in the absence of PARP-1 (Vodenicharov *et al.*, 2000). However evidence for the role of PARP-1 in BER does not implicate PARP-1 in the repair of topo I poison-mediated DNA damage.

Direct evidence for the role of PARP-1 in repair of DNA single strand breaks induced by topo I poisons was provided by work conducted in the NICR (Bowman PhD thesis,

1999, and Bowman *et al.*, 2001). The level of DNA single strand breaks induced by a 16 hour exposure of L1210 cells to camptothecin was increased 2.5-fold in the presence of 200 μ M NU1025. Exposure of L1210 cells to 60 nM camptothecin for 6 hours resulted in NAD⁺ depletion, which could be reduced by 200 μ M NU1025, showing that this effect was PARP-1-mediated. PARP-1 activity assays (measuring [³²P]-NAD incorporation) showed that treatment with 120 nM camptothecin for 6 hours caused statistically significant 4-fold activation of PARP-1. These data provide evidence that PARP-1 is activated following camptothecin-induced DNA damage and inhibition of PARP-1 increases strand breaks, implicating PARP-1 in the repair of these breaks. Similar results were obtained by Mattern *et al.*, (1987) who demonstrated that potentiation of camptothecin cytotoxicity by 3-AB was associated with an increase in the yield of DNA strand breaks. Exposure of L1210 cells to 1 or 5 mM 3-AB for 16 hours and subsequently to camptothecin for a further 60 mins in the presence of 3-AB resulted in a 2 to 3-fold increase in DNA single strand breaks. However, these workers proposed that the increase in DNA strand breaks and cytotoxicity was due to the prevention of PARP-1-mediated repression of topo I activity.

Evidence for the role of PARP-1 in the repair of topo I poison-mediated DNA damage is scarce. However there is evidence connecting BER to the repair of camptothecin-induced damage therefore indirectly implicating PARP-1 via its role in BER. Most of this evidence has come from the use of cells deficient in the BER scaffold protein XRCC1. The EM9 Chinese hamster ovary cell line isolated on the basis of its increased sensitivity to EMS is a cell line deficient in XRCC1 that has been studied in relation to topo I poison-induced DNA damage. These cells have a reduced rate of DNA strand break rejoining following treatment with X-rays, EMS or MMS and a high baseline frequency of sister chromatid exchange (Thompson *et al.*, 1982). These cells are hypersensitive to many alkylating agents (Caldecott and Jeggo, 1991). The defect in XRCC1 results in a reduction in DNA ligase III activity (Ikejima *et al.*, 1984, Barrows *et al.*, 1998). Most interestingly, although these cells have normal levels of both topo I, and PARP-1, they are 2 to 5-fold hypersensitive to camptothecin, following long and short-term exposures and this sensitivity is independent of replication (Caldecott and Jeggo, 1991, Palitti *et al.*, 1993, Barrows *et al.*, 1998). This shows that BER is involved in the response to camptothecin-induced DNA damage.

Further evidence has been provided in support of the role of XRCC1 in the repair of topo I poison-mediated DNA damage. Plo *et al.*, (2003) established a connection between XRCC1 and tyrosyl DNA phosphodiesterase (Tdp1) a protein responsible for the removal of the topo I peptide linked to 3'-DNA terminus by hydrolysing the covalent bond between the topo I tyrosyl residue and the 3'-DNA phosphate. They showed that XRCC1-complemented EM9 cells were able to repair topo I poison-induced DNA damage faster than the XRCC1 deficient EM9 cells. Following a 1 hour exposure to camptothecin and 30 mins repair in drug-free medium, levels of single strand breaks were approximately 3-fold higher in EM9 cells compared to XRCC1 complemented EM9 cells. This corresponded to enhanced Tdp1 activity in the complemented cells. Polynucleotide kinase (PNK) activity was enhanced in the XRCC1-complemented cells compared to the deficient line. PNK is a protein associated with the long patch BER pathway that is used to remove a 3'-phosphate produced as a result of removal of the topo I, or by other means, and replace it with a 3'-hydroxyl terminus that can be extended by DNA pol β and ligated. It was also shown that XRCC1 immunoprecipitates contained both Tdp1 and PNK peptides and activity, suggesting a functional link between the XRCC1 strand break pathway and the repair of topo I covalent complexes.

Further evidence for the role of XRCC1 and thus the BER pathway has been provided by Park *et al.*, (2002). These authors made cell lines resistant to camptothecin by exposure to increasing concentrations of camptothecin, revertant cell lines were also derived from the resistant cells by removing them from camptothecin-containing growth medium. These revertant cell lines were still 2-fold resistant compared to the parental KB cell line (Biedler *et al.*, 1995). The resistant cell line was shown to be over-expressing XRCC1 greater than 5-fold compared to the revertant cell line. The degree of resistance was related to the amount of XRCC1 present in the cell. Interestingly, resistance to camptothecin was reduced by ~20% when these cells were exposed to 1 mM 3-AB, therefore suggesting that the effect of XRCC1 on camptothecin resistance was modulated by PARP-1. This study therefore provides evidence for the role of PARP-1 in the response to camptothecin via the BER pathway, and its interaction with XRCC1.

5.2 Aims

In this chapter the aim was to investigate the second hypothesis for the role of PARP-1 in the response to topo I poisons; that PARP-1 is involved in the repair of topo I poison-mediated DNA damage. To investigate this hypothesis, the levels of DNA single strand breaks formed in response to treatment with camptothecin and AG14361 were determined. Single strand breaks were measured as these are the primary DNA lesions caused by treatment. Exposure times of 30 mins and 16 hours were used to correspond with the exposures used in the cytotoxicity assays in section 3 in order to see if the potentiation of cytotoxicity was related to increases in DNA strand breaks.

The effect of scheduling of AG14361 on levels of strand breaks formed in response to treatment with camptothecin was also investigated. This aimed to determine whether maximal strand breaks could be achieved when PARP-1 was inhibited for 16 hours before or after exposure to camptothecin for 30 mins as described by Mattern *et al.*, (1997). Results presented in chapter 3 showed that 30 mins exposure to camptothecin was sufficient to cause growth inhibition in K562 cells, but a 16 hour exposure to AG14361 was required for significant potentiation of camptothecin-induced cytotoxicity and growth inhibition. Therefore the studies described in this chapter were aimed to determine whether cytotoxicity was related to the levels of DNA strand breaks present following these exposures. These studies were also predicted to give an insight into the mechanism of enhancement of cytotoxicity by PARP-1. If enhancement of strand break levels was observed with exposure to AG14361 prior to camptothecin, this would suggest that a modification of topo 1 activity by poly(ADP-ribosylation) and/or poly(ADP-ribosylation) of other acceptor proteins may be required. Whereas increases in DNA strand breaks following a exposure to AG14361 after camptothecin would indicate that PARP-1 might play a role in the repair of topo I associated damage. The repair of camptothecin-induced DNA damaged after shorter repair times was also studied in the presence or absence of AG14361.

5.3 Results.

5.3.1 Effect of AG14361 on camptothecin-induced DNA single strand breaks.

PARP-1 inhibitors have been shown to increase the number of DNA strand breaks produced by exposure to camptothecin (Mattern *et al.*, 1987, Bowman *et al.*, 1998). The inhibitors used in these previous studies (3-AB, NU1025) were less potent than AG14361, but were able to increase the levels of DNA strand breaks induced by camptothecin by 2 to 3 fold. However these studies did not address the question as to whether the increased strand breaks was due to increased break formation or decreased repair. Therefore these experiments were designed to confirm the previous results and investigate in more detail the effects of a more potent PARP-1 inhibitor in levels of DNA single strand breaks. The effect of drug scheduling on strand breaks and the repair of the lesions was also investigated.

5.3.1.1 Effect of AG14361 on DNA single strand break levels in K562 cells exposed to camptothecin for 16 hours.

The initial conditions for this experiment were based on the work by Bowman *et al.*, (1998). In this paper the effect of 200 μ M NU1025 on levels of DNA single strand breaks formed in L1210 cells following treatment with camptothecin for 16 hours was investigated by alkaline elution. Potentiation of camptothecin-induced DNA strand breaks by NU1025 was observed using 15 and 40 nM camptothecin corresponding to the LC₅₀, and LC₉₀ for cytotoxicity of camptothecin following 16 hours exposure in L1210 cells. These studies demonstrated a good correlation between the enhancement of camptothecin-induced DNA strand breaks and cytotoxicity so the initial studies in this thesis aimed to reproduce these conditions except for substitution of AG14361 for NU1025 and the K562 cell line for the L1210 cell line.

In this study, K562 cells were exposed to camptothecin in the presence or absence of 0.4 μ M AG14361 for 16 hours. Concentrations of 15, 40 and 100 nM camptothecin were used initially to correspond with the concentrations used by Bowman *et al.*, (2001). DNA single strand breaks levels were measured using alkaline elution. The alkaline elution method separates DNA fragments on the basis of size using

polycarbonate filters. Radiolabelled cells were treated, applied to the filters and lysed. The DNA was then eluted through the filter into fractions using a buffer at pH 12. DNA strand breaks were quantified by liquid scintillation counting (for further details see section 2.10). The elution profile of K562 cells exposed to 15, 40 and 100 nM camptothecin in the presence or absence of AG14361 for 16 hours is shown in Figure 5.2A. Unfortunately at both 40 and 100 nM camptothecin the levels of DNA strand breaks were at the maximal level that can be measured using this assay as indicated by the steep gradient of the elution profile at these concentrations. Therefore, any increase in strand breaks caused by PARP-1 inhibition could not be detected and was not significantly different from camptothecin alone. A small increase in the levels of strand breaks in the presence of AG14361 compared to camptothecin alone was seen using 15 nM camptothecin but this was not significant ($p = 0.1$ paired t-test).

As the concentration range used in Figure 5.2A produced strand breaks at the upper limits of detection of the assay, the effect of PARP-1 inhibition on camptothecin-induced DNA strand breaks at lower doses of camptothecin was investigated. Concentrations of camptothecin corresponding to 50, 90 and 95% survival (3, 10, and 30 nM, respectively) as measured in chapter 3, were used. The elution profile in Figure 5.2B shows that levels of DNA strand breaks below the uppermost limits of detection were achieved. DNA strand breaks were expressed as relative elution i.e. the proportion of [^{14}C]-associated activity eluted when half of the [^3H]-activity has eluted, compared to an untreated control as this accounts for variation in elution rate between assays (see section 2.10.5). Mean relative elution values from both of the concentration ranges used are summarised in Table 5.1. This shows that there was an increase in single strand breaks corresponding to increasing concentrations of camptothecin as has been shown previously by Mattern *et al.*, (1989) and Bowman *et al.*, (2000). 0.4 μM AG14361 increased the number of single strand breaks induced by camptothecin by a factor of 1.2 to 2.4 at all concentrations of camptothecin, with greatest increases at lower concentrations of camptothecin. However, due to the inherent variability of the assay this was only significant at 30 nM camptothecin ($p = 0.004$, paired t-test). There was no significant DNA strand breakage following exposure to 0.4 μM AG14361 alone. Although the possibility that some of the DNA breaks observed were due to apoptosis cannot be ignored, it has been shown previously that L1210 cells exposed to 120nM

camptothecin for 16 hours only resulted in 8% of cells showing morphology typical of apoptosis. Therefore the number of strand breaks observed here should be representative of breaks produced by camptothecin and not skewed by breaks caused by apoptosis.

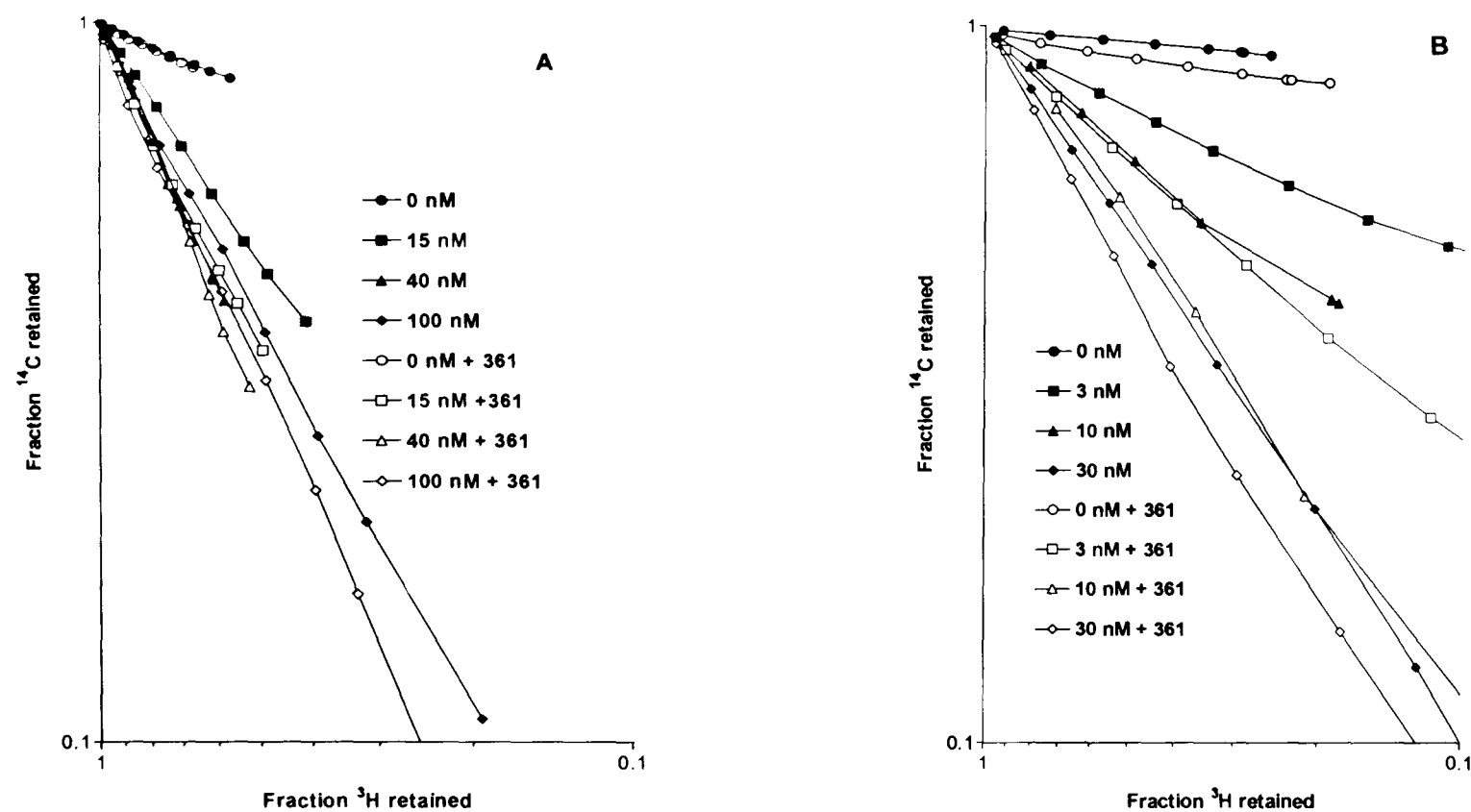


Figure 5.2 Effect of AG14361 on camptothecin-induced DNA single strand breaks.

K562 cells were exposed to (A) 15, 40, 100 nM or (B) 3, 10, 30 nM camptothecin in the presence or absence of 0.4 μ M AG14361 for 16 hours. DNA single strand breaks were measured by alkaline elution (see section 2.10). Representative elution profiles from each set of experiments are shown.

16 hour exposure	DNA single strand breaks (Relative Elution)		
Camptothecin (nM)	Camptothecin alone	Camptothecin + 0.4 μ M AG14361	Fold increase in strand breaks
3	0.021 \pm 0.02	0.08 \pm 0.05	2.4 \pm 0.7
10	0.12 \pm 0.05	0.15 \pm 0.04	1.6 \pm 0.5
15	0.17 \pm 0.06	0.23 \pm 0.02	1.6 \pm 0.4
30	0.20 \pm 0.04	0.26 \pm 0.04*	1.3 \pm 0.09
40	0.32 \pm 0.06	0.37 \pm 0.02	1.2 \pm 0.17
100	0.32 \pm 0.08	0.35 \pm 0.04	1.2 \pm 0.14

Table 5.1 Effect of AG14361 on levels of DNA single strand breaks induced by camptothecin.

K562 cells were exposed to camptothecin in the presence or absence of 0.4 μ M AG14361 for 16 hours prior to determination of DNA single strand breaks by alkaline elution (see section 2.10). Relative elution calculated by comparison with DMSO treated or 0.4 μ M AG14361 alone control as appropriate. Data are the mean \pm SEM for 3 independent experiments. Fold increase was calculated from mean RE values for individual experiments \pm SEM.

* p = 0.004 paired t-test.

5.3.1.2 Effect of AG14361 on DNA strand breaks formed by exposure to camptothecin for 30 min.

The 1.2 to 2.4-fold increase in camptothecin-induced DNA strand breaks by AG14361 following a 16 hour exposure corresponds reasonably well to the 2 to 3-fold potentiation of camptothecin-induced growth inhibition and cytotoxicity studies by AG14361 after 16 hours exposure described in chapter 3. In growth inhibition assays significant potentiation by AG14361 of a 30 min exposure to camptothecin was only seen at 100 nM camptothecin, even though 30 mins exposure to 0.4 μ M AG14361 was shown to be enough to reduce PARP-1 activity to less than 10% of normal (section 3.3.3). 30 mins was also the time taken to generate maximal levels of camptothecin-induced cleavable complexes (Padget *et al.*, 2000a), and camptothecin-induced DNA single strand breaks (Covey *et al.*, 1989). To determine whether the reduced level of potentiation observed following 30 mins exposure was related to levels of DNA strand breaks it was necessary to measure DNA strand breaks after a 30 min exposure to camptothecin in the presence or absence of AG14361.

To investigate this, K562 cells were exposed to a range of concentrations of camptothecin in the presence or absence of 0.4 μ M AG14361 for 30 mins. Following this DNA single strand breaks were measured by alkaline elution. A representative bar chart of relative elution values is shown in Figure 5.3 and pooled relative elution values from 3 independent experiments are shown in Table 5.2. These data show that there was no significant difference between those cells treated with camptothecin and AG14361 compared to those treated with camptothecin alone at any of the concentrations used.

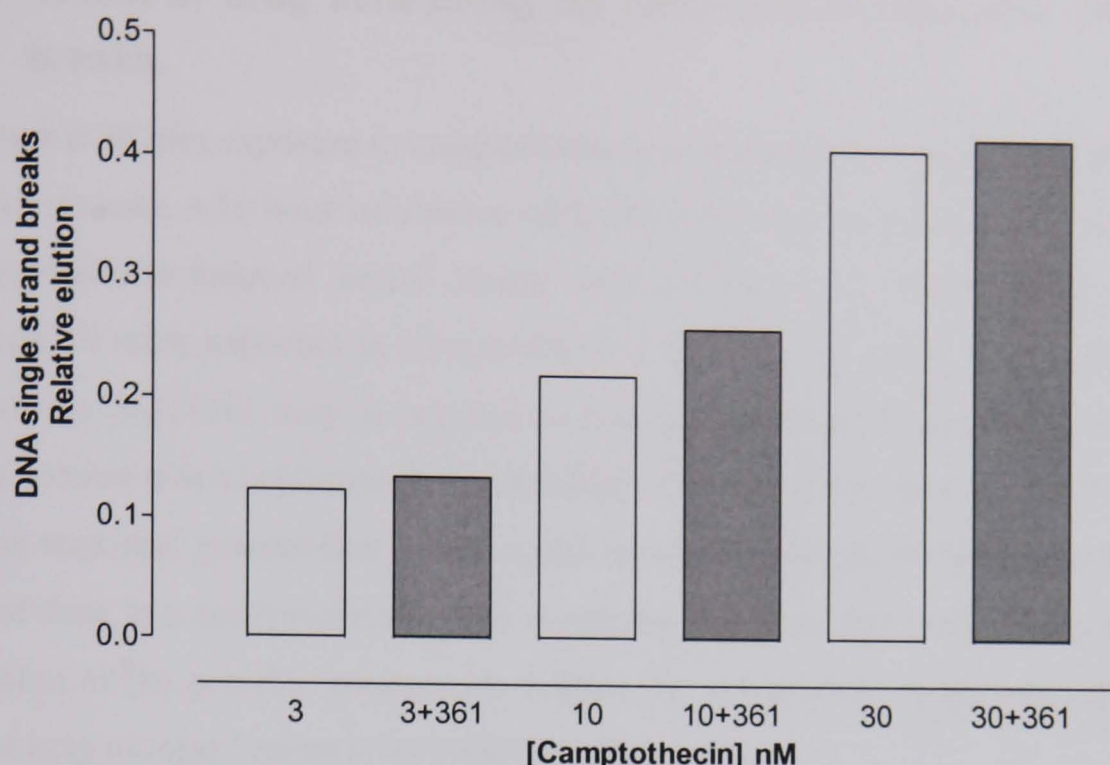


Figure 5.3 Effect of AG14361 on DNA strand breaks formed following 30 min exposure to camptothecin

K562 cells were exposed to 3, 10, and 30 nM camptothecin in the presence or absence of 0.4 μ M AG14361 for 30 mins. DNA strand breaks were measured by alkaline elution (see section 2.10). Relative elution was calculated by comparison with DMSO or AG14361 alone control as appropriate. A bar chart of relative elution values from one representative experiment is shown.

30 min	DNA single strand breaks (Relative Elution)		
Camptothecin (nM)	Camptothecin alone	Camptothecin + 0.4 μ M AG14361	Fold increase
3	0.091 \pm 0.04	0.082 \pm 0.09	0.9 \pm 0.9
10	0.18 \pm 0.05	0.21 \pm 0.06	1.2 \pm 0.5
30	0.36 \pm 0.08	0.35 \pm 0.06	1.0 \pm 0.3

Table 5.2 Effect of AG14361 on DNA strand breaks formed following 30 min exposure to camptothecin.

K562 cells were exposed to 3, 10 and 30 nM camptothecin in the presence or absence of 0.4 μ M AG14361 for 30 mins before measurement of DNA single strand breaks by alkaline elution. Relative elution was calculated by comparison with DMSO or 0.4 μ M AG14361 alone control as appropriate. Data are mean RE values from 3 independent experiments \pm SEM.

5.3.2 Effect of drug scheduling on camptothecin-mediated DNA strand breaks.

Although a 30 min exposure to camptothecin was sufficient to cause DNA strand breaks and cytotoxicity, a 16 hour incubation with AG14361 was required to detect an increase in camptothecin-induced strand breaks and cytotoxicity. Therefore it seems that although 30 mins exposure to camptothecin is sufficient to cause cytotoxicity a longer exposure to AG14361 may be required to maximally potentiate camptothecin. The aim of this section was to optimise the scheduling of camptothecin and AG14361 in order to achieve maximal potentiation. This could have implications for administration of this class of drug in a clinical setting. The results produced in this section may also give an indication of the possible mechanism behind the potentiation of growth inhibition and cytotoxicity of topo I poisons by PARP-1 inhibition.

Firstly, cells were exposed to AG14361 for 16 hours, and exposed to camptothecin for only the final 30 mins (pre-exposure, see Figure 5.4A). Although it was shown in section 3 that PARP-1 is inhibited in cells within 10 mins of drug exposure, it may take longer for the effects of PARP-1 inhibition to be measurable in the cell. Therefore treatment with AG14361 for 16 hours prior to administration of camptothecin, ensured that PARP-1 was fully inhibited for long enough to exert any down-stream effects by loss of poly(ADP-ribosylation) of target proteins, including topo I.

The effect of a 16 hour exposure to AG14361 following exposure to camptothecin for the first 30 mins was also investigated (post-exposure; see Figure 5.4B). 30 mins was sufficient to cause high levels of DNA strand breaks (Figure 5.2). Using a post exposure to AG14361 for 16 hours allows investigation into the effects of AG14361 on repair or reversal of these breaks. Any significant result under these conditions would provide implication of a role for PARP-1 in repair of topo I poison-induced DNA strand breaks.

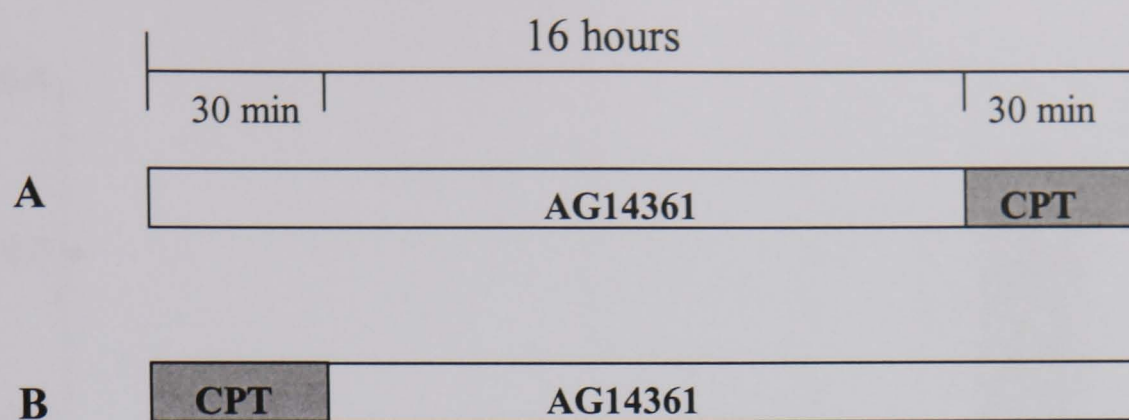


Figure 5.4 Dosing schedule for pre (A) and post (B) exposure to AG14361.

5.3.2.1 Effect of a 16 hour pre-exposure to AG14361 on camptothecin-induced DNA strand breaks.

K562 cells were exposed to 0.4 μ M AG14361 for 16 hours before the addition of a range of concentrations of camptothecin in the presence or absence of AG14361 for a further 30 mins. Figure 5.5 shows a representative bar chart of relative elution values, pooled data for 3 experiments are shown in Table 5.3. Increases in DNA strand break levels were observed, particularly at low concentrations of camptothecin, but overall there was no significant effect of PARP-1 inhibition on DNA single strand break levels when PARP-1 was inhibited prior to topo I poisoning by camptothecin.

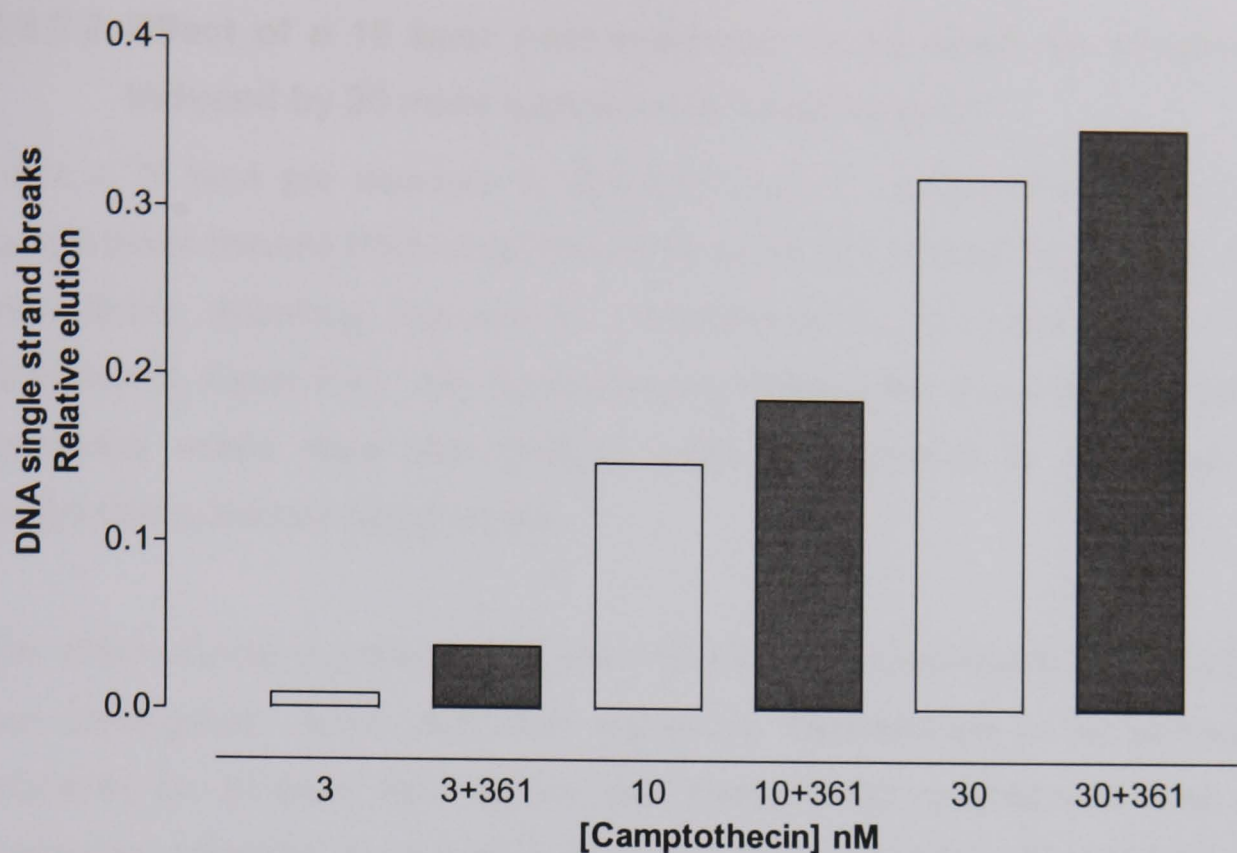


Figure 5.5 Effect of pre-exposure to AG14361 on camptothecin-induced DNA strand break levels.

K562 cells were exposed to 0.4 μ M AG14361 for 16 hours before the addition of 3, 10, or 30 nM camptothecin for a further 30 mins. DNA strand breaks were measured by alkaline elution. Relative elution was calculated by comparison with DMSO or 0.4 μ M AG14361 alone control as appropriate. A bar chart of relative elution values from one representative experiment is shown.

Camptothecin (nM)	DNA single strand breaks (Relative Elution)		Fold increase
	Camptothecin alone	Camptothecin + 0.4 μ M AG14361	
3	0.046 \pm 0.02	0.072 \pm 0.03	1.6 \pm 0.8
10	0.16 \pm 0.01	0.19 \pm 0.001	1.2 \pm 0.08
30	0.28 \pm 0.02	0.32 \pm 0.02	1.1 \pm 0.1

Table 5.3 DNA strand break levels in K562 cells treated with AG14361 for 16 hours followed by camptothecin for a further 30 mins.

Mean relative elution values \pm SEM from 3 independent experiments are shown.

5.3.2.2 Effect of a 16 hour post exposure to AG14361 on strand breaks induced by 30 mins exposure to camptothecin.

Since a 16 hour pre exposure to AG14316 had no significant effect on levels of camptothecin-induced DNA strand breaks the effect of a 16 hour exposure to AG14361 immediately following exposure to camptothecin for 30 mins was investigated (Schedule B, Figure 5.4). Any significant potentiation seen with AG14361 under these conditions would show that PARP-1 might be involved in the repair of the camptothecin-induced strand breaks.

The effect of post exposure to 0.4 μ M AG14361 on camptothecin treated K562 cells was investigated. K562 cells were exposed to camptothecin or camptothecin with AG14361 for 30 mins; the drug was then removed and replaced with fresh medium containing AG14361, for a further 16 hours. The levels of single strand breaks were then determined using alkaline elution (see section 2.10). Initially concentrations of 3, 10, and 30 nM camptothecin were used to correspond with the data shown in section 5.3.1.1, but it was found that there was very little detectable DNA damage remaining after 16 hours (data not shown). This is probably because of the rapid reversal of the cleavable complexes and the repair of any DNA strand breaks. Following this, the dose was escalated up to a maximum of 300 nM camptothecin. The results in Figure 5.6 show that there was a small increase in levels of DNA single strand breaks in those cells treated with AG14361 compared to those treated with camptothecin alone. The greatest increase was observed at 300 nM; giving relative elution values of 0.04 for camptothecin alone compared to 0.1 with camptothecin and AG14361. This was not quite statistically significant ($p = 0.06$ paired t-test).

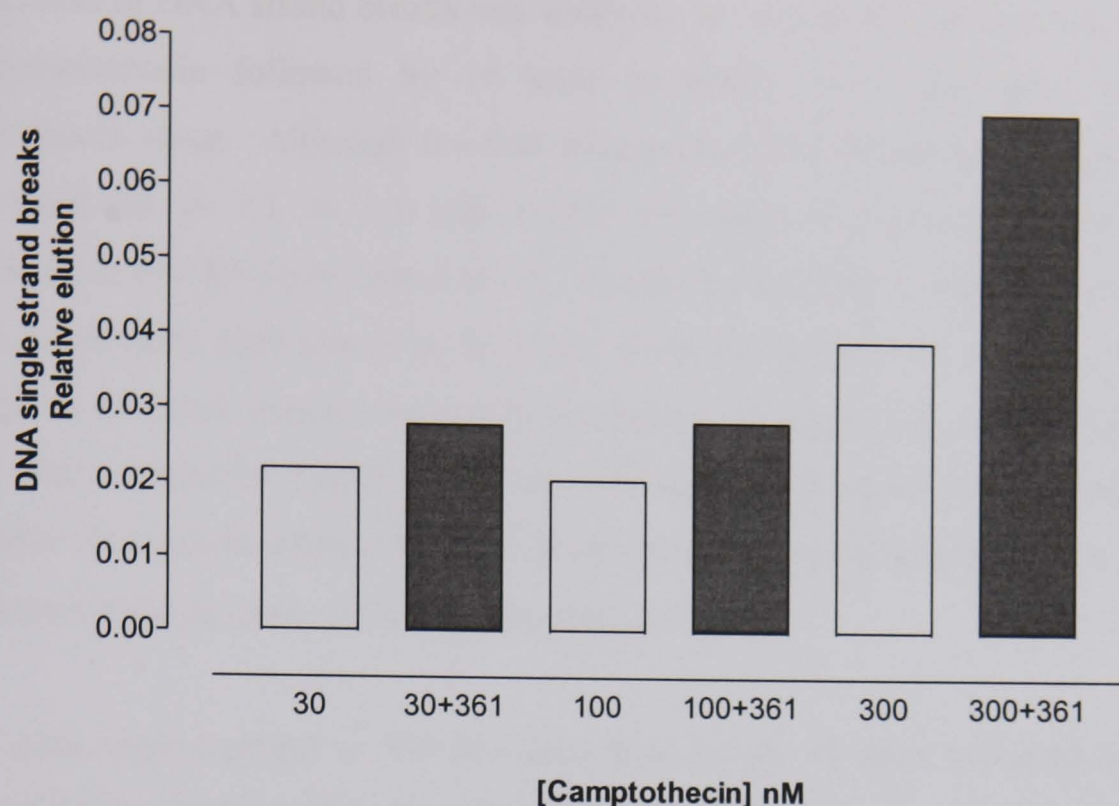


Figure 5.6 Effect of post exposure to AG14361 on 30 mins exposure to camptothecin.

K562 cells were exposed to 30, 100 and 300 nM camptothecin in the presence or absence of 0.4 μ M AG14361 before the drug was removed and the cells were returned to fresh medium or medium containing 0.4 μ M AG14361. DNA strand breaks were measured by alkaline elution. Relative elution was calculated by comparison with DMSO or AG14361 alone control as appropriate. A bar chart of one representative experiment with duplicate samples is shown.

DNA single strand breaks (Relative Elution)			
Camptothecin (nM)	Camptothecin alone	Camptothecin + 0.4 μ M AG14361	Fold increase
30	0.013 \pm 0.01	0.041 \pm 0.008	3.2 \pm 2.5
100	0.027 \pm 0.0037	0.079 \pm 0.029	2.9 \pm 1.1
300	0.040 \pm 0.034	0.10 \pm 0.04 ⁺	2.5 \pm 2.3

Table 5.4 DNA strand breaks in K562 cells treated with camptothecin for 30 mins followed by AG14361 for a further 16 hours.

Mean relative elution values \pm SEM are given.

⁺ p = 0.06 paired t-test compared to camptothecin alone.

An increase in DNA strand breaks was observed as a result of a 30 min exposure to 300 nM camptothecin followed by 16 hour incubation with AG14361 compared to camptothecin alone. Although the fold increase in DNA strand breaks was 2.5 to 3.2-fold compared to 1.1 to 1.6-fold in the pre-exposure experiments, this was not significant at the 95% confidence level. However, the relative elution values obtained in this experiment were almost at the lower limits of detection for the assay presumably because at 16 hours repair was largely complete. To verify the putative proposal that repair was retarded by PARP-1 inhibition levels of DNA strand breaks were measured at shorter time points where the level of strand breaks remaining would be greater and thus increase the accuracy of the results obtained.

K562 cells were exposed to 300 nM camptothecin for 30 mins followed by 1 and 16 hour incubation in the presence or absence of AG14361. The results in Figure 5.7 show a representative bar chart of relative elution values. The mean RE values given in Table 5.5 show that the majority of the DNA strand breaks were repaired within the first hour of drug removal. There was a significant increase in strand breaks at both 1 and 16 hours after removal of camptothecin in the presence of AG14361 indicating that inhibition of PARP-1 retards repair.

Since the majority of strand breaks were reversed within the first hour of drug removal, consistent with previous published data (Covey *et al.*, 1989), in order to detect strand breaks at physiologically relevant camptothecin concentrations a shorter time of exposure to AG14361 after the camptothecin was investigated. The time course of reversal of camptothecin-induced DNA strand breaks was studied to find out the optimum time to measure the effect of AG14361 on the level of camptothecin-induced reversal of DNA strand breaks, preferably at a time when half of the breaks are remaining. K562 cells were exposed to 30 nM camptothecin (which corresponds to ~50 and >5% survival after 0.5 and 16 hours exposure respectively and as used in the DNA strand break assays in section 5.3.1), for 30 mins and allowed to reverse in drug free medium before determination of the levels of DNA strand breaks. The results in Figure 5.8 show that DNA strand breaks were totally reversed following a 30 min incubation in drug-free medium with no further detectable change for up to 4 hours. Given that most of the DNA strand breaks had been reversed within 30 mins of drug removal, it was practical to look at earlier time points to examine the effects of PARP-1 inhibition.

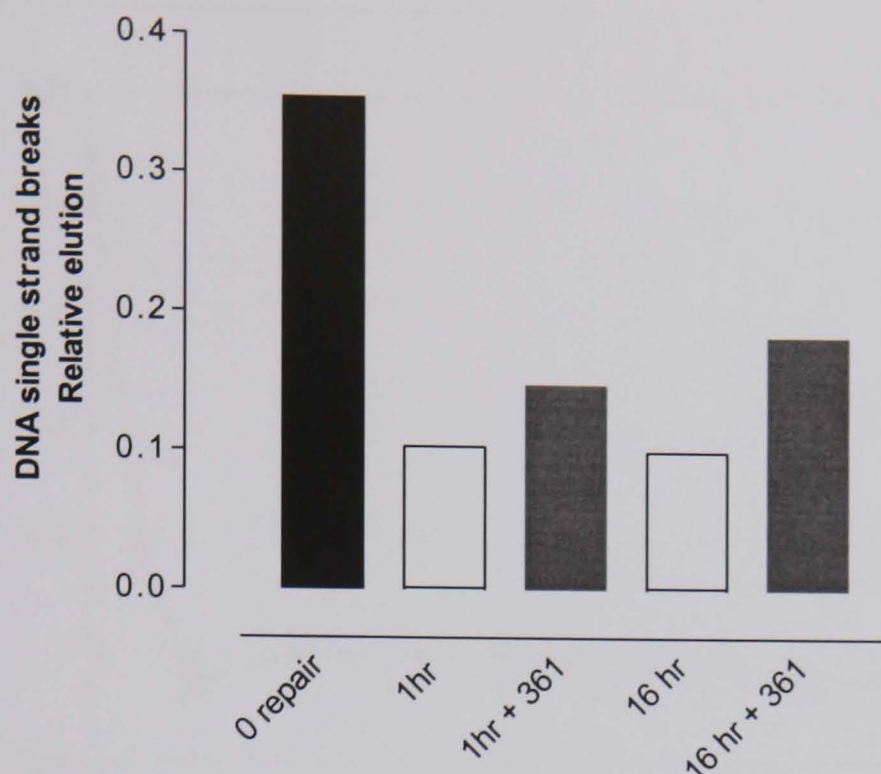


Figure 5.7 Effect of AG14361 on repair of camptothecin-induced DNA strand breaks. K562 cells were exposed to 300 nM camptothecin \pm 0.4 μ M AG14361 for 30 mins, after this time the drug was removed and replaced with fresh medium or medium containing 0.4 μ M AG14361 for a further 1 or 16 hours. Bar chart shows results from one representative experiment.

	DNA single strand breaks (Relative Elution)	
Repair time (hours)	Camptothecin / control medium	Camptothecin + 0.4 μ M AG14361 / AG14361
0	0.28 ± 0.08	0.29 ± 0.05
1	0.062 ± 0.024	0.12 ± 0.018 *
16	0.04 ± 0.034	0.10 ± 0.04 +

Table 5.5 Effect of 1, and 16 hour post-exposure to AG14361 following 30 mins exposure to 300 nM camptothecin.

Mean relative elution values calculated from 3 independent experiments \pm SEM are given.

* $p = 0.023$ paired t-test compared to camptothecin alone.

+ $p = 0.06$ paired t-test compared to camptothecin alone.

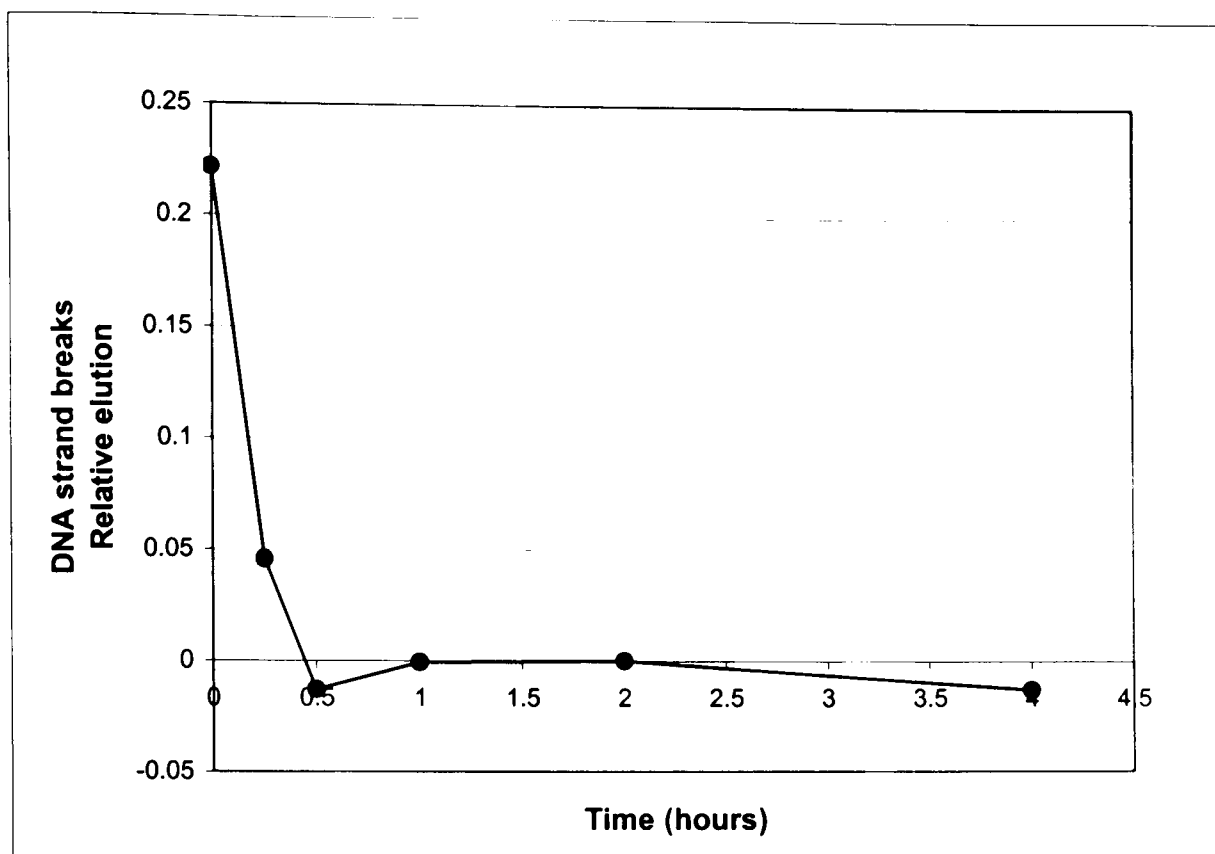


Figure 5.8 Time course of reversal of DNA strand breaks induced by 30 mins exposure to 30 nM camptothecin.

K562 cells were exposed to 30 nM camptothecin for 30 mins before removal into drug free medium for 10 min, 30 min, 1, 2, and 4 hours. DNA strand breaks were measured by alkaline elution. Relative elution was calculated by comparison with untreated control. A representative repair profile is shown.

5.3.2.3 Effect of AG14361 on repair of camptothecin-induced DNA strand breaks.

The time course of repair of damage induced by 30 mins exposure to 30 nM camptothecin indicated that the majority of strand breaks had been repaired within 30 min of removal of camptothecin (Figure 5.8). Therefore, the effect of AG14361 on DNA strand breaks at a 10 and 20 min time point after camptothecin removal was investigated.

K562 cells were exposed to 30 nM camptothecin for 30 mins in the presence or absence of 0.4 μ M AG14361. This was followed by removal of camptothecin and incubation for a further 10 or 20 mins in fresh medium or medium containing AG14361. DNA strand breaks were measured by alkaline elution. The bar chart in Figure 5.9 shows that there was no difference in the level of strand breaks present following 30 mins exposure to camptothecin alone or camptothecin plus AG14361, as shown previously. Following drug removal, the level of breaks decreased, such that at 10 mins, 20% of breaks remained. The repair was significantly retarded by AG14361, such that at 10 mins 50% of breaks remained. Thus, PARP-1 inhibition retards the repair of camptothecin induced single strand ~2.5- fold following a 10 min repair period. A similar, but non-significant, trend was followed at 20 mins after drug removal. 78% of DNA strand breaks were repaired 20 mins after drug removal in the presence of AG14361, whereas 84% were repaired in drug free medium (see Table 5.6).

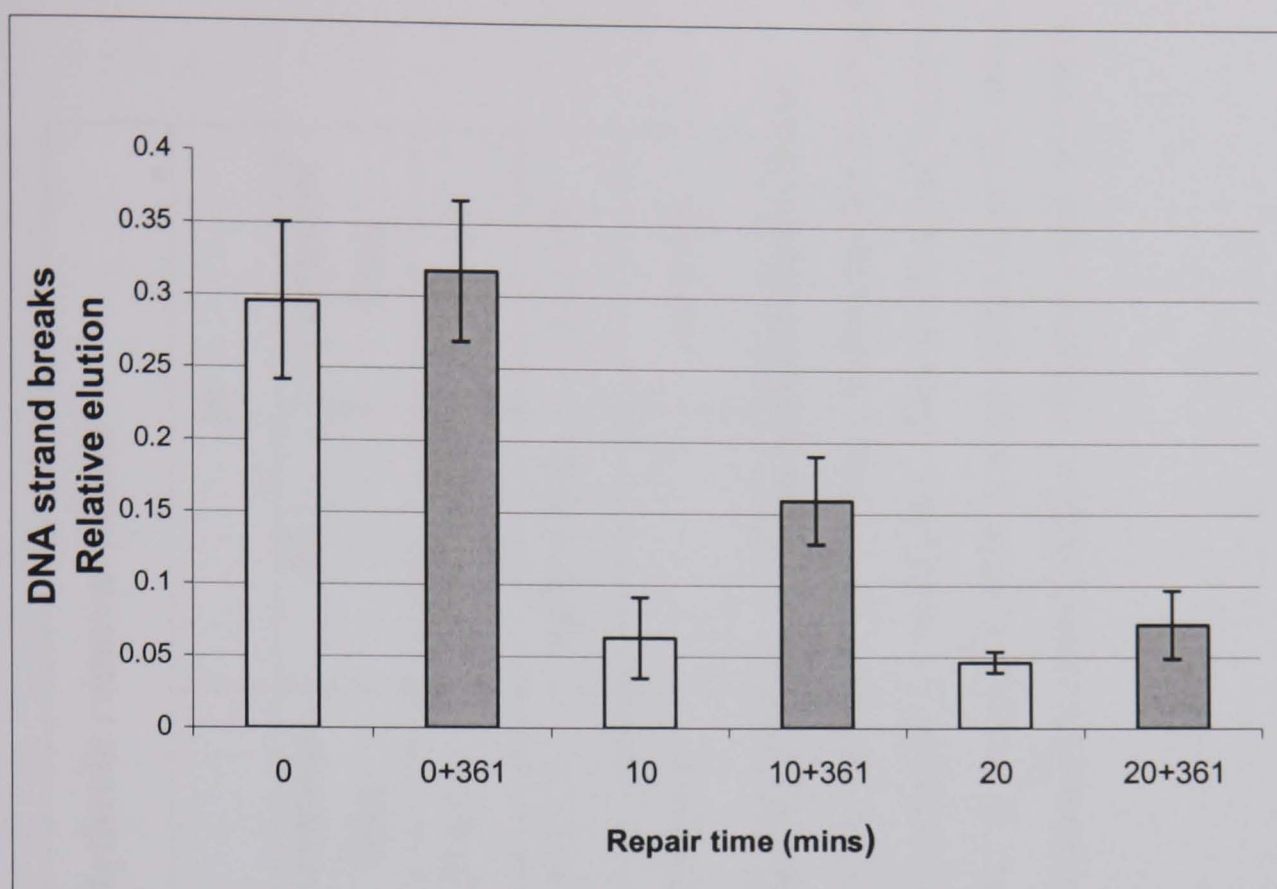


Figure 5.9 Effect of AG14361 on the repair of camptothecin-induced strand breaks.

K562 cells were exposed for 30 mins to 30 nM camptothecin followed by repair in drug free medium or medium containing 0.4 μ M AG14361 for 0, 10 or 20 mins. Relative elution was calculated by comparison with DMSO or 0.4 μ M AG14361 alone control as appropriate. Data are the mean of 3 independent experiments \pm SEM.

	Time after camptothecin removal (mins)				
	0	10		20	
	RE	RE	% unrepaired DNA	RE	% unrepaired DNA
Camptothecin	0.29 ± 0.05	0.063 ± 0.03	20 ± 5.4	0.046 ± 0.007	16 ± 2.8
Camptothecin + AG14361	0.32 ± 0.05	0.16 ± 0.03*	50 ± 1.7	0.073 ± 0.02	22 ± 4.9
Fold increase in strand breaks remaining			2.5 ± 0.2		1.4 ± 0.4

Table 5.6. Effect of AG14361 on repair of DNA single strand breaks formed following a 30 min exposure to 30 nM camptothecin.

K562 cells were exposed to 30 nM camptothecin in the presence or absence of 0.4 µM AG14361 for 30 mins. Following this the drug was removed and replaced with fresh medium or medium containing 0.4 µM AG14361 for a further 10 or 20 mins. DNA single strand breaks were measured by alkaline elution. Data shown are mean relative elution values ± SEM. % unrepaired DNA was calculated from RE values for strand breaks remaining after 10 or 20 mins, expressed as a percentage of the relevant unrepaired control (with or without 0.4 µM AG14361).

*p = 0.001 paired t-test; compared to camptothecin alone.

% breaks remaining was calculated by the equation

$$\frac{\text{RE at time (t)}}{\text{RE at time (0)}} \times 100$$

5.3.3 Effect of AG14361 on repair of camptothecin-induced DNA damage in PARP-1 wild-type and null cells.

In K562 cells AG14361 increased both the cytotoxicity and the level and persistence of DNA strand breaks induced by camptothecin by 2 to 3-fold. This suggested that the increase in camptothecin-induced growth inhibition by AG14361 was due to the AG14361-induced increase in persistence of camptothecin-induced single strand breaks. PARP-1 wild type and null cells were used to measure whether there were differential levels of strand breaks formed in response to treatment with camptothecin, to confirm a role for PARP-1 in the response to camptothecin. AG14361 was used with these cell lines to demonstrate whether there was a differential effect of AG14361 on the PARP-1 wild type and null cells. Therefore this would show that any effect observed was mediated by the inhibition of PARP-1 by AG14361 rather than an effect of AG14361 on some other factor associated with the repair of camptothecin-induced DNA damage.

5.3.3.1 Effect of camptothecin on DNA strand breaks in PARP-1 wild type and null cells.

As in the previous studies on DNA strand breaks, a concentration of camptothecin and incubation period had to be determined that was suitable for the measurement of strand breaks. This had to be a concentration that produced measurable strand breaks and whose damage was not repaired in less than 10 mins after drug removal (the minimum time that was practical for measurement of strand breaks). Initial experiments indicated that the concentration and/or time points used for the K562 cells (30 mins 30 nM camptothecin followed by 30 mins repair in drug free medium) were not sufficient as DNA strand breaks were barely detectable after a 30 min repair of damage caused by exposure to 30 nM camptothecin (data not shown). PARP-1 wild-type and null cells were exposed to increasing concentrations of camptothecin for 30 mins, to determine an appropriate concentration to produce the required levels of DNA strand breaks to study repair. Figure 5.10 shows that in the PARP-1 null cell line there was an increase in strand breaks that begins to plateau at 1 μ M, but levels of breaks still increase to 10 μ M, the maximum concentration used in these experiments. Similar results were obtained for the PARP-1 wild type cells (data not shown).

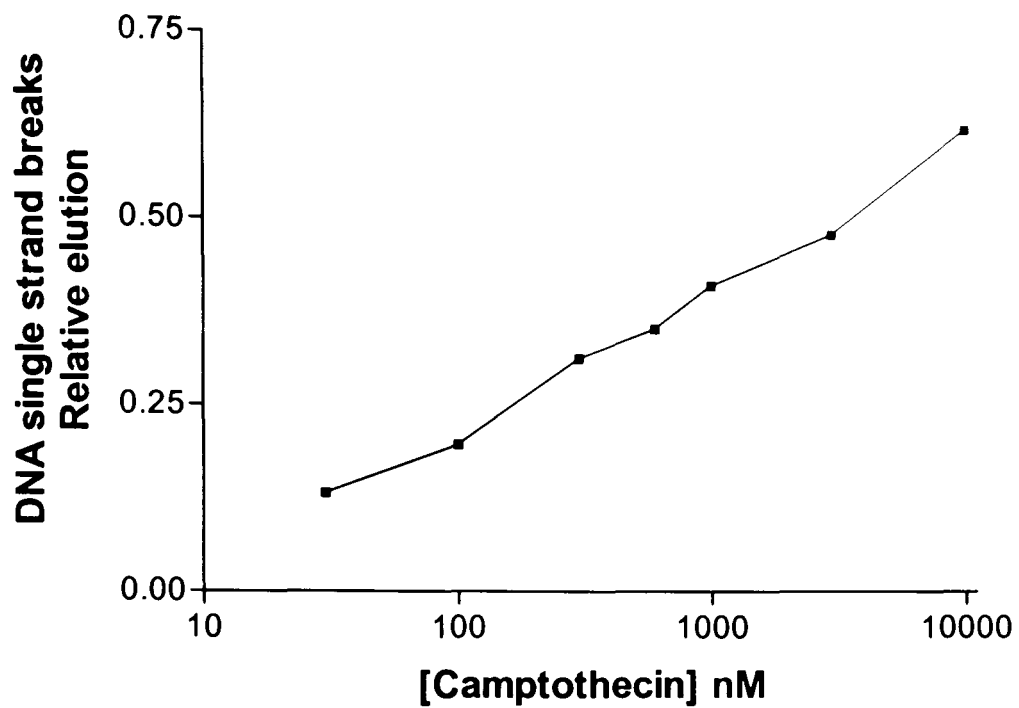


Figure 5.10 DNA single strand breaks induced by increasing concentrations of camptothecin in PARP-1 null cells.

Cells were exposed to 0, 30, 100, 300, 600, 1,000, 3,000 and 10,000 nM camptothecin for 30 mins before measurement of DNA strand breaks by alkaline elution. Data are from one representative experiment.

5.3.3.2 Effect of PARP-1 status of cell lines on levels of camptothecin-induced DNA single strand breaks.

The PARP-1 wild-type and null cells were exposed to 10 μ M camptothecin for 30 min before measurement of DNA strand breaks by alkaline elution. Mean relative elution values show that after a 30 min exposure, there were significantly higher levels of DNA strand breaks in the PARP-1 null cells ($RE = 0.44 \pm 0.04$) compared to the PARP-1 wild type cells ($RE = 0.36 \pm 0.03$, $p = 0.002$ paired t-test). This suggests that the observed hypersensitivity to topo I poisons seen in the PARP-1 null cell line seen in section 3.3.4 could indeed be due to an increase in the number of DNA strand breaks.

5.3.3.3 Effect of AG14361 on repair of camptothecin-induced DNA single strand breaks in PARP-1 wild type and null cells.

To confirm that the increase in strand breaks seen in the presence of AG14361 was due to PARP-1 inhibition rather than an effect of AG14361 on other cellular processes the effect of AG14361 on the PARP-1 wild type and null cells was studied. Initial experiments were conducted to determine the optimum repair time following a 10 μ M camptothecin for 30 mins. It was shown that repair for 60 mins resulted in easily detectable and reproducible levels of strand breaks in both cell lines as 20-50 % of the DNA damage was still detectable, and that repair seemed to be faster in the wild-type compared to the null cells (Figure 5.11). Therefore, PARP-1 wild type and null cells were exposed to 10 μ M camptothecin in the presence or absence of AG14361 for 30 mins followed by a 60 min repair incubation in the absence of camptothecin. The results are shown in Figure 5.12 for PARP-1 wild type cells and Figure 5.13 for PARP-1 null cells. In the PARP-1 wild type cells 48.2 ± 4.3 % of the DNA strand breaks induced by a 30 min exposure to 10 μ M remained following 60 mins repair in drug free medium, compared to $57.3 \pm 5.8\%$ that remained in these cells treated with AG14361. In the PARP-1 null cells, 21.1 ± 2.5 % of the strand breaks induced by the 30 min incubation with camptothecin remained after 60 mins incubation in fresh medium compared to $21.0 \pm 3.4\%$ in those PARP-1 null cells treated with AG14361. These data show that AG14361 caused a small but significant inhibition of repair at 60 mins in PARP-1 wild type cells ($p = 0.03$, paired t-test), but not in the PARP-1 null cells ($p = 0.8$ paired t-test). From these data it appeared that the PARP-1 wild type cells repaired more slowly than the null cells. The PARP-1 wild type cells achieved ~50 % repair compared to ~80% for the PARP-1 null cells after 60 mins repair in drug free medium. This is not consistent with the initial time course experiments shown in Figure 5.11 where it would seem that the wild type cells repaired the damage much faster than the PARP-1 null cells. However, in neither of these studies were both of cell lines investigated simultaneously and the contradictory nature of these data may reflect inter-assay variation. This was investigated in the next section.

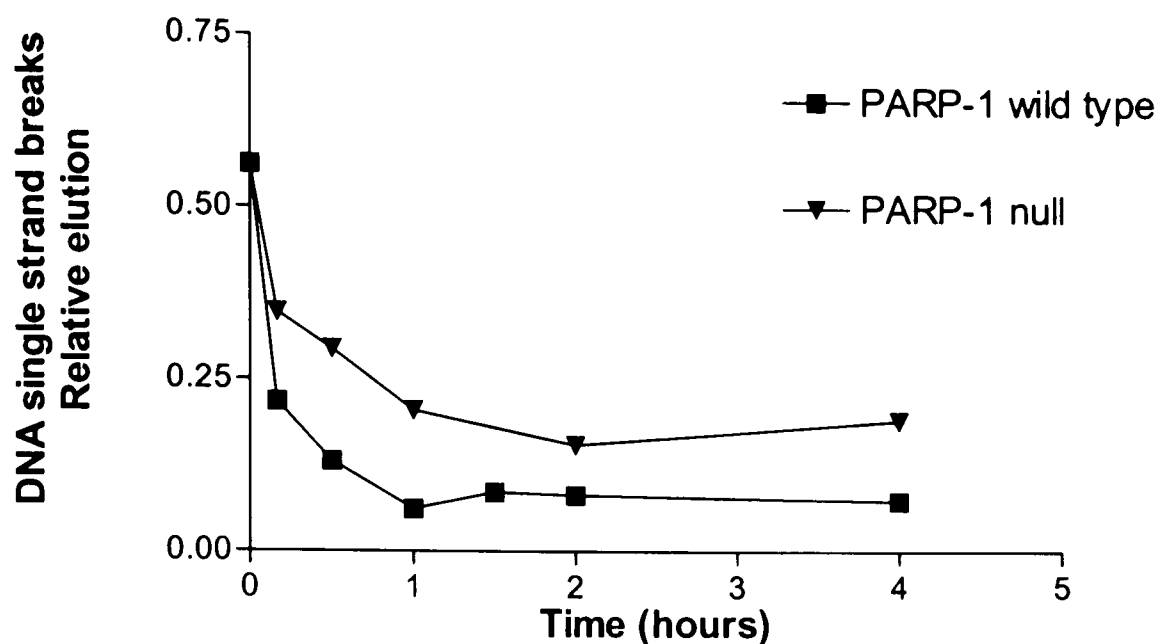


Figure 5.11 Repair of PARP-1 wild type and null cells following treatment with camptothecin.

PARP-1 wild type and null cells were treated with 10 μ M camptothecin for 30 mins. The drug was removed and replaced with fresh medium for a further, 10, 30 60, 120, 240 mins, before measurement of DNA strand breaks by alkaline elution. The repair of each cell line was studied in independent experiments and the data presented are representative of two independent experiments.

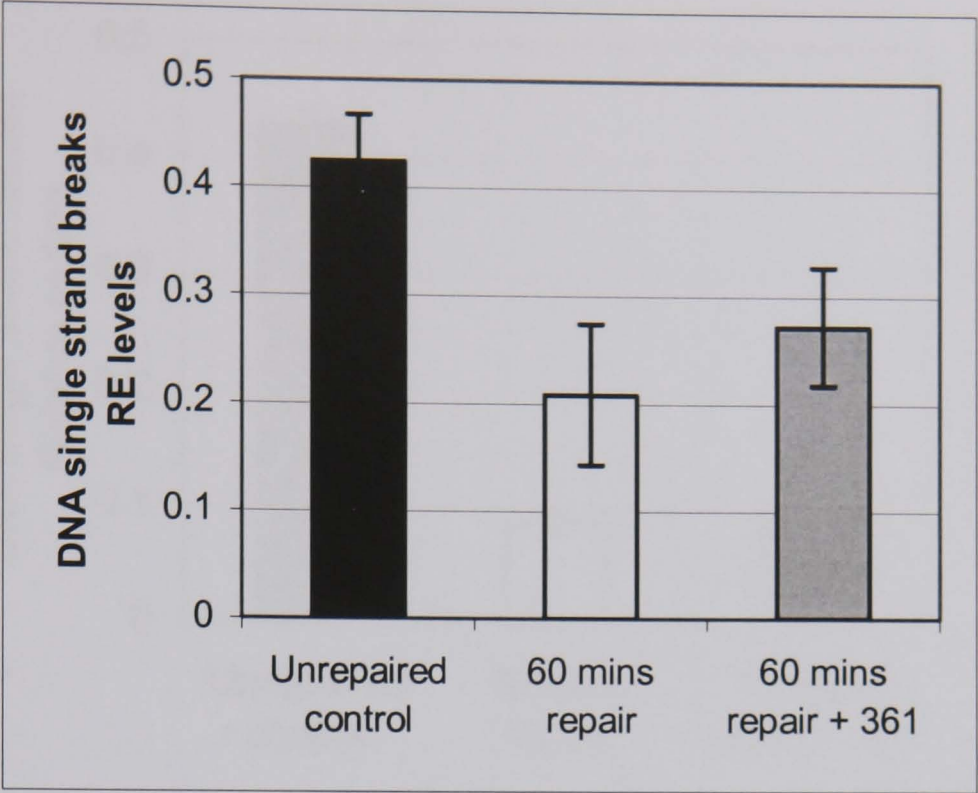


Figure 5.12 Effect of AG14361 on camptothecin-induced single strand breaks in PARP-1 wild type cells.

PARP-1 wild type cells were exposed to 10 μ M camptothecin for 30 mins in the presence or absence of 0.4 μ M AG14361. Following this the drug was removed and the cells washed once in Dul A. Fresh medium or medium containing 0.4 μ M AG14361 was then added to the cells for a further 60 mins. DNA single strand breaks were measured by alkaline elution. Relative elution values for each condition were calculated by comparison with the appropriate untreated or 0.4 μ M AG14361 alone control. Data are the mean of 3 independent experiments \pm SEM.

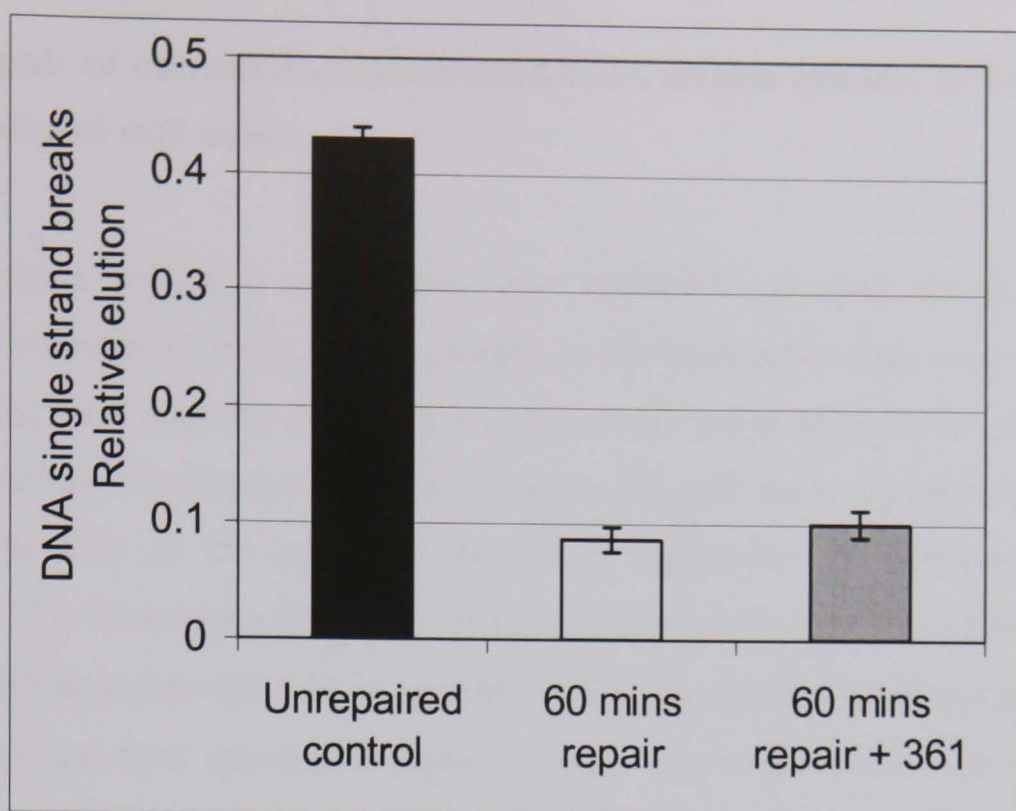


Figure 5.13 Effect of AG14361 on camptothecin-induced single strand breaks in PARP-1 null cells.

PARP-1 null cells were exposed to 10 μ M camptothecin for 30 mins in the presence or absence of 0.4 μ M AG14361. Following this the drug was removed and the cells washed once in Dul A. Fresh medium or medium containing 0.4 μ M AG14361 was then added to the cells for a further 60 mins. DNA single strand breaks were measured by alkaline elution. Relative elution values for each condition were calculated by comparison with the appropriate untreated or 0.4 μ M AG14361 treated control. Data are the mean of 3 independent experiments \pm SEM.

5.3.4 Repair of camptothecin-induced DNA strand breaks in PARP-1 wild type and null cells.

In the previous section it was shown that AG14361 increases the persistence of camptothecin-induced strand breaks present at 60 mins after drug removal. It also appeared that there might be a difference in the rate of repair between the two cell lines. As the previous experiments did not compare the cell lines simultaneously it was necessary to look at the repair in the same experiment to eliminate inter-assay variability. To investigate the repair of camptothecin-induced DNA strand breaks in PARP-1 wild-type and null cells in parallel, cells were exposed to 10 μ M camptothecin for 30 mins and then allowed to repair in drug-free medium for 1 or 4 hours. A representative bar chart of relative elutions and summary of percent damage remaining after drug removal relative to an unrepaired control are shown in Figure 5.14 and Table 5.7, respectively. These data show that there was no significant difference between the ability of the PARP-1 wild type or null cells to repair camptothecin-induced DNA strand breaks. The difference in levels of strand breaks remaining between this experiment and the previous one (Figure 5.12 and Figure 5.13) may be due to the use of different passage numbers of the cell lines and different batches of media, as these experiments were carried out several months apart.

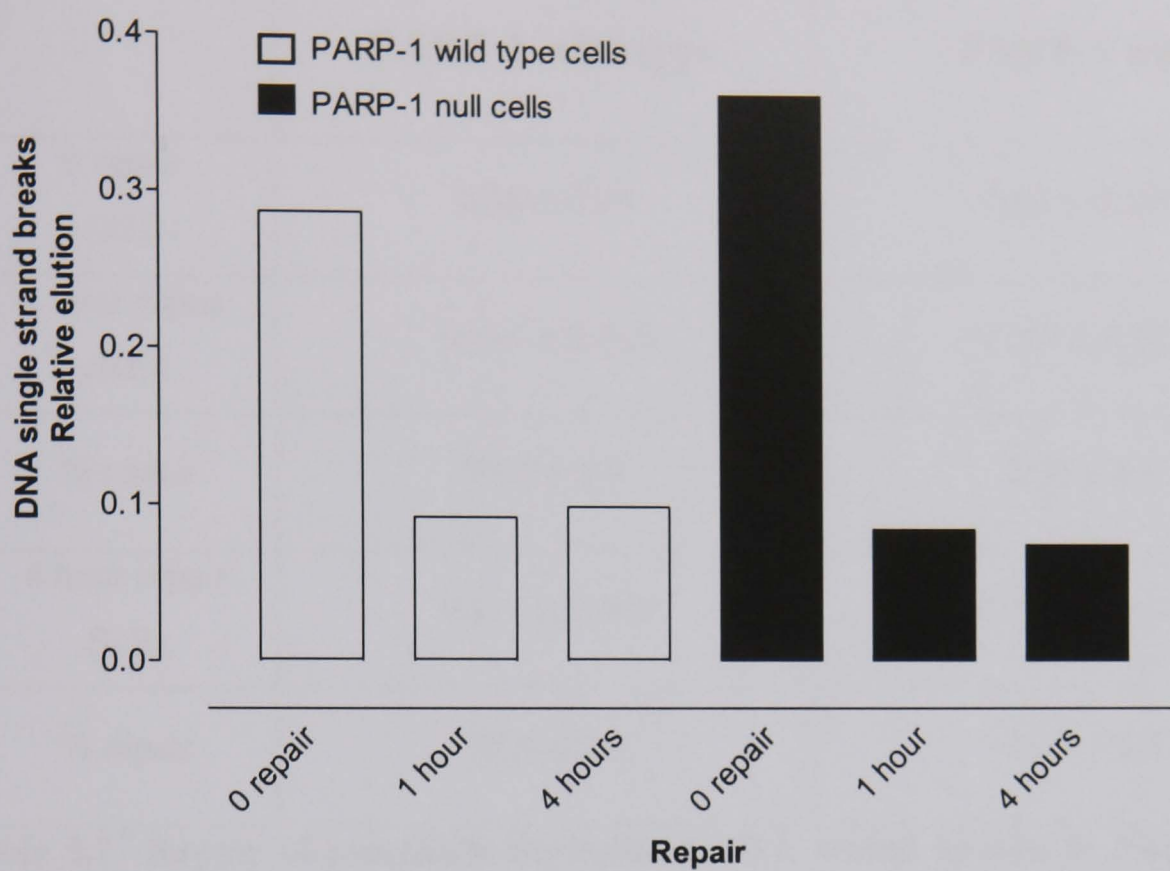


Figure 5.14 Repair of camptothecin-induced DNA strand breaks in PARP-1 wild type and null cells.

PARP-1 wild-type and null cells were exposed to 10 μ M camptothecin for 30 mins, camptothecin was then removed and replaced with fresh medium for 0, 1 or 4 hours before determination of DNA strand breaks by alkaline elution (see section 2.10). Relative elution values are given from one representative experiment.

	PARP-1 wild type	PARP-1 null
0 repair (RE)	0.36 ± 0.03	0.44 ± 0.04*
1 hour repair (RE)	0.114 ± 0.023	0.109 ± 0.039
% repair	67.8 ± 5.8	72.9 ± 9.5
4 hour repair (RE)	0.111 ± 0.007	0.101 ± 0.016
% repair	72.9 ± 2.9	75.2 ± 3.2

Table 5.7 Repair of camptothecin-induced DNA strand breaks in PARP-1 wild type and null cells.

Values are RE and % repair following the indicated period of repair relative to an unrepaired control from 3 independent experiments ± SEM.

(*) p = 0.002 paired t-test compared to PARP-1 wild type cells.

5.4 Discussion.

The studies in this chapter were conducted to determine whether PARP-1 was involved in the repair of topo I poison-mediated DNA damage. If PARP-1 inhibition could inhibit the repair of DNA strand breaks caused by camptothecin this could provide an explanation for the potentiation of growth inhibition seen in chapter 3 and data previously reported in the literature. To address this, the effect of AG14361 on the level and persistence of camptothecin-induced DNA single strand breaks was investigated in the human leukaemia K562 cell line and murine PARP-1 wild type and null cells.

In K562 cells AG14361 significantly increased the levels DNA single strand breaks caused by a 16 hour exposure to camptothecin by ~30% (table 5.1), suggesting that the increase in DNA strand breaks was a major factor in the potentiation of growth inhibition and cytotoxicity observed in these cells as described in chapter 3. The increase in DNA strand breaks and cytotoxicity were remarkably similar following a 16 hours exposure to 3, 10, and 30 nM camptothecin. AG14361 caused a 2.5, 1.6 and 1.3-fold increase in DNA strand breaks 1.8, 1.9 and 1.5 fold increase in cytotoxicity respectively. Moreover, exposure to AG14361 for only 30 mins failed to significantly increase DNA damage induced by a 30 min exposure to camptothecin, this corresponding to the lack of potentiation of camptothecin-induced growth inhibition (section 3.3.5). Potentiation of camptothecin-induced cytotoxicity by AG14361 was however seen at higher concentrations of camptothecin but unfortunately these could not be used in strand break assays as the levels of breaks induced by concentrations higher than 30 nM camptothecin were at the upper limit of detection of the assay. Previous authors have shown a similar time-dependent effect on strand breaks. Increases in DNA single strand breaks by inhibition of PARP-1 have been reported by Mattern *et al.*, (1987), using 3-AB where it was shown that there was no increase in the level of strand breaks formed after a 60 min exposure to camptothecin in the presence or absence of 3-AB, however an increase in strand breaks could be detected after 16 hours.

It is interesting that strand breaks were only increased after a 16 hour exposure to AG14361 because AG14361 is able to inhibit PARP-1 within 10 mins of exposure (figure 3.7), and 30 mins has been shown to be sufficient for the formation of maximum

levels of topo I-DNA complexes in response to camptothecin (Padget *et al.*, 2000a). Therefore this may suggest that the increase in the level of strand breaks is related to down-stream effects of PARP-1 or the cumulative effect of the inhibition of poly(ADP-ribosylation) of topo I or other proteins, or on the repair of topo I damage. Alternatively, the increase in total DNA strand breaks could be a reflection of a gradually accumulating increase in break formation or a decrease in reversal/repair. Further experiments were designed to investigate this.

To investigate if a cumulative loss of poly(ADP-ribosylation) from target proteins was required to permit a greater induction of DNA breaks by camptothecin, or if prolonged PARP-1 inhibition was required for the inhibition of downstream processing of camptothecin-induced breaks, the effect of scheduling of AG14361 on a 30 min exposure to camptothecin was studied. These experiments demonstrated that a 16 hour pre-exposure to AG14361 had no significant effect on the level of camptothecin-induced strand breaks produced by a 30 min exposure to camptothecin (table 5.3). However a 16 hour post exposure to AG14361, did increase the level of strand breaks remaining after exposure to camptothecin (table 5.4). This would suggest that PARP-1 plays a role in the reversal or repair of camptothecin-induced strand breaks, rather than their generation. Furthermore, as a pre-exposure had little effect, this suggests that increased DNA breaks are not due to modulation of topo I activity by poly(ADP-ribosylation) in agreement with the data presented in chapter 4, rather, they reflect an effect down stream of the DNA damage i.e. in repair.

As a 16 hour post exposure to AG14361 caused a significant increase in the persistence of camptothecin-induced strand breaks detected but the breaks remaining at that time were near the lower limits of detection, shorter post-exposure times were investigated. This aimed to increase the amount of detectable breaks and therefore provide more accurate results. As was previously shown, co-exposure to AG14361 did not affect camptothecin-induced DNA strand breaks following a 30 min exposure. However, AG14361 significantly increased the level of strand breaks remaining after a 10 min incubation in drug free medium following drug exposure by 2 to 3-fold (table 5.6). This shows that AG14361 retards the repair of camptothecin-induced DNA strand breaks, implicating a role for PARP-1 in the repair of such damage. After 20 mins, there were still more strand breaks present in those cells treated with AG14361, although these

were not significantly different from those without AG14361. The reduced enhancement of damage seen 20 mins after drug removal may be due to the fact that any differences in strand break levels were undetectable as most of the DNA damage had been repaired by this point.

The PARP-1 wild-type and null cells were used to verify that the increased sensitivity of PARP-1 null cells to topo I poisons was due to PARP-1-mediated repair of topo I poison-induced DNA damage, and furthermore, that the increased level of strand breaks seen in the presence of AG14361 was indeed due to PARP-1 inhibition. The results presented here show that there were significantly more single strand breaks detectable following exposure to camptothecin in the PARP-1 null cells than the wild-type cells. This differential sensitivity demonstrates that PARP-1 is involved in the response to camptothecin-induced DNA strand breaks and the increased level of breakage most probably leads to the hypersensitivity of the null cells to TP as shown in chapter 3. Furthermore, AG14361 increased the level of camptothecin-induced single strand breaks in the PARP-1 wild type but not in the PARP-1 null cells. This differential effect between the cell lines seen in response to AG14361 shows that the effect of AG14361 on the repair of camptothecin-induced DNA single strand breaks is due to inhibition of PARP-1 rather than on some other factor involved in the processing of topo I poison-induced DNA damage.

Further studies presented here have shown the PARP-1 null cells were not deficient in the repair of camptothecin-induced DNA single strand breaks. This may be a reflection of the time points studied as there may be a rapid, PARP-1-dependent repair phase followed by a slower PARP-1 independent phase. It is also possible that PARP-1-independent pathways can function to repair this damage in the absence of PARP-1 and these could possibly be upregulated to compensate for the lack of PARP-1 in these cells. It has been shown by some authors that BER is active in the absence of NAD⁺ or PARP-1 in *in vitro* and whole cell studies, which could suggest that the hypersensitivity of PARP-1 null cells was related to the lack of poly(ADP-ribosylation) of other cellular targets and not related to BER (Allinson *et al.*, 2003, Vodenicharov *et al.*, 2000). Allinson *et al.*, also showed that that PARP-1 null cell extracts repaired DNA damage at a faster rate than the PARP-1 wild type cell extracts, consistent with data presented in this thesis. However it is widely accepted that PARP-1 is involved in BER (see chapter

1), and has been shown that the long patch BER pathway cannot function in the absence of PARP-1. However, the short patch mechanism is still partly functional in the absence of PARP-1 (Dantzer *et al.*, 2000) and therefore could serve to repair the camptothecin-induced damage seen in this study. Therefore, in the absence of PARP-1 it is possible that the camptothecin-induced damage could still be repaired by a PARP-1 independent mechanism that is not normally the primary mechanism of repair. This may be an adaptive response to the removal of PARP-1. It is known that PARP-2 can participate in the BER pathway performing a similar role as PARP-1 (Schreiber *et al.*, 2002). It may be that there is redundancy in the BER pathway and that BER can operate in the absence of PARP-1 by using PARP-2. However, AG14361 is known to inhibit PARP-2 (Karen Maegely (Pfizer), personal communication) as well as PARP-1, thus this cannot account for the repair seen in the presence of AG14361.

It should be noted that single strand breaks are not the only lesion produced following exposure to camptothecin. Had more time been available, it would be useful to investigate levels of double strand breaks that are produced following collision with replication forks, as PARP-1 is able to bind double as well as single strand breaks. As camptothecin induced damage can occur independently of replication, most likely due to collision with the transcription machinery, it would also be interesting to study the effect of PARP-1 inhibition on replication-independent camptothecin-induced DNA damage.

The studies in this chapter demonstrate that exposure to AG14361 not only increases the level of camptothecin-induced single strand breaks, but also slows the repair of these breaks upon drug removal, confirming that PARP-1 is involved in the repair of topo I poison-mediated DNA damage. This finding could have implications if a combination of topo I poison and PARP-1 inhibitor should ever be used in the clinic. It would be important to ensure that PARP-1 inhibition was maintained for a period of time after topo I poison exposure for the effect of PARP-1 inhibition on cellular cytotoxicity to be maximised.

Summary

- AG14361 increases the levels of camptothecin-induced DNA strand breaks via inhibition of PARP-1 in K562 and PARP-1 wild-type cells under certain conditions.
- Reversal of camptothecin-induced strand breaks is delayed by AG14361 in K562 cells.
- Camptothecin-induced single strand breaks can be repaired in the absence of PARP-1, demonstrating that there are PARP-1-independent mechanisms to repair this damage.

Chapter 6

**Effect of PARP-1 inhibition on topoisomerase I
poison induced cytotoxicity in cell lines deficient
in DNA repair.**

6.1 Introduction.

In the previous chapters it was shown that AG14361 could potentiate the growth inhibitory and cytotoxic effects of topo I poisons, and that this was most likely to be via modulation of DNA repair. The aim of this chapter was to determine how inhibition of PARP-1 was affecting the repair of topo I poison-mediated DNA damage. For example, whether the inhibition of PARP-1 prevented the repair of the lesion via the BER pathway or some other repair pathway such as non-homologous end-joining or homologous recombination.

Many DNA repair pathways have been implicated in the repair of topo I poison-mediated DNA damage. The major cytotoxic lesion created following exposure to topo I poisons occurs upon collision of the stabilised cleavable complex with the replication fork (Hsaing *et al.*, 1989). Such a collision results in three different types of DNA damage as shown in Figure 6.1. Firstly, there is an irreversible protein-DNA covalent complex with topo I covalently linked to the 3'-terminus of the break. This covalent complex has been shown to be removed by a 3'-tyrosyl DNA phosphodiesterase (TDP-1, Yang *et al.*, 1996). This protein can cleave the phosphotyrosyl bond between the enzyme and the DNA. Although genetic inactivation of TDP-1 sensitised yeast to topo I poisons, the degree of sensitisation was less than expected suggesting that there are other ways to remove the cleavable complex (Pouliot *et al.*, 1999, Liu *et al.*, 2002). Secondly, there is a DNA double strand break consisting of the 5'-end of the cleaved strand annealed to the newly synthesised strand. The double strand breaks may be repaired by either of the double strand break repair pathways, HR or NHEJ. Finally, there is a single stranded region of the partially replicated lagging DNA strand. The single strand section may be repaired by BER (reviewed by Pourquier and Pommier 2001).

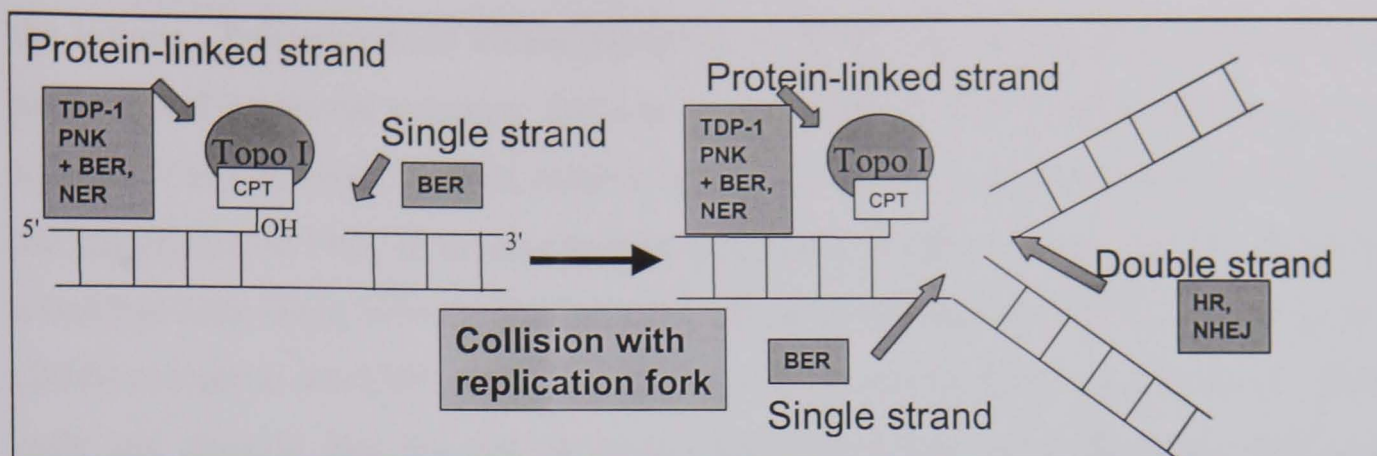


Figure 6.1 DNA damage caused in response to topo I poisons. Arrows indicate types of DNA damage, and the pathways and enzymes used to repair them are shown in boxes.

The most likely mechanism of interaction between PARP-1 and the repair of topo I poison-mediated DNA damage is via the BER pathway. As has been reviewed previously in this thesis, the role of PARP-1 in BER has been demonstrated although not yet fully understood. BER is the pathway that is responsible for the repair of DNA single strand breaks caused by excision of damaged bases e.g. following exposure to alkylating agents or IR (see section 1.6.7). BER has been implicated in the repair of topo I poison-induced DNA damage, as cells deficient in BER through a mutation in the BER scaffold protein, XRCC1 (EM9 cells) are hypersensitive to topo I poisons independently of replication (Caldecott and Jeggo, 1991, Barrows *et al.*, 1998). In addition to this KB cells that have been made resistant to camptothecin, through exposure to increasing concentrations of camptothecin, have been shown to over-express XRCC1. The degree of resistance of these cells was directly related to the level of XRCC1 in the cell line (Park *et al.*, 2002).

It is possible that PARP-1 is involved in the repair of the other forms of damage. Recently a link has been suggested between the repair of the cleavable complex and the BER pathway. TDP-1 is the enzyme that specifically cleaves the chemical bond that joins the active site tyrosine of topo 1 to the 3'-end of DNA allowing removal of the cleavable complex (Yang *et al.*, 1996). This enzyme is widely conserved between eukaryotes, which suggests that it plays an important role. However this enzyme does not have the 3'-phosphatase activity that is required to produce a 3'-hydroxyl DNA end for the extension of DNA by repair polymerases and therefore can only repair some of

the lesions. Polynucleotide kinase phosphatase (PNK) can remove the phosphate and produce a 3'-hydroxyl terminus that can be extended by DNA pol β and ligated by ligases. Yeast deficient in PNK exhibit hypersensitivity to camptothecin demonstrating the importance of PNK in the response to camptothecin (Meijer *et al.*, 2002). Recently a link has been made between PNK, TDP-1 and the scaffold protein XRCC1. Plo *et al.*, (2003) compared the EM9, XRCC1 deficient cell line and XRCC1-complemented EM9 cells and showed that the camptothecin-sensitivity observed in the EM9 cells was related to reduced single strand break repair. The XRCC1-transfected EM9 cell line also exhibited and enhanced TDP and PNK activities. XRCC1 was also shown to immunoprecipitate with TDP and PNK. An interaction between XRCC1 and PNK has previously been shown using yeast-2-hybrid technology and further investigation revealed that XRCC1 stimulated PNK activity (Whitehouse *et al.*, 2001). These findings indicated that there might be a functional link between the BER repair pathway and the repair of topo I cleavable complexes. It was hypothesised that XRCC1 may act as a scaffold protein to recruit TDP-1, to sites of breakage, as it does with other repair enzymes. Once the topo I had been excised by TDP-1 and the DNA ends prepared by PNK, then the BER pathway could religate the break (see figure 6.2). XRCC1 is known to associate with PARP-1 via BRCT domains present in both proteins, and possibly the zinc-finger domain of PARP-1. (Masson *et al.*, 1998). Therefore it is possible that PARP-1 could be involved in the repair following the removal of the cleavable complex by TDP-1.

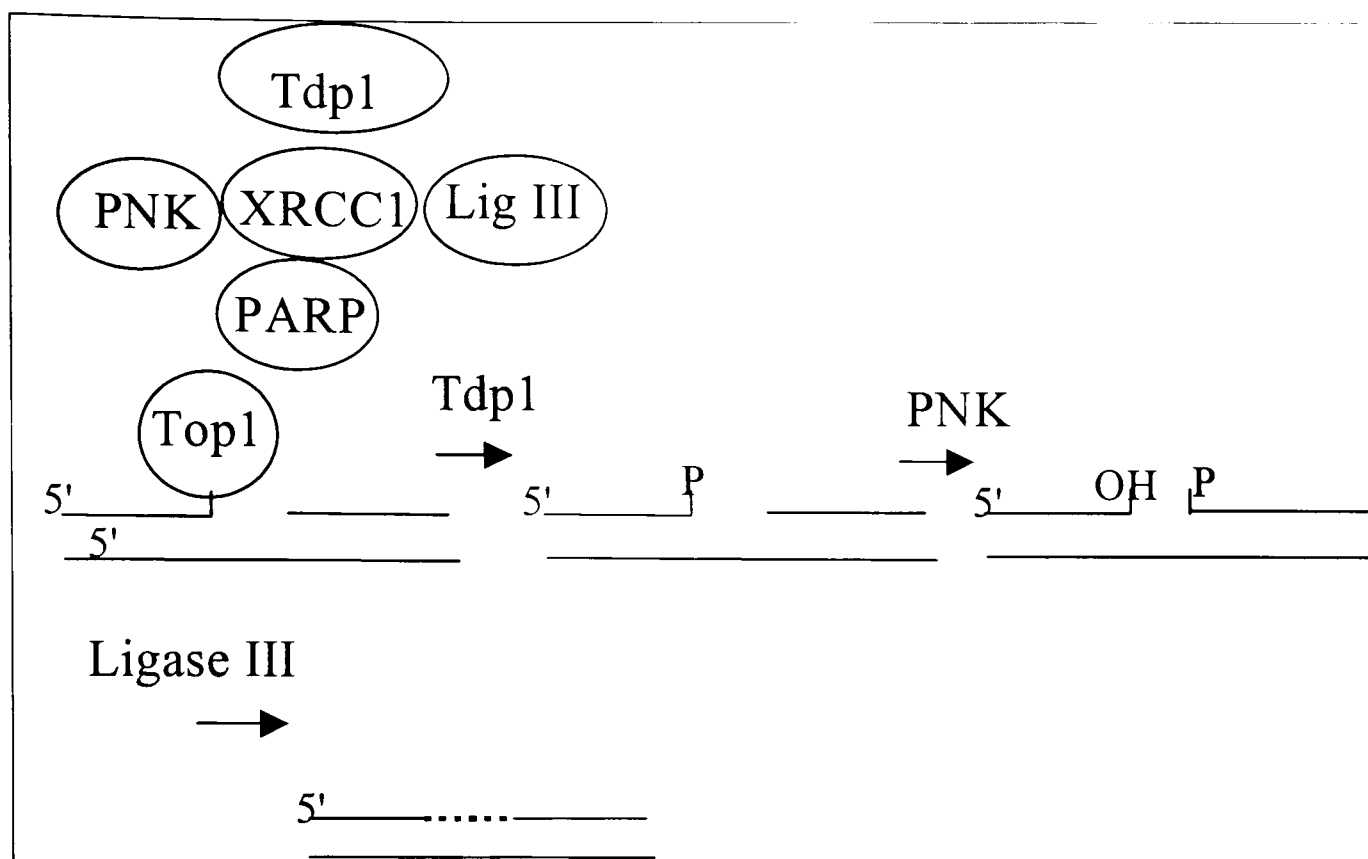


Figure 6.2 Proposed mechanism for the repair of topo I cleavable complexes by an XRCC1-dependent pathway. The repair complex is shown at the top and is coordinated by the scaffold protein, XRCC1, to repair the DNA strand break. Tdp1 hydrolyses the 3'-phosphotyrosyl bond, then PNK hydrolyses the 3'-phosphate and phosphorylates the 5'-hydroxyl. The gap is sealed by ligase III. Adapted from Plo *et al.*, (2003).

There is evidence that the homologous recombination repair pathway (HR) is involved in the repair of camptothecin-induced DNA double strand breaks. HR is described in section 1.5.3.1. Briefly, HR is an error-free mechanism of DSB repair that uses the sister chromatid as a template. This process involves the Rad50/MRE11/NBS-1 complex and Rad52. The involvement of HR in the response to camptothecin has been demonstrated using cells deficient in a number of components of the HR pathway. Yeast deficient in homologous recombination through a mutation in Rad52 are hypersensitive to camptothecin (Nitiss and Wang, 1988). Cells deficient in NBS-1, part of the Rad50/Mre11/NBS1 complex, are three-fold hypersensitive to camptothecin (Kraakman-van der Zwet *et al.*, 1999). The CHO cell line irs1SF, deficient in the HR protein XRCC3, has been shown to be 5-fold sensitive to camptothecin. Arnaudeau *et al.*, (2001) and Hinz *et al.*, (2003) have made a comparison of sensitivities of NHEJ and HR-deficient cells to camptothecin. The HR deficient irs1SF cells were shown to be more sensitive to a 24 hour exposure to camptothecin than NHEJ-deficient V3 cells,

with LC₉₀ values of 10 nM and 50 nM respectively, compared to 100 nM in the parental AA8 cell line. In these papers it was suggested that HR played a more important role in the response to camptothecin than NHEJ due to relative sensitivities of the cell lines.

Recently, a role for PARP-1 in the HR pathway has been described. PARP-1 deficient cells have an increased level of sister chromatid exchange suggesting a hyper recombination phenotype. Therefore a role for PARP-1 in HR was investigated. Rad51 foci form at sites of HR, and are an indicator of an efficient HR pathway; cells deficient in HR do not form foci. Rad51 foci form in PARP-1 deficient cells and in general PARP-1 does not co-localise with Rad51 foci. Repair of DSB by HR was not affected in the PARP-1 deficient cells. However, the PARP-1 null cells displayed a 30% increase in spontaneous Rad51 foci and inhibition of PARP-1 by 3-AB, ISQ or NU1025, increased the number of cells with Rad51 foci in the PARP-1 proficient cell line but not the PARP-1 deficient line. Therefore this shows that Rad51 foci are induced in the absence of PARP-1 or as a consequence of PARP-1 inhibition. These data suggest that PARP-1 does not participate in HR directly but may have a role in controlling the DNA damage recognised by HR (Schultz *et al.*, 2003). Therefore as HR is involved in the repair of camptothecin-induced damage and PARP-1 may be involved in HR, it is possible that PARP-1 exerts some effect on topo I cytotoxicity via the HR pathway.

Camptothecin-induced DNA double strand breaks can be repaired via the NHEJ pathway. NHEJ is reviewed in section 1.5.3.2. This process is more error-prone and involves the rejoining of the DNA double strand breaks by DNA-PK, XRCC4 and DNA ligase IV, without the synthesis of new DNA. Much of the evidence for the role of NHEJ in the response to camptothecin involves the nuclear serine-threonine kinase DNA-PK, which is activated by DNA double strand breaks, and is the end-binding complex of the NHEJ pathway. DNA-PK activity was increased 5-fold in HT-29 cells in response to 1 hour treatment with camptothecin. Also, human glioblastoma MO-59J cells, deficient in the catalytic subunit of DNA-PK are hypersensitive to camptothecin (Shao *et al.*, 1999 values not quoted). The V3 cell line also deficient in DNA-PK has been shown to be ~2-fold more sensitive to camptothecin than the parental AA8 cell line (Arnaudeau *et al.*, 2003). This demonstrates that NHEJ is involved in the response to camptothecin.

PARP-1 and DNA-PK have been shown to interact by a number of authors (reviewed by de Murcia and Shall, 2000). Both of these enzymes have similar properties in the single and double strand break repair pathways. Both bind DNA strand interruptions and are activated by strand breaks, however DNA-PK is only activated by double strand breaks (Blier *et al.*, 1993), whereas PARP-1 is activated by a variety of breaks, both double and single strand (Benjamin and Gill, 1980). PARP-1 poly(ADP-ribosylates) DNA-PK, leading to activation of the protein. DNA-PK phosphorylates PARP-1 *in vitro* without any consequence (Ruscetti *et al.*, 1998). PARP-1, DNA-PKs and the Ku proteins have also been shown to co-immunoprecipitate (Morrisson *et al.*, 1997). Since there is definitely a functional interaction between these proteins, such an interaction may regulate a pathway that is involved in the repair of camptothecin-induced DNA damage, and it is therefore possible that PARP-1 may mediate its effect on topo I activity via the NHEJ pathway.

Topo I poison-mediated DNA damage may also be repaired by the nucleotide excision repair pathway (NER) pathway. NER is described in detail in section 1.5.2. NER is responsible for the repair of damage that distorts DNA such as thymidine dimers caused by UV light and other bulky adducts. This process involves many proteins including XPC, XPG, CSA, CSB and RPA. Cells deficient in either of the two transcription coupled-NER proteins associated with Cockayne syndrome (CSA and CSB), are sensitive to camptothecin (Squires *et al.*, 1993). Camptothecin-resistant MCF/C4 cells have also been shown have enhanced nucleotide excision repair activity (Fujimori *et al.*, 1996). However, cells deficient in other NER factors such as the XP factors are not hypersensitive to camptothecin (Squires *et al.*, 1993). PARP-1 is not thought to have a role in the NER pathway as 3-AB was unable to potentiate UV damage (Cleaver *et al.*, 1983). Since it has been reported that PARP-1 does not exert its effect on topo I poison-mediated cytotoxicity via the NER pathway, this pathway was not investigated in this study.

PARP-1 is primarily thought to be involved in BER, although the evidence presented above may implicate a role for PARP-1 in the HR and NHEJ pathways as well. As multiple DNA lesions are formed in response to damage with camptothecin which may

be repaired by any of these pathways, it is therefore possible that the modulation of repair of DNA strand breaks by PARP-1 may be mediated by one or all of these pathways. Therefore the aim of this chapter is to elucidate which pathway or pathways are involved in the response of PARP-1 to camptothecin-mediated DNA damage.

6.2 Aims.

In the previous chapters it has been shown that AG14361 increases the cytotoxic and growth inhibitory effects of topo I poisons. Investigations into the mechanisms underlying this have shown that PARP-1 is most likely to effect topo I poison-induced cytotoxicity via modulation of DNA repair. The aim of the experiments described in this chapter was to try to identify the repair pathways that PARP-1 was involved in, to cause the modulation of camptothecin-induced cytotoxicity. In this chapter the effect of AG14361 on camptothecin-mediated cytotoxicity in BER, HR and NHEJ deficient cell lines was investigated as PARP-1 has been implicated in these pathways as described above. Also the effect of AG14361 on the repair of camptothecin-induced DNA damage in BER deficient cells was investigated. The theory behind these studies was that if a cell line was already deficient in a repair pathway then further inhibition of this pathway should not result in potentiation of cytotoxicity.

Cell lines used in this chapter.

The cell lines used in this chapter were the parental AA8 Chinese hamster ovary cell line, the base excision repair deficient EM9 cell line, non-homologous end joining deficient V3 cell line and the homologous recombination deficient irs1SF cell line.

The CHO EM9 cell line is deficient in base excision repair. This cell line was isolated on the basis of their hypersensitivity to killing by ethyl methanesulfonate (EMS) (Thompson *et al.*, 1980). These cells have ~10-fold sensitivity to EMS and MMS, moderate sensitivity to H₂O₂ and camptothecin (2 to 5-fold), and weak sensitivity to IR, ENU, MNNG, mitomycin C, UVC, UVA, near visible and blue light and heavy metals. They also have a reduced rate of DNA-strand break rejoining following treatment with X-rays, EMS or MMS, as well as a high baseline frequency of sister chromatid exchange compared to the parental AA8 cell line (Thompson *et al.*, 1982). It had been

demonstrated that hypersensitivity is mediated via a mutation in the XRCC1 gene, resulting in a deficiency in base excision repair. (Thompson *et al.*, 1990). The gene coding for XRCC1 in the EM9 cells has been shown to contain a C to T base change in codon 221, which introduces a termination codon one third of the way into the sequence. This results in the expression of a truncated XRCC1, which does not contain either of the BRCT domains (Shen *et al.*, 1998).

The V3 CHO cell line is deficient in NHEJ via a deficiency in DNA-PK. The V3 cell line does not express DNA-PKcs due to an inactivating mutation in the C-terminal region of one allele of the DNA-PKcs gene (XRCC7) (Blunt *et al.*, 1995). These cells have been shown to be 2-fold more sensitive to camptothecin than the parental AA8 cell line (Arnaudeau *et al.*, 2003).

The irs1SF cell line was isolated because of their 2-fold sensitivity to x-rays. These cells have been shown to have cross-sensitivity to UV (2.5-fold), EMS (2.3-fold), camptothecin (5-fold), and also the cross-linking agent mitomycin C, cisplatin, nitrogen mustard, and melphalan (between 20 to 60-fold). The irs1SF cells have also been reported to have a ~50% reduced efficiency of repair of single strand breaks, and an increased levels of spontaneous chromosome aberrations (10-24% abnormal cells). (Caldecott and Jeggo, 1991, Fuller and Painter, 1988). The irs1SF cells have been shown to be deficient in the HR protein, XRCC3 (Tebbs *et al.*, 1995). These cells show an altered death and cell cycle checkpoint responses following treatment with camptothecin (Hinz *et al.*, 2003).

6.3 Results

6.3.1 Effect of AG14361 on camptothecin-induced cytotoxicity in AA8, EM9 and V3 cell lines.

To investigate the repair pathways involved in the effect of AG14361 on topo I poison induced damage, cells deficient in DNA repair were obtained. The cell lines were deficient in BER, HR, and NHEJ pathways, the three pathways for which there is evidence of interaction with PARP-1 (Table 6.1). The cell lines were selected on the basis of their common parental cell line to allow comparison between cell lines. Since a human model set of cell lines were not available, Chinese hamster ovary cell lines were used as these cells have a well defined genotype and phenotype as described in section 6.2. The repair deficient cells were used to define which pathway or pathways involve PARP-1.

Cell Line	Repair Deficiency	Genotype
AA8		Parental CHO cell line
EM9	BER	Deficient in XRCC1
V3	NHEJ	Deficient in DNA-PKcs
irs1SF	HR	Deficient in XRCC3

Table 6.1 Cell lines used in this chapter and their characteristics

To investigate the effect of AG14361 on camptothecin-induced cytotoxicity in AA8, EM9 and V3 cell lines, clonogenic survival assays were used (see section 2.4.4). Initial studies with a range concentrations of camptothecin defined the appropriate concentration range for investigation of the impact of 0.4 μ M AG14361 on camptothecin-induced cytotoxicity. Cells were exposed to camptothecin for 16 hours before harvesting, counting and re-plating a defined number of cells for colony formation in drug-free medium (Figure 6.3). Cell survival was expressed as a percent of untreated control.

Figure 6.3 shows that the irs1SF cells were the most sensitive to camptothecin, being 9.3 ± 2.8 -fold more sensitive to camptothecin than the AA8 cells ($p = 0.003$ unpaired t-test). The EM9 cells were 4.5 ± 1.2 -fold more sensitive to camptothecin than the AA8

cells ($p = 0.0007$, unpaired t-test). The V3 cells were 1.6 ± 0.4 -fold more sensitive to camptothecin than the AA8 cells ($p = 0.03$, unpaired t-test). The EM9 cells were 2.9 ± 0.9 -fold more sensitive to camptothecin than the V3 cells ($p = 0.03$, unpaired t-test). These sensitivities are consistent with previous reports (Arnaudeau *et al.*, 2001, Caldecott and Jeggo, 1991). The significant sensitivities of all three repair-deficient cell lines to camptothecin relative to the repair-proficient parental cells implicate all three of the repair pathways in the cellular response to topo I poisons, with HR being the most important and NHEJ the least. In order to determine which pathways involve PARP-1, the effect of AG14361 on camptothecin induced cytotoxicity was investigated in these cells. Initial revealed that the irs1SF cells were hypersensitive to AG14361 alone and combination experiments with these cells are described in section 6.3.2. The following section describes studies with V3 and EM9 cells in comparison with AA8 cells.

The effect of co-incubation with $0.4 \mu\text{M}$ AG14361 on the cytotoxicity of a 16 hour exposure to an appropriate range of camptothecin concentrations was investigated. Survival curves of mean data from AA8, V3 and EM9 cell lines exposed to camptothecin \pm AG14361 for 16 hours are shown in Figure 6.4, Figure 6.4, and Figure 6.5, respectively. Pooled data from all cell lines are shown in Table 6.2. AG14361 significantly potentiates the cytotoxicity of camptothecin by 2.25-fold in AA8 cells, and 2.0-fold in V3 cell lines ($p = 0.005$ and 0.04 respectively paired t-test). This was comparable with the 2 to 3-fold potentiation seen in the K562 and PARP-1 wild type cell lines in chapter 3 and potentiation of other cell lines by PARP-1 inhibitors as reported in the literature. Potentiation of camptothecin-induced cytotoxicity by AG14361 in the V3 cells suggests that there are other camptothecin-induced damage repair pathways besides NHEJ that involves PARP-1. AG14361 did increase the sensitivity of EM9 cells to camptothecin 1.8-fold, however, this increase was not significant ($p = 0.18$, paired t-test). Examination of the individual experiments shows that there was no potentiation in of camptothecin-induced cytotoxicity by AG14361 in 3 of the 5 experiments. This would suggest that BER was the major PARP-1 dependent pathway for repair of camptothecin-induced DNA damage. However as potentiation was seen in some experiments there is still a possibility that there are other PARP-1-dependent pathways that lead to survival following exposure to camptothecin, besides BER.

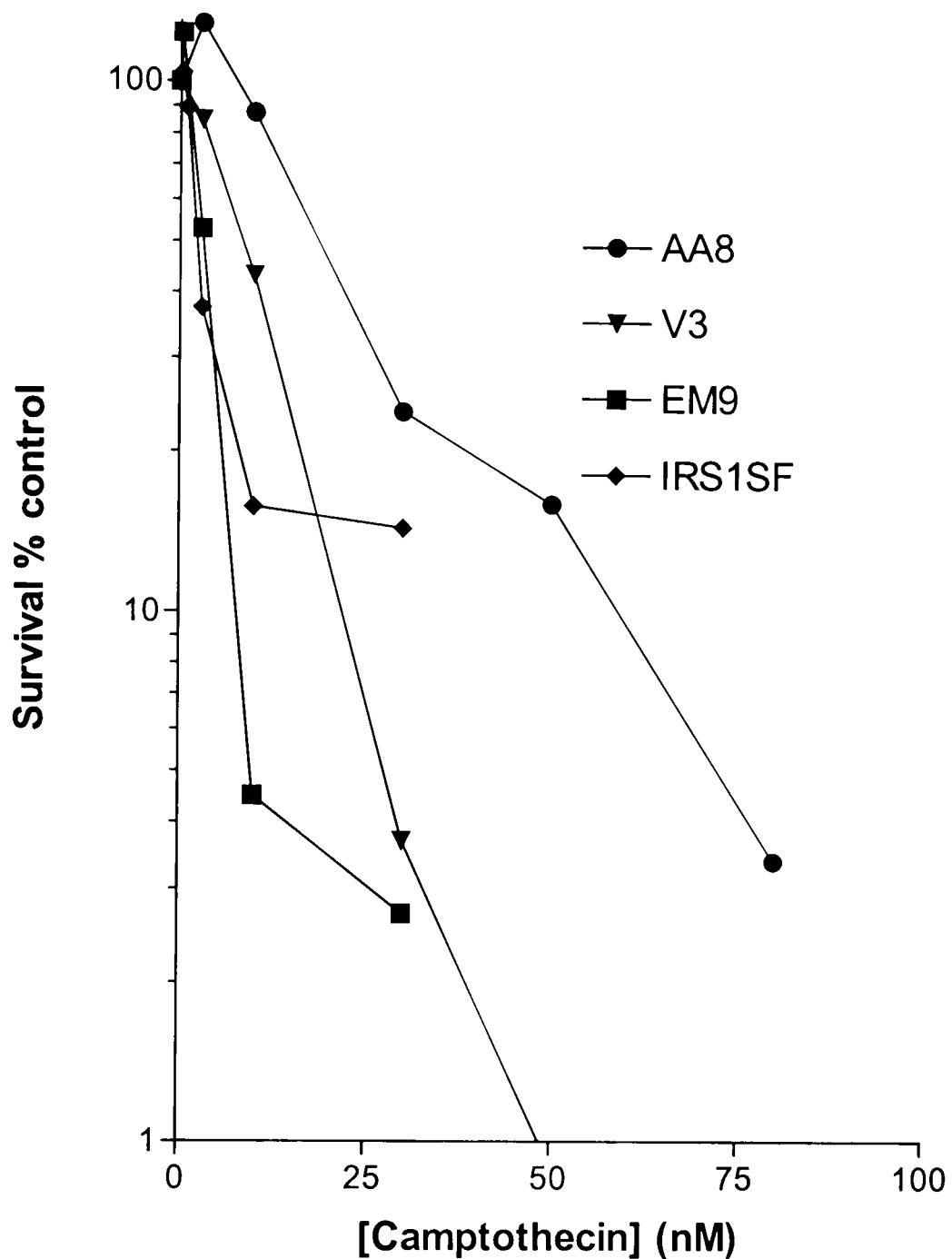


Figure 6.3 Relative sensitivities of AA8, V3, EM9 and irs1SF cells to camptothecin.

Cells were exposed to a range of concentrations of camptothecin for 16 hours. Cell survival was determined by the clonogenic assay (see section 2.4.4). The number of colonies formed was expressed as a percentage of the untreated control. Data are representative curves from one individual experiment using triplicate samples, they are not from the same experiment and not all examined at the same time.

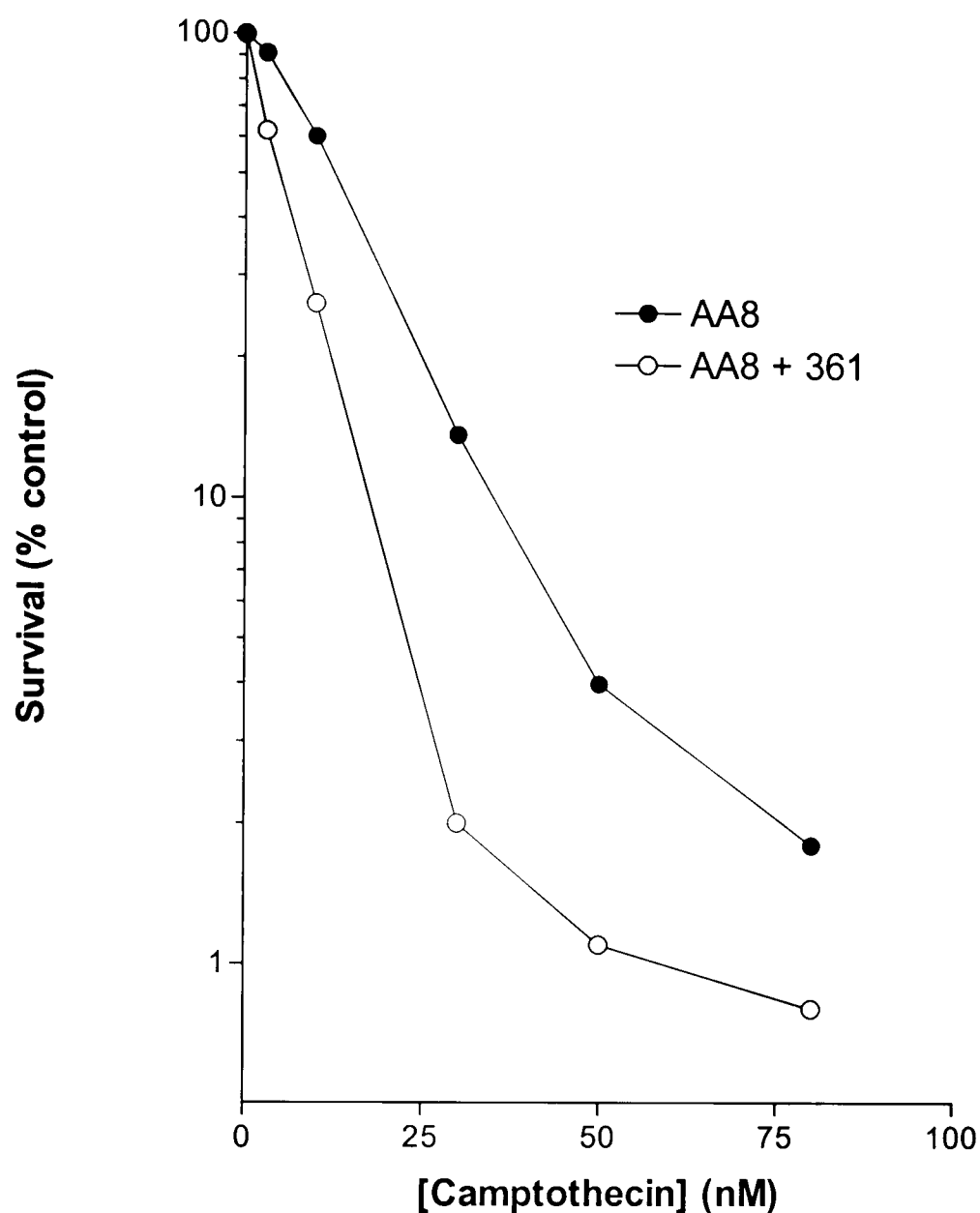


Figure 6.4 Effect of AG14361 on camptothecin-induced cytotoxicity in AA8 cells.

AA8 cells were exposed to 0, 1, 3, 10, 30, 50 and 80 nM camptothecin in the presence or absence of 0.4 μ M AG14361 for 16 hours. Cell survival was determined using the clonogenic assay (see section 2.4.4). The number of colonies formed was expressed as a percentage of the untreated or 0.4 μ M AG14361 alone control. Data are from one representative experiment.

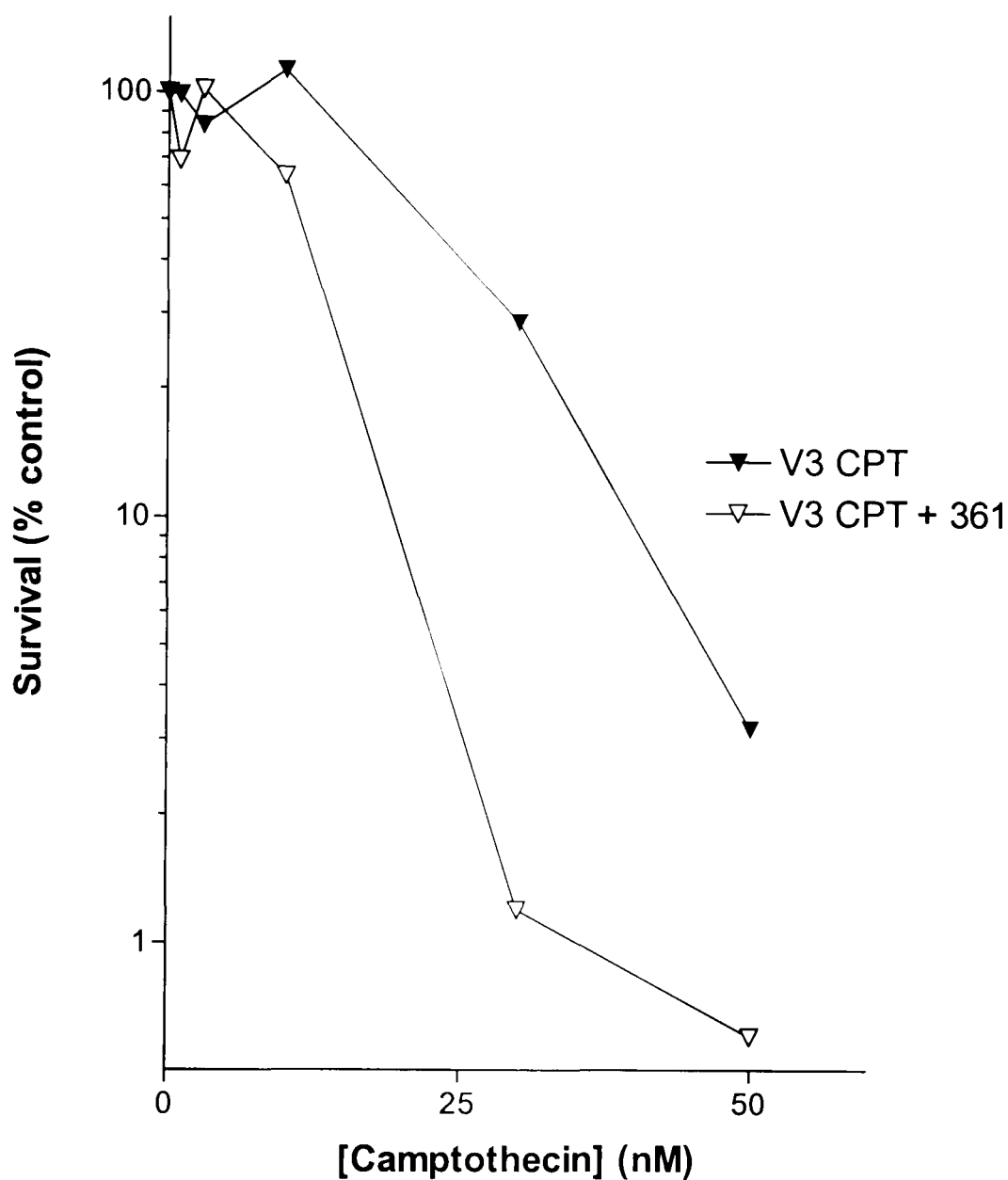


Figure 6.5 Effect of AG14361 on camptothecin-induced cytotoxicity in V3 cells.

V3 cells were exposed to 0, 1, 3, 10, 30, and 50 nM camptothecin in the presence or absence of 0.4 μ M AG14361 for 16 hours. Cell survival was determined by the clonogenic assay. The number of colonies formed was expressed as a percentage of the relevant untreated or 0.4 μ M AG14361 alone control. Data are from one representative experiment.

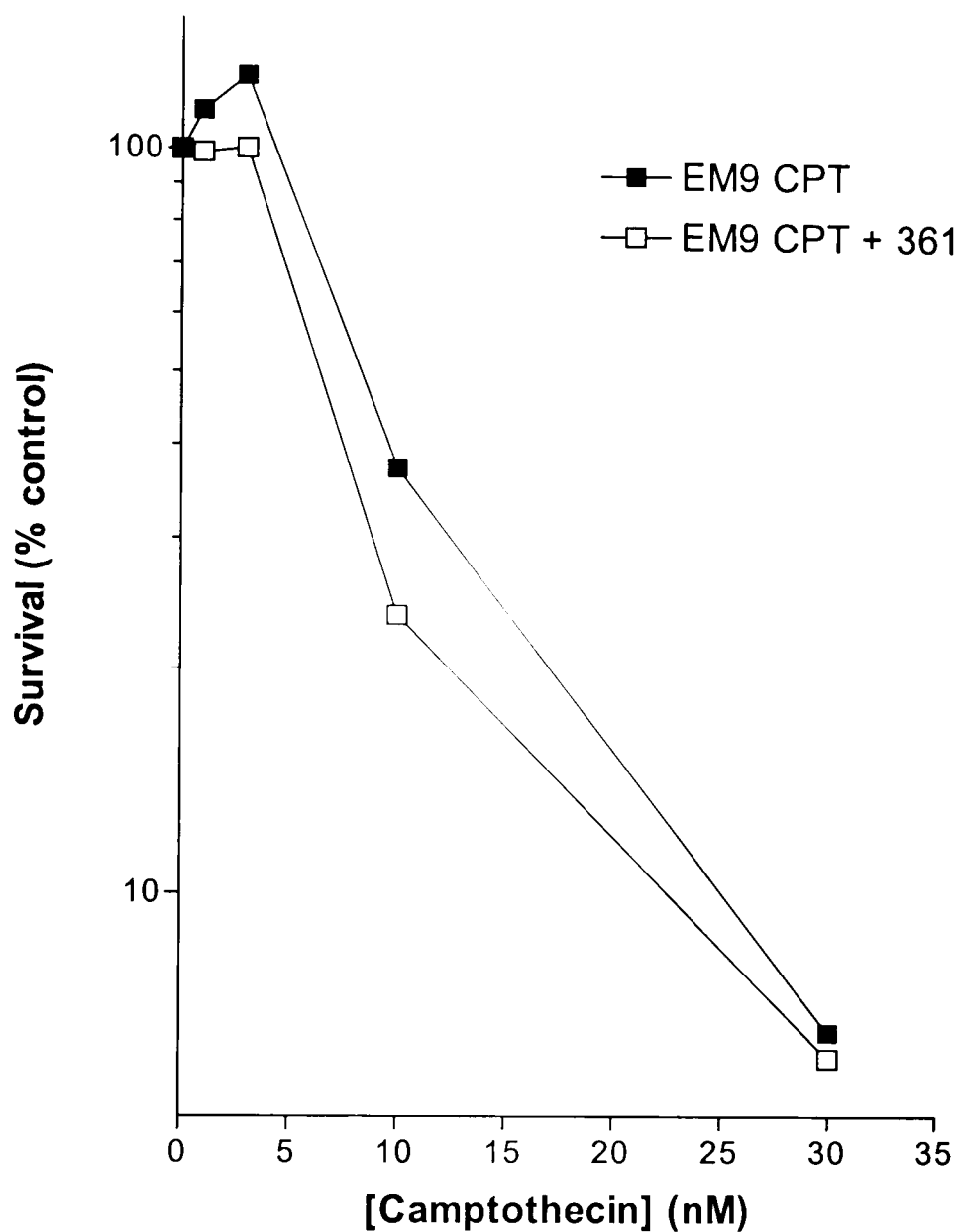


Figure 6.6 Effect of AG14361 on camptothecin-induced cytotoxicity in EM9 cells.

EM9 cells were exposed to 0, 1, 3, 10, and 30 nM camptothecin in the presence or absence of 0.4 μ M AG14361 for 16 hours. Cell survival was determined by clonogenic assay. The number of colonies formed was expressed as a percentage of the untreated or 0.4 μ M AG14361 alone control. Data are from one representative experiment.

Cell Line		LC ₅₀ (nM)	PF ₅₀ (nM)
AA8	Camptothecin	25.0 ± 3.5	2.25 ± 0.31
	Camptothecin + AG14361	12.2 ± 2.4 **	
EM9	Camptothecin	5.6 ± 1.2	1.85 ± 0.63
	Camptothecin + AG14361	4.0 ± 1.1 ^{NS}	
V3	Camptothecin	16.1 ± 4.0	2.0 ± 0.50
	Camptothecin + AG14361	10.2 ± 3.6*	

Table 6.2 Survival of AA8, EM9 and V3 cell lines following a 16 hour exposure to camptothecin in the presence or absence of AG14361.

Mean LC₅₀ values from at least 4 independent experiments are given ± SEM. Mean PF₅₀ ± SEM values calculated using LC₅₀ values from individual experiments.

NS = not significantly different from camptothecin alone, * p < 0.05, ** p< 0.01 compared to camptothecin alone, paired t-test.

6.3.2 Effect of AG14361 on camptothecin-induced cytotoxicity in the irs1SF (homologous recombination-deficient) cell line.

The effect of AG14361 on homologous recombination deficient cells was also investigated. The irs1SF cell line was used, which has a deficiency in homologous recombination that can be corrected by transfection of XRCC3 into the cell. This cell line has previously been shown to be hypersensitive to camptothecin and are unable to rejoin single strand breaks (Caldecott and Jeggo, 1991, Fuller and Painter, 1988). It has also been shown that these cells are hypersensitive AG14361 alone (S Kyle, NICR personal communication). Therefore it was necessary to identify a concentration of AG14361 that would not cause significant cytotoxicity compared to untreated control in a cell survival assay, but still inhibited PARP-1 activity.

The cytotoxic effects of AG14361 on the irs1SF cell line were determined by clonogenic survival assay (section 2.4.4). The survival of irs1SF cells following a 16 hour exposure to increasing concentrations of AG14361 is shown in Figure 6.7. Survival of irs1SF cells was reduced by < 50% by 0.4 μ M AG14361. At concentrations below 100 nM there was >90% survival. In order to determine if this hypersensitivity was due to altered PARP-1 activity and to ensure that an adequate concentration of AG14361 to inhibit PARP-1 activity was used in subsequent clonogenic survival assays, PARP-1 activity was determined in the presence and absence of AG14361 by [32 P]-NAD incorporation as described in section 2.6. The effect of a 10 min exposure to a range of concentrations of AG14361 on PARP-1 activity is shown in Figure 6.8. Based on these data, PARP-1 activity in these cells was 70 pmol/ 10^6 cells. Concentrations of AG14361 (15 and 70 nM) that inhibited PARP-1 by 50 and 90% respectively, were chosen for the determining the impact of PARP-1 inhibition on camptothecin-induced cytotoxicity in irs1SF cells. These concentrations of AG14361 had minimal effect on cell survival and corresponded to a 26 and 6-fold lower concentration of AG14361 than used in the other cell lines.

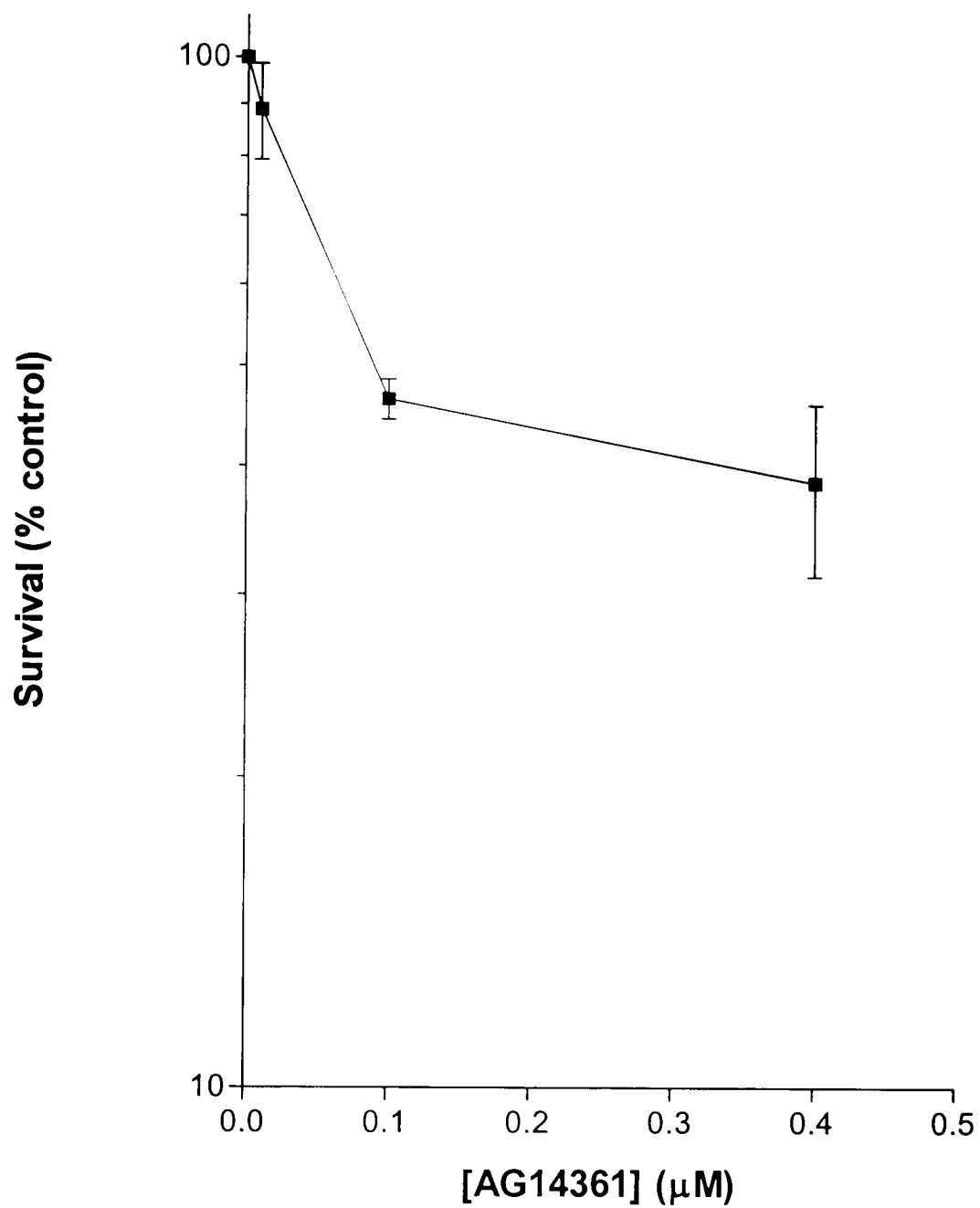


Figure 6.7 Effect of AG14361 on cell survival in the irs1SF cell line.

irs1SF cells were exposed to 0.01, 0.1 and 0.4 μM AG14361 for 16 hours. Cytotoxicity was determined by clonogenic assay (section 2.4.4). The number of colonies formed was expressed as a percentage of the untreated control. Data from one experiment is shown.

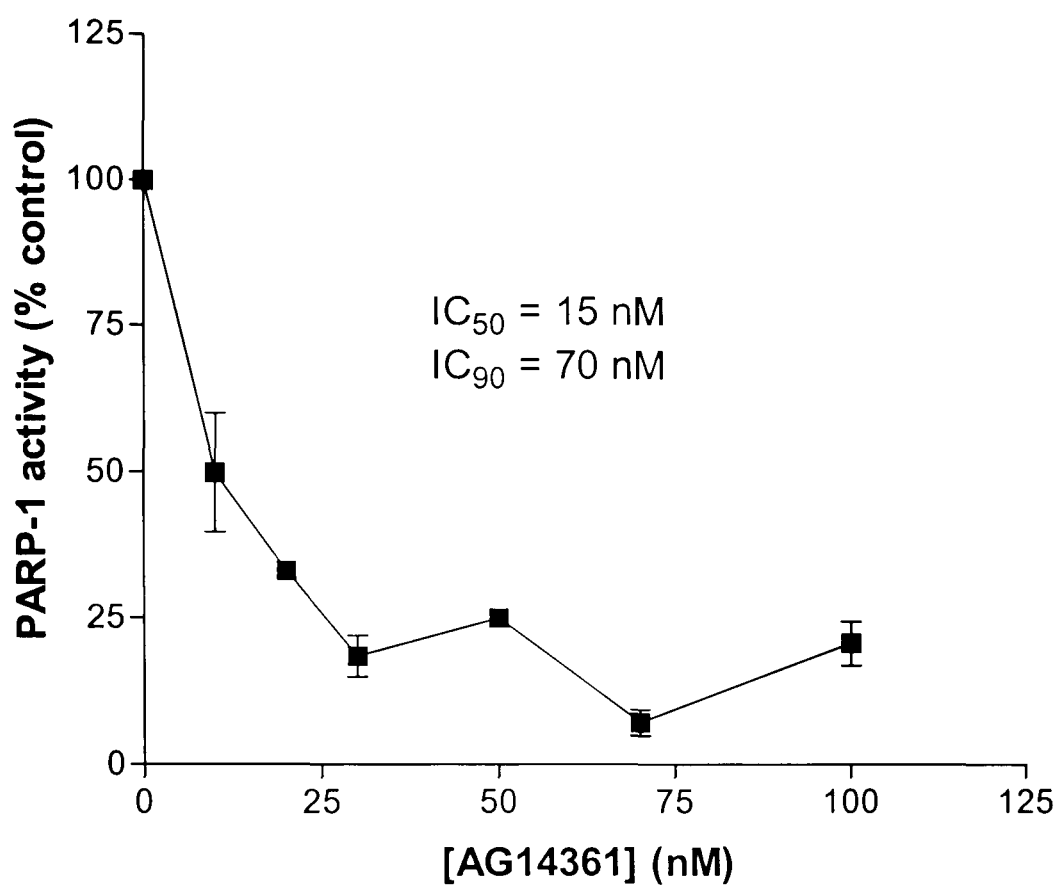


Figure 6.8 Inhibition of PARP-1 activity by AG14361 in the irs1SF cell line.

irs1SF cells were exposed to 0, 10, 20, 30, 50, 70, and 100 nM AG14361 for 10 mins. PARP-1 activity was determined by [32 P]-NAD incorporation assay (see section 2.6). Data are the mean of three independent experiments \pm SEM.

6.3.3 Effect of AG14361 on survival of irs1SF cells treated with camptothecin.

The clonogenic survival of irs1SF cells in response to 16 hours treatment with camptothecin in the presence or absence of 15 or 70 nM AG14361 was determined. The survival of irs1SF cells is shown in Figure 6.9 and mean LC₅₀ values are given in Table 6.3. These data show that there was no significant potentiation of camptothecin induced cytotoxicity in the presence of either of the concentrations of AG14361 used ($p > 0.2$ paired t-test). The combination of acute hypersensitivity to both camptothecin and AG14361 in these cells has made it difficult to determine if there was any additive effect of AG14361 on camptothecin cytotoxicity. Since much lower AG14361 concentrations had to be used in these experiments it is difficult to compare these data with those in the other cell lines. Nevertheless, looking at figure 6.9, 70 nM AG14361 did cause a similar degree of potentiation to that seen in the AA8 and V3 cell lines, suggesting that HR-independent mechanisms are involved in AG14361-mediated potentiation of camptothecin.

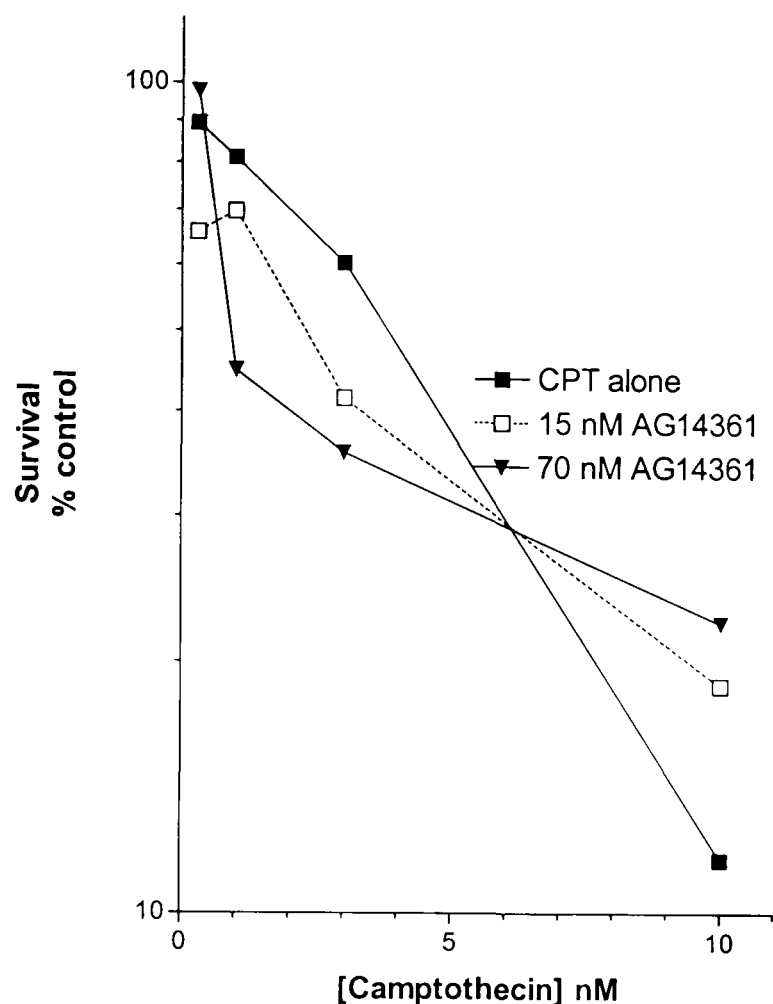


Figure 6.9 Effect of AG14361 on camptothecin-induced cytotoxicity in irs1SF cells.

irs1SF cells were exposed to 0, 1, 3, 10, and 30 nM camptothecin in the presence or absence of 15 or 70 nM AG14361 for 16 hours. Cell survival was measured using the clonogenic assay (see section 2.4.4). The number of colonies formed was expressed as a percentage of the untreated, 15 or 70 nM AG14361 alone control. Data are from a single representative experiment.

	LC ₅₀ Camptothecin (nM)	LC ₅₀ Camptothecin + 15 nM AG14361 (nM)	LC ₅₀ Camptothecin + 70 nM AG14361 (nM)
	2.69 ± 0.69	1.66 ± 0.43	1.43 ± 0.42
PF ₅₀		1.97 ± 0.72	2.29 ± 0.79

Table 6.3 Effect of AG14361 on camptothecin induced cytotoxicity in irs1SF cells.

Mean IC₅₀ values from 4 independent experiments ± SEM are shown. PF₅₀ values calculated from IC₅₀ values from individual experiments ± SEM.

6.3.4 DNA damage repair in AA8 and EM9 cell lines.

In the previous section it was found that AG14361 significantly enhanced camptothecin-induced cytotoxicity in repair competent, NHEJ and HR-deficient cells but in the camptothecin-sensitive, BER-deficient, EM9 cells, potentiation by AG14361 was not significant. This suggested that (a) BER was implicated in the repair of camptothecin-induced DNA damage and (b) that PARP-1 dependent repair/survival was conducted via BER. To investigate this further at the level of DNA repair, the effect of AG14361 on repair of camptothecin-induced DNA strand breaks in AA8 and EM9 cells was determined by alkaline elution.

EM9 cells had been reported to be slow at rejoining single strand breaks (Thompson *et al.*, 1982). Therefore an appropriate time point to measure the repair in these cells was determined. Initial experiments revealed that the EM9 cells had completed ~70% repair of single strand breaks induced by 10 μ M camptothecin after 60 mins repair in drug free medium. This was comparable to the results obtained using the PARP-1 wild-type and null cells where 48 and 57% repair was achieved after 60 mins in drug free medium. Therefore, 60 mins was thought to be a suitable time point to measure repair in these cells in comparison with the AA8 cells. AA8 and EM9 cells were treated with 10 μ M camptothecin for 30 mins in parallel, the drug was removed and the cells were allowed to repair in drug free medium or medium containing AG14361 for a further 60 mins. Representative elution profiles and table summarising data for triplicate experiments is shown in Figure 6.10 and Table 6.4, respectively. The EM9 cells had significantly more DNA strand breaks than the AA8 cells after a 30 min exposure to camptothecin without repair; relative elution in EM9 cells = 0.63 ± 0.04 compared to 0.44 ± 0.04 in AA8 cells ($p = 0.05$ paired t-test), in agreement with the retarded repairing in these cells reported previously (Thompson *et al.*, 1982). These data show that AG14361 significantly retarded DNA strand break ligation in the AA8 cell line at 60 mins ($p = 0.03$, paired t-test). In the EM9 cells, despite the initial higher level of DNA breaks compared to the AA8 cells, the rate of repair in the presence and absence of AG14361 was very similar to that observed in the AA8 cells (Table 6.4), i.e. in both cell lines ~25% breaks remained after a 60 min in control medium and ~40% in AG14361-containing medium.

However the effect of AG14361 on breaks rejoining was not significant in the EM9 cells ($p = 0.09$ paired t test).

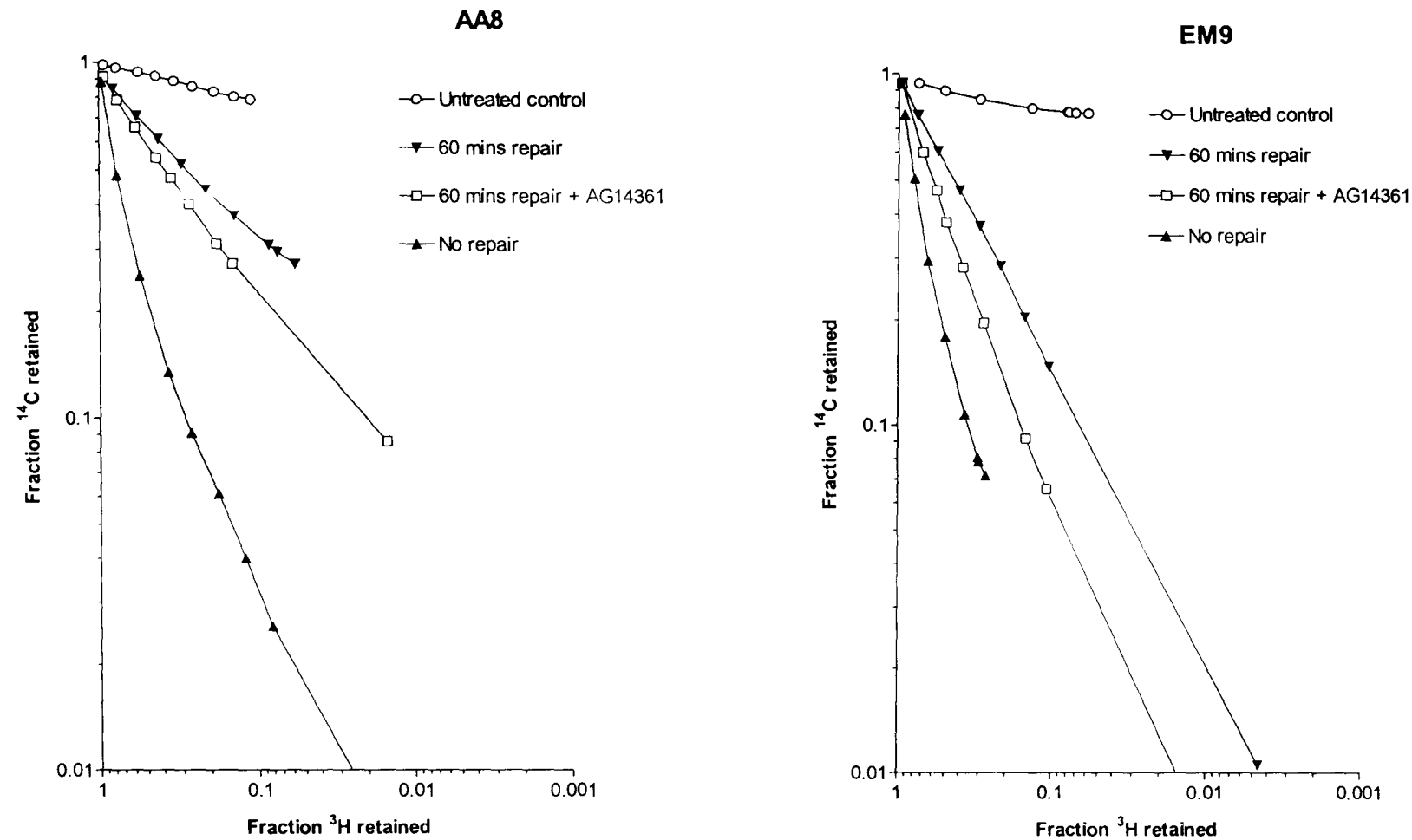


Figure 6.10 Effect of AG14361 on repair of camptothecin-induced DNA strand breaks in AA8 and EM9 cells.

AA8 and EM9 cells were exposed to 10 μ M camptothecin in the presence or absence of AG14361 followed by removal of the drug and a further 60 mins repair in fresh medium or medium containing 0.4 μ M AG14361. Elution profiles from one representative experiment are shown.

	AA8	EM9
No repair (Relative Elution)	0.49 ± 0.04	0.63 ± 0.04
60 min repair (Relative elution)	0.12 ± 0.011	0.16 ± 0.014
% DNA strand breaks remaining	25.8 ± 2.9	25.1 ± 2.9
60 min repair + AG14361 (Relative elution)	$0.19 \pm 0.003 *$	$0.25 \pm 0.023^+$
% DNA strand breaks remaining	39.7 ± 1.7	38.4 ± 2.9

Table 6.4 Effect of AG14361 on repair of camptothecin-induced DNA strand breaks in AA8 and EM9 cells.

Cells were exposed to 10 μ M camptothecin in the presence or absence of AG14361 followed by removal of the drug and a further 60 mins repair in medium \pm 0.4 μ M AG14361. Data are mean relative elution values from 3 independent experiments \pm SEM. % DNA strand breaks was calculated using relative elution values for samples and expressing these as a percentage of a camptothecin treated control that was not allowed to repair.

Significant differences from RE value in absence of AG14361 are given by: ⁺ p < 0.01, * p < 0.05.

6.4 Discussion

Topo I poison-mediated DNA damage has been reported to be repaired by a number of different pathways including BER, HR, and NHEJ (reviewed in Pourquier and Pommier, 2001, Caldecott and Jeggo, 1991, Arnaudeau *et al.*, 2001). The aim of this chapter was to try to determine by which repair pathways PARP-1 was acting to increase the amount of DNA damage caused by topo I poisons thus enhancing cytotoxicity. PARP-1 may play a role in all of these pathways as described in the introduction to this chapter and therefore the effect of AG14361 on cells deficient in BER, NHEJ and HR was investigated.

The data presented in this chapter showed that cells deficient in BER, NHEJ and HR were hypersensitive to topo I poisons compared to the parental AA8 cell line. The *irs1SF* cells were 9-fold more sensitive, EM9 cells were 4.5-fold more sensitive, and the V3 cells were 1.5-fold more sensitive to camptothecin than the parental AA8 cell line (table 6.2). This is consistent with previous data showing hypersensitivity of these cell lines to topo I poisons. Caldecott and Jeggo (1991) showed that the EM9 cells were 4-5 fold more sensitive to camptothecin than the parental AA8 cell line following a 24 hour exposure and the *irs1SF* cells were more sensitive than the EM9 cells (figures not available). Arnaudeau *et al.*, (2001) compared the V3 and *irs1SF* cells to the AA8 line, and showed that they were ~2 and 10-fold more sensitive to camptothecin, respectively. This would suggest that all of these DNA repair pathways are involved in the repair of topo I-mediated DNA damage. These data also suggest that HR was the predominant repair pathway for the repair of camptothecin-induced DNA damage followed by BER and NHEJ.

AG14361 was used to investigate in which pathway of topo I poison-induced DNA damage repair PARP-1 was involved. In theory, if PARP-1 was involved in only one of these pathways then in a cell line already deficient in this particular pathway AG14361 should not potentiate the cytotoxicity of camptothecin. In other words, if a cell had already lost a particular repair pathway that involved PARP-1 then inhibiting PARP-1 should not have any effect. The effect of AG14361 on camptothecin-mediated

cytotoxicity was investigated in all of the DNA repair deficient cell lines mentioned above

AG14361 caused a significant ~2-fold potentiation of camptothecin-mediated cytotoxicity in the AA8 cells (table 6.2) consistent with the levels seen in other repair competent cells, e.g. the K562 (1.9-fold), PARP wild type cells (3.4-fold) (chapter 3) SW620 (1.7-fold) and LoVo (1.6-fold) (Calabrese et al JNCI in press). AG14361 also caused 2-fold potentiation of camptothecin cytotoxicity in the V3 cell line. This would suggest that PARP-1 may mediate its effect on camptothecin-induced cytotoxicity via NHEJ-independent pathways

AG14361 caused a 0.7 to 4.3-fold increase in camptothecin-induced cytotoxicity in EM9 cells however (table 6.2), the cytotoxicity of camptothecin and AG14361 was not significantly different from the cytotoxicity of camptothecin alone in EM9 cells (4 out of 5 PF_{50} values fell in the range of 0.7-1.7). This may suggest that the involvement of PARP-1 in BER is at least in part responsible for the potentiation of camptothecin-induced cytotoxicity by AG14361. Nevertheless, since potentiation was occasionally observed, albeit not significantly (due to experimental variation), it is possible that PARP-1 may be involved in other pathways as well. Interestingly, the level of potentiation caused by AG14361 in AA8 cells treated with camptothecin was not equivalent to a loss of BER (by comparison of LC_{50} for AA8 + 361 12.0 nM, and EM9 camptothecin alone 5.6 nM). This indicates that inhibition of PARP-1 does not have such a marked effect on survival after exposure to camptothecin as loss of XRCC1, and suggests that the BER pathway may function to a limited extent in the absence of PARP-1 activity. PARP-1 has been shown to be more or less essential for long patch BER but only about 50% of short patch repair (Dantzer *et al.*, 2000). Indeed, some authors have shown that PARP-1 is not essential for BER. Vodenicharov *et al.*, (2000) showed that extracts prepared from wild-type and PARP-1 null cells were able to repair plasmid DNA damaged by either X-rays or MNNG. Similarly PARP-1 null cells were also able to repair MNNG-induced plasmid DNA damage as efficiently as the wild-type cells. Therefore it is possible that BER can function in the absence of PARP-1 explaining why the effect of loss of XRCC1 and hence BER was more detrimental than lack of PARP-1. Alternatively, XRCC1 could be involved in other repair pathways in which PARP-1 does not participate. Thus, the relative sensitivities of EM9 and AA8

cells to camptothecin and potentiation of camptothecin by AG14361 suggests that (a) PARP-1 activity facilitates, but is not essential (b) PARP-1 may be involved in XRCC1-independent repair pathways.

The irs1SF cells were intrinsically sensitive to AG14361 alone (figure 6.7). This suggests that PARP-1 can compensate for HR in resolution of spontaneous DNA damage or that in the absence of HR, DNA lesions are resolved by pathways dependent on PARP-1 activity. The possibility that the sensitivity of these cells to AG14361 was because they had upregulated PARP-1 activity, in response to loss of HR, was investigated. However, total stimutable PARP activity in these cells is ~70 pmol/million cells was comparable to that in K562 (113 pmol/million cells) and PARP wild-type cells (78 pmol/million cells, data not shown)

As the irs1SF cells were hypersensitive to AG14361, concentrations of AG14361 were determined that were PARP-1 inhibitory but not growth inhibitory for use in the cytotoxicity assay. These concentrations of AG14361 were not able to significantly potentiate the cytotoxicity of camptothecin following a 16 hour exposure (table 6.4). This may suggest that PARP-1 is involved in the repair of camptothecin-induced DNA strand breaks via the HR pathway. Schultz *et al.*, (2003) has shown that PARP-1 may play a role in the recognition of the DNA damage repaired by the HR machinery as a deficiency in PARP-1 leads to an increase in the spontaneous generation of Rad 51 foci. These foci are central to the HR process. Therefore this evidence suggests that PARP-1 may play a role in the recognition of camptothecin induced double strand breaks and target them for repair by the HR pathway.

The lack of potentiation of camptothecin cytotoxicity by AG14361 in irs1SF cells may simply be due to the fact that lower concentrations of AG14361 had to be used because of its intrinsic cytotoxic effect in these cells. The concentrations of AG14361 used with these cells were between 6 and 26 times lower than that used in the other cell lines in this study. It may be that the concentration of AG14361 being used in these cells is not enough to cause potentiation of cytotoxicity. PARP-1 inhibition was shown to be 50 and 90% for 15 and 70 nM AG14361 respectively. The inhibition seen at 70 nM AG14361 is comparable to the ~95% inhibition seen in response to 0.4 μ M AG14361 in

the other cell lines studied. If more time had been available, it would have been useful to investigate the potentiation of camptothecin by 70 nM AG14361 in AA8, EM9 and V3 cells. to aid in the interpretation of the results obtained with the irs1SF cells.

The lower (and not statistically significant) levels of potentiation of camptothecin cytotoxicity in the EM9 cells, compared the other cell lines suggested that PARP-1 was primarily involved in BER-mediated repair of camptothecin-induced DNA lesions. Therefore the effect of AG14361 on repair of camptothecin- induced DNA damage was investigated in the EM9 cells compared to the wild type AA8 cells. If more time had been available the other cell lines would also have been investigated.

The EM9 cells formed an increased number of single strand breaks in response to treatment with camptothecin compared to the AA8 cell line. This increase could explain the hypersensitivity of these cells to camptothecin. However, a difference in the level of DNA single strand breaks was not shown by Plo *et al*, (2003), comparing the effects of a one hour exposure to 1 μ M camptothecin in EM9 and XRCC1-complemented EM9 cells. The difference in these findings may be due to the cell lines used and the different experimental procedure used.

The EM9 cells have been reported to be deficient in the repair of single strand breaks (Thompson *et al.*, 1982). However, under the conditions used here (measurement of DNA breaks 60 mins after a 30 min pulse with 10 μ M camptothecin) the repair of single strand breaks in the EM9 cells was similar to that seen in the AA8 cells i.e. 70-75%. This is in opposition to Plo *et al.*, (2003), who showed that repair was delayed in the EM9 cells compared to the XRCC1-complemented cells after 15 and 30 mins. It is possible that the time point that was used in this study was too long after drug removal, and the BER dependent stage of repair occurred immediately following drug exposure therefore accounting for the conflicting studies. Comparable experiments with PARP-1 wild type and null cells also exposed to a 30 min pulse with 10 μ M camptothecin indicated that only 50-60% of the DNA strand breaks had been resolved by 60 mins, which is similar to the results obtained with the AA8 and EM9 cells. Therefore, the proportion of DNA breaks remaining at different times may be due to the concentration of camptothecin used and hence the initial level of breaks. Much more rapid repair was

seen after 10 min repair in the K562 cells exposed to 30 nM camptothecin (chapter 5) in which 80% of the damage was repaired within 10 mins following drug removal. The observation that DNA breaks immediately after camptothecin-exposure (without repair incubation) were ~30% higher in the EM9 cells than the AA8 cells may be due to reduced repair, if there is a dynamic equilibrium between induction and repair of camptothecin-induced DNA strand breaks. If the rate of induction of breaks was the same in both cell lines but the rate of repair was slower in the EM9 cells then more breaks would accumulate in these cells.

AG14361 caused a significant increase in the number of single strand breaks remaining at 60 min after camptothecin removal in the AA8 cell line. This is consistent with data presented for the K562 and PARP-1 wild type cells in this thesis (see chapter 5). AG14361 also caused a similar increase in the EM9 cells but this was not statistically significant. This combined with the lack of statistically significant potentiation of camptothecin in EM9 cells could implicate PARP-1 in XRCC1-dependent (presumably BER) pathways of DNA repair. However, the fact that both retardation of DNA repair and increased cytotoxicity was observed suggests the involvement of PARP-1 in other DNA repair pathways, such as NHEJ and HR, possibly to a lesser extent than BER. The involvement of PARP-1 in these repair pathways is described in the introduction of this chapter.

Summary.

1. V3, EM9 and irs1SF cells are 1.5, 4.5 and 9-fold more sensitive to camptothecin than AA8 cells indicating that HR is the most important pathway for repair of camptothecin-induced DNA damage, followed by BER, with NHEJ playing a minor role.
2. AG14361 significantly potentiates the cytotoxicity of camptothecin to a similar extent in the AA8 and V3 cell lines, therefore suggesting that PARP-1 is involved in NHEJ-independent pathways.
3. AG14361 potentiated camptothecin-induced cytotoxicity in EM9 cells to a lesser degree than the other cell lines and the potentiation was not statistically significant. Retardation of repair of camptothecin-induced DNA damage in EM9 cells, although apparently similar to the retardation of repair in AA8 cells, was also not statistically

significant. These data would suggest that PARP-1 is involved in BER-mediated repair of topo I poison-induced DNA damage, consistent with its well known role in this pathway in response to IR and alkylating agent-induced DNA damage. Nevertheless, the fact that repair does appear to be retarded and cytotoxicity potentiated by AG14361 (albeit without statistical significance) suggests a role for PARP-1 in other pathways as well.

4. *irs1SF*, HR deficient, cells are hypersensitive to AG14361 and this is not due to altered PARP-1 activity in these cells or sensitivity to inhibition by AG14361.
5. AG14361 does not significantly potentiate camptothecin-induced cytotoxicity in *irs1SF* cells, this may suggest that PARP-1 may play a role in the HR pathway or that the concentration of AG14361 was too low.

**PAGE
MISSING
IN
ORIGINAL**

Chapter 7.

Summary and Future Directions.

The cytotoxicity and anti-tumour effects of topo I poisons such as camptothecin, topotecan and irinotecan can be enhanced by inhibition of PARP-1 *in vitro* and *in vivo*. As new combinations of chemotherapy are always being sought to overcome the problems of resistance and reduce side effects, the combination of topo I poison and PARP-1 inhibitor may have a role in the clinic. In order to design studies that may enable the clinical use of this combination to be optimised, the molecular mechanisms underlying this potentiation of cytotoxicity need to be elucidated.

There were two hypotheses put forward to explain the effect of PARP-1 on topo I poison mediated cytotoxicity. Firstly that PARP-1 inhibited the activity of topo I via poly(ADP-ribosylation) which, by virtue of the negative charge conferred by the polymer on the enzyme, caused topo I to be repelled from the DNA. The second hypothesis was that PARP-1 was involved in the repair of topo I poison-mediated DNA damage, probably via its role in the base excision repair pathway. In this study these hypotheses have been tested using AG14361, a novel potent inhibitor of PARP-1, developed by the Experimental Therapeutics group at the Northern Institute for Cancer Research, University of Newcastle upon Tyne in collaboration with Pfizer GRD.

A role for PARP-1 in the response to topo I poison-induced cytotoxicity and growth inhibition has been confirmed. The inhibition of PARP-1 by AG14361 caused a ~2-fold potentiation of topo I poison-induced cytotoxicity or growth inhibition in all of the wild type cells used in this thesis (PARP-1 wild type MEFs, K562 and AA8 cells, see figures 3.8, 3.12 and 6.4). This effect was achieved at a concentration of AG14361 (0.4 μ M) that inhibited PARP-1 activity by >90% without affecting cellular proliferation or survival (table 3.2). PARP-1 null MEF cells were 2 to 3-fold hypersensitive to topotecan, a similar degree to that seen in PARP-1 wild-type cells treated with AG14361 (figure 3.8). This confirms a role for PARP-1 in the response to topo I poisons. AG14361 was unable to significantly potentiate the cytotoxicity of topotecan in PARP-1 null cells. However, the residual PARP activity that was detected in the null cells, possibly due to PARP-2, could be inhibited by AG14361 (table 3.2).

AG14361 was able to significantly potentiate camptothecin-mediated growth inhibition in K562 cells following a 16 hour exposure. However, after 30 mins exposure,

AG14361 did not significantly reduce the GI_{50} for camptothecin. This suggested that the effect of PARP-1 on topo I poison-mediated growth inhibition was time dependent. The difference in potentiation between these two time points was not related to modulation of topo I activity. Topo I activity was determined by measurement of DNA relaxation activity; and levels of cleavable complexes were measured using the TARDIS and K-SDS assays. Using the relaxation assay AG14361 did not significantly alter topo I activity following either a 30 min and 16 hour exposure (figure 4.1 and 4.2). Cleavable complexes were not increased by AG14361 following exposure to camptothecin for either 30 mins (figure 4.6 and 4.9) or 16 hours (figure 4.10). Neither was the persistence of the complexes following drug removal (table 4.1 and figure 4.11). It had previously been reported that PARP-1 poly(ADP-ribosylated) topo I following IR (Boothman *et al.*, 1994), however exposure to IR prior to treatment with camptothecin had no significant effect on the level of cleavable complexes (figure 4.8). Neither did AG14361 have an effect on the level of cleavable complexes produced by exposure to IR and camptothecin compared to treatment with camptothecin alone. This suggested that PARP-1 did not exert its effect on topo I poison-mediated cytotoxicity by modulation of topo I activity via poly(ADP-ribosylation).

To address the second hypothesis, that PARP-1 is involved in the repair of topo I poison-mediated DNA damage, the levels of DNA single strand breaks were measured in response to treatment with camptothecin. AG14361 significantly increased the level of single strand breaks by ~30 % following a 16 hour exposure to camptothecin (table 5.1). There was no detectable difference in DNA single strand breaks induced by a 30 minute exposure to camptothecin verses camptothecin and AG14361 (table 5.2). This was consistent with the growth inhibition data where there was no reduction in the GI_{50} for camptothecin by AG14361 after only 30 mins (figure 3.11). A study of different schedules of exposure 30 min exposure to camptothecin with or without 16 hours exposure to AG14361 showed that AG14361 increased the level of strand breaks when cells were treated with AG14361 after camptothecin but not when the exposure to AG14361 preceded camptothecin (table 5.3 and 5.4). Thus, the increase in strand breaks was shown to be a reflection of decreased repair of strand breaks rather than increased formation. The repair of camptothecin-induced strand breaks following a 10 min repair interval was significantly retarded by AG14361 such that there were 28% more strand breaks remaining in those cells incubated in AG14361-containing medium,

compared to control medium, following a 30 min pulse with camptothecin (figure 5.9). Thus it would seem that PARP-1 has a role in the repair of DNA damage caused by camptothecin.

DNA single strand break levels were also studied in the PARP-1 wild type and null cells. Exposure to camptothecin for 30 mins resulted in the accumulation of ~20% more DNA single strand breaks in the PARP-1 null cells compared to the PARP-1 wild type cells (table 5.7), showing that PARP-1 is involved in increasing the levels of DNA strand breaks in response to treatment with camptothecin. This may provide the explanation for the differential sensitivities of the PARP-1 wild type and null cells treated with topotecan (figure 3.8). The increase in DNA strand breaks caused by AG14361 in camptothecin treated PARP-1 wild type cells was surprising as inhibition of PARP-1 by AG14361 did not significantly increase the levels of strand breaks following a 30 min exposure in K562 cells although small increases were detectable in these cells. It may therefore be that difference between strand break levels in K562 cells treated with camptothecin and AG14361 were not high enough to be significantly different to those treated with camptothecin alone. AG14361 significantly increased the levels of DNA strand breaks remaining 60 mins after drug removal in PARP-1 wild type cells. AG14361 did not increase the persistence of strand breaks in the PARP-1 null cells therefore confirming that AG14361-induced accumulation of DNA single strand breaks was due to PARP-1 inhibition. The increased strand breakage caused by AG14361 observed in the PARP-1 wild type cells was very small compared to those in the K562 cells, which may be a reflection of the cell type, or due to differences in the repair period (60 verses 10 mins). Had more time been available the conditions might have been optimised to enable better detection of the effect of AG14361 or lack of PARP-1 on rate of repair.

The lack of a significant effect of AG14361 on camptothecin-induced strand breaks in K562 cells following a 30 min exposure may be due to the limits of sensitivity of the assay. The level of strand breaks is a reflection of both the rate of formation and reversal/repair. Therefore, after a 30 min exposure the decreased repair of the breaks in PARP-1 inhibited cells may not be detectable if the rate of formation of the breaks is equivalent or greater than the rate of repair. Over time the balance between formation and reversal will result in an accumulation of strand breaks if the breaks are not repaired

as fast as they are formed. The greater accumulation of camptothecin-induced breaks in the presence of AG14361 most likely arises from an inhibition of repair, thus tipping the balance in favour of formation. Similarly, in the cytotoxicity assays, in the 30 min exposure period there may be insufficient time to accumulate a greater number of breaks in PARP-1 inhibited cells (compared to control) that could lead to an increase in cytotoxicity following drug removal.

The PARP-1 null cells were not deficient in the repair of camptothecin-induced strand breaks as might be expected. Extracts from PARP-1 null cells have been shown previously to be able to repair single strand plasmid DNA damage by Vodenicharov *et al.*, 2000, and Allinson *et al.*, 2003, in a NAD⁺-independent manner. This would suggest that PARP-1 is not essential for BER. This has been shown by Satoh *et al.*, (1993) where PARP-1 deficient cell extracts were able to conduct BER in an NAD-independent manner. However, extracts containing inhibited PARP-1 (either by 3-AB or NAD⁺-depletion) were unable to conduct efficient BER, this was thought to be due to obstruction of access of the repair proteins to the site of damage as PARP-1 is unable to be removed from the nick site via poly(ADP-ribosylation). In this study, it has been demonstrated that repair of camptothecin-induced DNA strand breaks is possible in the presence of inhibited PARP-1, opposing the results of Satoh *et al.*, prompting the need for alternative explanations. The BER pathway has two sub-pathways that can cross over therefore it is possible that BER could be accomplished in the absence of PARP-1 by using an alternative mechanism. PARP-2 is also able to perform the same role in BER as PARP-1, therefore a NAD⁺-dependent BER could still function in the absence of PARP-1. It has been shown by Dantzer *et al.*, (2000) that PARP-1 null cells demonstrate a 90% deficiency in long patch BER, but still retain 50% of the short patch capacity compared to the wild type cells. This confirms the data presented in this thesis showing that BER does function in the absence of PARP-1 activity. In addition, as there are a number of different lesions produced in response to treatment with camptothecin (single, double and protein-linked strand breaks), it is possible that camptothecin-induced DNA damage could be repaired by a variety of different pathways including BER, HR and NHEJ.

The mechanism by which PARP-1 may be exerting its effect on the repair of topo I poison-mediated cytotoxicity was also investigated. PARP-1 has been shown to be

involved in the BER pathway. There are also reports suggesting that it may function in the HR and NHEJ pathways as well. To investigate which pathway or pathways are involved in the cellular response to camptothecin and in which PARP-1 acts by, cells deficient in BER, (EM9) HR (irs1SF) and NHEJ (V3) were used. All of these cell lines were hypersensitive to camptothecin compared to the parental AA8 cell line. The irs1SF were most sensitive (9-fold), followed by EM9 (4.5-fold) and then V3 (1.5-fold) (figures 6.4, 6.5 and 6.6) consistent with results obtained previously by Caldecott and Jeggo, (1991), Arnaudeau et al (2001) and Hinz et al (2003). This suggested that the HR pathway was the most important pathway in the repair of topo I poison mediated DNA damage, followed by BER and NHEJ. AG14361 was able to potentiate the cytotoxicity of camptothecin in the V3 cells suggesting that PARP-1-dependent repair of camptothecin-induced DNA damage did not overlap with the NHEJ pathway. AG14361 did not significantly potentiate the cytotoxicity of camptothecin or significantly retard repair of camptothecin-induced DNA strand breaks in the EM9 cells (table 6.2). Therefore this suggests that PARP-1 is involved in the repair of camptothecin-induced DNA strand breaks via the BER pathway. However, since AG14361 caused a modest (not significant) potentiation of camptothecin-induced cytotoxicity and retardation of repair of camptothecin-induced DNA single strand breaks, it is possible that PARP-1 is involved in other pathways as well.

AG14361 did not potentiate the cytotoxicity of camptothecin in the HR deficient cells (table 6.3). Although, these results are hard to interpret as lower concentrations of AG14361 had to be used due to the sensitivity of HR-deficient cells to treatment with AG14361 alone. This may suggest that PARP-1 is involved in the HR pathway, as has been suggested by Schultz et al (2003) where it was proposed that PARP-1 may serve to control the DNA damage recognised by the HR pathway. It may also suggest that in the absence of PARP-1, HR acts to repair damage normally repaired by PARP-1-dependent pathways, and thus in the absence of both pathways there is hypersensitivity. It may also be that the concentration of camptothecin used was too low to exert an effect. To determine whether this was the case it would have been useful to conduct cytotoxicity assays with the lower concentration of AG14361 used with the irs1SF cells on other wild type cells to see if this concentration was sufficient to potentiate cytotoxicity. The results from this would help to determine whether AG14361 had an effect on camptothecin induced cytotoxicity in these cells.

Possibly the most plausible mechanism by which PARP-1 can modulate topo I cytotoxicity is via its role in BER. As has been shown here there was no significant potentiation of cytotoxicity or retardation of strand break repair in cells deficient in BER. The BER pathway may repair the single strand break formed on collision with the replication fork, or it may be involved in processing the single strand break formed following removal of the cleavable complex. The last proposal is supported by the observation that the tyrosyl DNA phosphodiesterase (TDP) responsible for the removal of the topo I cleavable complex associates with the BER scaffold protein XRCC1 (Plo *et al.*, 2003). Thus PARP-1 may be involved in the processing of the strand break via the BER pathway, and through its association with XRCC1 as PARP-1 has been shown to be necessary for the formation of XRCC1 nuclear foci, in response to DNA damage (El-Khamisy *et al.*, 2003). This theory would be consistent with the increased strand breaks seen 10 mins after removal of camptothecin in those cells treated with AG14361 (figure 5.9). The level of complexes in those cells treated with AG14361 would be the same as those treated with camptothecin alone as the action of the TDP should be the same in the presence or absence of AG14361, which is also consistent with the observations made in this study. PARP-1 could be involved in the recruitment of XRCC1 to the break formed following or prior to removal of the complex by TDP, or down stream of XRCC1 in the recruitment of other repair enzymes (illustrated in figure 7.1). To further determine whether this was the case it would be interesting to see if there was any interaction between PARP-1 and TDP. This could be investigated by immunoprecipitation, or by searching the amino acid sequence of TDP to see if there was a poly(ADP-ribose) binding motif, although, actual interaction between these proteins may not actually be necessary, as both proteins interact with XRCC1. It may also be interesting to see if PARP-1 locates to the sites of damage repaired by TDP, by studying the foci formed in response to damage caused by topo I poisons.

The increased potentiation of cytotoxicity seen after 16 hours may just be due to the accumulation of damage, but may also be a reflection of the involvement of PARP-1 in other repair pathways apart from BER. After a 16 hour exposure collision of the camptothecin-stabilised cleavable complex with the replication fork is likely to have occurred in at the least 50% of the cells as the doubling time for K562 cells is ~20 hours, therefore there will be double strand breaks as well as single strand breaks. As

was demonstrated by the hypersensitivity of the *irs1SF* cells to camptothecin and their lack of potentiation by AG14361, there may be a role for PARP in the HR pathway. As mentioned previously, Schultz *et al* (2003) has suggested that PARP-1 may serve to control the repair recognised by HR. This hypothesis could be tested by studying the repair of double strand breaks following 16 hours incubation. If PARP-1 was involved in this pathway then AG14361 may increase double strand breaks. Similarly the *irs1SF* cells could be used to compare the effect of camptothecin on this pathway in comparison with the AA8 cells in the same way that single strand breaks have been studied in the EM9 cells compared to the AA8 cells. Although there may be difficulties in obtaining meaningful results as the *irs1SF* cells are hypersensitive to AG14361 therefore other cell lines deficient in HR could be used.

It would be interesting to investigate the intrinsic sensitivity of the *irs1SF* cells to AG14361. It has been shown in this study that the levels of PARP-1 activity in these cells is comparable to other wild type cells such as the K562 and PARP-1 wild-type therefore the sensitivity of these cells is not due to decreased PARP-1 activity. PARP-1 could be involved in the repair pathways that do function in these cells, or HR could be a back-up mechanism that acts in the absence of PARP-1. Further characterisation of the repair pathways functioning and the levels of the repair proteins in PARP-1 null cells may provide insight into the sensitivity of these cells to AG14361.

To summarise, the studies contained within this thesis show that PARP-1 is involved in the response to topo I poisons. This is likely to be via repair of the single strand breaks formed on removal of the topo I from the DNA, via the base excision repair pathway. There are also indications that other pathways may be involved, in particular the homologous recombination pathway. These possible methods of interaction of PARP-1 in the response to topo I poisons are summarised in figure 7.1.

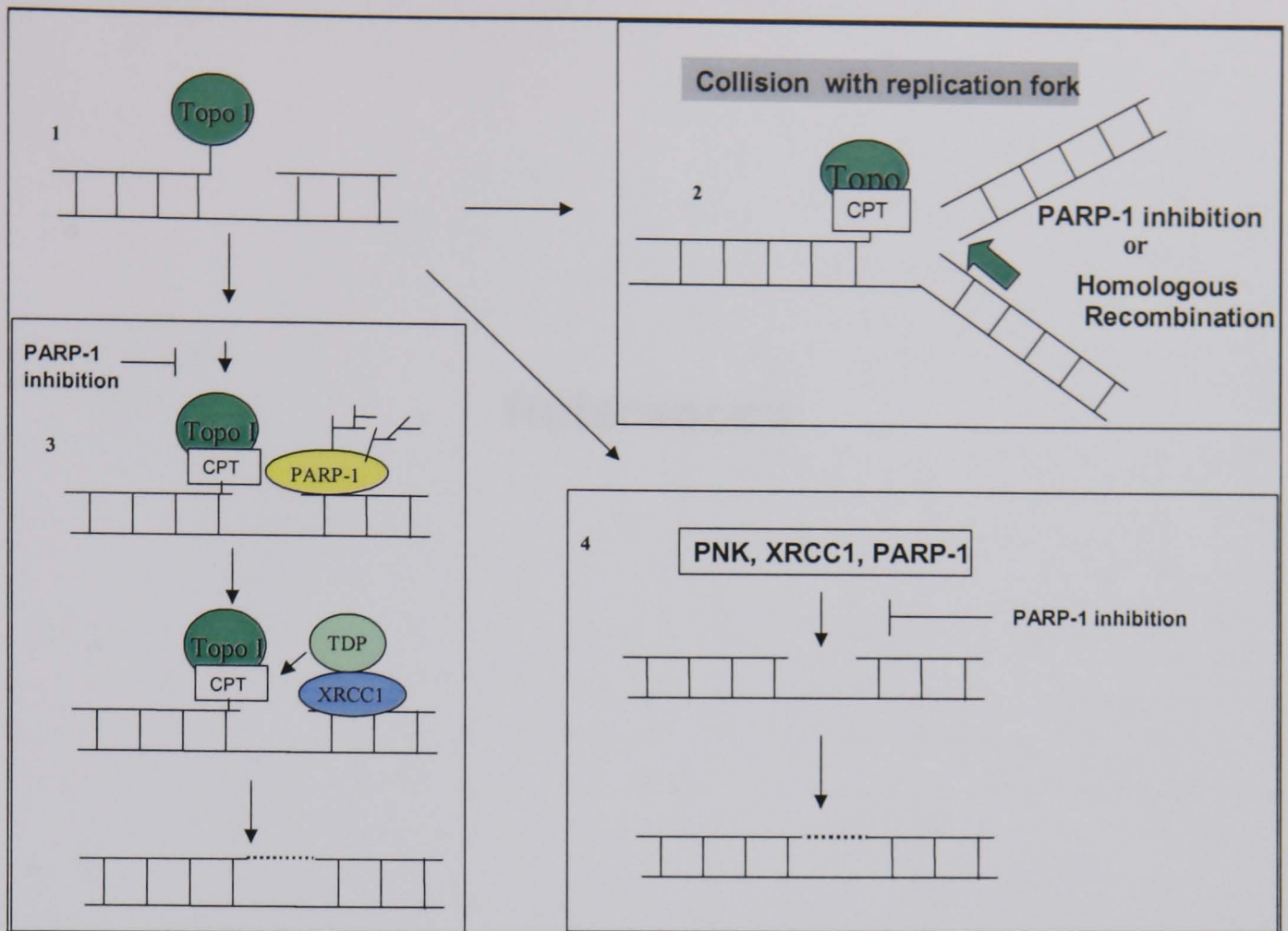


Figure 7.1 The role of PARP-1 in topo I poison-mediated cytotoxicity.

(1) Topo I binds to DNA forming a protein linked single strand break that can be stabilised by camptothecin. (2) Persistence of strand breaks may cause collision of the complex with the replication fork. Double strand breaks are formed that can be repaired by HR. In the absence of PARP-1 this damage may be repaired by the HR pathway. (3) PARP-1 may be stimulated in response to topo I-related DNA single strand breaks. Poly(ADP-ribose) polymers are formed and recruit XRCC1. TDP via its association with XRCC1 may be recruited to remove the topo I. The remaining gap may then be repaired by PNK, pol β and ligase III, according to the BER pathway. Inhibition of PARP-1 would prevent the recruitment of the DNA repair enzymes. (4) An alternative pathway may involve the removal of topo I by TDP, and the remaining single strand break may be repaired by XRCC1 and the other members of the BER pathway involving PARP-1. Inhibition of PARP-1 may delay repair (4) and cause persistence of the strand break, which may collide with the replication fork causing double strand breaks and eventual cell death.

References

8. References

- Adameitz P., and Rudolph A. (1984) ADP-ribosylation of nuclear proteins *in vivo*. Journal of Biological Chemistry. **256**:6841-6846
- Allinson, S. L., Dianova, I. I., and Dianov, G. L. (2003) Poly(ADP_ribose)polymerase in base excision repair: always engaged, but not essential for DNA damage processing. Acta Biochimica Polonica, **50**: 169-179
- Althaus F.R., Hofferer L, Kleczkowska H. E., Malanga, M., Naegeli, H, Panzeter P. L., Realini C. A., (1994). Histone shuttling by poly (ADP-ribosylation). Molecular and Cellular Biochemistry. **138** (1-2): 53-59
- Alvarez-Gonzalez R, Althaus F. R. (1989) Poly(ADP-ribose) catabolism in mammalian-cells exposed to DNA-damaging agents. Mutation Research **218** (2): 67-74
- Ame, J. C., Rolli, V, Schreiber, V, Neidergang, V, Apiou, F, Decker, P, Muller, S, Hoger, T, Menissier de Murcia J, de Murcia G (1999). PARP-2, A novel mammalian DNA damage dependent Poly(ADP-ribise) Polymerase. J. Biol Chem **274**: 17860-17868.
- Arnaudeau, C., Lundin, C., and Helleday (2001). DNA double-strand breaks associated with replication forks are predominately repaired by homologous recombination involving and exchange mechanism in mammalian cells. J. Mol. Biol **307**: 1235-1245
- Arundel-Suto, C. M., Scavone, S. V., Turner, W. R., Suto, M. J., and Seebolt-Leopold, J. S. (1991) Effects of PD128763, a new potent inhibitor of poly(ADP-ribose) polymerase, on X-ray induced cellular recovery processes in Chinese hamster V79 cells. Radiation Research **126**: 367-371
- Bale, A E, and Brown S, J.(2001) Etiology of Cancer: Cancer Genetics, Chapter 13 Cancer: Principles and Practice of Oncology Ed. De Vita LW & W
- Banasik, M., Komura, H., Shimoyama, M., and Ueda, K. (1992) Specific inhibitors of poly(ADP-ribose) synthetase and mono(ADP-ribosyl)transferase. Journal of Biological Chemistry. **267**: 1569-1575
- Barrows, L. R., Holden, J. A., Anderson, M., and D'Arpa, P. (1998) The CHO XRCC1 mutant, EM9, deficient in DNA ligase III activity, exhibits hypersensitivity to camptothecin independent of DNA replication. Mutation Research **408**: 103-110
- Beidler, D. R., and Cheng, Y-C. (1995). Camptothecin induction of a time- and concentration-dependent decrease of topoisomerase I and its implication in camptothecin activity. Molecular Pharmacology **47**: 907-914

- Beidler, D. R., Chang, J-Y., Zhou, B-S., and Cheng, Y-C. (1996). Camptothecin resistance involving steps subsequent to the formation of protein-linked DNA breaks in human camptothecin-resistant KB cell lines. *Cancer Research* **56**: (2) 345-353
- Ben-Hur, E., Utsami, H., Elkind, M. M. (1984) Inhibitors of poly(ADP-ribose synthesis enhance X-ray killing of log phase Chinese hamster cells. *Radiation Research*. **97**: 546-555
- Benjamin, R. C., and Gill, D.M. (1980). ADP-ribosylation in mammalian cell ghosts. Dependence of Poly(ADP-ribose) synthesis on strand breakage in DNA. *J. Biol. Chem.* **255**: 10493-10501.
- Berger J. M. (1998) Structure of DNA topoisomerases. *Biochimica et Biophysica Acta*. **1400**: 3-18
- Berger N. A (1985) Poly(ADP-ribose) in the cellular-response to DNA damage *Radiation Research*. **101** (1): 4-15
- Bjornsti, M. A., Benedetti P, et al. (1989). Expression of human DNA topoisomerase I in yeast cells lacking yeast DNA topoisomerase I: restoration of sensitivity of the cells to the antitumor drug camptothecin. *Cancer Research* **49**(22): 6318-23.
- Blier P. R., Griffith A. J., Craft J, Hardin, J. A., (1993) Binding of Ku protein to DNA-measurement of affinity for ends and demonstration of binding to nicks. *Journal of Biological Chemistry* **268** (10): 7594-7601.
- Blunt, T., Finnie, N. J., Taccioli, G. E., Smith, G. C., Demengeot, J., Gottlieb, T., T., Mizuta, R., Varghese, A.J., Alt, F. W., and Jeggo, P. A. (1995) Defective DNA-dependent protein kinase activity is linked to V(D)J recombination and DNA repair defects associated with the murine scid mutation. *Cell* **80**: 813-823
- Boothman, D. A., Fukunaga, N., and Wang, M. (1994). Down-regulation of Topoisomerase I in mammalian cells following ionising radiation. *Cancer Research* **54**: 4618-4626
- Boothman, D. A., Wang, M. Z., Schea R. A., Burrows H. L., Strickfaden S, Owens, J. K. (1992) Post-treatment Exposure To Camptothecin Enhances The Lethal Effects Of X-Rays On Radioresistant Human-Malignant Melanoma-cells. *International Journal Of Radiation Oncology Biology Physics* **24** (5): 939-948
- Bouchard, V. J., Rouleau, M., and Poirier, G. (2003) PARP-1 a determinant of cell survival in response to DNA damage. *Experimental Haematology* **31**: 446-454
- Boulton, S., Pemberton, L.C., Porteous, J.K., Curtin, N.J., Griffin R.J., Golding, B.T., and Durkacz B.W. (1995) Potentiation of temozolamide-induced cytotoxicity: A comparative study of the biological effects of poly(ADP-ribose) polymerase inhibitors. *British Journal of Cancer* **72**: 849-856
- Bowman, J., Newell, D.R. and Curtin, N.J. (2001). Differential effects of the poly(ADP-ribose) polymerase (PARP) inhibitor NU1025 on topoisomerase I and II inhibitor cytotoxicity. *British*

Journal of Cancer **84**(1): 106-112.

Bowman, K. J., White A., (1998). Potentiation of anti-cancer agent cytotoxicity by the potent poly(ADP-ribose) polymerase inhibitors NU1025 and NU1064. *British Journal of Cancer* **78**(10): 1269-77.

Burkle, A., Schreiber, V., Dantzer F., Olivier, F. J., Neidergang, C., de Murcia, G., and menissier de Murcia, J. (2000) Biological significance of poly(ADP)ribosylation reactions: molecular and genetic approaches. Chapter 3 in *from DNA damage and stress signalling to cell death: poly (ADP-ribosylation reactions*. Ed de Murcia G., and Shall S. Oxford University Press

Calabrese, C. R., Batey, M. A., Thomas, H. D., Durkacz, B. W., Wang, L-Z., Kyle, S., Skaltzky, D., Li, J., Zhang, C., Boritzky, T., Maegley, K., Calvert, A. H., Hostomsky, Z., Newell, D. R., and Curtin, N. J. (2003) Identification of potent non-toxic poly(ADP-ribose) polymerase-1 inhibitors: Chemopotential and Pharmacological studies. *Clinical Cancer Research* **9**: 2711-2718.

Caldecott K. W., Aoufouchi S., Johnson P., Shall S. (1996) XRCC1 polypeptide interacts with DNA polymerase beta and possibly poly(ADP-ribose) polymerase, and DNA ligase III is a novel molecular 'nick-sensor' in vitro. *Nucleic Acids Research*. **24** (22): 4387-4394

Caldecott KW, Aoufouchi S, Johnson P, Shall S (1996) XRCC1 polypeptide interacts with DNA polymerase beta and possibly poly (ADP-ribose) polymerase, and DNA ligase III is a novel molecular 'nick-sensor' in vitro. *Nucleic Acids Res*. **24**(22):4387-94

Caldecott, K. (2003). XRCC1 and DNA strand break repair. *DNA Repair*, **2**: 955-969

Caldecott, K. and Jeggo, P. (1991) Cross sensitivity of γ -ray-sensitive hamster mutants to cross-linking agents. *Mutation Research: DNA Repair*, **255**: 111-121

Callebaut, I., and Mornon, J.P (1997). From BRCA1 to RAP1: a widespread BRCT module closely associated with DNA repair. *FEBS Letters* **400**: 25-30.

Camilloni, G., Di Mauro, E., Casterta, M., Di Mauro, E. (1988) Eukaryotic DNA topoisomerase I reaction is topology dependent. *Nucleic Acids Research* **16** (14B) 7071-7085

Carmichael, J. and Ozols, R.F. (1997). Topotecan, an active new antineoplastic agent: review and current status. *Exp Opin Invest Drugs* **6**(5): 593-608.

Chambon, P, Weil J D, and Mandel P (1963). Nicotinamide mononucleotide activation of a new DNA-dependant poly -adenylic acid synthesising nuclear enzyme. *Biochem. Biophys. Res. Commun.* **11**: 39-43

Champoux JJ. (1978) Mechanism of the reaction catalyzed by the DNA untwisting enzyme: attachment of the enzyme to 3'-terminus of the nicked DNA. *J Mol Biol.*; **118**(3):441-

Champoux, J.J. (1998) Domains of human topoisomerase I and associated functions. *Prog*

- Chang J. Y., Dethlefsen, L. A., Barley, L. R., Zhou, B. S., Cheng Y. C. (1992) Characterization of camptothecin-resistant Chinese-hamster lung-cells *Biochemical Pharmacology* **43** (11): 2443-2452
- Chatterjee, S., Cheng, M-F., Trivedi, D. Petzold, S.J., and Berger, N. A. (1990) Camptothecin hypersensitivity in poly(adenosine diphosphate-ribose) polymerase-deficient cell lines. *Cancer Communications* **1**: 389-394
- Chatterjee, S., Hirschler N. .Petzold V, Berger, S. J.Berger, N. A. (1989). Mutant cells defective in poly(ADP-ribose) synthesis due to stable alterations in enzyme activity or substrate availability. *Experimental Cell Research* **184**(1): 1-15.
- Chen A.Y., Okunieff P., Pommier Y., Mitchell J. B. (1997) Mammalian DNA topoisomerase I mediates the enhancement of radiation cytotoxicity by camptothecin derivatives. *Cancer Research* **57** (8): 1529-1536
- Chiarugi A. (2002) Poly(ADP-ribose) polymerase: killer or conspirator? The 'Suicide hypothesis' revisited. *Trends In Pharmacological Sciences* **23** (3): 122-129
- Cleaver, J.E., (1984) Differential toxicity of 3-aminobenzamide to wild type and 6-thioguanine-resistant Chinese hamster cells by interference with the pathways of purine biosynthesis. *Mutation Research*, **131**: 123-127
- Covey, J. Jaxel, C. Kohn, K., and Pommier, Y. (1989) Protein-linked DNA strand breaks induced in mammalian cells by camptothecin an inhibitor of topoisomerase I. *Cancer Research* **49**: 5016-5022
- D'Arpa P, Beardmore C., Liu L. F. (1990) Involvement Of Nucleic-Acid Synthesis In Cell Killing Mechanisms Of Topoisomerase Poisons. *Cancer Research* **50** (21): 6919-6924
- D'Amours, D., Desnoyers, S. D'Silva, I, Poirier, G. G. (1999). Poly(ADP-ribosyl)ation reactions in the regulation of nuclear functions. *Biochemical Journal* **342**(Pt 2): 249-268.
- Danks M. A., Garrett, K. E., Marion, R. C. and Whipple, D. O. (1996) Subcellular redistribution of DNA topoisomerase I in anaplastic astrocytoma cells treated with topotecan. *Cancer Research* **56**: 1664-1673
- Dantzer, F, Schreiber V, Niedergang, C, Trucco, C, Flatter, E., De La Rubia, G , Oliver, J.Rolli, V. Menissier-de Murcia, J. de Murcia, G.. (1999). Involvement of poly(ADP-ribose) polymerase in base excision repair. *Biochimie* **81**(1-2): 69-75.
- Dantzer, F., de la Rubia Menissier de Murcia, J, Hostomsky, Z, de Murcia, G, Schreiber, V. (2000). Base excision repair is impaired in mammalian cells lacking poly(ADP-ribose)polymerase. *Biochemistry* **39**: 7559-7569.
- de Jonge, M.J. , Sparreboom A., and Verweij, J. (1998). The development of combination therapy involving camptothecins: a review of preclinical and early clinical studies. *Cancer*

Treatment Reviews **24**: 205-220.

De Laat, W. L., Jaspers, N. G., and Hoeijmakers J. H. (1999) Molecular Mechanism of Nucleotide Excision Repair. *Genes Dev.* **13** 768-785.

de Murcia, G. and Shall S.(2000). From DNA damage and stress signalling to cell death, Oxford University Press.

de Murcia, G. and. Menissier de Murcia J (1994). Poly(ADP-ribose) polymerase: a molecular nick-sensor [published erratum appears in *Trends Biochem Sci* 1994 Jun;19(6):250]. *Trends in Biochemical Sciences* **19**(4): 172-176.

de Murcia, G., Huletskym, A., Lamarre, D., Gaudreau, A., Pouyet, J., Daune, M., Poirier, G. (1986) Modulation of chromatin superstructure induced by poly(ADP-ribose) synthesis and degradation. *Journal of Biological Chemistry*, 261: 7011-7017

de Murcia, G., Schreiber, V., Molinete, M., Saulier, B., Poch, O, Masson, M, Niedergang, C.,Menissier de Murcia, J. et al. (1994). Structure and function of poly(ADP-ribose) polymerase. *Molecular & Cellular Biochemistry* **138**(1-2): 15-24.

De Vita, (2001) *Cancer: Principles and Practice of Oncology* LW & W

Delaney, C. A., Wang L.-Z., Kyle, S, White, A WCalvert, A H, Curtin, N, J, Durkacz BW, Hostomsky Z, Newell D R (2000). Potentiation of temozolamide and topotecan growth inhibition and cytotoxicity by novel poly(ADP-ribose)polymerase inhibitors in a panel of human tumour cell lines. *Clinical cancer research* **6**: 2860-2867.

Desai, S. D., Li T-K., Rodriguez-Bauman, A. Rubin, E. H., and Liu, L. (2001) ubiquitin/26S proteasome-mediated degradation of topoisomerase I as a resistance mechanism to camptothecin in tumour cells. *Cancer Research* **61**: 5926-5932

Desai, S. D., Liu, L.F., Vazquez-Abad, D., and D'Arpa P.(1997) Ubiquitin-dependent destruction of topoisomerase I is stimulated by the antitumour drug camptothecin. *Journal of Biological Chemistry* **272**: 24159-24164

Desnoyers, S., Kaufmann, S., and Poirier, G. (1996) Alteration of the localisation of PARP upon treatment with transcription inhibitors. *Experimental Cell Research* **227**: 146-153.

Dianov G, Bischoff C, Piotrowski J, Bohr VA (1998) Repair pathways for processing of 8-oxoguanine in DNA by mammalian cell extracts. *J Biol Chem*; 273(50):33811-6

Ding, R. and Smulson, M. (1994) Depletion of nuclear poly(ADP-ribose) polymerase by antisense RNA expression: influences on genomic stability, chromatin organisation and carcinogen cytotoxicity. *Cancer Research*, **54**: 4627-4634

Ding, R., Pommier, Y., Kang, V.H., and Smulson, M. (1992) Depletion of poly(ADP-ribose) polymerase by antisense RNA expression results in a delay in DNA strand break rejoining. *Journal of Biological Chemistry*, **267**: 12804-12

- Dodson ML, Michaels ML, Lloyd RS. (1994) Unified catalytic mechanism for DNA glycosylases. *J Biol Chem*; 269: 32709-32712
- Durkacz, B. W., Omidiji, O., Gray, D. A., and Shall, S. (1980) (ADP-ribose) participates in DNA excision repair. *Nature* **283**: 593-596
- El-Khamisy, S. F., Masutani, M., Suzuki, H., and Caldecott, K. W. (2003) A requirement for PARP-1 for the assembly or stability of XRCC1 nuclear foci at sites of oxidative DNA damage. *Nucleic Acids Research* **31**:5526-5533
- Eriksson, C., Busk, L., and Brittebo, E.B. (1996) 3-Aminobenzamide: effects on cytochrome P450-dependent metabolism of chemicals and on the toxicity of dichlobenil in the olifactory mucosa. *Toxicol. Appl. Pharmacol.* **136**: 324-331
- Errington F., Willmore E., Tilby M. J., Li L., Li G., Li W., Baguley B. C., Austin C. A. (1999) Murine transgenic cells lacking DNA topoisomerase II beta are resistant to acridines and mitoxantrone: Analysis of cytotoxicity and cleavable complex formation. *Molecular Pharmacology* **56** (6): 1309-1316
- Ferro, A. M., and Olivera, B. M. (1984). Poly(ADP-ribosylation) of DNA topoisomerase I from Calf Thymus. *Journal of Biological Chemistry* **259**: 547-554
- Ferro, A. M., Higgins, N., and Olivera, B. M. (1983) Poly(ADP-ribosylation) of DNA topoisomerase. *Journal of Biological Chemistry* **258**: 6000-6003
- Ferro, A. M., McElwain, M. C. Olivera, B.M. (1984). Poly(ADP-ribosylation) of DNA topoisomerase I: a nuclear response to DNA-strand interruptions. *Cold Spring Harbour Symp. Quant. Biol.* **49**(6): 683-690.
- Frank, A. J., Proctor S. J., Tilby, M.J. (1996). Detection and quantification of melphalan-DNA adducts at the single cell level in haematopoietic tumour cells. *Blood* **88**(3): 977-984.
- Froelich-Ammon, S. J. and Osheroff, N (1995). Topoisomerase Poisons: Harnessing the Dark side of enzyme mechanism. *J. Biol Chem* **270**: 21429-21432.
- Fujimori A., Gupta M., Hoki Y., Pommier Y. (1996) Acquired camptothecin resistance of human breast cancer MCF-7/C4 cells with normal topoisomerase I and elevated DNA repair. *Molecular Pharmacology* **50** (6): 1472-1478
- Fujimori A., Harker W.G., Kohlhagen G., Hoki Y., Pommier Y. (1995) Mutation at the catalytic site of topoisomerase-I in CCEM/C2, a human leukemia-cell line resistant to camptothecin. *Cancer Research* **55** (6): 1339-1346
- Fuller L. F., Painter R. B. (1988) A Chinese-hamster ovary cell-line hypersensitive to ionizing-radiation and deficient in repair replication. *Mutation Research* **193** (2): 109-121

- Gerrits, C. J., de Jonge M. J., Schellens, J. H., Stoter, G., Verweij, J.. (1997). Topoisomerase I inhibitors: the relevance of prolonged exposure for present clinical development. *British Journal of Cancer* **76**(7): 952-62.
- Gobert, C., Sklandanowski A., and Larsen, A. K. (1999) The interaction between p53 and DNA topoisomerase I is regulated differently in cells with wild-type p53. *PNAS* **96**: 10355-10360
- Goldwasser F., Bae I., Valenti M., Torres K., Pommier Y. (1995) Topoisomerase I-related parameters and camptothecin activity in the colon-carcinoma cell-lines from the National-Cancer-Institute anticancer screen. *Cancer Research* **55** (10): 2116-2121
- Goldwasser F., Shimizu, T., Jackman, J., Hoki, Y., O'Connor, P.M. Kohn, K.W. and Pommier, Y. (1996) Correlations between S and G2 arrest and the cytotoxicity of camptothecin in human colon carcinoma cells. *Cancer Research* **56**: 4430-4437
- Gonzalez, R. and. Althaus F. R (1989). Poly(ADP-ribose) catabolism in mammalian cells exposed to DNA-damaging agents. *Mutation Research* **218**(2): 67-74.
- Gottlieb, J. A., Guarino, A. M., and Call J. B. (1970) Preliminary pharmacologic and clinical evaluation of camptothecin sodium (NSC-100880). *Cancer Chemother Rep.* **54**: 461-70
- Gradwohl G., Demurcia J. M., Molinete M., Simonin F., Koken M., Hoeijmakers J. H. J., Demurcia G. (1990) The 2nd zinc-finger domain of poly(ADP-ribose) polymerase determines specificity for single-stranded breaks in DNA. *Proceedings of the National Academy of Sciences of the United States of America* **87** (8): 2990-2994
- Griesenbeck J., Ziegler M., Tomilin N., Schweiger M., Oei S. L (1999). Stimulation of the catalytic activity of poly(ADP-ribosyl) transferase by transcription factor Yin Yang I. *FEBS Letters* **443** (1): 20-24
- Griffin, R. J., Srinivasan, S. Griffin, R. J., Srinivasan, S., Bowman, K., Calvert, A., H., Curtin, N. J., Newell, D. R., Pemberton, L. C., Golding, B. T. (1998). Resistance-modifying agents. 5. Synthesis and biological properties of quinazolinone inhibitors of the DNA repair enzyme poly(ADP-ribose) polymerase (PARP). *Journal of Medicinal Chemistry* **41**(26): 5247-5256.
- Griffin, R. J., Curtin N. J, Curtin, N. J., Newell, D. R., Golding, B. T., Durkacz, B. W., Calvert, A. H.. (1995a). The role of inhibitors of poly(ADP-ribose) polymerase as resistance-modifying agents in cancer therapy. *Biochimie* **77**(6): 408-422.
- Griffin, R. J., Pemberton L. C, Pemberton, L. C., Rhodes, D., Bleasdale, C., Bowman, K., Calvert, A. H., Curtin, N. J., Durkacz, B. W., Newell, D. R., Porteous, J. K. (1995b). Novel potent inhibitors of the DNA repair enzyme poly(ADP-ribose)polymerase (PARP). *Anti-Cancer Drug Design* **10**(6): 507-514.
- Gupta, M., A. Fujimori, Fujimori, A., Pommier, Y. (1995). Eukaryotic DNA Topoisomerases I. *Biochem and Biophys Acta* **1262** 1-14.
- Halldorsson, H., Gray, D.A., and Shall, S. (1978) poly(ADP-ribose polymerase activity in

nucleotide permeable cells. *FEBS Letters*, **85**: 349-352

Hansen, W., K and Kelley, M R (2000). Review of mammalian DNA repair and translational implications. *J. Pharmacology and experimental therapeutics* **295**(1): 1-9.

Hatakeyama K., Nemoto Y., Ueda K., Hayaishi O. (1986) Purification and characterization of poly(ADP-ribose) glycohydrolase - different modes of action on large and small poly(ADP-ribose). *Journal Of Biological Chemistry* **261** (32): 4902-4911

Heck, M. M., Hittelman W. N, Earnshaw, W.C.et al. (1988). Differential expression of DNA topoisomerases I and II during the eukaryotic cell cycle. *PNAS* **85**(4): 1086-1090.

Hellman, S. (2001) Principles of Cancer Management: Radiation Therapy Chapter 16 in De Vita, Cancer: Principles and Practice of oncology LW & W

Herceg, Z. and Wang, Z-Q (2001). Functions of poly(ADP-ribose) polymerase (PARP) in DNA repair, genomic integrity and cell death. *Mutation Research* **477**: 97-110.

Hertzberg R. P., Busby R. W., Caranfa M. J., Holden K.G., Johnson R.K., Hecht S. M., Kingsbury W. D. (1990) Irreversible trapping of the DNA-topoisomerase-I covalent complex - affinity labeling of the camptothecin binding-site. *Journal of Biological Chemistry* **265** (31): 19287-19295

Hinz, J. M., Helleday, T., and Meuth, M. (2003). Reduced apoptotic response to camptothecin in CHO cells deficient in XRCC3. *Carcinogenesis* **24**: 249-253

Hoejmakers J, H, J. (2001) Genome maintenance mechanisms for preventing cancer. *Nature* **411**: 366-374

Holl, V., Coelho, D., Weltin, D., Hyun, J-W., Dufour, P, and Bischoff, P. (2000) Modulation of the antiproliferative activity of anti-cancer drugs in hematopoietic tumour cell lines by the poly(ADP-ribose) polymerase inhibitor 6(5H)-phenanthridinone. *Anticancer Research*. **20**: 3233-3242

Houghton P. J., Cheshire, P. J., Myers, L., Stewart, C. F., Synold, T. W., Houghton, J. A., (1992) Evaluation of 9-dimethylaminomethyl-10-hydroxycamptothecin against xenografts derived from adult and childhood solid tumours. *Cancer Chemother Pharmacol*. **31**: 229-39

Hsaing, Y., Lui, L Wall ME., Wani MC., Kirshenbaum S., Silber R., Potmesil M. (1989). DNA topoisomerase I-mediated DNA cleavage and cytotoxicity of camptothecin analogues. *Cancer Research* **49**: 4385-4389.

Hsaing, Y-H., and Liu, L. F. (1988) Identification of mammalian DNA topoisomerase as an intracellular target of the anticancer drug camptothecin. *Cancer Research* **48**: 1722-1726.

Hsaing, Y-H., Hertzberg, R., Hecht, S., and Liu, L. Camptothecin induces protein-linked DNA breaks via mammalian DNA topoisomerase I. (1985) *Journal of Biological Chemistry* **260**: 14873-14878

- Huet J., and Laval, F. (1985) Influence of poly(ADP-ribose) synthesis inhibitors on the repair of sub-lethal and potentially lethal damage in gamma-irradiated mammalian cells. *Int J Radiat BiolRelat Stud Phys Chem Med.* **47**: 655-62
- Husain I., Mohler J. L., Seigler H. F., Besterman J. M., (1994) Elevation of topoisomerase-I messenger-RNA, protein, and catalytic activity in human tumours - demonstration of tumor-type specificity and implications for cancer-chemotherapy. *Cancer Research* **54** (2): 539-546
- Hwu, P., (2001) Gene Therapy. Section 62.1 in De Vita, Cancer: Principles and Practice of Oncology LW & W
- Ikejima M., Noguchi S., Yamashita R., Ogura T., Sugimura T., Gill D. M., Miwa M. (1990) The zinc fingers of human poly(ADP-ribose) polymerase are differentially required for the recognition of DNA breaks and nicks and the consequent enzyme activation - other structures recognize intact DNA. *Journal Of Biological Chemistry* **265** (35): 21907-21913
- Ikejima, M., Bohannon, D., Gill, D. M., and Thompson, L. H. (1984) Poly(ADP-ribose) metabolism appears normal in EM9, a mutagen-sensitive mutant of CHO cells. *Mutation Research* **128**: 213-220
- Jacobson MK, Meter RG, Meyer-Ficca ML, Coyle DL, Kim H, Oliveeira MA, Slama JT, and Jacobson EL. (2003) PARG as a therapeutic target for modulation of cellular responses to genotoxic stress. *Medical Science Monitor* **9** (1) Abstract 29
- Jacobson, M. K. and. Jacobson E. L. (2001). Discovering new ADP-ribose polymer cycles: protecting the genome and more. *TIBS* **24**: 415-417.
- Jaxel C, Capranico G, Kerrigan D, Kohn Kw, Pommier Y (1991) Effect of local DNA-sequence on topoisomerase-I cleavage in the presence or absence of camptothecin. *Journal Of Biological Chemistry.* **266** (30): 20418-20423
- Jean, L., Risler, J L, Nagase, T T, Coulouarn, N, Nomura, J P, Sailier, J P. (1999). The nuclear protein PH5P of the inter-alpha-inhibitor superfamily: a missing link between poly(ADP-ribose) polymerase and the inter-alpha-inhibitor family and a novel actor of DNA repair? *FEBS Letters* **446**: 6-8.
- Johansson, M. (1999). A human poly(ADP-ribose)polymerase gene family (ADPRTL): cDNA cloning of two novel poly(ADP-ribose)polymerase homologues. *Genomics* **57**: 442-445.
- Johnson, R. T., Gotoh, E., Mullinger, A. M., Ryan, A. J., Shiloh Y., Ziv, Y., and Squires, S. Targetting double-strand breaks to replicating DNA identifies a subpathway of DSB repair that is defective in Ataxia-Telangiectasia cells. (1999) *Biochem and Biophys Res Comm.* **261**: 317-325.
- Jongstra-Bilan, J., Ittel, M-E., Neidergang, C., Vosberg, H-P., and Mandel, P. (1983). DNA topoisomerase I from calf thymus is inhibited in vitro by poly(ADP-ribosylation). *European Journal of Biochemistry*, **136**: 391-396

- Juan, C., Hwang. J, Jui. AA, Whang-Peng J, Knutsen T, Huebner K, Croce CM, Zheng JC, Wang JC and Lui LF (1988). Human Topoisomerase I is encoded by a single-copy gene that maps to chromosome 20q12-13.2. *PNAS* **85**: 8910-8913.
- Kameshita, I., Z. Matsuda, Tanigushi, T., .Shizuta, Y. (1984). Poly (ADP-Ribose) synthetase. Separation and identification of three proteolytic fragments as the substrate-binding domain, the DNA-binding domain, and the automodification domain. *J. Biol Chem* **259**: 4770-4776.
- Kanaar R., Hoeijmakers J. H. J., van Gent D. C. (1998) Molecular mechanisms of DNA double-strand break repair. *Trends in Cell Biology* **8** (12): 483-489
- Kane CM and. Linn S (1981) Purification and characterization of an apurinic/apyrimidinic endonuclease from HeLa cells. *J. Biol. Chem.* **256**, pp. 3405–3414
- Kanofsky, J. R. and Sima, P. D. (2000) Preferential cytotoxicity for multidrug-resistant K562 cells using the combination of a photosensitiser and a cyanide dye. *J. Photochem. Photobiol.* **54**:136-144
- Kaufmann S. H., Desnoyers S., Ottaviano Y., Davidson N. E., Poirier G. G (1993) Specific proteolytic cleavage of poly(ADP-ribose) polymerase - an early marker of chemotherapy-induced apoptosis *Cancer Research* **53** (17): 3976-3985
- Kaufmann, S. H. (1998). Cell death induced by topoisomerase-targetted drugs: more questions than answers. *Biochemica et Biophysica Acta* **1400**: 195-211.
- Kaufmann, S., Charron M., Burke P.J., Karp JE. (1995). Changes in Topoisomerase I levels and localisation during myeloid maturation in vitro and in vivo. *Cancer Research* **55**: 1255-1260.
- Kawato, Y., Aonuma, M.,Hirota, Y.,Kuga,. H. and Sato, K (1991). Intracellular roles of SN-38, a metabolite of the camptothecin derivative CPT-11, in the antitumour effect of CPT-11. *Cancer Research* **51**: 4187-4191.
- Khanna K. K, Jackson S P (2001) DNA double-strand breaks: signaling, repair and the cancer connection. *Nature Genetics* **27** (3): 247-254
- Kingsbury W. D., Boehm J. C., Jakas D. R., Holden K. G., Hecht S. M., Gallagher G., Caranfa M. J., McCabe F. L., Faucette L. F., Johnson R. K., Hertzberg R. P. (1991) Synthesis of water-soluble (aminoalkyl)camptothecin analogs - inhibition of topoisomerase-I and antitumor-activity. *Journal of Medicinal Chemistry* **34** (1): 98-107
- Kjeldsen, E., Svejstrup, J. Q., Gromova I. I., Alsner, J., and Westergaard, O. (1992). Camptothecin inhibits both the cleavage and religation reactions of eukaryotic DNA topoisomerase I. *J. Mol. Biol.* **228**: 1025-1030
- Kleczkowska H. E., Malanga M., Szumiel I., Althaus F. R. (2002). Poly ADP-ribosylation in two L5178Y murine lymphoma sublines differentially sensitive to DNA-damaging agents. *Int J Radiat Biol.* **78**(6): 527-34.

- Klugland, A. and Lindahl, T. (1997) Second pathway for completion of human DNA base excision repair: reconstruction with purified proteins and requirement for DNase IV (FEN1). *EMBO*, 16: 3341-3348
- Koch S. S. C., Thoresen L. H., Tikhe J. G., Maegley K.A., Almassy R. J., Li J. K., Yu X. H., Zook S. E., Kumpf R. A., Zhang C., Boritzki T. J., Mansour R. N., Zhang K. E., Ekker A., Calabrese C.R., Curtin N. J., Kyle S., Thomas H. D., Wang L. Z., Calvert A. H., Golding B. T., Griffin R. J., Newell D. R., Webber S. E., Hostomsky Z. (2002) Novel tricyclic poly(ADP-ribose) polymerase-1 inhibitors with potent anticancer chemopotentiating activity: design, synthesis, and X-ray co-crystal structure. *Journal of Medicinal Chemistry* **45** (23): 4961-4974
- Koh, Y. Nishio, K., and Saijo, N. Mechanisms of Action of Cancer Chemotherapeutic Agents: Topoisomerase Inhibitors. thecancerhandbook.net
- Kohn, K. W., Ewig, R., Erickson, L., and Zwelling L. (1981) Measurement of strand breaks and cross-links by alkaline elution. *DNA repair a manual of research techniques* ed. Friedberg and Hanawalt. New York Marcel Dekker.
- Kraakman-van der Zwet, M., Overkamp, W. J. I., Friedl, A. A., Klein, B., Verhaegh, G. W. C. T., Jaspers, N. G. J., Midro, A. T., Eckardt-Schupp, F., Lohman, P. H. M., Zdzienicka, M. Z. (1999) Immortalisation and characterisation of Nijmegen Breakage syndrome fibroblasts, *Mutation Research* **434**: 17-27.
- Krokan, H. E., Nilsen, H Skorpen, F., Otterlei, M., Slupphaug G. (2000). Base excision repair of DNA in mammalian cells. *FEBS Letters* **476**: 73-77.
- Krupitza, G. and Cerutti P (1989). ADP-ribosylation of ADPR-transferase and topoisomerase I in intact mouse epidermal cells JB6. *Biochemistry* **28**(5): 2034-2040.
- Kubota N., Kanzawa F., Nishio K., Takeda Y., Ohmori T., Fujiwara Y., Terashima Y., Saijo N. (1992) Detection of topoisomerase-I gene point mutation in CPT-11 resistant lung-cancer cell-line. *Biochemical and Biophysical Research Communications* **188** (2): 571-577
- Kubota, N. (1992) Detection of DNA topoisomerase gene point mutation in CPT-11 resistant lung cancer cell line. *Biochem Biophys Research Commun*: **188** 571-577
- Kupper J. H., Muller M., Jacobson M. K., Tatsumimiyajima J., Coyle D. L., Jacobson E. L., Burkle A. (1995) Transdominant inhibition of poly(ADP-ribosyl)ation sensitizes cells against gamma-irradiation and n-methyl-n'-nitro-n-nitrosoguanidine but does not limit DNA-replication of a polyomavirus replicon. *Molecular and Cellular Biology* **15** (6): 3154-3163
- Lautier, D., Lagueux, J Thibodeau, J., Menard, L., Poirier, G. G. (1993). Molecular and biochemical features of poly (ADP-ribose) metabolism. *Molecular & Cellular Biochemistry* **122**(2): 171-93.
- Lavrik, O. I., Prasad, R., Sobol, R. W., Horton, J. K., Ackerman, E. J., and Wilson, S. H. (2001) Photoaffinity labelling of mouse fibroblast enzymes by a base excision repair

- intermediate. *Journal of Biological Chemistry* **276**: 25541-25548
- Leppard, J. B., Dong, Z., Mackey, Z. B., and Tomkinson, A. E. (2003) Physical and functional interaction between DNA ligase II α and poly(ADP-ribose) polymerase I in DNA single-strand break repair. *Molecular and Cellular Biology* **23**: 5919-5927
- Lindahl T. (1974) An N-glycosidase from *Escherichia coli* that releases free uracil from DNA containing deaminated cytosine residues. *Proc Natl Acad Sci USA*; **71**: 3649-3653.
- Lindahl, T., Satoh M. S., Poirier, G. G., Klungland, A.. (1995). Post-translational modification of poly(ADP-ribose) polymerase induced by DNA strand breaks. *Trends in Biochemical Sciences* **20**(10): 405-411.
- Liu, C., Pouliot, J. J., and Nash, H. A. (2002) Repair of topoisomerase I covalent complexes in the absence of the tyrosyl-DNA phosphodiesterase Tdp1. *PNAS* **99**: 14970-14975.
- Longley D.B., Harkin D.P., and Johnston P.G. (2003) 5-Fluorouracil: mechanisms of action and clinical strategies. *Nature Reviews in Cancer* **3**: 330-337
- Loprinzi, C. L., and Erlichman C. (2001) Hormonal Therapies. Section 20.3 in De Vita, Cancer: Principles and Practice of oncology LW & W
- Lozzio C. B. and Lozzio B. B. (1975) Human chronic myelogenous leukaemia cell-line with positive Philadelphia chromosome. *Blood*, **45**: 321-334
- Madden, K. R. and Champoux J.J (1992). Overexpression of human topoisomerase I in baby hamster kidney cells: hypersensitivity of clonal isolates to camptothecin. *Cancer Research* **52**(3): 525-532.
- Mao, Y. Sun, M., Desai, S. D., and Liu, L. SUMO-1 conjugation to topoisomerase I: a possible repair response to topoisomerase-mediated DNA damage. *PNAS* **97**: 4046-4051
- Marintchev, A., Robertson, A., Dimitriadis E. K., Prasad, R., Wilson, S. H., and Mullen G. P., (2000) Domain specific interaction in the XRCC1-DNA polymerase beta complex. *Nucleic Acids research*. **28**: 2049-2059
- Marks D I, and Fox R M. (1991). DNA damage, poly(ADP-ribosyl)ation and apoptotic cell death as a potential common pathway of cytotoxic drug action. *Biochemical Pharmacology*. **42** 1859-1867
- Masson M., Menissier de Murcia J., Mattei, M., J., de Murcia G., and Niedergang, C. P. (1997) Poly(ADP-ribose) polymerase interacts with a novel human ubiquitin conjugating enzyme hUbc9. *Gene*, **190**: 287-296
- Masson, M., Niedergang C, Schreiber, V., Muller, S., Menissier de Murcia, J., de Murcia. G. (1998). XRCC1 is specifically associated with poly(ADP-ribose) polymerase and negatively regulates its activity following DNA damage. *Mol. Cell. Biol.* **18**: 3563.-3571
- Matsutani, M., Nozaki, T., Nishiyama, E., Shimokawa, T., Tachi, Y., Suzuki, H., Nakagama,

- H., Wakabayashi, K., and Sugimura M. (1999) Function of poly(ADP-ribose) polymerase in response to DNA damage: gene disruption study in mice. *Mol Cell Biochem.* **193**: 149-52
- Mattern, M.R, Mong, S-M, Bartus, H, F, Mirabelli, C, K, Crooke, S T and Johnson, R K. (1987). Relationship between the intracellular effects of camptothecin and the inhibition of DNA topoisomerase I in cultured L1210 cells. *Cancer Research* **47**: 1793-1798.
- Meijer, M., Karimi-Busheri, F., Huang, T. Y., Weinfeld, M., Young, D. (2002) Pnk1, a DNA kinase/phosphatase required for normal response to DNA damage by gamma-radiation or camptothecin in *S. pombe*. *Journal of Biological Chemistry.* **277**: 4050-4055
- Menissier de Murcia, J., Molinette, M., Gradwohl, G., Simonin, F., and de Murcia G. (1989) Zinc-binding domain of poly(ADP-ribose)polymerase participates in the recognition of single strand breaks on DNA. *Journal of Molecular Biology,* **210**: 229-233
- Menissier de Murcia, J., Ricoul, M., Tartier, L., Neidergang, C., Huber, A., Dantzer, F., Schreiber, V., Ame, C. J., Dierich, A., Le Meur M., Sabatier, L., Chambon P., and de Murcia, G. (2003). Functional interaction between PARP-1 and PARP-2 in chromosome stability and embryonic development in mouse. *EMBO* **22** (9) 2255-2263
- Mennisier-de Murcia, J., Neidergang C., Trucco, C., Ricoul, M., Dutrillaux B., Mark, M., Oliver, F.J., Masson, M., Dierich A., Lemeur M., Waltzinger, C., Chambon P., de Murcia G. (1997). Requirement of poly(ADP-ribose) polymerase in recovery from DNA damage in mice and in cells. *PNAS* **94**: 7303-7307.
- Miknyoczki, S., Jones-Bolin, S., Pritchard, S., Hunter, K., Zhao, H., Wan, W., Ator, M., Bihovsky, R., Hudkins, R., Chatterjee, S., Klein-Szanto, A. Dionne, C., and Ruggeri, B. (2003) Chemopotentiation of temozolamide, irinotecan and cisplatin activity by CEP-6800, a poly(ADP-ribose)polymerase inhibitor. *Molecular Cancer Therapeutics.* **2**: 371-382
- Milam, K.M, Thomas G, H, and Cleaver, J, E. (1986). Disturbances in DNA precursor metabolism associated with exposure to an inhibitor of Poly(ADP-ribose) synthetase. *Exp. Cell. Res.* **165**: 260-268
- Mo, Y-Y., Yu, Y., Shen, Z., and Beck, W.T. (2002) Nuclear delocalisation of human topoisomerase I in response to topotecan correlates with sumoylation of the protein. *Journal of Biological Chemistry* **277**(4):2958-2964.
- Moertal C. G., Schutt, A. J., Reitmeier R. J., Hahn, and R. J. (1972) Phase II study of camptothecin (NSC-100880) in the treatment of advanced gastrointestinal cancer. *Cancer Chemother Rep.* **56**: 95-101
- Molinette, M., Vermeulen W., Burkle, A, Menissier-de Murcia J, Kupper, J H, Hoeijmakers J H, de Murcia G. (1993). Overproduction of the poly(ADP-ribose)polymerase binding domain blocks alkylatiion-induced DNA repair synthesis in mammalian cells. *EMBO* **12**(5): 2109-2117.
- Morrison, C., Smith, G.S., Stingl, L., Jackson, S., Wagner, E.F., and wang, Z.Q. (1997) genetic

- link between PARP and DNA-PK in V(D)J recombination and tumourigenesis. *Nature Genetics* **17**: 479-482
- Nash R. A., Caldecott, K. W., Barnes, D. E., and Lindahl T. (1997) XRCC1 protein interacts with one of two distinct forms of DNA ligase III. *Biochemistry* **36**: 5207-5211
- Nie, J., Sakamoto, S., Song, D.m Qu, Z., Ota, K., and Taniguchi, T. (1998) Interaction of Oct-1 and automodification domain of poly(ADP-ribose) synthetase. *FEBS Letters*, **424**: 27-32
- Nitiss, J., and Wang, J.C. (1988). DNA topoisomerase-targeting antitumor drugs can be studied in yeast. *PNAS USA* **85**: 7501-7505.
- Oei, S. L., Griesenbeck J, Schweiger, M. (1997). The role of poly(ADP-ribosyl)ation. *Reviews of Physiology Biochemistry & Pharmacology* **131**: 127-73.
- Padget, K. Carr R, Pearson, ADJ, Tilby MJ, Austin CA. (2000a). Camptothecin-stabilised Topoisomerase I-DNA complexes in Leukaemia cells visualised and quantified in situ by the TARDIS assay (Trapped in agarose DNA immunostaining). *Biochem. Pharmacol* **59**: 629-638.
- Padget, K., Stewart, A., Charlton, P., Tilby, M J., and Austin C. A. (2000b) An investigation into the formation of N-[2-(dimethylamino)ethyl]acridine-4-carboxamide (DACA) and 6-[2-(dimethylamino)ethylamino]-3-hydroxy-7H-indenol[2,1-C]quinolin-7-onedihydrochloride (TAS-103) stabilised DNA topoisomerase I and II cleavable complexes in human leukaemia cells. *Biochem Pharmacol* **60**: 817-821
- Palatti, F., Cortes, F. Bassi, L., Di Chiara, D., Fiore, M. and Pinero, J. (1993) Higher G2 sensitivity to the induction of chromosomal damage in the CHO mutant EM9 than its parental line AA8 by camptothecin an inhibitor of DNA topoisomerase I. *Mutation Research* **285**: 281-285
- Park, S-Y., Lam, W., and Cheng, Y-C. (2002) X-ray repair cross-complementing gene I protein plays an important role in camptothecin resistance. *Cancer Research* **62**: 459-465
- Payne, C. M., Crowley, C., Washo-Stultz, D., Briehl, M., Bernstein, H., Bernstein, C., beard, S., Holubec, H., and Warneke, J. (1998) The stress-response proteins poly(ADP-ribose) polymerase and NF-kB protect against bile salt induced apoptosis. *Cell Death and Differentiation* **5**: 623-636
- Pizzolato J. F., and Saltz L. B. (2003). The camptothecins. *The Lancet*. **361**: 2235-2242
- Pleschke, J. M., Kleczkowska, H. E., Strohm, M., and Althaus, F. (2000). Poly(ADP-ribose) binds to specific domains in DNA damage checkpoint proteins. *Journal of Biological Chemistry* **275**:40974-40980
- Plo, I., Liao, Z-Y., Barcelo, J. M., Kohlhagen, G., Caldecott, K. W., Weinfield, M., Pommier, Y. (2003) Association of XRCC1 and tyrosyl DNA phosphodiesterase (Tdp1) for the repair of topo I-mediated DNA lesions. *DNA Repair* **2** 1087-1100

- Pommier Y., Kerrigan, D., Hartman, K. D., and Glazer, R. I. (1990) Phosphorylation of mammalian DNA topoisomerase I and activation by protein kinase C. *J. Biol. Chem.* **265**: 9418-9422
- Pommier, Y, Pourquier P, Fan, Y., Strumberg, D. (1998). Mechanism of action of eukaryotic DNA topoisomerase I and drugs targeted to the enzyme. *Biochimica et Biophysica Acta* **1400**(1-3): 83-105.
- Pommier, Y. (1998). Diversity of DNA topoisomerases I and inhibitors. *Biochimie* **80**(3): 255-70.
- Pouliot, J.J., Yao, K.C., Robertson, C.A., and Nash, H.A. (1999) Yeast gene for a Tyr-DNA phosphodiesterase that repairs topoisomerase I complexes. *Science*, **286**: 552-555
- Pourquier P., and Pommier, Y. (2001) Topoisomerase I-mediated DNA damage. *Advances in Cancer Research*, **80**: 189-216
- Prasad, R., Lavrik, O. I., Kim, S-J., Keder, P., Yang, Y-P., Vande Berg, B. J., and Wilson, S. H. (2001) DNA polymerase β -mediated long patch base excision repair: Poly(ADP-ribose) polymerase-1 stimulates strand displacement DNA synthesis. *Journal of Biological Chemistry* **276** (35):32411-32414
- Purnell, M. R., and Whish, W. J. D. (1980) Novel inhibitors of poly(ADP-ribose) synthase. *Biochemical Journal* **185**: 775-777
- Purnell, M. R., Kidwell, W. R., Minshall, L., and Whish, W. J. D. (1985) Specificity of poly(ADP-ribose) Synthetase Inhibitors. *ADP-ribosylation of Proteins* ed. Althaus F. R., Hilz, H., and Shall, S. Springer-Verlag, Berlin.
- Redinbo, M. R., Stewart, L., Champoux, J. J., and Hol, W. G. J. (1999). Structural flexibility in human topoisomerase I revealed in multiple non-isomorphous crystal structures. *J. Mol. Biol.* **292**: 685-696
- Rhallabhandi P., Hashimoto, K., Mo, Y-Y., Bech, W. T., Moitra, P. K., and D'Arpa, P. Sumoylation of topo I is involved in its partitioning between nucleoli and nucleoplasm and its clearing from nucleoli in response to camptothecin. *Journal of Biological Chemistry* **277**(42):40020-40026.
- Riott, I.M. (1956) The inhibition of carbohydrate metabolism in ascites tumour cells by ethyleneimines. *Biochemical Journal*. **63**: 300-307
- Robertson, E. M. (1987) Embryo-derived stem cell lines. In "Teratocarcinomas and Embryonic stem cell lines: a practical approach". Edited by E. J. Robertson, p71-112
- Roca, J. (1995). The mechanism of DNA topoisomerases. *TIBS* **20**: 156-160.
- Rosenberg, S.A. (2001) Principles of Cancer Management: Surgical Oncology Chapter 15 in DeVita, Cancer: Principles and Practice of oncology LW & W

- Rountree MR, Bachman KE, Herman JG, Baylin SB. (2001) DNA methylation, chromatin inheritance, and cancer. *Oncogene* **20**(24):3156-65.
- Ruscetti, T., Lehnert, B. E., Halbrook, J., Trong, H. L., Hoekstra, M. F., Chen, D. J., and Peterson, S. R. (1998) Stimulation of the DNA protein kinase by poly(ADP-ribose) polymerase. *Journal of Biological Chemistry* **273**: 14461-14467
- Saleem, A., Edwards, T. K., Rasheed, Z., and Rubin E., H. (2000) Mechanisms of resistance to camptothecins. *Annals of the New York Academy of Sciences*, **55**: 46-55
- Samuels, D. S., Shimizu, N., Nakabayashi, T., Shimizu, N. (1994) Phosphorylation of DNA topoisomerase I is increased during the response of mammalian cells to mitogenic stimuli. *Biochemica and Biophysica Acta* **1223**(1): 77-83.
- Samuels, D.S., Shimizu, Y., and Shimizu, N. (1989) Protein kinase C phosphorylates DNA topoisomerase I. *FEBS Letters*, **259**: 57-60
- Sander M and Hsieh T (1983) Double strand DNA cleavage by type II DNA topoisomerase from *Drosophila melanogaster*. *J Biol Chem*. **258**(13):8421-8.
- Sastry S. and Ross B. M. (1998) Mechanisms for the processing of a frozen topoisomerase-DNA conjugate by human cell free extracts. *Journal of Biological Chemistry*. **273**: 9942-9950
- Satoh, M. S., and Lindahl, T. (1992) Role of poly(ADP-ribose) formation in DNA repair. *Nature*. **356**: 356-358
- Satoh, M. S., Poirier, G., and Lindahl, T. (1993) NAD⁺-dependent repair of damaged DNA by human cell extracts. *Journal of Biological Chemistry*. **268**: 5480-5487
- Schultz, N., Lopez, E., Saleh-Gohari, N., and Helleday, T. (2003). PARP-1 has a controlling role in homologous recombination. *Nucleic Acids Research* **31** (17) : 4959-4964.
- Scudiero, D.A., Shoemaker, R.H., Paull, K.D., Monks, A., Tierney, S., Nofziger, T.H., Currrens, M.J., Seniff, D., and Boyd, M.R. (1988) Evaluation of a soluble tetrazolium/formazan assay for cell growth and drug sensitivity in culture using human and other tumour lines. *Cancer Research*. **45**: 4827-4833
- Sebolt-Leopold, J. S. and Scavone S. V. (1992). Enhancement of alkylating agent activity in vitro by PD128763, a potent poly(ADP-ribose) synthetase inhibitor. *Int J Radiat Oncol Biol Phys* **22**: 619-621.
- Seeberg, E., Eide L, Bjoras M. (1995). The Base excision repair pathway. *TIBS* **20**: 391-397.
- Shall, S. (1975) Experimental manipulation of the specific activity of poly(ADP-ribose) polymerase. *Journal of Biochemistry*. **77**: 2
- Shall, S. and de Murcia G (2000). Poly(ADP-ribose) polymerase-1: what have we learned from the deficient mouse model? *Mutation Research* **460**(1): 1-15.
- Shao, R-G., Cao, C-X., Zhang, H. Kohn, K. W., Wold, M. S. and Pommier Y. (1999).

Replication-mediated DNA damage by camptothecin induces phosphorylation of RPA by DNA-dependent protein kinase and dissociates RPA:DNA-PK complexes. *EMBO* **18**: 1397-1406

Shen, M. R., Zdzienicka, M. Z., Mohrenweiser, H., Thompson, L.H., and Thelen, M. P. (1998) Mutations in hamster single-strand break repair gene XRCC1 causing defective DNA repair. *Nucleic Acids Research* **26**: 1032-1037

Simbulan-Rosenthal, C. M., Ly, D.H., Rosenthal, D.S., Konopka, G., Luo, R., Wang, Z-Q., Schultz, P.G., and Smulson, M.E. (2000). Misregulation of gene expression in primary fibroblasts lacking poly(ADP-ribose) polymerase. *PNAS* **97**(21): 11274-11279.

Simbulan-Rosenthal, C. M., Rosenthal, D.S., Hilz, H., Hickey, R., Malkas, L., Applegren, N, Wu, Y., Bers, G., and Smulson, M.E. (1996) The expression of poly(ADP-ribose) during differentiation-linked DNA replication reveals that it is a component of the multiprotein DNA replication complex. *Biochemistry* **35**: 11622-11633.

Skalitzky, D. J., Marakovits, J. T., Maegley, K. A., Ekker A., Yu, X., Hostomsky, Z., Webber, S. E., Eastman, B. W., and Almassy, R., Li, J. (2003). Tricyclic Benzimidazoles as potent Poly(ADP-ribose) polymerase-1 inhibitors. *J. Med Chem.* **46**: 210-213

Skehan, P., Storeng R. D., Scudiero, A., Monks, J., McMahon, D., Vistica J. T., Warren Bokesch S Kenney MR Boyd. (1990). New Colormetric Assay for Anticancer-Drug Screening. *Journal of the National Cancer Institute* **82**(13): 1107-1112.

Slichenmyer, W. J., Rowinsky E K, Donehower, R. C., Kaufmann, S. H. (1993). The current status of camptothecin analogues as antitumor agents. *Journal of the National Cancer Institute* **85**(4): 271-291.

Smith, H. M., and Grosovsky, A. J. (1999) Poly(ADP-ribose)-mediated regulation of p53 complexes with topoisomerase I following ionising radiation. *Carcinogenesis* **20**: 1439-1443

Smith, S. (2001). The world according to PARP. *TIBS* **26**(3): 174-179.

Smith, S. and. de. Lange T (2000). Tankyrase promotes telomere elongation in human cells. *Current Biology* **10**: 1299-1302.

Smith, S., Giriat I, Scmitt, A, de Lange,T (1998). Tankyrase, a poly(ADP-ribose)polymerase at human telomeres. *Science* **282**: 1484-1487.

Southan, G.J. and Szabo, C. (2003) Poly(ADP-ribose) polymerase inhibitors. *Current Medicinal Chemistry*, **10**: 321-340

Squires, S., Ryan, A.J., Strutt, H.L. nad Johnson, R.T. (1993) Hypersensitivity of Cockayne's syndrome cells to camptothecin is associated with the generation of abnormally high levels of double strand breaks in nascent DNA. *Cancer Research*, **53**: 2012-2019

- Srivastava, D.K., Berg, B.J., Prasad, R., Molina, J.T., Beard, W.A., Tomkinson, A.E., and Wilson S.H. (1998) Mammalian abasic site base excision repair. Odentification of the reaction sequence and rate-determining steps. *Journal of Medicinal Chemistry*. **273**: 21203-21209
- Staron, K., Kowalska-Loth, B., and. Szumiel, I. (1994) The sensitivity to camptothecin of DNA topoisomerase I in L5178Y-S lymphoma cells. *Carcinogenesis* **15**: 2953-2955
- Staron, K., Kowalska-Loth, B., Nieznanski, K and. Szumiel, I (1996) Phosphorylation of topoisomerase I in L5178Y-S cells is associated with poly(ADP-ribose) metabolism. *Carcinogenesis* **17**: 383-387
- Staron, K., Kowalska-Loth, B., Zabek, J., Czerwinski, R. M., Nieznanski, K., and. Szumiel, I (1995) Topoisomerase I is differently phosphorylated in two sublines of L5178Y mouse lymphoma cells. *Biochim. Biophys. Acta*. **1260**: 35-42
- Stewart, L, Redinbo, M, R, Qui, X, Hol, W, G, J, Champoux, J.(1998). A model for the mechanism of Human Topoisomerase I. *Science*, **27**: 1534-1541
- Stewart, L. and. Champoux. J. J. (2000). Assaying DNA topoisomerase I Relaxation activity. *Methods in Molecular Biology*, Vol 95: DNA topoisomerase Protocols, Part II: Enzymology and Drugs. N. a. B. Osheroff, M.A., Humana Press Inc: 1-11.
- Stewart, L., Ireton, G. C., Parker, L.H., Madden, K. R., and Champoux, J. J. (1996) Biochemical and biophysical analyses of recombinant forms of human topoisomerase I.. *Journal of Biological Chemistry* **271**: 7593-7601
- Sugimoto, Y., Tsukahara, S., Oh-hara, T., Isoe, T., and Tsuruo, T. (1990) decreased expression of DNA topoisomerase in camptothecin-resistant tumour cell lines as determined by a monoclonal antibody. *Cancer Research*, **50**: 6925-6930
- Sugimura, T. and Miwa M (1994). Poly(ADP-ribose): historical perspective. *Molecular & Cellular Biochemistry* **138**(1-2): 5-12.
- Suto, M. J., Turner, W. R., Arundel-Suto, C. M., Werbel, I. M., and Seebolt-Leopold, J. S. (1991) Dihydroisoquinolines: the design and synthesis of a new series of potent inhibitors of poly(ADP-ribose polymerase. *Anticancer Drug Design*. **7**: 107-117
- Svejstrup, J.Q., Christiansen K., Gromova, H., Anderson, A.H., and Westergaard, O. (1991) new technique for uncoupling the cleavage and religation reactions of eukaryotic topoisomerase I. The mode of action of camptothecin at a specific recognition site. *Journal of Molecular Biology*. **222**: 669-678
- Takasuna, K., Hagiwara, T., and Hirohashi, M. (1996) Involvement of beta-glucoronidase in intestinal microflora in the intestinal toxicity of the antitumour camptothecin derivative irinotecan hydrochloride (CPT-11) in rats. *Cancer Research* **56**: 3752-3757
- Takimoto, C.H., and Arbuck, S.G. (1997) Clinical status and optimal use of topotecan.

Oncology, **11**: 1635-1646, 1649-1651 and 1655-1657

Tanizawa, A., Bertrand, R., Kohlhagen, G., Tabichi, A., Jenkins, J., and Pommier Y. (1993) Cloning of Chinese hamster DNA topoisomerase I cDNA and identification of a single point mutation responsible for camptothecin resistance. *J. Biol. Chem.* **268**: 25463-24568

Tebbs, R. S., Zhao, Y., Tucker, J. D., Scheerer, J. B., Siciliano, M. J., Hwang, M., Liu, N., Legerski, R. J., and Thompson, L. H. (1995). Correction of chromosomal instability and sensitivity to diverse mutagens by a cloned cDNA of the XRCC1 DNA repair gene. *PNAS* **92**: 6354-6358.

ten Bokkel Huinink, W., Carmichael J, Armstrong, D., Gordon, A., Malfetano, J.. (1997). Efficacy and safety of topotecan in the treatment of advanced ovarian carcinoma. *Seminars in Oncology* **24**(1 Suppl 5): S5-19-S5-25.

Tentori, L., Leonetti, C., Scarsella, M., d'Amati, G., Portarena, I., Zupi, G., Bonmasser, E., and Graziani, G. (2002) *Blood*, **99**: 2241-2244

Tentori, L., Portarena, I., and Graziani, G. (2002) Potential clinical applications of poly(ADP-ribose) polymerase inhibitors. *Pharmacological Research*, **45**: 73-85

Thompson L.H., Borrkman, K.W., Dillehay, L.E., Carrano, A.V., Mazrima Mooney, C. L., and Minkler, J. L. (1982) A CHO-cell strain having hypersensitivity to mutagens, a deficiency in DNA strand-break repair, and an extraordinary baseline frequency of sister chromatid exchange. *Mutation Research* **95**: 427-440

Thompson T. H., Fong, S., and Brookman, K. (1980) Validation of conditions for efficient detection of HPRT and APRT mutations in suspension-cultured Chinese hamster ovary cells. *Mutation research*, **74**: 21-36

Trucco, C., Olivier, J. F., de Murcia, G., Menissier de Murcia J. (1998) DNA repair defect in poly(ADP-ribose) polymerase-deficient cell lines. *Nucleic Acids Research* **26**: 2644-2649

Tsao, Y., Russo, A., Nyamuswa, G., Silber, R., and Liu, L.F. (1993). Interaction between replication forks and topoisomerase I-DNA cleavable complexes: Studies in a cell-free SV40 DNA replication system. *Cancer Research* **53**: 5908-5914.

Tse-Dinh, Y-C., Wong, T. W., and Goldberg, A. R., (1984) Virus- and cell-encoded tyrosine protein kinases inactivate DNA topoisomerases *in vitro*. *Nature*, **312**, 785-786

Ulukan H., and Swann P. W. (2002). Camptothecins: A review of their Chemotherapeutic potential. *Drugs* **62**: 2039-2057

Veuger, S. J., Curtin, N. J., Richardson, C. J., Smith, G. C. M., and Durkacz, B. W. (2003). Radio sensitisation and DNA repair inhibition by the combined use of novel inhibitors of DNA-dependent protein kinase and poly(ADP-ribose) polymerase-1. *Cancer Res.* 2003 **63**: 6008-6015.

- Virag, L., and Szabo, C. (2002) The therapeutic potential of poly(ADP-ribose) polymerase inhibitors. *Pharmacology Review*, **54**: 375-429
- Vodenicharov, M. R, Sallmann F.R, Satoh, M.S., Poirier G.G.. (2000). Base excision repair is efficient in cells lacking poly(ADP-ribose)polymerase 1. *Nucleic acids research* **28**(20): 3887-3896.
- Voigt, W., Vanhoeffter U., Yin M.B., Minderman, H., Schmoll, H. J., and Rustum, Y. M. (1997). Evaluation of topoisomerase I catalytic activity as determinant of drug response in human cancer cell lines. *Anticancer Research* **17**: 3707-3712
- Wall, M.E., Wani, M.C., Cooke, C.E. Palmer, K.H., McPhail, A.T, Slim, G.A. Am., (1966). *J Am Chem Soc* **88**: 3888-3890.
- Wang, J. C., (1996) Topoisomerases. *Annual Review of Biochemistry*, **65**: 635-692
- Wang, Z.Q., Auer, B., Stingl, L., Berghammer, H., Haidacher, D., Schweiger, M., and Wagner, E. W. (1995) Mice lacking ADPRT and poly(ADP) ribosylation develop normally but are susceptible to skin disease. *Genes Dev.* **9**: 509-520
- Weiner, L. M., Adams G. P., Mehren M. Therapeutic Monoclonal Antibodies: General Principles. Section 20.5 in De Vita, Cancer: Principles and Practice of oncology LW & W.
- Weltin, D., Holl, V., Hyun, J., Marchal, J., Bischoff, P., and Dufour, P. (1997) Effects of treatments combining 6(5H)-phedanthridinone, a new poly(ADP-ribose) polymerase inhibitor, and anticancer agents upon murine and human tumour cell lines. *Proc. Am. Assoc. Can. Res.* **38**: 1485
- Whish, W. J. D., Davies, M. I., and Shall, S. (1975) Stimulation of poly(ADP-ribose) polymerase activity by the anti-tumour antibiotic, streptozotocin. *Biochem. Biophys Res Commun.* **65**: 772-30
- Whitehouse, C.J., Taylor, R.M., Thistlethwaite, A., Zhang, H., Karim-Busheri, F., Lasko, D.D., Weinfeld M., and Caldecott, K.W. (2001) XRCC1 stimulates human polynucleotide kinase activity at damaged DNA termini and accelerates DNA single strand break repair. *Cell*, **104**: 107-117
- Willmore E., Frank A. J., Padget K., Tilby, M. J., and Austin C. A. (1998). Etoposide targets topoisomerase II α and II β in leukemic cells: isoform-specific cleavable complexes visualised and quantified *in situ* by a novel immunofluorescence technique. *Molecular Pharmacology* **53**: 78-85
- Wu, J and Liu, L.F. (1997) Processing of topoisomerase I cleavable complexes into DNA damage by transcription. *Nucelic Acids Research*, **25**: 4181-4186

Yang, S-W., Burgin, A. B., Huizenga, B. N., Robertson, C. A., Yao, K. C., and Nash H. A. (1996) A eukaryotic enzyme that can disjoin dead-end covalent complexes between DNA and type I topoisomerases. PNAS **93**: 11534-11539

Yu, S.W., Wang, H., Poitras, M.F., Coombs, C., Bowers, W.J., Federoff, H.J., Poirier, G.G., Dawson, T.M., and Dawson V.L. (2002) Mediation of poly(ADP-ribose) polymerase-1-dependent cell death by apoptosis-inducing factor. Science, **297**: 259-263

Zhang, H. DeArpa P, and Lui, L.F (1990). A model for tumour killing by topoisomerase poisons. Cancer Cells **2**: 23-27